The Responsive Approach: an Integrated Socially-Sustainable Technically-Optimal Decision Model

THÈSE N^{O} 4251 (2008)

PRÉSENTÉE LE 17 DÉCEMBRE 2008

À LA FACULTE ENVIRONNEMENT NATUREL, ARCHITECTURAL ET CONSTRUIT
LABORATOIRE DE MAINTENANCE, CONSTRUCTION ET SÉCURITÉ DES OUVRAGES
PROGRAMME DOCTORAL EN STRUCTURES

ÉCOLE POLYTECHNIQUE FÉDÉRALE DE LAUSANNE

POUR L'OBTENTION DU GRADE DE DOCTEUR ÈS SCIENCES

PAR

James Denman BIRDSALL

acceptée sur proposition du jury:

Prof. J.-P. Lebet, président du jury
Prof. E. Brühwiler, directeur de thèse
Dr R. Hajdin, rapporteur
Dr O. Lateltin, rapporteur
Prof. V. November, rapporteur

ÉCOLE POLYTECHNIQUE
FÉDÉRALE DE LAUSANNE

Suisse
2009

Executive Summary

Motivation

Over the past 30 years, within the field of infrastructure management, as infrastructure systems have grown more complex, the level of managerial and financial oversight has increased, and the computation power has become less expensive and more readily available, infrastructure managers have increasingly turned to computerized infrastructure management systems to aid in the management of the built infrastructure. An infrastructure management system acts as an infrastructure manager's 1) inspection database detailing the current state of the built infrastructure, 2) infrastructure performance simulation platform modeling the potential future infrastructure performance, 3) infrastructure deterioration and provided service estimator evaluating the equivalent financial loss associated with infrastructure deterioration and decreased provided levels of service, and 4) infrastructure maintenance action development engine formulating and scheduling technically and financially optimal infrastructure maintenance solutions.

Historically, the performance simulation module of infrastructure management systems has focused primarily upon modeling gradual infrastructure deterioration processes, such as corrosion, and the infrastructure provided service estimator has employed nominal values for quantifying the public's evaluation of the provided infrastructure performance. These approaches have caused infrastructure managers to focus their attention and funding towards combating gradual infrastructure deterioration while giving priority maintenance status to infrastructure objects that place the largest nominally evaluated total performance impact on society.

While this approach has helped infrastructure managers to more efficiently manage the built infrastructure, such an approach is only efficient if it is unfailingly implemented over multiple decades. Unfortunately, the current limited infrastructure management system scope has exposed infrastructure managers to two potentially disruptive forces – potential unforeseen natural hazard induced technical failures and potential political and/or financial funding support failures due to incongruent evaluation of the provided level of performance between the infrastructure manager's nominal evaluation measures and the experiencing society. While these two disruptive forces originate in two very different elements of an infrastructure management system, they both can induce the same result – undermining of the intended technically and financially optimal infrastructure management solution.

Objective and originality

To work towards rectifying both of these limitations, the current work has developed methodologies for both quantifying the long-term infrastructure natural hazard risk exposure and estimating an individual's experience-based evaluation of the provided level of infrastructure performance.

The methodology for assessing natural hazard induced technical infrastructure failures has focused around developing an infrastructure component potential failure assessment procedure which employs data within existing infrastructure and transportation management systems and currently under development natural hazard identification maps. This failure assessment procedure is designed to identify the locations and estimate the associated consequences of potential natural hazard induced failures. This failure probability and failure consequence information is then employed to quantify an annualized and a multi-year infrastructure link risk exposure.

The methodology for estimating an individual's experience-based evaluation of the provided level of infrastructure performance has been developed by employing research findings from the fields of psychology and behavioral economics to develop the affective assessment approach, a variance-based evaluation tool. This evaluation tool employs an individual's range and quality of experienced infrastructure performance in time to predict the individual's current induced affect and future sensitivity to the provided levels of infrastructure performance. As this is a constructed evaluation approach, employing the affective assessment approach directly in the third infrastructure management module, evaluating equivalent financial loss associated with decreased provided levels of service, can be computationally prohibitive as each potential sequence would need to be modeled. It is, therefore, proposed to use the affective assessment approach as a reality check against which the developed technically and financially optimal management solution can be assessed and solutions which provide too low or inconsistent levels of infrastructure performance can be identified, reevaluated or discarded.

Results and benefits

With this additional technical information and perspectives, infrastructure managers are able to actively consider an object's natural hazard risk exposure in modeling the infrastructure deterioration and in developing optimal maintenance actions. Furthermore, infrastructure managers are able to determine the annual funding that should be invested and made available to respond to current and future natural hazard induced object failures. By, calibrating and implanting the affective assessment approach, infrastructure managers can also study how proposed technically optimal solutions may be socially received and can select solutions which best maintain social support throughout the duration of the maintenance solution.

Within the field of infrastructure management, the past 30 years has been invested in developing standardized and computerized infrastructure management systems. With these systems implemented, infrastructure managers are starting to observe their strengths but also their limitations. This work has focused on formulating quantitative methods to develop solutions for two of these limitations. It is hoped that these methods might be further developed, calibrated and implemented to improve existing infrastructure management systems and the infrastructure and society they manage.

Key Words:

Infrastructure management, component failure assessment, natural hazard risk management, experience-based evaluation, affective assessment approach

Résumé

Motivation

Les 30 dernières années ont vu, le domaine des systèmes de gestion d'infrastructures se complexifier, le niveau de veille financière et de gestion augmenter, la puissance de calcul devenir plus accessible et moins coûteuse, et les gestionnaires d'infrastructure se tourner vers une utilisation croissante des systèmes de gestion d'infrastructures assistés par ordinateur. Un système de gestion d'infrastructure fonctionne comme un gestionnaire d'infrastructures en ayant recours à : 1) une base de donnée répertoriant l'état des structures 2) des simulations modélisant les performances de potentielles infrastructures 3) l'estimation des pertes financières équivalentes, dues à la détérioration de l'infrastructure ainsi qu'à la baisse des niveaux de service, et 4) à un moteur de développement d'actions de maintenance d'infrastructures, formulant et planifiant les solutions financières et techniques optimales de maintenance.

Historiquement, les modules de simulation de performance des systèmes de gestion d'infrastructures se sont concentrés dans un premier temps, sur la modélisation des processus de dégradation progressive de l'infrastructure, comme la corrosion, et des valeurs statistiques étaient utilisées par les estimateurs de service d'infrastructure pour quantifier l'évaluation publique des performances de l'infrastructure. Ces approches ont dirigé l'attention et le financement des gestionnaires d'infrastructures à combattre contre la détérioration progressive de l'infrastructure, ce en rendant prioritaires les statuts de maintenance des composants d'infrastructures ayant l'impact nominal le plus important lors de leur l'évaluation au cours de l'étude de l'impact sociétal de l'infrastructure.

Cependant, malgré l'augmentation d'efficacité pourvue aux gestionnaires d'infrastructure, cette approche ne peut être efficace que si elle est implémentée de manière continue au cours de plusieurs dizaines d'années. Malheureusement l'étendue actuellement limitée des systèmes de gestion d'infrastructures, expose les gestionnaires d'infrastructures à deux forces potentiellement disruptives - l'induction potentielle de défaillances techniques par d'imprévisibles catastrophes naturelles et des baisses potentielles de support politique et/ou financier, dues à des évaluations incongrues des niveaux de performance entre les évaluations statiques du gestionnaire d'infrastructures et ceux rencontrés par la société. Malgré les origines très différentes de ces forces disruptives, elles peuvent toutes deux conduire au même résultat - la sape financière et technique de la solution intentée de gestion de l'infrastructure.

Objectifs et originalité de la démarche

Dans une optique de rectification de ces limites, ce travail a développé des méthodologies de quantifications de l'exposition à long terme aux risques naturels et à l'estimation du niveau de performance de l'infrastructure basé sur l'expérience personnelle d'un individu.

La méthode d'assertion de risques induits par des catastrophes naturelles causant des défaillances techniques c'est concentré autour du développement d'une procédure d'évaluation de potentielle défaillance de composants de l'infrastructure, utilisant des données provenant des systèmes de gestion des infrastructures et de transport ainsi que des cartes de risque naturels en cours de développement. Ces procédures d'identification de risque de défaillance se proposent d'identifier les zones et d'estimer les conséquences corollaires de potentielles défaillances induites par les risques

naturels. Les informations provenant des probabilités de défaillance et leurs conséquences sont alors utilisées pour quantifier un lien d'exposition aux risques annuel et pluriannuel.

La méthodologie utilisée pour l'estimation des l'évaluation des performances de structures, basée sur l'expérience d'un individu, ont été développées en utilisant des résultats expérimentaux provenant des domaines de la psychologie et de l'économie comportementale afin de développer un modèle d'évaluation de l'affectif, basé sur un outil d'analyse de la variance. Cet outil d'évaluation utilise un classement des individus selon le nombre et la qualité des expériences sur les performances d'infrastructures rencontrées au cours du temps. Ceci pour prédire les influences actuelles et futures de l'affectif dans l'analyse des niveaux de performance de l'infrastructure. Cette approche évaluative construite, utilisant directement l'approche d'évaluation affective dans le troisième module de gestion d'infrastructures, servant à évaluer la perte financière équivalente associée en fonction de la baisse des niveaux de service, peut-être limitant du point de vue calculatoire sachant que chaque séquence potentielle devrait être modélisée. Il est, cependant, proposé d'utiliser l'approche d'évaluation affective comme un vérificateur de réalité grâce auquel les solutions de gestion technique et financière optimales pourront être évaluées, ainsi les solutions proposant des niveau de performance d'infrastructure trop bas ou inconsistants pourront être réévaluées ou retirées.

Résultats et bénéfices

Avec ces perspectives et ces informations techniques additionnelles, les gestionnaires d'infrastructures sont capables de considérer activement l'exposition aux risques naturels d'un composant en modélisant la détérioration de l'infrastructure et en développant des actions de maintenance optimales. En outre, les gestionnaires d'infrastructure sont capables de déterminer la somme annuelle devant être mise à disposition et investie afin de répondre aux défaillances induites les risques naturels présents et futurs. En calibrant et implantant l'approche par évaluation affective, les gestionnaires d'infrastructure peuvent alors étudier quelles seront les solutions techniques acceptées socialement et ainsi choisir les solutions socialement optimales durant toute la durée de l'intervention de maintenance.

Dans le domaine de la gestion de structure, les 30 dernières années ont été investies à développer des systèmes de gestion d'infrastructure informatisés et standardisés. Une fois ces systèmes implémentés, les gestionnaires d'infrastructures pourront alors observer leurs avantages mais aussi leurs limites. Ce travail c'est concentré sur la formulation de méthodes quantitatives afin de fournir des solutions sur deux limites de ces systèmes. Il est à espérer qu'un développement, une calibration, et une implémentation ultérieure de ces systèmes de gestion seront effectués avec comme objectif l'amélioration de la gestion des infrastructures et des sociétés.

Mots-clés :

Gestion d'infrastructure, évaluation de rupture de composants, gestion de risque naturel, évaluation basée sur l'expérience, approche d'évaluation affective

Zusammenfassung

Motivation

Während in den vergangenen 30 Jahren Verkehrsinfrastruktursysteme immer komplexer geworden sind, das Mass an betriebswirtschaftlicher und finanzieller Übersicht gewachsen und Rechenleistung erschwinglicher und leichter verfügbar geworden ist, haben sich Infrastrukturmanager mehr und mehr computergestützten Infrastrukturmanagementsystemen zugewandt, um die Verwaltung der gebauten Infrastruktur zu bewältigen. Infrastrukturmanagementsysteme fungieren 1) als Inspektionsdatenbanken, die den aktuellen Zustand der gebauten Infrastruktur erfassen, 2) als Plattform zur Simulation der zukünftigen Leistungsfähigkeit von Infrastruktursystemen, 3) als Hilfsmittel zur Abschätzung des Schädigungsausmasses und der Nutzbarkeit der Infrastruktur, das den äquivalenten finanziellen Verlust, der mit der Infrastrukturschädigung und der reduzierten Nutzbarkeit verbunden ist auswertet und 4) als technische und finanzielle Planungshilfe für optimale Unterhaltsarbeiten.

Früher zielten die Module von Infrastrukturmanagementsysteme zur Modellierung der Leistungsfähigkeit vornehmlich auf die Vorhersage der fortschreitenden Infrastrukturschädigung durch beispielsweise Korrosion ab. Die Nutzbarkeitsabschätzung verwendete statische Werte für die Quantifizierung der öffentlichen Bewertung der verfügbaren Leistungsfähigkeit der Infrastruktur. Diese Ansätze bewirkten, dass Infrastrukturmanager ihre Aufmerksamkeit und Mittel auf die Bekämpfung der fortschreitenden Infrastrukturschädigung richteten, wobei Priorität der Unterhalt von den Infrastrukturkomponenten bevorzugt wurde, die die grössten nominell bewerteten Gesamtauswirkungen auf die Leistungsfähigkeit der Gesellschaft haben.

Während dieser Ansatz Infrastrukturmanagern geholfen hat die gebaute Infrastruktur effizienter zu bewirtschaften, ist ein solcher Ansatz nur dann effizient, wenn er über mehrere Jahrzehnte konsequent angewendet wird. Leider hat der aktuell begrenzte Funktionsumfang der Infrastrukturmanagementsysteme Infrastrukturmanager zwei möglicherweise zerstörerischen Kräften ausgesetzt – dem potentiellen durch unvorhergesehene Naturgefahren hervorgerufenen technischen Versagen und dem potentiellen Verlust politischer und/oder finanzieller Unterstützung aufgrund einer inkongruenten Beurteilung des verfügbaren Leistungsfähigkeitsniveaus durch die statischen Bewertungsmethoden des Infrastrukturmanagers einerseits und der wahrnehmenden Öffentlichkeit andererseits. Während diese beiden zerstörerischen Kräfte ihren Ursprung in zwei sehr verschiedenen Elementen eines Infrastrukturmanagementsystems haben, können beide das gleiche Ergebnis bewirken – die Unterwanderung der vorgesehenen technisch und finanziell optimalen Infrastrukturmanagementlösung.

Zielstellung und Originalität

Zur Aufhebung dieser beiden Einschränkungen, wurden in der vorliegenden Arbeit Methoden entwickelt, um die langfristige Risikoexposition der Infrastruktur gegenüber Naturgefahren zu quantifizieren und um die individuelle, erfahrungsbasierte Beurteilung der verfügbaren Infrastrukturleistungsfähigkeit abzuschätzen.

Die Methodik um technische Ausfälle der Infrastruktur durch Naturgefahren abzuschätzen, richtet sich auf die Entwicklung eines Beurteilungsverfahrens für das mögliche Versagen von Infrastrukturkomponenten, das Daten aus bestehenden Infrastruktur- und Transportmanagementsystemen und gegenwärtig im Entstehen begriffene Karten zur Identifizierung

von Naturgefahren verwendet. Dieses Verfahren zur Versagensabschätzung erlaubt es den Ort zu lokalisieren und die mit einem möglichen Schadensfall durch Naturgefahren verbundenen Konsequenzen zu bewerten. Die Versagenswahrscheinlichkeit und die Information über die Schadensfolgen wird dann angewendet, um die Risikoexposition der Infrastruktur im Jahresmittel und Mehrjahreszeitraum zu quantifizieren.

Die Methodik um die individuelle, erfahrungsbasierte Bewertung der verfügbaren Infrastrukturleistungsfähigkeit einzuschätzen, wurde unter Verwendung von Forschungsergebnissen aus dem Gebiet der Psychologie und der Verhaltensökonomie entwickelt, um den affektiven Bewertungsansatz, ein varianzbasiertes Beurteilungswerkzeug, aufzustellen. Dieses Beurteilungswerkzeug berücksichtigt frühzeitig den Erfahrungsbereich und die Erfahrungsqualität des Einzelnen bezüglich der Infrastrukturleistungsfähigkeit, um den gegenwärtigen Affekt und die zukünftige Sensibilität des Einzelnen in Bezug auf die Infrastrukturleistungsfähigkeit vorherzusagen. Da dies ein konstruierter Beurteilungsansatz ist, der den affektiven Bewertungsansatz direkt im dritten Infrastrukturmanagementmodul ansiedelt, ist die Auswertung der äquivalenten finanziellen Verluste, die mit einem gesunkenen Nutzbarkeitsniveau verbunden sind, berechnungsseitig nahezu unmöglich, da jede potentielle Sequenz modelliert werden müsste. Daher wird vorgeschlagen, den affektiven Bewertungsansatz als einen Realitätscheck anzuwenden dem die erarbeitete technisch und finanziell optimale Managementlösung gegenübergestellt werden kann. Lösungen, die zu niedrige oder inkonsistente Niveaus der Infrastrukturleistungsfähigkeit liefern, können damit identifiziert, neu beurteilt oder verworfen werden.

Ergebnisse und Nutzen

Mit diesen zusätzlichen technischen Informationen und Perspektiven sind Infrastrukturmanager in der Lage die Risikoexposition einer Komponente durch Naturgefahren in der Modellierung der Infrastrukturschädigung aktiv zu berücksichtigen und optimale Erhaltungsmassnahmen zu ergreifen. Darüber hinaus sind sie in der Lage, die jährliche Finanzierung festzulegen, die aufgewendet und zur Verfügung gestellt werden sollte, um auf den aktuellen und zukünftigen Ausfall von Infrastrukturkomponenten durch Naturgefahren zu reagieren.

Durch Kalibrierung und Implementierung des affektiven Bewertungsansatzes können Infrastrukturmanager ebenso untersuchen, wie vorgeschlagene technisch optimale Lösungen gesellschaftlich aufgenommen werden und können somit Lösungen auswählen, die die grösste gesellschaftliche Unterstützung während der Dauer der Erhaltungsmassnahmen erfahren.

Auf dem Gebiet des Infrastrukturmangements wurden die vergangenen 30 Jahre in die Entwicklung standardisierter und computergestützter Infrastrukturmanagementsysteme investiert. Mit der fortlaufenden Anwendung dieser Systeme beginnen Infrastrukturmanager die Systemstärken und -grenzen zu ermitteln. Die vorliegende Arbeit zielt darauf ab, quantitative Methoden für die Behebung zwei dieser Einschränkungen zu formulieren. Es besteht die Hoffnung, dass diese Methoden weiterentwickelt, kalibriert und implementiert werden, um bestehende Infrastrukturmanagementsysteme und die Infrastruktur und Gesellschaft, denen sie dienen, zu verbessern.

Schlüsselwörter:

Infrastrukturmanagement, Bauteilversagensbeurteilung, Rsikiomanagement von Naturgefahren, Erfahrungsbasierte Bewertung, Affektiver Beurteilungsansatz

Table of Contents

Foreword

The field of infrastructure management has made significant progress over the last 20 years. Infrastructure management systems have been developed focusing primarily on modelling of deterioration processes. While this approach certainly helped infrastructure managers to manage more efficiently the built infrastructure, it lacks considering the more and more relevant questions of 1) hazard situations due to natural hazards and 2) insufficient support for funding of infrastructure maintenance (which might be due to inadequate consideration of the user's evaluation of infrastructure performance).

In his thesis, Mr Birdsall provides engineering methods and approaches for 1) quantifying the exposure to natural hazards and 2) considering the user's evaluation of the performance of the infrastructure system, which are validated by means of case studies. This research covers a broad range of disciplines ranging from failure behaviour of structures to topics from psychology and economics while dealing with computational aspects of infrastructure management tools. Bringing all these disciplines together in a research work devoted to one topic, i.e. infrastructure management, was a real challenge. The result is very satisfying since this thesis provides methods useful for the infrastructure manager and for implementation into infrastructure management tools.

Mr Birdsall provides the proof of his capabilities to conduct a scientific study and to solve complex problems. In the name of the whole team of MCS, I thank him for his thorough and constant investment to the thesis topic as well as for his professional skills and personal qualities.

Lausanne, December 2008 Professor Eugen Brühwiler

Acknowledgements

This work was conducted at the Laboratory of Maintenance and Safety of Structures (MCS), a laboratory within the Structural Engineering Institute at the École Polytechnique Fédérale de Lausanne and at the Infrastructure Management Consultants, a Zurich based infrastructure consulting firm. This research was funding by a École Polytechnique Fédérale de Lausanne university scholarship and the Swiss National Science Foundation National Research Program NRP 54 – Sustainable Development of the Built Environment.

During my doctoral research, I have had the opportunity to professionally and personally interact with and learn from a number of particular individuals. I would like to take a moment to acknowledge a number of individuals who have significantly contributed to the development of this work and of my professional and personal perspectives.

I would first like to thank Professor Eugen Brühwiler for the opportunity to conduct research within his laboratory, for the chance to learn his 'examineering' perspective, and for the latitude to question and research a number of domains not traditionally considered within the traditional civil engineering domain. Secondly, I would like to thank Dr. Rade Hajdin and Dr. Bryan Adey for their friendship, advice and benevolent tempering of these research activities.

In developing the comprehensive risk assessment approach, I would like to thank Dr. Marzio Giamboni, Dr. Andreas Meier, Willy Eyer and Dr. Blaise Duvernay for aiding me in gaining an understanding for the natural hazard and risk management approaches currently employed within Switzerland.

I would also like to thank Professor Jean-Paul Lebet, Professor Valerie November and Dr. Olivier Lateltin for serving on my doctoral defence committee. Additionally, I would like to thank Mme. Christine Benoit, the MCS laboratory secretary, for her assistance in tackling all sorts of administrative and every-day questions.

Furthermore, I would like to thank my fellow master and doctoral students with whom I have had the honor and enjoyment of working with – Daniel Lenggenhanger, Dr. Aicha Kamen, Alix Grandjean, Alexsis Kalogeropoulos, Talayeh Noshiravani, Aga Switek, Dr. David Conciatori, Dr. Andrin Herwig, Dr. Danijel Mocibob and especially Dr. John Wuest.

Most importantly, I would like to thank my wife and partner, Jenn, and my son, Nathaniel, for their advice, help, patience and loving support over the seemingly unending days, nights and weekends invested in bringing this work to fruition.

In closing, my family and I would like to thank Switzerland for warmly welcoming us into their communities and homes. We have truly found our home here and we hope that we will maintain the Swiss way of life in the years to come.

Table of Figures

Table of Tables

Table of Examples

Table of Case Studies

Glossary

Term	Abbreviation	Definition
Affect		the positive or negative quality of an interaction
Attenuation factor		a continuous exposed object length reduction factor for a specific infrastructure component an natural hazard
Bounded rationality		a form of decision making where an individual's finite faculties limits the range of reality considered
Consequences		are the expected direct and indirect consequences of the reduced structural and/or function performance of an infrastructure object
Construct		a discrete mental concept of an individual's experience reality
Direct consequences		the financial valuation of the repair activities required to return the infrastructure object's structural performance to its original state
EPA		environmental protection agency
ESA		endangered species act
Evaluation norm		the perceived summary of the set of all previous interactions with a specific parameter
Experienced reality		the subset of reality which an individual personally interacts with
Experience-based risk assessment		a form of risk assessment in which an individual's personal experience is used to quantify the uncertainty of given risk source
Experience practitioners		an individual who has amassed an expert level of knowledge repairing and maintaining infrastructure systems
Exposure length		the length of an infrastructure object exposed to a specified hazard
Failure of an infrastructure object		the state of reduced structural and/or functional performance of the infrastructure object
Failure mode	m_n	the process through an infrastructure object failure is induced
Failure scenario		the process by which a hazard can cause structural or functional damage to an infrastructure object
FEMA		United States Federal Emergency Management Agency
Functional performance		the functional state of the infrastructure object

Geographic information systems	*GIS*	an geographically-based approach to presenting data and conducting analyses
HCP		habitat conservation plans
Hazard	*H*	a potentially damaging phenomenon
Hazard parameter	*h*	a variable quantifying a hazard (e.g. flood depth)
Hazard parameter intensity	*x*	the magnitude of a hazard parameter
HAZards United States	*HAZUS-MH*	a geographic information systems based computerized natural hazard risk assessment tool distributed by FEMA
hedonic psychology		the study of what makes interactions pleasant or unpleasant
Indirect consequences		the financial valuation of the losses and additional expenditures incurred from transport and societal related impacts of an infrastructure object's reduced functional performance
Induced affect		the induced emotion of a given interaction
Interaction		the direct personal usage of a public transportation system
LSGIs		local self-governing institutions
National Bridge Inventory Database	*NBI*	an inventory of all bridges within the United States with a span longer than 6 meters
NYDOT		New York State Department of Transportation
Return period	*RP*	an estimate of the average time interval between equivalent intensity events [years]
Risk of failure	R_i^H	the probabilistic quantification of the consequences a potentially damaging phenomenon, a hazard (*H*), can cause failure of an infrastructure object (*i*)
SilvaProtect		a natural hazard indication mapping resource for determining the largest possible extent of gravity-induced natural hazards
StorMe		a nationally supported, cantonally administrated natural hazard event documentation database
Structural performance		the structural state of the infrastructure object
Service interruption duration		the time required to return a failed infrastructure object to a fully functional state
Swiss highway structures database	*KUBA*	an infrastructure management system developed to manage the swiss highway structures
Swiss transportation model	*STM*	a subset of over 51,000 transportation links which are a minimum of 2.8m wide and have the capacity to carry a reasonable amount of traffic

SwissTopo	Swiss national office for geographic information systems
Vector25	an object type-based geographic vectorization of the Swiss transportation systems at a scale of 1:25000
Vulnerability	the consequences a hazard parameter of a given intensity can cause failure of an infrastructure object

Table of Symbols

Latin Upper Case

Symbol	Definition
A	the number of non-depreciated interactions [ ]
A_{BSE}	area of bridge superstructure exposed to the hazard [m^2]
A_{GW}	the hazard induced axial wall forces [kN]
A_s	the area of the tensile reinforcement within the width b [mm^2]
A_s'	the area of the compression reinforcement within the width b [mm^2]
A_{sBD}	tensile reinforcement area within the width b_{BD} of the bridge deck [mm^2]
$A_s'_{BD}$	compression reinforcement area within the width b_{BD} of the bridge deck [mm^2]
A_{sBP}	the bridge pier tensile reinforcement [mm^2]
A_{sBP}'	the bridge pier compression reinforcement [mm^2]
A_{sBS}	tensile reinforcement area within the bridge deck width b_{BD} [mm^2]
$A_s'_{BS}$	compression reinforcement area within the bridge deck width b_{BD} [mm^2]
A_{sGR}	the gallery roof tensile reinforcement area within the width b_{GRM} [mm^2]
$A_s'_{GR}$	the gallery roof compression reinforcement area within the width b_{GRM} [mm^2]
A_{sGRM}	the gallery roof structural member tensile reinforcement area within the width b_{GRM} [mm^2]
$A_s'_{GRM}$	the gallery roof structural member compression reinforcement area within the width b_{GRM} [mm^2]
A_{sGW}	the gallery wall tensile reinforcement area within the width b_{GWM} [mm^2]
$A_s'_{GW}$	the gallery wall compression reinforcement area within the width b_{GWM} [mm^2]
A_{sGWM}	the gallery wall structural member tensile reinforcement area within the width b_{GWM} [mm^2]
$A_s'_{GWM}$	the gallery wall structural member compression reinforcement area within the width b_{GWM} [mm^2]
AB	Bernoulli's initial value of goods
AC, AD, AD, AF	Bernoulli's future potential value of goods (sequentially increasing)
AF	the affective assessment factor
AS_i	the potential induced affect for interaction i given the interaction intensity, the perceived mean and the perceived standard deviation of experience of all previous interactions.
AV	the NYSDOT bridge safety assurance program bridge abutment vulnerability [ ]
B	width of the concrete compression face [mm]
B_{BH}	total bridge bearing horizontal capacity [kN]
B_{BV}	the bridge bearing vertical capacity [kN]
b_{GR}	the gallery roof concrete compression face width [mm]

BF	the NYSDOT bridge safety assurance program bridge structural assessment of the bridge foundation [ ]
BP	Bernoulli's value of the potential action
$C_{A,B}$	the correlation factor between the greater magnitude hazard risk A and the lesser magnitude hazard risk B [ ]
C_B	bridge clearance measured between the bottom of the superstructure and the average water level or surrounding earth [m]
$Cost$	HAZUS estimated replacement cost of the given bridge class detailed in Table 2-3 [USD]
CS	the NYSDOT bridge safety assurance program bridge classification score [ ]
D_{50}	median diameter of bed material [m]
D_{84}	diameter of 84% bed material is smaller [m]
D_{BA}	abutment or pier depth measured from the ground surface at the downhill side of the abutment[m]
D_{BP}	bridge pier depth [m]
D_H	hazard rupture surface depth at the retaining wall location [m]
D_j	the memory depreciation factor for the considered interaction j [ ]
D_L	landslide rupture surface depth measured from the ground surface at the downhill side of the abutment [m]
D_{RWF}	retaining wall foundation depth [m]
$Damage$	the HAZUS total anticipated direct financial loss resulting from a bridge failure due to scour [USD]
$DC_{i,mn}^{x}$	the financial valuation of the repair activities required to return object i's failure in mode m_n with respect to the hazard parameter intensity x to object i's original state [CHF]
DC_{mn}^{HI0}, DC_{mn}^{HI1}, DC_{mn}^{HI2} DC_{mn}^{HI3}	estimated direct consequences for the given component class and failure mode as a function of the hazard parameter intensity [CHF/100m]
$DC_{mn}(x)$	the direct consequence function fitted to the estimated direct consequences [CHF]
DD_A	avalanche deposited depth [m]
DD_H	hazard deposited depth [m]
DD_L	landslide deposited depth [m]
DD_R	rockfall deposited depth [m]
DD_T	torrent deposited depth [m]
$E(n, X \leq x, t)$	the number of events less than or equal to a given threshold event x occurring within time t
E_{BD}	the bridge deck modulus of elasticity [N/mm^2]
E_{BP}	the bridge pier modulus of elasticity [N/mm^2]
E_{GRC}	the gallery roof cushioning material modulus of elasticity [N/mm^2]
E_{GWM}	the gallery wall member modulus of elasticity [N/mm^2]
E_R	rockfall kinetic energy [kJ]
E_{RW}	the retaining wall modulus of elasticity [N/mm^2]
ED_F	flood induced bank erosion depth [m]
$EL_i(x)$	the exposed object section i length as a function of the hazard parameter intensity [m]

F	estimated direct consequence extrapolation factor (typically 0.333) [ ]
$F_{i,mn}^{x}$	the structural state of object *i* failing in mode m_n to the hazard parameter intensity *x*
$F_{Xn}(X)$	the cumulative distribution function for the annual maximum hazard parameter intensity
$F_{XN}(X)$	the cumulative distribution function for the largest hazard parameter intensity during the time perspective *N*
FC	the NYSDOT bridge safety assurance program bridge potential failure consequences [ ]
FK_1	footing nose shape correction factor [ ]
FK_2	angle of flow attack correction factor [ ]
FK_3	bed condition scour depth correction factor [ ]
FK_4	footing armoring scour depth correction factor [ ]
G	estimated service interruption duration extrapolation factor (typically 0.333) [ ]
H_b	clearance between the lowest superstructure point and the non-scoured stream bed [m]
H_{BD}	bridge deck height [m]
H_C	height of the culvert inlet [m]
H_F	flood height [m]
H_G	the gallery height [m]
H_G'	the uphill gallery wall height measured from the surrounding earth [m]
H_{GRC}	the height of the gallery roof cushioning material [mm]
H_{RWB}	the height of the retaining wall brace [m]
H_T	torrent height [m]
H_{TU}	the height of the lowest tunnel electrical, communication or ventilation utilities [m]
HA	the NYSDOT bridge safety assurance program bridge vulnerability to the given hazard [ ]
HI_0, HI_1, HI_2, HI_3	reference hazard parameter intensities employed in the consequence estimation [ ]
I	infrastructure link reference variable [ ]
$IC_{i,mn}^{x}$	the financial valuation of the incurred transport and societal losses and additional expenditures due to infrastructure object *i*'s reduced functional performance by failing in mode m_n [CHF]
$IC_{I,daily}$	the daily financial valuation of the losses and additional expenditures incurred from transport and societal related impacts of infrastructure link *I*'s reduced functional performance [CHF]
J	the applicable object length natural hazard specific attenuation factor [ ]
K	exposed object section length extrapolation factor (typically 0.333) [ ]
K_w	wide pier in shallow flow correction factor [ ]
k	hazard reference variable
K_u	hydraulic constant (19.63) [ ]
L	redefined LQI considering work-leisure tradeoffs
L_B	bridge span length between two adjacent supports [m]

L_{BT}	total bridge length measured from end to end or expansion joint to expansion joint [m]
L_G	the spacing distance between the gallery structural frames [mm]
L_i^{hi0}, L_i^{hi1}, L_i^{hi2}, L_i^{hi3}	object section exposed lengths determined from the geographic coincident analysis [m]
L_{max}	the total length of the object section [m]
L_0	the original life quality index [$/person]
L_x	total number of years lived in age interval [years]
L_{x1}	modified total number of years lived in age interval [years]
$LC^{A,B}$	the correlation factor specifying the correlation between the initial hazard *A* and the secondary hazard *B*, both within the same inferior hierarchical level
Link_Risk	the financial equivalent link risk exposure considering direct and indirect consequences [CHF]
$Link\_Risk_{DC}$	the link direct consequence risk due to all hazard specific continuous risks [CHF]
$Link\_Risk_{SI}$	link risk level service interruption duration risk with respect to all five hazards [days]
LS	the NYSDOT bridge safety assurance program bridge vulnerability to the given hazard [ ]
M_{ABS}	maximum bridge superstructure avalanche induced moment [Nmm]
M_{AGWM}	the gallery structural wall member maximum avalanche induced moment [Nmm]
M_{GW}	the hazard induced moment wall forces [kNm]
M_{HBD}	the maximum hazard induced moment force within the bridge deck [Nmm]
M_{HGR}	the gallery roof maximum hazard induced moment [Nmm]
M_{HGRM}	the gallery structural roof member maximum hazard induced moment [Nmm]
M_{HGW}	the gallery wall maximum hazard induced moment [Nmm]
M_{HHPH}	hazard induced horizontal moment [kNm]
M_{HHBS}	hazard induced horizontal moment [kNm]
M_{HRW}	the retaining wall maximum hazard induced moment [kNm]
M_{HRWF}	the retaining wall foundation maximum hazard induced moment [kNm]
M_{LGWM}	the gallery structural wall member maximum landslide induced moment [Nmm]
M_{RBD}	the bridge deck maximum rockfall induced moment [Nmm]
M_{RGR}	the gallery roof maximum rockfall induced moment [Nmm]
M_{RHBP}	the bridge pier maximum rockfall induced moment [Nmm]
M_{RBS}	the bridge superstructure maximum rockfall induced moment [Nmm]
M_{RGW}	the gallery wall maximum rockfall induced moment [Nmm]
M_{RGWM}	the gallery roof member maximum rockfall induced moment [Nmm]
M_{RHBS}	the bridge superstructure maximum rockfall induced moment [Nmm]
M_u	the ultimate moment resistance [Nmm]
M_{uBD}	the ultimate moment resistance of the bridge deck [Nmm]
M_{UBPH}	bridge pier ultimate horizontal moment capacity [kNm]
M_{uBS}	bridge superstructure ultimate moment resistance [Nmm]

M_{UBSH}	bridge superstructure ultimate horizontal moment capacity [kNm]
M_{uGR}	the gallery roof ultimate moment resistance [Nmm]
M_{uGRM}	the gallery roof structural member ultimate moment resistance [Nmm]
M_{uGW}	the gallery wall ultimate moment resistance [Nmm]
M_{uGWM}	the gallery wall structural member ultimate moment resistance [Nmm]
M_{URW}	the retaining wall ultimate moment capacity [kNm]
M_{URWF}	the retaining wall foundation ultimate moment capacity [kNm]
M_x	observed death rate [years^{-1}]
M_{x1}	modified death rate [years^{-1}]
N	the considered time perspective [years]
N_{BP}	the number of bridge piers within the considered bridge or bridge section [ ]
P	hazard reference variable
$P(n,t)$	the probability of n events in period t
$P(n, X \leq x, t)$	the probability of n events in period t that are less in intensity than or equal to a threshold intensity x [ ]
P_{AH}	avalanche horizontal pressure [kN/m^2]
P_{BBHi}	horizontal capacity of bridge bearing or load path i [kN]
P_{BBVi}	vertical capacity of bridge bearing i [kN]
P_{fA}^{B}	the failure probability of object A with respect to hazard B [ ]
$P_{fi,mn}^{x}$	the failure probability of object i failing in mode m_n with respect to the hazard parameter intensity x [ ]
$P_{failure}$	the HAZUS probability of failure detailed in Table 2-2 [ ]
P_{HH}	total horizontal applied force [kN]
P_{RGRM}	the rockfall force applied on the gallery roof member [kN]
P_{RGWM}	the rockfall force applied on the gallery roof member [kN]
P_{RHBP}	the rockfall horizontal force applied to the bridge pier [kN]
P_{RRW}	the rockfall force applied on the retaining wall [kN]
P_{RVBD}	the rockfall vertical force applied to the bridge deck [kN]
P_{TV}	the torrent vertical pressure [N/mm^2]
PK_1	pier nose shape correction factor [ ]
PK_2	angle of flow attack correction factor [ ]
PK_3	bed condition scour depth correction factor [ ]
PK_4	pier armoring scour depth correction factor [ ]
PV	the NYSDOT bridge safety assurance program bridge pier vulnerability [ ]
Q_C	culvert design discharge [m^3/s]
R	rockfall hazard reference variable [ ]
R_{DH}	hazard running depth [m]
R_{HRW}	the retaining wall brace maximum hazard induced force assessed parallel to the slope [kN]
R_I^{H1}	the continuous object I's risk to avalanche hazards [CHF]
R_I^{Hi}, R_I^{Hj}, R_I^{Hk}, R_I^{Kl}	the continuous object I's risk to the four hazards (flood, landslide rockfall, torrent) are called in decreasing risk magnitude [CHF]
$R_{I,SI}^{1}$	superior hierarchical level service interruption duration risk with respect to avalanche hazard [days]

$R_{I,SI}^{k}$	superior hierarchical level service interruption duration risk with respect to hazard *k* [days]
$R_{i,mn}^{x}$	object *i*'s structural capacity with respect to the failure mode m_n and the hazard parameter intensity *x*
R_I^{Hz}	the individual hazard continuous object risks [CHF]
$R_{i,SI}^{'1}$	inferior hierarchical level continuous object and object section service interruption duration risk with respect to the avalanche hazard [days]
$R_{j,SI}^{'1}$	maximum inferior hierarchical level continuous object and object section service interruption duration risk with respect to the avalanche hazard [days]
$R_{q,SI}^{'k}$	maximum inferior hierarchical level continuous object and object section service interruption duration risk with respect to hazard *k* [days]
R_{URW}	the retaining wall brace ultimate capacity assessed parallel to the slope [kN]
RD_A	avalanche running depth [m]
RD_H	hazard running depth [m]
RD_{HB}	hazard running depth on top of the bridge superstructure [m]
RD_L	landslide running depth [m]
RD_R	rockfall running depth [m]
RES	reconstruction economies of scale [ ]
Rh	hydraulic radius [m]
$Risk_A^B$	the risk of failure of object *A* with respect to hazard *B* [CHF]
$Risk_{DC,T}^{H}$	the object direct consequence risk for a given hazard *H* over a time perspective of *T* years [CHF]
$Risk_{DC,T,N}^{H}$	the object direct consequence risk for a given hazard *H* over a time perspective of *T* years considering the maximum hazard parameter intensity in *N* years [CHF]
$Risk_i^H$	the risk of object section *i* with respect to hazard *H* [CHF]
$Risk_I$	the multi-hazard continuous object risk [CHF]
$Risk_{I,DC}^{h}$	the annual continuous object *I* direct consequence risk with respect to the hazard parameter *h* [CHF]
$Risk_{I,DC}^{H}$	continuous object *I*'s direct consequence risk exposure to hazard *H* [CHF]
$Risk_{I,SI}^{h}$	the annual continuous object *I* service interruption duration risk with respect to the hazard parameter *h* [days]
$Risk_{SI,T}^{H}$	the object service interruption duration risk for a given hazard *H* over a temporal horizon of *T* years [days]
$Risk_{SI,T,N}^{H}$	the object service interruption duration risk for a given hazard *H* over a time perspective of *T* years considering the maximum hazard parameter intensity in *N* years [days]
S_C	culvert slope [m/m]
S_i	the Gumbel Type I standard extreme variate for the given return period *i* [ ]
S_i	the measured intensity of the current interaction *i*
$SI_{i,mn}^{x}$	the time required to return infrastructure object *i* having failed in mode m_n to the hazard parameter intensity *x* to a fully functional state [days]
SI_{mn}^{HI0}, SI_{mn}^{HI1}, SI_{mn}^{HI2}, SI_{mn}^{HI3}	estimated service interruption durations for the given component class and failure mode as a function of the hazard parameter intensity [days/100m]

$SI_{mn}(x)$	the service interruption duration function fitted to the estimated service interruption durations [days]
T	footing thickness [m]
T	the risk assessment temporal horizon [years]
T_D	thickness of a torrent [m]
T_x	total number of years lived beyond age x [years]
T_{x1}	modified total number of years lived beyond age x [years]
V_1	average flow velocity immediate upstream of the pier [m/s]
V_2	adjusted flow velocity for spread footing induced scour calculations [m/s]
V_{50}	critical velocity of D_{50} sized material [m/s]
V_a	average flow velocity of D_{50} bed material before scour [m/s]
V_{ABS}	maximum bridge superstructure avalanche induced direct shear [N]
V_{AGWM}	the gallery structural wall member maximum avalanche induced shear force [N]
V_d	the ultimate direct shear capacity [N]
V_D	flow velocity of a torrent [m/s]
V_{dBD}	the ultimate direct shear capacity of the concrete deck [N]
V_{dBS}	bridge superstructure ultimate direct shear capacity [N]
V_{dGR}	the gallery roof ultimate direct shear capacity [N]
V_{dGRM}	the gallery roof structural member ultimate direct shear capacity [N]
V_{dGW}	the gallery wall ultimate direct shear capacity [N]
V_{dGWM}	the gallery wall structural member ultimate direct shear capacity [N]
V_F	average flow velocity below top of footing [m/s]
V_{GW}	the hazard induced gallery shear wall forces [kN]
V_{HBD}	the maximum hazard induced shear force within the bridge deck [N]
V_{HGR}	the gallery roof maximum hazard induced direct shear [N]
V_{HGRM}	the gallery structural roof member maximum hazard induced shear [N]
V_{HGW}	the gallery wall maximum hazard induced direct shear [N]
V_{HHBP}	hazard induced horizontal shear force [kN]
V_{HHBS}	hazard induced horizontal shear force [kN]
V_{HRW}	the retaining wall maximum hazard induced shear [kN]
V_{LGWM}	the gallery structural wall member maximum landslide induced shear [N]
V_{RBD}	the bridge deck maximum rockfall induced direct shear [N]
V_{RBS}	the bridge superstructure maximum rockfall induced direct shear [N]
V_{RGR}	the gallery roof maximum rockfall induced direct shear [N]
V_{RGRM}	the gallery roof member maximum rockfall induced direct shear [N]
V_{RGW}	the gallery wall maximum rockfall induced direct shear [N]
V_{RGWM}	the gallery wall member maximum rockfall induced direct shear [N]
V_{RHBP}	the bridge pier maximum rockfall induced horizontal direct shear [N]
V_{RHBS}	the bridge superstructure maximum rockfall induced horizontal direct shear [N]
V_{UBPH}	bridge pier ultimate direct horizontal shear capacity [kN]
V_{UBSH}	bridge superstructure ultimate direct horizontal shear capacity [kN]
V_{URW}	the retaining wall ultimate shear capacity [kN]

VS	the NYSDOT bridge safety assurance program bridge vulnerability rating score [ ]
$Vulnerability_i^H(x)$	the vulnerability function of object *i* with respect to hazard *H* [CHF]
$Vulnerability_{i,mn}^{x}$	the vulnerability of object *i* failing in mode m_n with respect to a hazard parameter intensity *x* [CHF]
$Vulnerability_{I,DC,mn}^{h}$	the continuous object *I* direct consequence vulnerability with respect to the hazard parameter *h* assuming each object section responds in the identical failure mode m_n [CHF]
$Vulnerability_{I,SI,mn}^{h}$	the continuous object *I* service interruption duration vulnerability with respect to the hazard parameter *h* assuming each object section responds in the identical failure mode m_n [CHF]
W_{BS}	weight of the bridge superstructure [kN]
W_{BP}	bridge pier width [m]
W_{DH}	weight of the displaced hazard volume [kN]
W_G	the gallery width [m]
W_H	the hazard width [m]
W_{RW}	the retaining wall width [m]
X_n	the maximum annual hazard parameter intensity [ ]
X_N	the maximum hazard parameter intensity during the considered time perspective *N* [ ]

Latin Lower Case

Symbol	**Definition**
a	pier width [m]
a_{BD}	the horizontal position of the rockfall impact point measured from the closest bridge superstructure beam [mm]
a_{BS}	the lateral position of the rockfall impact point measured from the uphill gallery wall [m]
a_{BS}	the longitudinal position of the rockfall impact point measured from the closest support or expansion joint [mm]
a_C	culvert cross-sectional area [m^2]
a_f	spread footing width [m]
a_{GRM}	the horizontal position of the rockfall impact point measured from the closest gallery roof structural frame [mm]
a_{GWM}	the horizontal position of the rockfall impact point measured from the closest gallery structural frame [mm]
a_x	death rate factor [$years^{-1}$]
$aEL_i(x)$	the effective exposed length of object section *i* as a function of the hazard parameter intensity *x* [m]
$aEL_I(x)$	the effective exposed length of continuous object *I* as a function of the hazard parameter intensity [m]
b_{BD}	width of the concrete compression face of the concrete deck [mm]
b_{BD}	the horizontal spacing of the bridge superstructure beams [mm]
b_{BS}	bridge superstructure concrete compression face width [mm]

b_{GR}	the lateral position of the rockfall impact point measured from the uphill gallery wall [m]
b_{GRM}	the gallery roof structural member concrete compression face width [mm]
b_{GW}	the gallery wall concrete compression face width [mm]
b_{GWM}	the gallery wall structural member concrete compression face width [mm]
$consequences_A^B$	the consequences of object *A* failing due to hazard *B* [CHF]
$consequences_{i,mn}^x$	the consequences of object *i* failing in mode m_n to the hazard parameter intensity *x* [CHF]
d	the distance from the extreme compression fiber to the centroid of the tensile reinforcement [mm]
d'	the distance from the extreme compression fiber to the centroid of the compression reinforcement [mm]
d_{BD}	the distance from the extreme compression fiber to the centroid of the tensile reinforcement of the bridge deck [mm]
d'_{BD}	the distance from the extreme compression fiber to the compression reinforcement centroid of the bridge deck [mm]
d_{BS}	distance from the extreme compression fiber to the centroid of the tensile reinforcement within the bridge superstructure [mm]
d'_{BS}	distance from the extreme compression fiber to the compression reinforcement centroid of the bridge superstructure [mm]
d_{cGRM}	the distance between the centroids of the compression and tensile reinforcement within the gallery roof member [mm]
d_{GR}	the distance from the extreme compression fiber to the tensile reinforcement centroid within the gallery roof [mm]
d'_{GR}	the distance from the extreme compression fiber to the compression reinforcement centroid within the gallery roof [mm]
d_{GRM}	the distance from the extreme compression fiber to the centroid of the tensile reinforcement within the gallery roof structural member [mm]
d'_{GRM}	the distance from the extreme compression fiber to the centroid of the compression reinforcement within the gallery roof structural member [mm]
d_{GW}	the distance from the extreme compression fiber to the tensile reinforcement centroid within the gallery wall [mm]
d'_{GW}	the distance from the extreme compression fiber to the compression centroid reinforcement within the gallery wall [mm]
d_{cGWM}	the distance between the centroids of the compression and tensile reinforcement within the gallery wall member [mm]
d_{cRW}	the distance between the retaining wall compression and tensile reinforcement centroids [mm]
d_{GWM}	the distance from the extreme compression fiber to the centroid of the tensile reinforcement within the gallery wall structural member [mm]
d_{GWM}	the distance between the extreme compression fiber and the centroid of the tensile reinforcement within the gallery wall member [mm]
d'_{GWM}	the distance from the extreme compression fiber to the centroid of the compression reinforcement within the gallery wall structural member [mm]
d_T	the deposited torrent debris density [N/m^3]

de	the new safety regulation impact on the life expectancy at birth
dg	the financial investment required to implement this new safety regulation per exposed individual
dL	the change of the LQI as a function of a new safety regulation
d_{RW}	the distance between the retaining wall extreme compression fiber and tensile reinforcement centroid [mm]
d_x	number of deaths
e	the life expectancy at birth [years]
e_x	life expectancy [years]
e_{x1}	modified life expectancy [years]
f	lateral footing extension measured from edge of pier [m]
f'_{dc}	the dynamic ultimate compressive strength of concrete [N/mm^2]
f'_{dcBD}	the dynamic ultimate compressive strength of concrete in the bridge deck [N/mm^2]
f'_{dcBD}	the bridge deck dynamic ultimate compressive concrete strength [N/mm^2]
f'_{dcBP}	the bridge pier ultimate compressive concrete strength [N/mm^2]
f'_{dcBS}	the dynamic ultimate compressive strength of the bridge structural deck [N/mm^2]
f'_{dcGR}	the gallery roof dynamic ultimate concrete compressive strength [N/mm^2]
f'_{dcGRM}	the gallery roof structural member dynamic ultimate concrete compressive strength [N/mm^2]
f'_{dcGW}	the gallery wall dynamic ultimate concrete compressive strength [N/mm^2]
f'_{dcGWM}	the gallery wall structural member dynamic ultimate concrete compressive strength [N/mm^2]
f_{ds}	dynamic design stress for reinforcement [N/mm^2]
f_{dsBD}	dynamic design stress for reinforcement of the bridge deck [N/mm^2]
f_{dsBS}	bridge superstructure reinforcement dynamic design stress [N/mm^2]
f_{dsGR}	the gallery roof reinforcement dynamic design stress [N/mm^2]
f_{dsGRM}	the gallery roof structural member reinforcement dynamic design stress [N/mm^2]
f_{dsGW}	the gallery wall reinforcement dynamic design stress [N/mm^2]
f_{dsGWM}	the gallery wall structural member reinforcement dynamic design stress [N/mm^2]
$f_{Xn}(X)$	the probability density function for the annual maximum hazard parameter intensity
$f_{Xn,i}(X)$	the probability density function for the largest annual hazard parameter intensity at the considered object section i
$f_{XN}(X)$	the probability density function for the largest hazard parameter intensity during the time perspective N
g	9.807 gravitation acceleration [m/s^2]
g	the real gross domestic product per capita [$/person/year]
h	hazard parameter reference variable [ ]
h_0	elevation of bottom of footing measured from stream bed [m]
hi_0, hi_1, hi_2, hi_3	reference hazard parameter intensities employed within the geographic coincident analysis [ ]

i	infrastructure object section reference variable [ ]
j	maximum inferior hierarchical level continuous object and object section service interruption duration risk reference variable with respect to a given hazard
j	the number of interactions between the considered interaction and the current interaction [ ]
l	hazard reference variable
l_x	number of survivors
m	hazard reference variable
m	the number of ways the respective action can be achieved in Bernoulli's measurement of risk
m_n	failure mode reference variable [ ]
n	the total number of object sections located within the continuous object [ ]
n	failure mode reference variable [ ]
n	the number of continuous objects and object sections in the inferior hierarchical level
n	the number of events [ ]
n	the number of ways the respective action can be achieved in Bernoulli's measurement of risk
n	the memory depreciation rate [ ]
n	steel reinforcement to concrete modulus of elasticity ration [ ]
n_C	Manning's roughness coefficient for the given culvert [ ]
n_x	interval duration [years]
p	the number of ways the respective action can be achieved in Bernoulli's measurement of risk
p_{AV}	the avalanche vertical pressure [N/mm^2]
p_{HH}	hazard horizontal pressure [kN/mm^2]
p_{HV}	the hazard vertical pressure [N/mm^2]
p_{LV}	the landslide vertical pressure [N/mm^2]
$p\mu_{i-1}$	the perceived mean experience for all previous interactions (1 to i-1)
$p\sigma_{i-1}$	the perceived standard deviation of experience for the previous interactions (1 to i-1)
$p\sigma_{min}$	the minimum perceived standard deviation of experience [ ]
q	maximum inferior hierarchical level continuous object and object section service interruption duration risk reference variable with respect to a given hazard
q	the number of ways the respective action can be achieved in Bernoulli's measurement of risk
q_F	flood specific discharge [m^2/s]
q_x	probability of death [ ]
q_{x1}	modified probability of death [ ]
r	maximum inferior hierarchical level continuous object and object section service interruption duration risk reference variable with respect to a given hazard
r_R	the radius of the boulder at the contact point [mm]

$rate_{DC}$	the direct consequence discount rate [ ]
$rate_{SI}$	the service interruption discount rate [ ]
rp_i	the return period for hazard parameter intensity event *i* [ ]
s	maximum inferior hierarchical level continuous object and object section service interruption duration risk reference variable with respect to each hazard [ ]
t	maximum inferior hierarchical level continuous object and object section service interruption duration risk reference variable with respect to a given hazard [ ]
t	the considered time period [years]
u_n	the characteristic largest value of the initial variate X_n [ ]
u_N	the Gumbel Type I characteristic largest value of the initial variate X_N [ ]
v_c	the punching shear stress capacity [N/mm^2]
v_{cBD}	the punching shear stress capacity of the bridge deck [N/mm^2]
v_{cBS}	the punching shear stress capacity of the bridge structural deck [N/mm^2]
v_{cGR}	the gallery roof punching shear stress capacity [N/mm^2]
v_{cGRM}	the gallery roof structural member punching shear stress capacity [N/mm^2]
v_{cGWM}	the gallery wall structural member punching shear stress capacity [N/mm^2]
v_{cRW}	retaining wall punching shear stress capacity [N/mm^2]
v_{RBD}	the bridge deck ultimate rockfall induced punching shear [N/mm^2]
v_{RGRM}	the gallery roof member ultimate rockfall induced punching shear [N/mm^2]
v_{RGWM}	the gallery wall member ultimate rockfall induced punching shear [N/mm^2]
v_{RRW}	rockfall induced punching shear stress [N/mm^2]
w	the average amount of an individual's lifetime invested in working [ ]
w_{BS}	bridge superstructure weight per square meter [kN/m^2]
w_{DH}	distributed buoyancy force per square meter [kN/m^2]
x	hazard parameter intensity [ ]
x	a threshold or reference intensity [ ]
x	age interval [years]
y	distance between the neutral axis and the extreme compression fiber [mm]
y_1	average upstream main channel depth prior to contraction scour [m]
y_2	adjusted flow depth for spread footing induced scour calculations [m]
y_f	elevation bottom of footing measured from stream bed [m]
$y_{sfooting}$	local scour depth induced by the footing geometry [m]
y_{spier}	local scour depth induced by the pier geometry [m]
$y_{spressure}$	depth of vertical contraction scour measured from the non-scoured stream bed [m]
y_{stotal}	total scour depth adjacent to the pier measured from the non-scoured stream bed [m]

Greek Letter

Symbol	Definition
α_B	the bridge uphill slope [rad]
α_G	the gallery uphill slope [rad]

α_n	an inverse measure of the dispersion of the maximum annual hazard parameter intensity X_n [ ]
α_N	the Gumbel Type I inverse measure of the dispersion of X_N [ ]
α_R	the rockfall angle of attack measured from the vertical
α_{RH}	the rockfall angle of attack measured from the horizontal [rad]
α_{RRW}	the rockfall angle of attack measured from a line perpendicular to the retaining wall surface [rad]
φ_{GRC}	the gallery roof cushioning material internal friction angle [rad]
γ_H	the hazard's specific gravity [kN/m^3]
ν	the event occurrence rate [years]$^{-1}$
v_i^x	the probability of the hazard parameter intensity x affecting object i [ ]
ρ_H	hazard density [kN/m^3]

1 Introduction

1.1 Management of transportation infrastructure systems

Transportation infrastructure systems are composed of links connecting geographically dispersed communities, towns and cities. When these systems operate as designed, they form the foundation upon which commerce, trade and the serviced communities' well-being can flourish (Gramlich, 1994). But when the availability of these systems is jeopardized by gradual deterioration (e.g. corrosion induced deterioration) or by sudden failure (e.g. avalanche induced link failure), the communities they service can likewise suffer. The dependent relationship between the systems and the communities they services is so extensive that the threat of transportation system service interruptions can induce the serviced populations to publicly protest or even relocate (Omar, 2001). Thus, it is important to maintain the functionality and performance of these transportation infrastructure systems in the eyes of engineers and the serviced populations.

Historically, this maintenance has taken the form of local community leaders and engineers personally maintaining limited areas of the transportation infrastructure system. But, as the systems have become more extensive, the sheer scale of the systems has required a rethinking of the management approach of transportation infrastructure systems. For example, the federal, state and local roadway systems in the United States of America are comprised of over 6.3 million km of roads and the paved Swiss roadway system is comprised of 83,000 km of roads (US Department of Transportation - Federal Highway Administration, 2008) (National Office of Topography Swisstopo, 2008).[1]

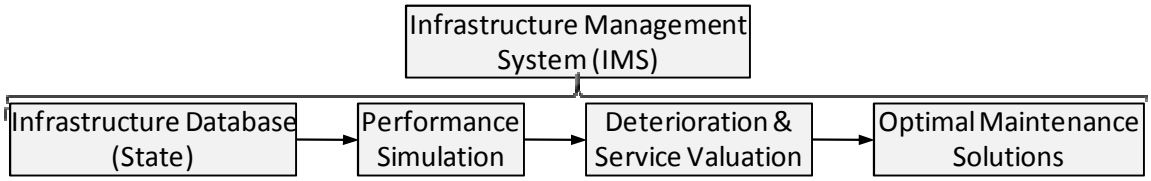

Figure 1-1: General framework of an infrastructure management system.

To meet these changing needs, over the past thirty years, civil engineers have developed infrastructure management systems (IMS), as shown in Figure 1-1, to collate inspection data specifying the current state of infrastructure objects (e.g. roads, bridges, tunnels), to simulate future deterioration processes, to evaluate the consequences of this deterioration and to develop optimal infrastructure management approaches. Infrastructure management systems use detailed criterion-based inspection and evaluation approaches, such as the approach employed by the United States Federal Highway Administration in conducting bi-annual bridge inspections, to identify and quantify the signs and indications of these deterioration processes (Hartle, Ryan, Mann, Danovich, Sosko, & Bouscher, 2002). Example infrastructure management systems include PONTIS, developed in conjunction with the United States Federal Highway Administration (FHWA) for managing the United States highway bridges, and KUBA, developed by the Swiss National Roads Office to manage road

[1] While these total roadway lengths do appear to be considerably different, the road length to citizen ratio is almost identical with 21 and 10.9 m/citizen respectively for the United States of America and Switzerland.

structures within the Swiss National Highway System (Thompson, Small, Johnson, & Marshal, 1998)(Hajdin, 2001).

Through implementing infrastructure management systems, one can develop optimized management approaches for various foreseeable funding levels and predict the resulting performance. With this funding-performance linked information, engineers can approach political decision makers and infrastructure owners with hard, transparent evidence documenting the implications of different levels of funding. Such transparent management approaches can help to induce more optimal investment in transportation infrastructure. But unfortunately the hidden signs of deterioration combined with semi-rigid taxation and budgetary structures can undermine the political motivation for changing infrastructure funding. This commonly results in the out-right denial of such funding requests. Unfortunately, it is common for such funding requests to only be completely fulfilled in the aftermath of a significant deterioration related infrastructure object failures as were the cases in the British railroad management policies following deregulation-linked deterioration and the Minnesota highway system management following the recent Minnesota I-35 bridge collapse (Vickerman, 2004)(The Economist, 2007).

1.2 Limitations of current infrastructure management systems

Infrastructure management systems are not without areas for improvement. These structural problems appear on two levels: 1) as a product of the complexities of managing such large infrastructure systems and 2) within the approaches used to analyze such systems. Concerning the complexities of managing such systems, infrastructure management systems sometimes: a) struggle to avoid being an administrative requirement rather than an active analysis tool, b) result in additional bureaucratic complexity than rather improved transparency in managing such systems, and c) overlook local issues affecting the transportation infrastructure objects, which are not perceivable from the more general approach taken by infrastructure management systems.

Concerning the approaches employed to analyze infrastructure management systems, while the infrastructure management approach has helped infrastructure managers to more efficiently manage the built infrastructure; such approaches are only efficient if they are unfailingly implemented over the management duration which can extend from multiple years to multiple decades. Unfortunately, the current infrastructure management system limited scope has exposed infrastructure managers to two potentially disruptive forces: 1) potential unforeseen natural hazard induced technical failures and 2) potential political and/or financial funding support failures due to incongruent evaluation of the provided level of performance between the infrastructure manager's nominal evaluation measures and the experiencing society. While these two disruptive forces originate in two very different elements of an infrastructure management system, they both can induce the same result – undermining of the intended analytically and financially optimal infrastructure management solution.

As the first three limitations mentioned are structural problems associated with the context in which infrastructure management systems are implemented, this work will focus on the analytical limitations concerning natural hazard assessment and social experience-based evaluation.

To work towards rectifying both of these limitations, as presented in Figure 1-2, the current work has employed a two part approach – first by developing a methodology for quantifying the long-term natural hazard risks to the built infrastructure and secondly by formulating an approach for

simulating an individual's experience-based evaluation of the provided level of infrastructure performance. As each part has its own detailed introduction, the remaining portion of this general introduction provides an overview of both parts and identifies the key challenges to and extensions of the current state of knowledge in infrastructure management and civil engineering made within this work.

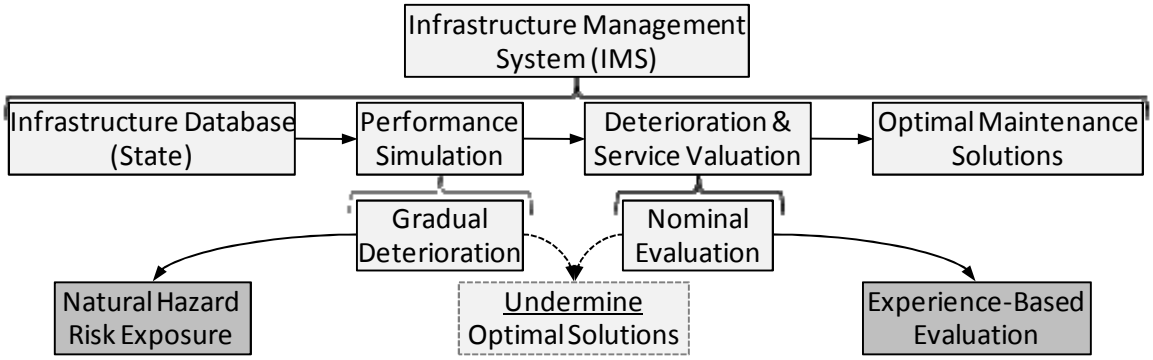

Figure 1-2: Rectifying infrastructure management limitations – natural hazard risk exposure assessment methodology and experience-based evaluation simulation approach.

1.3 A comprehensive risk assessment methodology

While gradual deterioration induced failure modes have been studied extensively and incorporated into infrastructure management systems, potential natural hazard induced failure modes have not been studied in detail or incorporated into infrastructure management systems. The most common natural hazard management approach employed is to conduct localized or regional transportation natural hazard risk assessment and mitigation projects, commonly following natural hazard events (Eyer, 2007a). Unfortunately the limited geographic, political and temporal scope of these local assessment projects significantly decreases the investment efficiency of the mitigation funds and resources as only potential failures within the considered scope are analyzed. It also means the natural hazard risk assessments have remained on a local level.

As presented in detail in Chapter 2, there are a number of large-scale transportation infrastructure systematic risk assessment initiatives actively employed or under development including HAZUS-MH, the New York State Bridge Safety Assurance Program, Risk Map Germany, and RiskScape New Zealand. In order to conduct large-scale assessments, these approaches have either employed significant simplifications in their quantitative analysis or have shifted completely to a purely qualitative assessment. Unfortunately both of these simplifications produce risk assessment approaches which have insufficient accuracy to be directly integrated into an existing infrastructure management system. Thus to rectify the limitations of the deterioration process simulation module inherent in existing infrastructure management systems, a comprehensive risk assessment methodology must be developed.

A comprehensive risk assessment methodology must include the following aspects:

- A hazard module which assesses the hazard occurrence and intensity potential within a given location.
- An infrastructure module which quantifies the structural capacities of the analyzed infrastructure objects.

- A failure assessment procedure which determines if a given potential hazard intensity can induce the failure of an infrastructure object.
- A consequence assessment framework which assesses the consequences of the potential infrastructure object failures.
- A risk quantification procedure which details the equations employed to assess the object risk given the hazard, infrastructure object, failure assessment framework, and consequence data sources.

From the existing risk assessment resources within Switzerland, presented in Chapter 2, there are already well established practices and procedures developed within the natural hazard assessment and infrastructure management fields for respectively collecting hazard and infrastructure object data. Where this work extends the current state of knowledge is by developing failure assessment procedures for each transportation infrastructure component (i.e. bridge, gallery, retaining wall, roadway and tunnel), Section 3.3 and Appendix A. These failure assessment procedures are then employed to identify the additional required hazard and infrastructure object data. These failure assessment procedures are then employed to assess the potential modes in which an infrastructure object can fail given the potential hazard intensity. Additionally, a framework is developed for employing expert opinion to estimate the direct consequences and service interruption durations resulting from an infrastructure object's failure, Section 3.4. Lastly, a procedure for a) assembling the hazard, infrastructure object, failure assessment framework and consequence assessment data sources and b) calculating the resulting transportation infrastructure object and link vulnerability and risk is clearly identified, Sections 3.5 to 3.9. This comprehensive vulnerability and risk assessment approach is then employed in Chapter 4 to assess the vulnerability and risk of selected infrastructure objects located along the Jaun Pass and the A2 highway as it transverses the towns of Zofingen and Brittnau.

This methodology forms a foundation for conducting a system wide natural hazard risk assessment. When applied across an entire transportation infrastructure system, the infrastructure manager can actively consider an infrastructure object's potential natural hazard failure risk exposure in modeling the infrastructure deterioration and in developing optimal maintenance solutions. He can also determine the annual funding which should be invested and made available for natural hazard prevention and failure response. This is important because, currently, natural hazard induced failure responses are not directly funded or considered by infrastructure management systems. The expected end result is reduced infrastructure object failure potential, improved natural hazard protection systems, and a more stable funding and infrastructure management, barring funding failures due to incongruent evaluation of the level of infrastructure performance between the infrastructure manager's nominal evaluation and the experiencing society. These dynamics are introduced in the next section.

1.4 An experience-based evaluation assessment approach

Operating and maintaining an infrastructure system is a union of two dichotomous entities: the analytical civil engineer and the experiencing public. In a perfect society, the concerns of the former would be actively and completely supported by the latter, but in practice, this support is commonly incomplete. This support gap is a direct product of the respective assessment approaches the engineering community and the general society employs to evaluate the performance of an infrastructure system.

To assess the performance of an infrastructure system, civil engineers employ codes and guidelines developed from empirical experiments, laws, jurisprudence and industry practices to maintain the built infrastructure systems. To arrive at this level of expertise, a person must conduct extensive training over a number of years to learn how to quantify forces, stress, strains, deflections and eventually failure probabilities. Thus when a civil engineer views a bridge, he does not see an elevated roadway connecting two separate landmasses, he instead sees stresses and moments, cracks and corrosion. The engineering community has employed this analytically based perspective to develop the observation-based inspection and systematic assessment methods that form the foundation of current infrastructure management systems (Hartle, Ryan, Mann, Danovich, Sosko, & Bouscher, 2002).

Like a civil engineer, each person in society has also conducted extensive training, but rather than studying structural problems and analytical assessments, this training relies on the individual's personal interactions and experiences. This training starts soon after birth and continually develops and evolves as the individual increases his wealth of knowledge with each additional interaction within the bounds of the individual's mental and physical capacities (Simon, 1957). Following each interaction, the individual evaluates the observed interaction's result and ramifications against his previous range and depth of experience. The individual then employs this evolving and refining range of experience to evaluate subsequence interactions (Kahneman & Miller, 2002). The end result is an individualized evaluation tool that is a product of the individual's frequency, range, sequence and intensity of interactions (von Glasersfeld, 1996). Thus when an individual views a bridge he does not see an elevated roadway connecting two separate landmasses, he sees the traffic and roadway conditions on the bridge within the context of his previous experiences with the bridge and similar infrastructure objects.

When it comes to evaluating the consequences of an infrastructure object's deteriorated performance, it is not surprising that the engineering community recommends analytically analyzing the situation, assigning the potential consequences into quantifiable groups and employing nominal values to evaluate each potential consequence group – be it the loss of a life or additional travel time and distance (Nathwani, Lind, & Pandey, 1997) (Vrtic, et al., 2005). When individuals from society personally interact with this deteriorating performance, they do not employ the engineer's selected nominal value, but instead they employ their recent experiences as a base against which this additional interaction is evaluated. If the deterioration is gradual, the individual is unable to discern this change, but if this deterioration deviates significantly from the individual's previous experience, the individual consciously discerns this change. Thus the societal evaluation of the consequences resulting from deteriorating performance are as much influenced by the given deterioration consequence as it is influenced by the context in which this deterioration consequence is experienced.

Thus to rectify this limitation of the deterioration consequence evaluation module within existing infrastructure management systems, an experience-based evaluation simulation approach must be developed.

In developing this experience-based evaluation simulation approach, one must:

- Identify the infrastructure object parameters the public personally interacts with.
- Specify a process for modeling how the performance difference between subsequent interactions can be evaluated.

- Formulate an approach for incorporating additional experiences into the individual's evaluative norms.
- Examine the implications an experience-base evaluation perspective has for individuals with different experience histories and within environments with different deterioration rates.

This work extends the current state of knowledge by first analyzing the logic used to develop one of the consequence evaluation approaches employed by civil engineers – the Life Quality Index, an approach used to assess of the value of a life, Appendix B. The Life Quality Index proposes that a unified rationale should be developed for taking action in society's interest and once this rationale is known and accepted, the day-to-day risk decisions should be removed from the political arena where, in the Life Quality Index developers' opinion, they do not belong (Nathwani, Lind, & Pandey, 1997). While this and other foundational tenets employed in developing the Life Quality Index are good intentioned, they are in fact incorrect for by removing the day-to-day risk decisions from society, a risk manager is actively exposing himself and his decisions to potential differences between the analytically-based performance evaluation and societal experience-based performance evaluations.

To establish a better understanding of the dynamic nature of an individual's experience-based evaluation approach, a pair of case studies studying how an individual's experience-based assessments evolve in time as they interact with a changing infrastructure systems are then analyzed in Chapter 5. From these cases, infrastructure parameters are identified that can be influenced by an infrastructure manager's policies and that an individual personally interacts with when using the given infrastructure object.

With these additional perspectives, in Chapter 6 an experience-based evaluation approach – the affective assessment approach – is developed from findings within the behavioral economics and psychology fields. The affective assessment approach is then employed in Sections 6.4 and 6.5 to analyze two cases to better understand the implications an experience-based evaluation approach can have on the evaluations of a set of interactions. The feasibility of applying such an experience-based evaluation approach is assessed in Chapter 7 by conducting a pilot study. In this study, it was determined that pursuing a calibration study was not feasible within this work, but should be pursued in the immediate future.

This approach offers infrastructure managers a tool to assess how individuals using infrastructure objects would evaluate the future provided infrastructure performance (functionality). This is important because it assists infrastructure managers in selecting an analytically optimal solution that insures the provided performance does not undermine or dilute society's level of expected performance. This assists in keeping society's evaluation of future performance sufficiently high to ensure technically optimal maintenance solutions are fully implemented and funded. The funding link has not yet been calibrated but the link is strongly suspected to exist especially in direct democracy funding situations as are found in Switzerland.

1.5 Conclusion

As can be seen in Figure 1-3, the improvements proposed within this work addresses the analytical limitations of current infrastructure management systems enabling infrastructure managers to: a) improve performance simulation of potential natural hazard risks, thus actively considering an infrastructure object's natural hazard risk in modeling the infrastructure deterioration and in

developing optimal maintenance solutions, b) improve annual funding determinations, c) study how proposed technically optimal solutions may be socially received and can select solutions which best maintain their social support throughout the duration of the maintenance solution. These tools form a technically optimal, socially sustainable infrastructure management model.

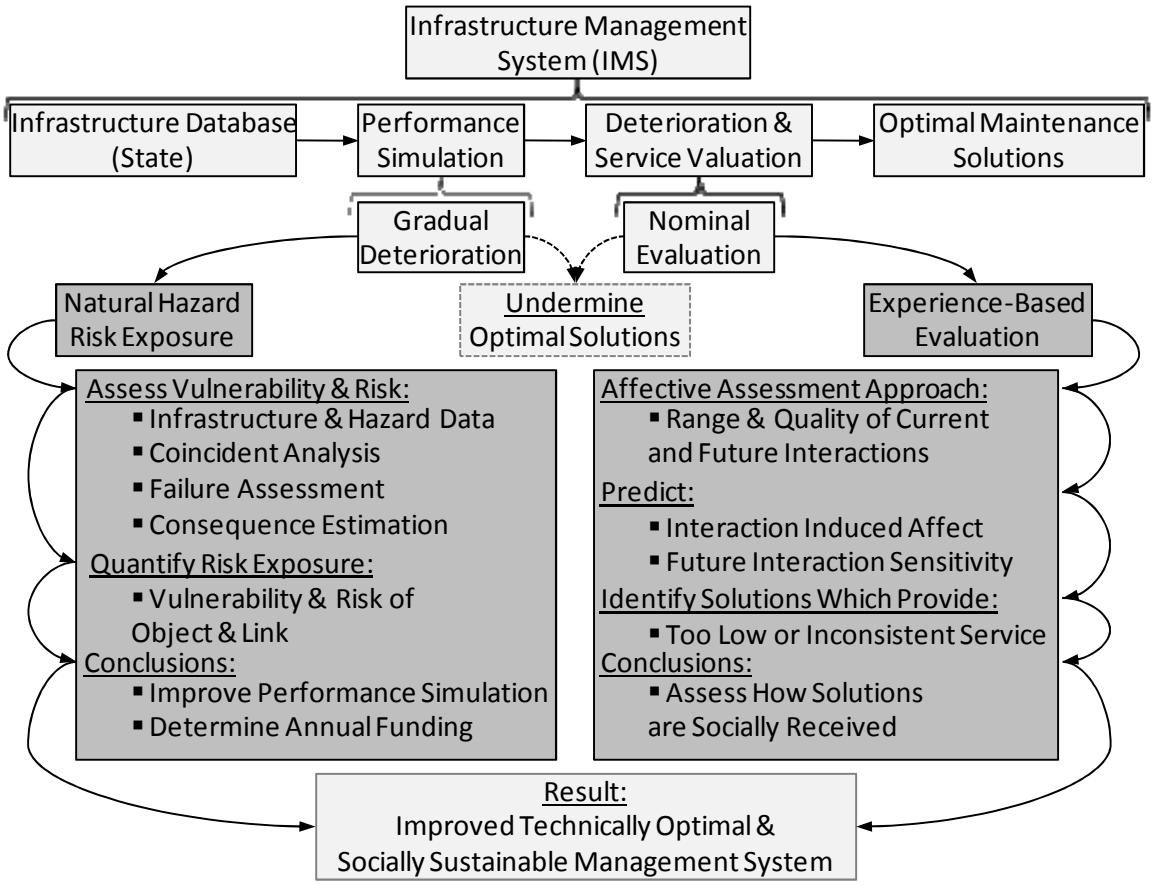

Figure 1-3: A technically optimal, socially sustainable management system.

2 Existing vulnerability assessment approaches

The management of potential natural hazard induced infrastructure failures has not enjoyed a comprehensive or system-wide management perspective as has the management of gradual deterioration induced failure modes. The most common approach is to conduct localized or regional transportation natural hazard risk assessment and mitigation projects, commonly following natural hazard events, resulting in localized management and mitigation approaches. Currently there are also a number of large-scale systematic risk assessment initiatives actively employed or under development. These assessment initiatives include HAZUS-MH, the New York State Bridge Safety Assurance Program, Risk Map Germany and RiskScape New Zealand. Through analyzing these existing risk assessment methods, one can gain a better understanding of the current state of practice and identify needed improvements.

2.1 HAZUS-MH

HAZUS, HAZards United States, is a Geographic Information Systems (GIS) based computerized natural hazard risk assessment tool developed in conjunction with the National Institute of Building Sciences and freely distributed by the United States Federal Emergency Management Agency (FEMA) for estimating building and infrastructure losses from natural hazards – specifically earthquake, wind and flood hazards. HAZUS-MH encompasses the risk assessment tasks of natural hazard intensity modeling, natural hazard-infrastructure object coincident analysis, and infrastructure loss estimation all in one platform (FEMA, 2004).

On the natural hazard assessment side, the HAZUS software is distributed with geographically based earthquake, wind and flood hazard intensities for each state in the United States of America. From the infrastructure side, HAZUS employs census data and national infrastructure databases such as the National Bridge Inventory Database (NBI) to define the location and general vulnerability parameters of private housing and public infrastructure. A geographic coincident analysis is then employed to determine which infrastructure elements (or statistically abstracted infrastructure representations) are affected by the given hazard intensities (FEMA, 2007).

The HAZUS methodology encourages end users to employ a three stage level of analysis. The first stage employs hazard and infrastructure data provided with the HAZUS software to establish a perspective of the general scope and scale of potential natural hazard losses. In the second stage, the end user moves the analysis from a general perspective to a specific analysis by personally specifying additional infrastructure vulnerability data such as specifying detailed vulnerability data for specific infrastructure elements. The third stage of analysis graduates this specific analysis to a validated state by remodeling the potential losses by analyzing the same objects and hazards within a different analysis platform. The specific analysis is validated, or disproved, by comparing and contrasting the specific HAZUS analysis and the external analysis. This three stage process helps end users develop a general understanding of their risk level and tailor the risk assessment process to their specific regions and infrastructure objects (FEMA, 2002).

To better understand HAZUS's level of detail and analysis capabilities consider how this risk analysis platform assesses road transportation network exposure to natural hazards. While HAZUS does provide the hazard intensities for three different hazards, only the effects of flood hazards are considered in analyzing the road transportation network. This analysis qualitatively considers which

roadway objects can become submerged and which bridges may fail due to scour during a flooding event.

The first failure mode – roadway objects submerged by water – is assessed by conducting a purely visual coincident analysis between the flood hazard geographic extent and the geographic location of the roadway objects. Unfortunately these visual observations cannot be quantitatively captured, such as by formulating a list of which roads may become inundated during a flood event. This limitation hampers emergency management planners from quantitatively determining if all road transportation links to a location, or even a region, have been severed by rising flood waters (FEMA, 2007).

The second failure mode – bridge failure due to scour – is assessed by conducting a coincident analysis between the geographic extent of the flood waters and the location of the bridges specified within the National Bridge Inventory (NBI), an inventory of all bridges with a span longer than 6 meters. Bridges within reach of the flood waters are then considered for potential failure due to scour by employing NBI's "scour critical bridges" data field. The NBI identifies scour critical bridges during normal biannual bridge inspections with the framework detailed in Table 2-1. HAZUS then employs this scour classification to identify the bridges that have been identified as scour critical (0 < scour code ≤ 3) (FEMA, 2007). Unfortunately, this assessment does not consider bridges which have not been assessed for scour or bridges with unknown foundational conditions, scour codes = U and 6 respectively. HAZUS then estimates the probability of failure of a given bridge ($P_{failure}$) as a function of the bridge's structural configuration, the bridge's scour rating and the flood event return period using the fixed values presented in Table 2-2.

Table 2-1: National Bridge Inventory scour critical coding descriptions (FHWA, 1995, pp. 56-57).

Scour Code	Code Description
N	Bridge not over water
U	Bridge with 'unknown' foundation that has not been evaluated for scour. Since risk cannot be determine, flag for monitoring during flood events and, if appropriate, closure.
T	Bridge over 'tidal' waters that has not been evaluated for scour, but considered low risk. Bridge will be monitored with regular inspection cycle and with appropriate underwater inspections.
9	Bridge foundations (including piles) on dry land well above flood water elevations.
8	Bridge foundations determined to be stable for assessed or calculated scour conditions: calculated scour is above top of footing.
7	Countermeasures have been installed to correct a previously existing problem with scour. Bridge is no longer scour critical.
6	Scour calculation/evaluation has not been made. (bridges that have not been assessed for scour).
5	Bridge foundations determined to be stable for calculated scour conditions: scour within limits of footing or piles.
4	Bridge foundations determined to be stable for calculated scour conditions: field review indicates action is required to protect exposed foundations from effects of additional erosion and corrosion
3	Bridge is scour critical; bridge foundations determined to be unstable for calculated scour conditions; scour within limits of footing or piles, scour below spread-footing base or pile tips.
2	Bridge is scour critical: field review indicates that extensive scour has occurred at bridge foundations. Immediate action is required to provide scour countermeasures.
1	Bridge is scour critical; field review indicates that failure of piers/abutments is imminent. Bridge is closed to traffic.
0	Bridge is scour critical. Bridge has failed and is closed to traffic.

Likewise, HAZUS quantifies the value of the given bridge class (*Cost*) by evaluating the bridge type with the fixed values presented in Table 2-3.

Table 2-2: HAZUS single and continuous estimated bridge failure percentage per each NBI scour code value (FEMA, 2007, pp. 7-9).

	Single-Span Bridge Scour Code					Continuous-Span Bridge Scour Code				
Return Period	**1**	**2**	**3**	**4-8**	**9**	**1**	**2**	**3**	**4-8**	**9**
100	5	2	1	0	N/A	1.25	0.5	0.25	0	N/A
500	10	4	2	0	N/A	2.50	1.0	0.50	0	N/A
1000	15	6	3	0	N/A	3.75	1.5	0.75	0	N/A

The potential financial loss of each identified scour critical bridge is then computed with Equation (2.1).

$$Damage = (P_{failure})(0.25)(Cost) \tag{2.1}$$

Where:

Damage = the total anticipated direct financial loss resulting from a bridge failure due to scour.

$P_{failure}$ = the probability of failure detailed in Table 2-2.

Cost = the estimated replacement cost of the given bridge class detailed in Table 2-3.

0.25 = the scour failure cost reduction factor as HAZUS makes the assumption that scour failures will only result in 25% of the bridge's total replacement cost.

Table 2-3: HAZUS bridge replacement cost estimations as a function of the bridge type (FEMA, 2007, pp. 3-34).

Bridge Type	HAZUS Valuation (USD)
Major Bridge	20,000,000
Other Bridge (including all wood)	1,000,000
Other Concrete Bridge	1,000,000
Continuous Concrete Bridge	5,000,000
Other Steel Bridge	1,000,000
Continuous Steel Bridge	5,000,000

Example 2-1: Apply the HAZUS-MH risk assessment methodology to quantify the scour risk of 84 bridges presented in Table 2-4.

Table 2-4: Example assessment of 84 different bridges with the HAZUS methodology.

		# per Scour Class			Damage per Return Period (USD)		
Bridge Type	**Total #**	**3**	**2**	**1**	**100**	**500**	**1000**
Major	3	1	0	0	12,500	25,000	37,500
Other Concrete	34	5	3	1	40,000	80,000	120,000
Continuous Concrete	17	3	1	0	15,625	31,250	46,875
Other Steel	24	4	3	1	37,500	75,000	112,500
Continuous Steel	6	2	1	0	25,000	50,000	75,000
		Total Cost			**130,625**	**261,250**	**391,875**
		# Bridges Failed			**0.0863**	**0.1725**	**0.2588**

Applying the HAZUS methodology to assess the direct failure cost and determine the number of bridges expected to fail due to 100, 500 and 1000 return period floods, is shown in Table 2-4. In this example, 29 of the 84 bridges are rated as scour critical with these 29 bridges representing a total HAZUS reconstruction valuation cost of 92 million dollars. Even considering a 1000 year return

period, the HAZUS methodology estimates that the direct costs will accumulate to almost 400,000 USD, 0.43% of this subset's reconstruction value. Additionally, as the HAZUS methodology is statistically based, for a 1000 year flood, it estimates that 0.2588 bridges out of the total 84 bridges will fail. Therefore, it is nearly impossible, without further analysis, to identify which bridge is most prone to fail and what mitigation actions to implement except for attempting to mitigate all 29 scour critical bridges. Furthermore, HAZUS does not provide any estimation of indirect costs including additional travel time and loss of connectivity costs, thus it is difficult to identify which of the 29 scour critical bridges should be addressed first.

In evaluating the capabilities of the HAZUS methodology, it is essential to remember that HAZUS identifies vulnerable bridges as bridges that are within the reaches of the flood waters. As the water level within this zone can extend from a 1000 year flood level to a 1 year flood level, the range of potential hazard forces on the vulnerable structures also varies. With this said, one can start to understand why only 0.2588 out of 29 scour critical bridges are expected to fail under a 1000 year return period flood. Unfortunately, such allowances cannot be extended to include the fact that the only infrastructure component considered by HAZUS is the bridge component, the only bridge failure mode considered is failure due to scour, and only statistical replacement costs are considered. As seen within the recent Katrina Hurricane damage, there are a number of additional roadway objects vulnerable to flooding including roadways, culverts and tunnels, there are a number of additional ways that bridges can fail due to flooding including bearing failure and complete submersion, and indirect costs resulting from additional travel time and, most significantly, the severing of all transportation connectivity can exceed all direct transportation infrastructure damage. With these perspectives, one can observe that while HAZUS does provide for the first time on a region and nationwide scale the ability to geographically analyze the potential coincidence between natural hazard events and infrastructure objects, the methodology behind this analysis needs to be expanded and further developed (Okeil & Cai, 2008).

2.2 New York State bridge vulnerability assessment

2.2.1 Program overview

Starting in 1991, the New York State Department of Transportation (NYDOT) began developing an inspection based bridge vulnerability assessment program entitled the Bridge Safety Assurance Program. Within the Bridge Safety Assurance Program, vulnerability is defined as an assessment of the likelihood of sudden failure and a relative quantification of the resulting consequences. This vulnerability assessment program was initially developed to assess the potential occurrences and consequences of hydraulic induced failures (predominately flooding) but has since been broaden to include steel fatigue, live force overload, motor and maritime vehicle collision, concrete detail and seismic associated infrastructure vulnerabilities. Each assessment phase employs a two-pronged approach of first reviewing available hazard, object and infrastructure system documents and secondly conducting an onsite inspection by qualified personnel. The primary aim of this program is to identify vulnerability prone objects so funding for additional technical analysis and mitigative actions can be allocated to address the most pressing needs (Bridge Safety Assurance, 2008). In recent proposed revision of the PONTIS bridge management system, it was recommended to employ the Bridge Safety Assurance Program vulnerability assessment and prioritization methods to quantify a bridge's vulnerability to hydraulic hazards (Patidar, Labi, Sinha, & Thompson, 2007).

2.2.2 Hydraulic vulnerability assessment program

Turning to the hydraulic vulnerability assessment program, the most applicable program to the current project, one can observe that this program first starts with an initial screening of the existing bridges to determine which bridges are susceptible to hydraulic induced failures. Then the vulnerability of the susceptible bridges is assessed with a two-stage assessment process in which 1) the bridge vulnerability to the given hazard (*LS*) and 2) the potential failure consequences (*FC*) are assessed. The bridge vulnerability and failure consequence assessments are then summed, Equation (2.2), to produce a vulnerability rating score (*VS*) which is used to delegate bridges into urgency-based vulnerability mitigation programs (i.e. safety priority, capital program, no action).

$$VS = LS + FC \tag{2.2}$$

Bridge vulnerability – hydraulic assessment

A bridge's vulnerability to hydraulic hazards is composed of a hydraulic assessment of the bridge's location and a structural assessment of the bridge's foundation (Bridge Safety Assurance, 2008).

Hydraulic assessment of the bridge site (*HA*)

The hydraulic assessment (*HA*) rates the object hydraulic vulnerability as a function of the following ten categories:

- river slope/flow velocity (0-3)
- channel configuration (0-2)
- near a water body junction (0-1)
- existing evidence of scour (0-5)
- object opening capacity (0-2)
- channel floor material quality (0-4)
- debris/ice accumulation potential (0-4)
- within a backwater zone (0-1)
- historical maximum flood depths (1-2)
- object hydraulic overflow potential (0-1)

Each assessment category is separated into subcategories and delegated numerically increasing values as a function of their contribution to the overall object vulnerability. For example the river slope/velocity is separated into three subcategories – flat (slope (s) ≤ 0.004 ft/ft), medium (0.0004 < s < 0.0015 ft/ft) and steep (s ≥ 0.0015 ft/ft) with the respective numerical rating values of 1, 2 and 3. The hydraulic assessment ratings for the ten categories are then totaled – resulting in a hydraulic vulnerability rating ranging from a maximum of 25 to a minimum of 1.

Structural assessment of the bridge foundation (*BF*)

With the hydraulic assessment completed, the focus then shifts to assessing the vulnerability of the bridge foundation (*BF*). As with the hydraulic assessment, the bridge foundation vulnerability assessment is a category ranking system. This process separately assesses the vulnerability of each abutment and pier – with the most vulnerable element controlling the bridge's vulnerability.

The bridge abutment vulnerability (*AV*) is quantified with the following five categories:

- existing scour countermeasures (0-5)
- abutment location on river bend (0-1)
- embankment encroachment (0-4)
- abutment foundation (0-10)
- angle of inclination (0-4)

And the bridge pier vulnerability (PV) is quantified with the following seven categories:

- existing scour countermeasures (0-5)
- angle of attack (0-4)
- pier foundation (0-10)
- footing/pile bottom below streambed (0-1)

- pier width (0-5)
- simple spans (0-1)
- multiple piers in floodplain (0-2)

As with the hydraulic vulnerability assessment, each of these twelve categories are subdivided into subcategories with each subcategory being delegated a numerical rating value as a function of the subcategory's contribution to the overall element vulnerability. Thus the abutment vulnerability rating can range from a high of 24 to a low of 0 and the pier vulnerability rating can range from a high of 32 to a low of 1. The structural assessment of the bridge foundation (*BF*), Equation (2.3), is then the maximum abutment and pier vulnerability rating.

$$BF = MAX(AV, PV) \tag{2.3}$$

With the hydraulic and the bridge vulnerability assessments completed, the individual vulnerability scores are summed resulting in a bridge classification score (*CS*), Equation (2.4).

$$CS = HA + BF \tag{2.4}$$

This classification score is then employed to assign the various objects to one of three vulnerability classes which are in turn assigned object event likelihood scores (*LS*):

- *CS* > 35 = high vulnerability → *LS* = 10
- *CS* < 25 = low vulnerability → *LS* = 2
- 40 > *CS* > 20 = medium vulnerability → *LS* = 6

Failure consequence assessment

The potential failure consequences (*FC*) are then assessed by assigning rating values as a function of the following three categories:

- potential failure type (1-5)
- the exposed traffic volume (0-2)
- the object contribution to the transportation network (0-3)

The failure type and exposure categories are then summed producing a failure consequence score ranging from a maximum of 10 to a minimum of 1.

Vulnerability rating score

The vulnerability rating score (*VS*) is then computed as shown in Equation (2.5) by summing the object likelihood and failure consequence scores.

$$VS = LS + FC \tag{2.5}$$

This vulnerability score, ranging from a maximum of 20 to a minimum of 1, is used to separate the various bridges into urgency-based vulnerability mitigation programs with the following thresholds:

- safety priority (VS > 15)
- safety program (13 < VS < 16)
- capital program (9 < VS < 14)
- inspection program (VS < 15)
- no action (VS < 9)
- not applicable (VS = 0)

Within the New York State Department of Transportation system, bridges identified as safety priorities are failure prone structures whose potential failure modes should be mitigated immediately or as part of the 5-year capital program. Bridges assigned to the safety program are potentially failure prone bridges for which vulnerability reduction interventions, enhanced inspections or addition to the long-term capital program may be considered in the future. Bridges within the capital program are bridges prone to failure under only extreme events and thus the risk

level can be tolerated until the implementation of a normally schedule capital improvement project. Bridges included within the inspection program are non-failure prone bridges given the current conditions remain constant. Thus the bridge and environmental conditions should be reassessed during normally scheduled bridge inspections. Bridges identified as no action and not applicable are respectively bridges with an extremely remote probability of failure and bridges not exposed to the given risk source respectively.

Thus with such an approach, an infrastructure manager can prioritize a group of bridges into urgency based vulnerability mitigation programs.

Example 2-2: Employ the New York State Department of Transportation Bridge Safety Assurance Program to analyze three bridges in the Canton of Aargau.

To help evaluate the strengths and limitations of the bridge safety vulnerability assessment approach, consider the case study of three bridges (designated herein as bridges 1, 2, and 3) located in the Canton of Aargau in north-central Switzerland. These three bridges span the Wigger River and link the city of Zofingen to the adjacent towns of Strengelbach and Brittnau as shown in Figure 2-1. Bridges 1 and 2, built in 1977, are three-span continuous bridges with respective lengths of 69.3m and 73.6m and cross not only the Wigger River but also the A2 national highway located just adjacent to the Wigger River. Bridge 3 is a 20.0m simply-supported bridge located just east of Brittnau where it spans the Wigger River. At the time of the case study, this structure was being replaced as the existing structure was in a severely deteriorated state thus the Wigger River was placed into bypass conduits.

Figure 2-1: Elevation and plan images of Bridges 1, 2 and 3 spanning the Wigger River.

The vulnerability of the three bridges to potential flood induced damage was evaluated, as shown in Table 2-5, using the hydraulic vulnerability assessment during an onsite inspection. The hydraulic environment of all three bridges received ratings of 8 out of a potential score of 25. Additionally, the foundations of the three bridges received ratings of 6, 6, and 1 respectively out of potential ratings of 32, 32 and 24. When summed to determine the classification score, it was found that bridges 1 and 2 had classification scores of 14 and bridge 3 had a classification score of 9. Thus all of these three structures were determined to have a “low vulnerability.” On the consequence side, all three bridges are designed with horizontal shear keys and drilled piles at all support locations. Thus potential

structural failure consequences due to flooding are purely local structural damage. Within the network, bridges 1 and 3 are local roadways and bridge 2 is a collector roadway. Additionally bridges 1 and 2 carry between 4 and 25 thousand vehicles per day and bridge 3 carries less than 4 thousand vehicles per day. Therefore, the three bridges respectively received vulnerability ratings of 4, 5 and 3 out of a potential scour of 20. Thus, the Hydraulic Vulnerability Assessment manual would recommend that no action should be taken apart from continuation of biannual onsite hydraulic inspections.

Table 2-5: Example application of the Hydraulic Vulnerability Assessment.

Assessment Topic		Bridge 1		Bridge 2		Bridge 3	
Hydraulic Assessment	Streambed material	Cobbles	-	Cobbles	-	Cobbles	-
	River slope	Medium	1	Medium	1	Medium	1
	Channel bottom	Stable	1	Stable	1	Stable	1
	Channel configuration	Straight	0	Straight	0	Straight	0
	Debris/ice problems	None	0	None	0	None	0
	Near river confluence	No	0	No	0	No	0
	Affected by backwater	No	1	No	1	No	1
	History of scour	Small	1	Small	1	Small	1
	Historical max flood	> 3.3m	2	> 3.3m	2	> 3.3m	2
	Adequate opening	No	2	No	2	No	2
	Overflow relief available	Yes	0	Yes	0	Yes	0
	Hydraulic assess. total (*HA*)	- - - -	8	- - - -	8	- - - -	8
Abutment	Scour countermeasures	Sheet pile wall	0	Sheet pile wall	0	Sheet pile wall	0
	Abutment foundation	Long piles > 6m	0	Long piles > 6m	0	Long piles > 6m	0
	Location on river bed	Straight	0	Straight	0	Straight	0
	Angle of inclination	20-45 degs.	1	20-45 degs.	1	20-45 degs.	1
	Embankment encroachment	Small	0	Small	0	Small	0
	Abutment assess. total (*AV*)	- - - -	1	- - - -	1	- - - -	1
Pier Assessment	Scour countermeasures	Sheet pile wall	0	Sheet pile wall	0	- - - -	-
	Pier foundations	Concrete piles	0	Concrete piles	0	- - - -	-
	Footing/pile below stream bed	5-6m	1	5-6m	1	- - - -	-
	Angle of attack	0-20 degs	2	0-20 degs	2	- - - -	-
	Pier width	1-1.5m	2	1-1.5m	2	- - - -	-
	Simple spans	Yes	1	Yes	1	- - - -	-
	Multiple piers in floodplain	No	0	No	0	- - - -	-
	Pier assessment total (*PV*)	- - - -	6	- - - -	6	- - - -	-
	Likelihood scour total (*LS*)	*CS* = 6+8 = 14	2	*CS* = 6+8 = 14	2	*CS* = 1+8 = 9	2
Conseq.	Failure type	Structural Dmg.	1	Structural Dmg.	1	Structural Dmg.	1
	Exposure	4-25,000 ADT	1	4-25,000 ADT	1	< 4,000 ADT	0
	Functional class	Local road	0	Collector	1	Local Road	0
	Consequence score total	- - - -	2	- - - -	3	- - - -	1
	Vulnerability rating (*VS*)	- - - -	4	- - - -	5	- - - -	3

A vulnerable transportation infrastructure object is defined as an infrastructure object that can perform inadequately due to a set of potential natural hazard events. Considering the most common source of hydraulic risks, the existing rivers and streams, the bridge component is the component exposed to the highest hazard parameter intensities (i.e. flooding depth). Furthermore, a bridge is the infrastructure object with the largest potential post-failure interruption duration and reconstruction costs as the replacement of a single 45m bridge can take multiple weeks and cost hundreds of thousands of Swiss Francs. But bridges commonly only comprise less than 2 percent of a

given transportation system and while the other objects of a transportation infrastructure network (the roadways, culverts, retaining walls, galleries and tunnels) are less prone to hydraulic hazards than bridges, their structural resistance to hydraulic hazards is far less. These potential additional vulnerability sources become even more apparent when the scope of the potential hazards is broadened from purely hydraulic hazards to include rockfall, torrent, landslide and avalanche hazards, all common events in mountainous regions. Therefore, while the New York State Department of Transportation Bridge Assurance Program has developed a qualitative risk assessment approach which does address the infrastructure component most exposed to flood hazards, the bridge component, it does not consider any additional components or hazards, nor is it able to quantify the relative risk exposure. Thus, beyond serving as a tool to highlight potentially vulnerable bridges, the Bridge Safety Assurance Program is not detailed enough to be directly integrated into an infrastructure management platform.

2.3 Lifeline vulnerability assessment approach

The lifeline vulnerability assessment approach, originally developed within the earthquake engineering field, employs a multi-systems perspective to analyzing the vulnerability of the infrastructure systems upon which present-day life is dependent. Lifeline systems commonly include – communication lifelines (e.g. fiber optic cables, radio transmission, cellular towers), electrical lifelines (e.g. transition systems, power generation stations), fuel storage and distribution lifelines (e.g. natural gas and petroleum pipelines), and transportation lifelines (e.g. interstate highways, state highways, railroads). In conducting a lifeline vulnerability assessment, the response of each object contained within a given lifeline and each connection between separate lifelines to a defined hazard scenario or set of hazard scenarios is analyzed in detail. Through such an analysis, locations where a lifeline is directly vulnerable to a given hazard scenario or indirectly vulnerable through vulnerability of the required supporting systems can be identified. Once a given vulnerability is identified, the cost efficiency and effectiveness of potential strengthening or additional redundancy mitigation actions can be developed (Lowe, Scheffey, & Lam, 1991).

For example, to assess the direct vulnerability of an interstate highway lifeline and a fiber optic cable lifeline, which both cross the same bridge, one would first determine how the bridge structurally responds to the given hazard scenario (e.g. flooding of the bridge's substructure during the 100 year flood) and then assess what implications the bridge's structural response has for the interstate highway and fiber optic cable lifelines. This analysis is then expanded to include indirect vulnerability sources of the interstate highway and the fiber optic cable lifeline. This requires one to conduct a vulnerability assessment of all the systems required to ensure each lifeline remains functioning (e.g. the electrical power generation and distribution system). Thus, the given lifeline's vulnerability is not only a function of the direct vulnerability but also the indirect vulnerability introduced by vulnerabilities in the required supporting systems (e.g. vulnerability of a fiber optic cable lifeline resulting from a general electrical power outage).

Historically, lifeline vulnerability assessments have been conduced to analyze specific lifeline corridors or similarly limited scope infrastructure systems. These assessments do have the potential to identify previously unknown vulnerability sources and vulnerable objects. With such information, an infrastructure manager can implement strengthening or redundancy related mitigative actions to reduce the overall vulnerability of the specific lifeline. But the identification of potential vulnerability reduction measures only extends as a far as the geographic scope of the vulnerability assessment

which is commonly limited by geo-political boundaries, financial limitations and temporal limitations. Lastly, the quality of a lifeline vulnerability assessment is only as good as the methodology employed.

2.4 Currently under development risk assessment projects

Internationally, there are two major national comprehensive risk assessment platforms currently under development – Risk Map Germany and RiskScape New Zealand.

2.4.1 Risk Map Germany

Risk Map Germany is a multidisciplinary research and development project managed by Karlsruhe University. The primary objective of the Risk Map project is to conduct large scale quantification of natural and man-made risks. Towards this end, the Risk Map project has more than 41 professors, research scientists and doctoral students developing methods and procedures for quantifying hazard intensities including wind, earthquake, flood and man-made hazards, identifying approaches for estimating the vulnerability of infrastructure systems, developing estimations for private and business infrastructure assets, formulating methods for cross-comparing risks induced by different hazards, and establishing a GIS-based data management framework. The bulk of the Risk Map program focuses on assessing risks to private and business infrastructure, elements which are commonly the infrastructure objects directly insured by public or private insurance entities.

With respect to the public infrastructure, the roadways and railways, this risk research effort focuses on identifying critical transportation links by estimating the potential consequences that can result from the failure of a given infrastructure link. Critical transportation links are identified by assessing the link traffic load, the link demand and the post-failure link demand redistribution costs. Through comparing these values for each link, the most critical transportation links can be identified.

With the high consequence public infrastructure links identified, it is anticipated that the risk assessment process can be limited to this subset of the infrastructure network. While this approach will help to focus the risk assessment process to the majority of the high consequence links, it may overlook equivalent or even more at risk transportation links such as extremely hazard prone links with moderate or even low failure consequences (Risk Map, 2007). As the Risk Map Germany program is still a work in progress, it will be interesting to see if and how these issues are addressed.

2.4.2 RiskScape New Zealand

RiskScape is a New Zealand research program working to develop a loss-modeling software package for analyzing the potential impacts of natural hazards (flooding, earthquake, volcano, tsunami and wind) to improve natural hazard management. RiskScape is intended to include the following natural hazard risk assessment steps: natural hazard intensity assessment, identification of exposed infrastructure objects, evaluation of infrastructure vulnerability, assessment of damaged states, quantification of direct and indirect consequences, and evaluation of the resulting risk.

The RiskScape assessment methodology is build upon three primary modules: infrastructure databases, hazard modeling, and loss assessment. As no extensive infrastructure database exists in New Zealand, focused infrastructure field surveys and advanced data collection methods including satellite imagery and laser-scanning are being used to formulate the core of a pilot infrastructure database. The hazard modeling module is being formulated from previous recorded events and

computer simulation of potential future storms and events. To assess the potential hazard induced infrastructure damage, the RiskScape model is intending to employ vulnerability curves (Resse, King, Bell, & Schmidt, 2007). As this research program is under development, neither the extent (including the types of infrastructure objects considered) nor the depth (including the level of vulnerability analysis) is currently unknown.

2.5 Activities within Switzerland

2.5.1 Swiss federal railway (SBB)

The SBB is an extensive organization with over 28,000 employees charged with operating 9,000 trains daily and maintaining 3,000 km of railway lines (SBB, 2008). This infrastructure by definition is extremely geographically dispersed making it extremely exposed to potential natural hazards. Furthermore, the trains, electrical lines and communication lines are extremely vulnerable to natural hazard events. To combat the risks posed by natural hazards, the SBB employs a three pronged approach of documenting natural hazard events, implementing risk mitigation actions and repairing natural hazard induced infrastructure failures.

When natural hazard events occur, the SBB employee responsible for inspecting and maintaining the given rail section is primed to document the location and intensity of the given natural hazard event. The SBB is working to collate these numerous hazard event data points within a GIS platform and create natural hazard identification maps. When active natural hazard zones are identified or when infrastructure objects fail due to natural hazard events, risk mitigation and reconstruction efforts are immediately initiated. The SBB annually receives the financial equivalent of 1% of the current value of the built railway infrastructure from the Swiss national government to maintain the railway infrastructure. These maintenance funds are allocated by each of the four geographically based regions using semi-quantitative approaches. The primary pitfall that SBB is currently facing is that it does not have a complete inventory of its built infrastructure and thus is receiving a less than appropriate maintenance funding support (Meier, 2008).

2.5.2 Swiss federal roads authority (ASTRA)

Within the Swiss federal roads authority, the bridge research group is current working to prepare the decision foundation and methods to help guide financial resource allocation to maintain the required safety standards across the entire road transportation system. This decision foundation includes methods for evaluating and comparing risks from different sources (e.g. traffic, natural hazards, dangerous goods transport) and for formulating effective risk reduction interventions. The studied infrastructure system includes the road infrastructure structures and the vehicular traffic on the road infrastructure. The phases considered are construction, maintenance and system operation phases. Within ASTRA there is an increasing trend to use risk-based analysis in the planning and management of the built infrastructure. This trend extends far beyond the purely technical realm of analysis and into areas such as legal and code interpretation and revision aspects. The final goal of this program is to develop an actionable methodology which can serve as the foundation for the construction of a risk management system at ASTRA (Frey, Gerber, Kost, & Schneeberger, 2005).

2.5.3 Cantonal insurance companies

In Switzerland, 19 of the 26 Swiss Cantons each administers a cantonal fire insurance company which is charged with providing insurance for all public, corporate and private buildings against fire and natural hazards (i.e. avalanche, flood, landslide, mudslide and rockfall). While this insurance is mandatory, the individual premiums are not prorated on individual risk exposure and thus the total risk exposure is uniformly carried by all policy holders.

To aid current and future building owners in assessing their individual risk exposure and in determining if risk mitigation actions should be implemented to reduce the risk exposure of their respective buildings, the Cantonal Fire Insurance Companies have jointly formulated an application oriented manual for conducting building risk assessment with respect to natural hazards (Egli, 2005). For each of the considered hazards (avalanche, flood, landslide, mudslide and rockfall) the manual systematically presents, within a failure scenario format, the applicable hazard parameter intensities, the equations for assessing the forces applied to the buildings, quantification of the resulting consequences and identification of different mitigation actions which can be implemented by the building owner to reduce the building's risk exposure.

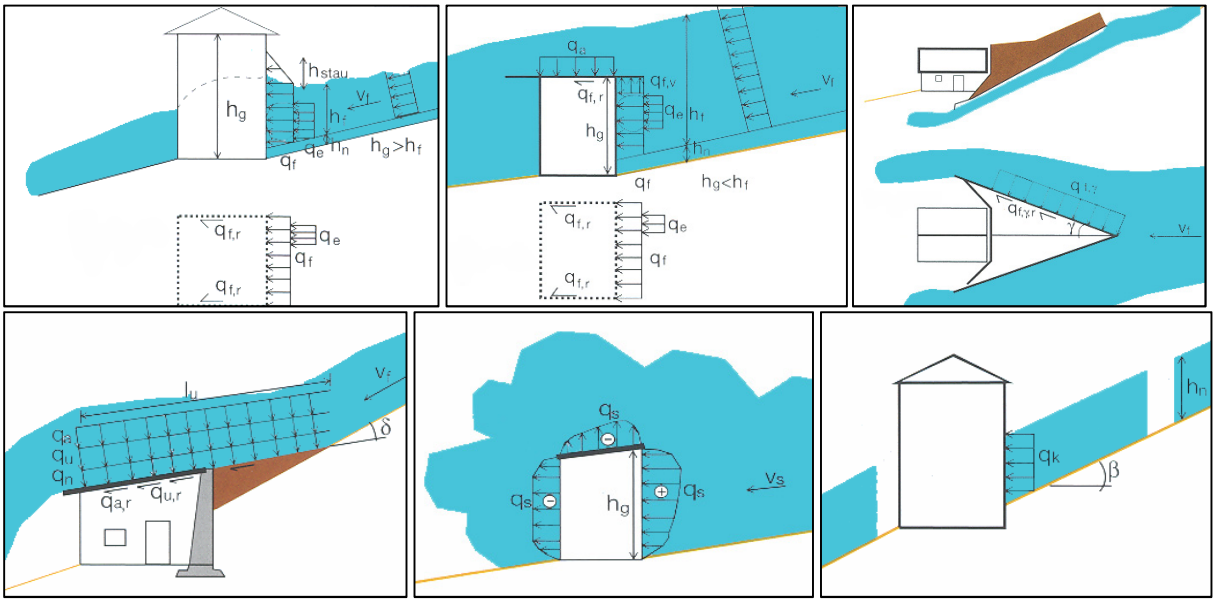

Figure 2-2: Cantonal Fire Insurance considered hazard-building interactions for the avalanche hazard.

A key aspect of this building risk assessment with respect to natural hazards is the considered hazard-building interactions. The hazard-building interactions for the avalanche hazard are presented in Figure 2-2 and from these images, one can observe how much influence the building geometry and configuration has on the resulting hazard-building interaction. Furthermore, such diagrams serve as the foundation for the building risk assessment with respect to natural hazards.

While neither the Cantonal Fire Insurance Companies nor the developed risk assessment manual addresses public transportation infrastructure risk with respect to natural hazards, as public transportation is beyond the Cantonal Fire Insurance Companies' charter, the general systematic risk assessment approach and employed hazard and infrastructure parameters have potential to be transferred, in spirit, to assessing transportation infrastructure risk with respect to natural hazards.

2.6 Hazard data sources in Switzerland

In reviewing the various vulnerability and risk assessment approaches presented in Sections 2.1 to 2.5, one can observe that each approach incorporates three different elements in quantifying vulnerability and risk – the hazard, the infrastructure object and the failure consequences. This section reviews a number of existing and under development resources for quantifying the natural hazard parameters and intensities within Switzerland – specifically SilvaProtect, StorMe, hazard identification maps and infrastructure specific hazard identification maps.

2.6.1 SilvaProtect

SilvaProtect is a natural hazard indication mapping resource for determining the largest possible geographic extent of gravity-induced natural hazards – specifically avalanche, landslide, rockfall and torrent hazards (Giamboni, 2007). Figure 2-3 presents the SilvaProtect hazard indication map for the center of Burgholz located in the Berne Canton. Within Figure 2-3, one can observe the key roadway and railway lines crossing Burgholz, shown orange and purple, transposed over a composite image of SilvaProtect avalanche, landslide, rockfall and torrent data.

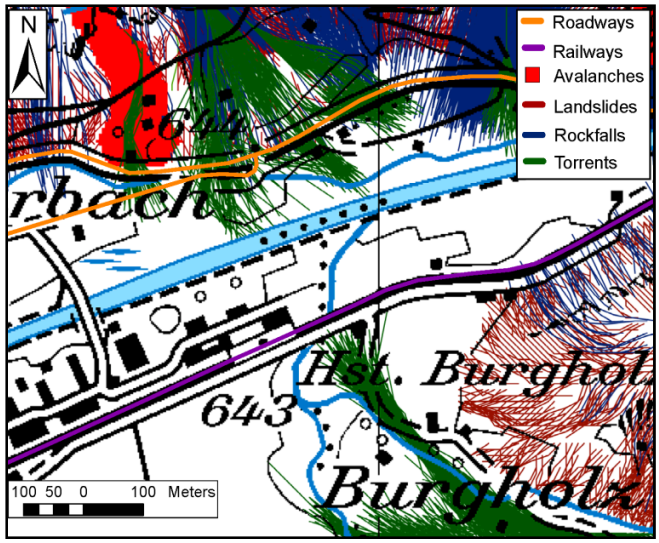

Figure 2-3: SilvaProtect hazard indication map – Burgholz.

The SilvaProtect data was developed by segmenting Switzerland into 20m x 20m parcels and assessing the gravitational stability of each parcel under conditions characteristic of each hazard given the local topography. Where instability is identified, the resultant kinetic energy driven path is computed and identified with a line. For example, individual potential landslide paths are well presented in the lower-right hand corner of Figure 2-3. As the path of a given hazard is influenced by the region's geographic contours, the path of some hazards – torrent and avalanche hazards in particular – can be channeled by the local topography. This potential channeling phenomenon can be observed in the torrent hazard at the bottom center of Figure 2-3.

To determine the maximum geographic reach of the various hazards, SilvaProtect employs a maximum possible event perspective (greater than 1000 years) and assumes that all slope stability and physical hazard prevention infrastructure is non-functional. Unfortunately, this maximum event perspective limits the potential application of the SilvaProtect data and thus it can only be employed to identify infrastructure objects which are or are not exposed to gravitationally induced hazards.

2.6.2 StorMe

StorMe is a nationally supported, cantonally administrated natural hazard event documentation database specifying the date, location and key aspects of previous natural hazard events. With over 17,500 entries, it is a testament to the detail required for accurately documenting previous natural hazard events (Eyer, 2007). Figure 2-4 presents over 100 natural hazard events in the region surrounding Spiez, located in the Berne Canton. Unfortunately, the level of participation and detail of information varies among the cantons, limiting the applicability of such a database for Swiss wide applications. Thus, the StorMe database can only be systematically employed as a tool for identifying potential object-hazard combinations and for assisting in developing hazard identification maps.

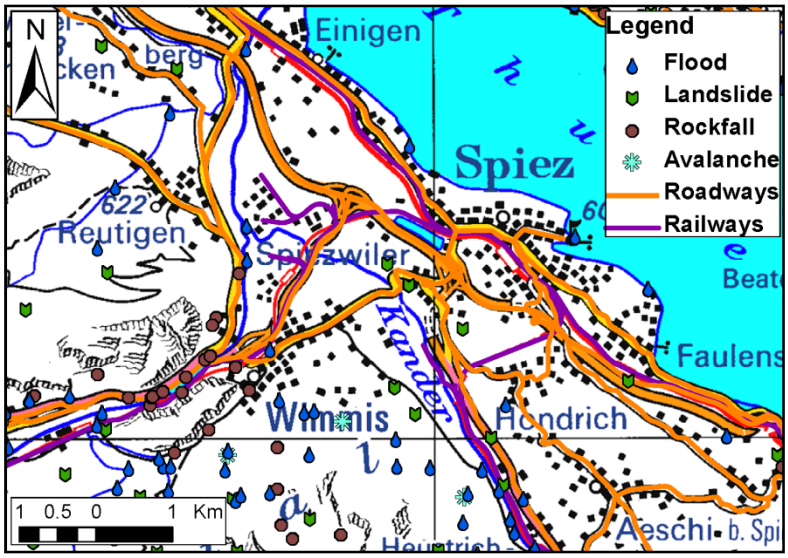

Figure 2-4: Geographical presentation of StorMe data in the Spiez region.

2.6.3 Swiss National hazard mapping initiative

A nationally mandated, cantonally implemented hazard indication map development initiative is currently underway within Switzerland. This initiative looks to develop, for all inhabited regions of

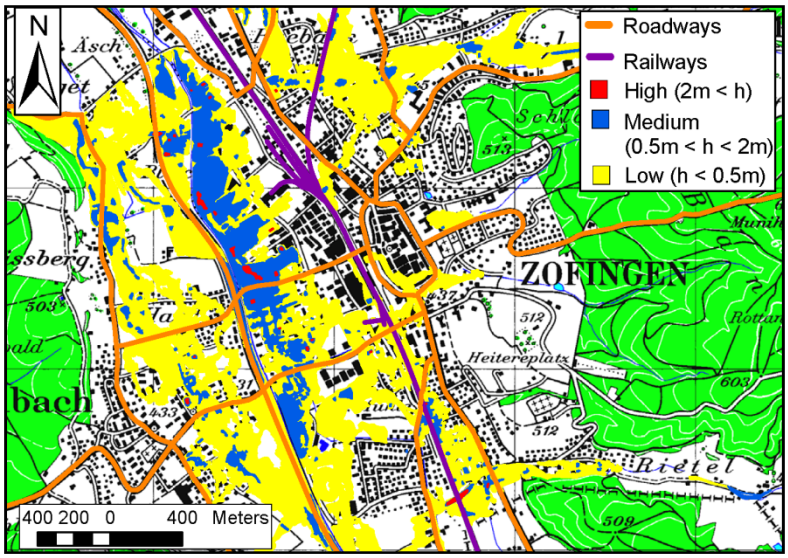

Figure 2-5: Hazard identification map example - Flood height intensity, 1000 yr return period.

Switzerland, avalanche, flood, landslide, rockfall and torrent hazard identification maps at a 1:5000 scale for 30, 100, 300 and 1000 year return periods for key hazard parameters presented in Table 2-6 (Loat, 2007). The project's specified completion date is December 2011. The hazard identification maps will specify the expected geographic scope and expected hazard parameter intensity for each of the four return periods. An example of the geographic and hazard parameter intensity detail of this information is presented in Figure 2-5.

To facilitate the Swiss National hazard mapping initiative, predefined hazard parameter intensity thresholds have been defined for each considered hazard parameter. As shown in Table 2-6, the Swiss National hazard mapping initiative has identified eight key hazard parameters for five different hazards (avalanche, flood, landslide, rockfall and torrent). Furthermore, the initiative has also identified threshold hazard intensities for each hazard parameter. For example, for the hazard parameter flood height, low, medium and high intensity thresholds of $H_F < 0.5$m, $0.5\text{m} < H_F < 2$m, and $2\text{m} < H_F$ respectively have been identified. Where applicable, these hazard parameter intensity threshold values can be directly employed to assess the vulnerability and risk of infrastructure objects. Currently, the mapping progress achieved by the various cantons does vary and thus already completed hazard intensity maps from the Cantons of Aargau and Fribourg are employed in Chapter 4 to demonstrate the developed vulnerability and risk assessment methodology.

Table 2-6: Hazard parameter intensity thresholds for the Swiss hazard identification maps (Loat, 2007).

Hazard	Hazard Parameter	Low Intensity	Medium Intensity	High Intensity
Avalanche	Horizontal Pressure	$P_{AH} < 3$ kN/m^2	$3 < P_{AH} < 30$ kN/m^2	$P_{AH} > 30$ kN/m^2
Flood	Bank Erosion Depth	$ED_F < 0.5$ m	$0.5 < ED_F < 2$ m	$ED_F > 2$ m
	Flood Height	$H_F < 0.5$ m	$0.5 < H_F < 2$ m	$H_F > 2$ m
	Specific discharge	$q_F < 0.5$m^2/s	$0.5 < q_F < 2$ m^2/s	$q_F > 2$ m^2/s
Landslide	Annual velocity	$V_L < 2$ cm/year	V_L: dm/year	$V_L >$ dm/day or > 1 m/event
Rockfall	Kinetic energy	$E_R < 30$ kJ	30 kJ $< E_R < 300$ kJ	$E_R > 300$ kJ
Torrent	Thickness and flow velocity	-	$T_D < 1$ m & $V_D < 1$ m/s	$T_D > 1$ m & $V_D > 1$ m/s

2.6.4 Infrastructure specific hazard maps

As the feasibility of developing hazard identification maps for extensive areas and the utility of these maps becomes more apparent, additional public entities are becoming interested in developing similar resources for their respective infrastructure systems. The key limitation of the Swiss National hazard mapping initiative, detailed in Section 2.6.3, is that it is focused on developing hazard identification maps for only the inhabited regions of Switzerland. Some infrastructure systems, transportation infrastructure systems in particular, extend beyond the limits of the inhabited regions of Switzerland. Therefore, to develop an exhaustive hazard identification map for a transportation infrastructure system, additional hazard parameter data must be collated and hazard parameters in previously undocumented regions must be assessed.

The Berne Cantonal Roads Authority, the agency charged at the time with operating and maintaining the Swiss highway system within the Canton of Berne, developed hazard parameter intensity maps for the National highways within the Berne Canton. Examples of the hazard identification maps for avalanche horizontal pressure and flood height intensities affecting the A8 national highway as it passes to the south of Erschwanden, just east of Interlaken, are presented in Figure 2-6 (Frick & Aeberhard, 2008).

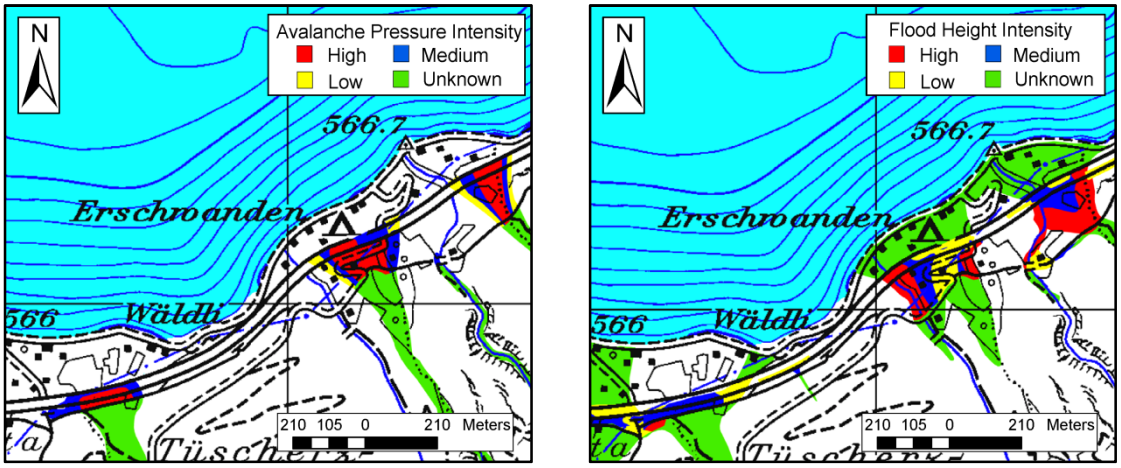

Figure 2-6: Geographical presentation of Berne Cantonal highway hazard parameter intensity maps for: a) avalanche horizontal pressure and b) flood height.

2.7 Infrastructure data resources in Switzerland

To assess the vulnerability and risk of an infrastructure object requires knowledge of three key elements – the hazard, the infrastructure object and the failure consequences. In Section 2.6, potential hazard data sources within Switzerland were reviewed. This section focuses on the second element required to quantify the vulnerability and risk of an infrastructure object – data specifying the location and key parameters of the objects contained within the considered infrastructure system. Currently, within Switzerland there are two key infrastructure object data sources – specifically the Vector25 and the KUBA databases. The details, strengths and limitations of these two databases are respectively discussed in Sections 2.7.1 and 2.7.2.

2.7.1 Transportation Link Vectorization – Vector25 & STM

SwissTopo, the Swiss National Office for Geographic Information Systems (GIS), has compiled an object type-based geographic vectorization of the Swiss transportation systems at a scale of 1:25000 entitled Vector25 (National Office of Topography Swisstopo, 2008). For the private transport system, the scope of this vectorization extends from Switzerland's major highways down to the smallest marked alpine walking paths and is comprised over 1.3 million links. A graphical presentation of this

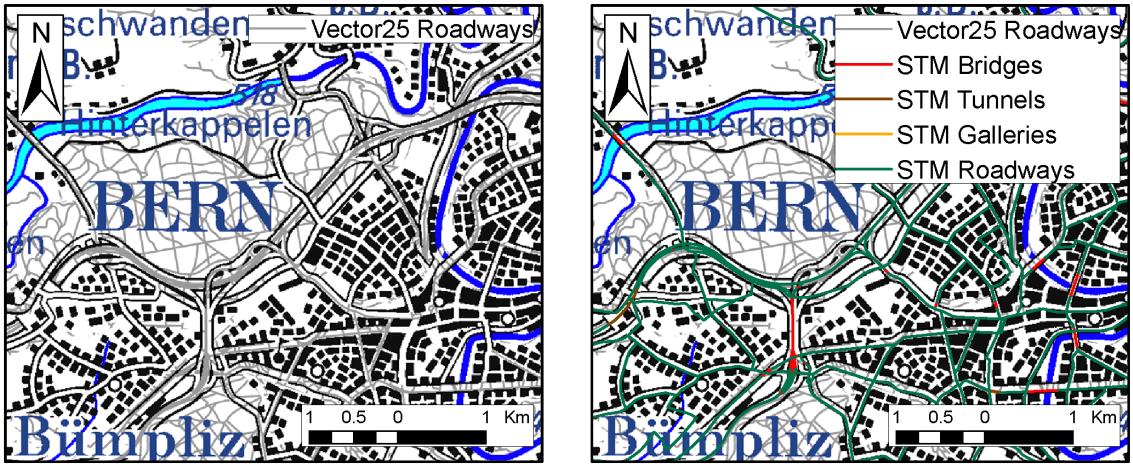

Figure 2-7: Geographic presentation of: a) Vector25 private transport data around Bern, b) the Swiss Transport Model Data tranposed over the Vector 25 Data.

Table 2-7: Considered Swiss Transportation Model functionality classes.

Class	Object Functionality Description	% of STM
Class 1	Principle roads, width > 6m, truck passing possible, slope < 10%	32.60%
Class 2	Secondary roads, width > 4m, car passing possible, slope < 15%	27.69%
Class 3	Tertiary roads, width > 2.8m, passing only in designated zones, services countryside	2.47%
Separated Highways	Limited access, high-speed roadway, each direction separated with a central median, no mixed traffic	12.34%
Non-Separated Highways	Limited access, high-speed roadway, not separated with a central median, no mixed traffic	3.94%
Connector Highways	Connector limited access, high-speed roadway, not separated with a central median, no mixed traffic	4.09%
Quarter Roads	Non-through traffic important roadways, width > 4m	2.09%

Vector25 data around the center of Bern is presented in Figure 2-7a. As this current work focuses developing a methodology to assess the Swiss Road Infrastructure System's vulnerability to natural hazards, a subset of over 51,000 transportation links which are a minimum of 2.8m wide and have the capacity to carry a reasonable amount of traffic are included in this analysis. Hereafter, this subset is referred to as the Swiss Transport Model (STM). A geographic presentation of the links included in the Swiss Transport Model with respect to the base Vector25 data (in gray) is shown in Figure 2-7b.

The links within the Swiss Transport Model (STM) are subcategorized by two different parameters – the given object's hierarchical functionality within the transportation network (e.g. Highway, Class 1 roadway, Class 2 roadway) and the link component type (i.e. bridge, gallery, roadway, tunnel).

The Swiss Transportation Model considers 35 different functionality classes, but only 7 classes, presented in Table 2-7, are located predominately within the borders of Switzerland and constitute at least one percent of the Swiss Transportation Model.

The links within these different functionality groups have then been identified with their respective component type. Analyzed as a whole, the four different components considered by the system and their representative percentages are presented in Table 2-8.

Table 2-8: Swiss Transportation Model component types.

Component	% of STM
Bridge	17.34
Gallery	0.78
Roadway	79.08
Tunnel	2.79

These functionality and component types presented within this section are useful resources for identifying properties and hazard parameter intensity based consequences to a given infrastructure class.

2.7.2 The Swiss highway structures database – KUBA

Over the past 19 years, the Swiss National Roads Office has developed and continues to expand an infrastructure database (KUBA) specifying the location, configuration, general dimensions and condition state of the various structures that comprise the Swiss National Highway System. This database is used to support the National Road's Authority in their decision making. KUBA's predictive

capabilities are currently oriented towards formulating optimal intervention strategies with respect to gradual deterioration.

In collecting and entering the data for KUBA, the various objects are first separated by component type (i.e. bridges, galleries, retaining walls, tunnels and water retention facilities) and then assigned to the one of more than 40 different structural configurations. Once assigned to a given structural configuration, the given practitioner is then primed to separate the given object into key elements. For the example of a two span continuous bridge, a practitioner is primed to separate the object into five key elements – left abutment, right abutment, central pier, superstructure and roadway deck. The practitioner then employs KUBA's semi-structured format of fifty-five different data fields to document the different elements within each object. In studying these fifty-five data fields, eleven data fields, detailed in Table 2-9, are directly applicable to quantifying an infrastructure object's resistance with respect to a hazard.

Table 2-9: Risk quantification applicable KUBA datafields.

Ref	Data Field	Ref	Data Field
1	Object type	7	Maximum clearance
2	Location	8	Load charge test
3	Total length	9	Discharge capacity
4	Total width	10	Pile type
5	Total surface	11	Distributed linear weight
6	Number of spans		

The initial three data fields, detailed in Table 2-9, can be obtained from the Vector25 data, but the additional eight data fields included within KUBA can help to further estimate an infrastructure object's resistance.

2.8 Failure consequence data resources in Switzerland

With the hazard and infrastructure object data sources within Switzerland detailed in Sections 2.6 and 2.7, the last element required to quantify the vulnerability and risk of an infrastructure object is information identifying the range of the potential consequences resulting from the potential failure of an infrastructure object. Within Switzerland, there are five primary sources of failure consequence data: local historical archives, public natural hazard event and infrastructure databases (StorMe and KUBA), private insurance databases, transportation system models and practitioner professional experience. Each source is herein detailed and its applicability to a comprehensive infrastructure object vulnerability and risk assessment methodology is assessed.

2.8.1 Local historical archives

Natural hazard events impact towns and communities in a number of ways including by damaging homes and severing local transportation links. These events commonly become defining points in a community's oral and written history. This history is informally contained within memories of the local residents who were present for each event and formally documented within the local historical archives and newspapers. While both of these resources contain extremely detailed information commonly documenting the event dates, natural hazard parameter intensity levels, direct consequences and indirect consequences, the time required to collect, compile and analyze this data from the vast number of resources undermines the potential of using these data resources for regional or national vulnerability and risk assessments.

2.8.2 Public natural hazard event and infrastructure databases

The StorMe natural hazard event and KUBA infrastructure databases contain venues for identifying the structural damage and indirect consequences resulting from natural hazards. Within StorMe this damage data is compiled quantitatively by noting if the natural hazard event resulted in any human fatalities, human injuries, animal fatalities, forest damage, or damage to protection structures. Additional data can be qualitatively included by adding a note to a given StorMe event entry. Unfortunately there is no standardized procedure or process for constructing a descriptive note and, other than noting the associated hazard (e.g. avalanche), there is no additional information provided concerning the hazard parameter intensity.

When infrastructure objects detailed within the KUBA database are damaged by a natural hazard, the practitioners are encouraged to note this damage in the KUBA database along with the gradual deterioration related damage. While KUBA has a venue for documenting structural damage, the instigator of this structural damage, the natural hazard parameter intensity, is not systematically recorded.

While both of the StorMe and KUBA databases do have venues for quantitatively and qualitatively recording the direct and/or indirect consequences of natural hazards, the fact that the hazard parameter intensity is not noted prevents one from relating a hazard parameter intensity to an infrastructure object's direct and indirect consequences.

2.8.3 Private insurance databases

Another potential source for quantifying the consequences of natural hazards is private and semi-private insurance company databases. Such databases are developed by an insurance company to document previous insurance claims and to predict the potential for future insurance claims. Therefore such databases are commonly central to the operation and financial stability of a given insurance company. Unfortunately, to the knowledge of the author, the current insurance companies focus predominately on private, corporate and governmental buildings which have different potential natural hazard induced failure modes as compared to transportation infrastructure objects. Furthermore, as these databases do directly or indirectly contain client information and as they are central to the financial profitability and stability of the given insurance firm, insurance companies are commonly reluctant to provide access to natural hazard insurance claim data. Thus the scope, privacy and general accessibility issues related to private and semi-private insurance databases limits their applicability to quantifying the potential consequences of a transportation infrastructure object failing due to a given hazard parameter intensity.

2.8.4 Transportation network models

An approach to quantify the indirect consequences due to the failure of an infrastructure object is to develop a model of the given system and to assess what implications the failure of the given object has on the system. Such a model specifying the traffic distribution aspects of the primary and secondary roadway systems in Switzerland is the Swiss Transportation Model (STM) (Vrtic, et al., 2005). This system, which has been derived from the Vector25 transportation link vectorization data, details the location, transportation capacity (e.g. number of vehicles at a given volume can cross a given link) and inter-link connectivity of over 51,000 transportation links. This system can be thus used to study how private transportation (e.g. cars, trucks and buses) deviate around a closed

transportation link and what implications this deviated traffic has for the general transportation system congestion, the total additional travel distance and the total additional travel time. Therefore, even though, the Swiss Transportation Model can only provide the unit daily transportation related impacts of a link closure (i.e. the total additional travel distance and travel time) when combined with the expected service interruption duration of a given infrastructure object failure, one can quantify the transportation related indirect consequences.

2.8.5 Practitioner professional experience

In the aftermath of natural hazards, the incurred private and public structural damage must be inspected, evaluated, and repaired. Within the private market, the responsibility of assessing and evaluating damaged homes and industrial buildings falls to general contractors. Within public market, the task of assessing the financial and service interruption duration implications of damaged roadways and railways falls to the local, cantonal and national road and rail infrastructure officials. It is these officials who, over numerous years, amass a wealth of professional experience assessing, evaluating and overseeing the repair of natural hazard induced structural damage. Unfortunately, this knowledge remains stored within the minds of these individuals, only to be applied when they are personally primed with pertinent questions and problems. Therefore, if a method for providing a context within which these experienced practitioners can formulate their direct damage and service interruption duration estimations and if a method for applying these consequence estimations in the vulnerability and risk assessment process were formulated, quantifying direct and indirect consequences from expert estimates can be a feasible method.

2.9 Critique of existing vulnerability and risk assessment approaches

As infrastructure systems have grown larger and the required level of oversight has increased, infrastructure managers have increasing turned to infrastructure management systems to transparently develop optimal management solutions to mitigate the gradual deterioration of the built infrastructure. The management of potential natural hazard induced infrastructure failures has not enjoyed such a comprehensive or system-wide management perspective. Rather, local or regional transportation natural hazard risk assessment and mitigation projects, commonly following natural hazard events, have been arbitrarily employed when a given infrastructure manager has deemed it appropriate.

To assess the risk of infrastructure systems to natural hazards, risk analysis platforms including HAZUS-MH and NYSDOT's Bridge Safety Assurance Program have been implemented. Unfortunately HAZUS-MH does not systematically consider the relative resistance of a specific transportation infrastructure object, other than scour, when conducting a risk assessment and the Bridge Safety Assurance Program provides only a qualitative risk assessment and inherently circumvents the ability to quantify in an equivalent monetary terms the relative annual risk exposure of an infrastructure object. Internationally, there are a number of national initiatives to develop comprehensive risk assessment platforms including Risk Map Germany and RiskScape New Zealand. Unfortunately, both of these initiatives are too early in development to adequately determine the intended analysis depth and scale.

Turning to risk assessment activities currently underway in Switzerland, one can observe that the cantonal insurance companies have developed and implemented a comprehensive assessment

approach to quantify the natural hazard risks to the existing building stock. Unfortunately, the cantonal insurance company charter prevents these governmental organizations from extending their scope of analysis and conducting comprehensive risk assessments of the built transportation infrastructure. Furthermore, the failure scenarios developed by the cantonal insurance company to analyze a building's response to a natural hazard are not directly applicable to assessing the potential failure of the built transportation infrastructure.

Looking closer at activities underway in Switzerland within the three domains required to quantify the risk of an infrastructure object – hazard, infrastructure and consequence assessment – it can be seen that a number of these elements have already been or are in the process of being developed. Within the hazard assessment domain, maximum scope of gravitational hazards can be determined with the SilvaProtect database and the local intensities of a set of hazard parameters within the habituated regions of Switzerland are currently being developed within the Swiss National hazard mapping initiative. Within the infrastructure assessment domain, a GIS vectorization of the Swiss transportation networks, component type identification and object class identification of each infrastructure object is publicly available within the Vector25 and STM data sets. Additionally, the Swiss highway infrastructure database – KUBA – details the location, configuration, general dimensions and condition state of the structures that comprise the Swiss National Highway System. Lastly within the consequence assessment domains, there are a number of potential sources of failure consequence data within Switzerland but the only sources which show potential for being applied on a nation-wide scale are practitioner professional experience to estimate the direct consequences and service interruption durations resulting from the failure of an infrastructure object and transportation network models to estimate the daily indirect traffic related consequences resulting from the failure of a transportation link.

In reviewing these available resources, one can observe that two key aspects required to assess the vulnerability and risk of an infrastructure network which still need to be developed are procedures to assess the potential failure of transportation infrastructure components to potential natural hazards and an overarching comprehensive vulnerability and risk assessment approach. These two limitations are addressed in Chapter 3 by developing failure assessment procedures for each private transportation infrastructure component and by proposing a comprehensive vulnerability and risk assessment approach. Additional, as each step of the vulnerability and risk assessment approach is introduced, an example is provided to demonstrate the intricacies, strengths and limitations of the proposed methodology. Lastly, the developed comprehensive vulnerability and risk assessment approach is employed in Chapter 4 to analyze the vulnerability and risk of selected objects within two different roadway links.

3 Comprehensively assessing vulnerability and risk of transportation infrastructure

3.1 Laying the foundation for a comprehensive vulnerability and risk assessment approach

In Chapter 2, a number natural hazard data sources, infrastructure data sources, consequence assessment methods, and risk assessment methods are presented. Each of these sources and methods have their own applications but, separately or combined, none of the information presented can provide a comprehensive assessment of a transportation infrastructure network's vulnerability and risk to natural hazards. Without such a comprehensive assessment methodology, infrastructure managers are unable to identify high risk infrastructure objects and links and quantify the risk of the various links within their infrastructure network.

The driving motivation of this chapter is, thus, to develop a transportation infrastructure vulnerability and risk assessment methodology from existing or shortly available hazard, infrastructure and transportation network data resources. The final product is intended to be fully actionable within a maximum time horizon of five years. This chapter lays the methodology's foundation by first defining, from a general perspective, risk, vulnerability and the associated supportive terms, in Sections 3.1.1 and 3.1.3. To assist in the explanation of risk and vulnerability, Section 3.1.1 applies these fundamentals to the vulnerability and risk assessment of an infrastructure object (i.e. a roadway). With these terms defined from a general perspective, in Section 3.1.3, the sequential steps of the methodology are presented in Sections 3.2 to 3.9.

3.1.1 Analytically quantifying risk – a general perspective

The failure of an infrastructure object (e.g. a roadway becoming buried in rockfall debris) is the state of reduced structural and/or functional performance of the infrastructure object. The risk of failure is the probabilistic quantification of the consequences a hazard, can cause on a part of the built infrastructure. Herein, a hazard is described as a function of its respective attributes, the hazard parameters. Furthermore the magnitude of a given hazard and hazard parameter are respectively referred to as the hazard intensity and hazard parameter intensity. The consequences of failure include direct consequences and indirect consequences. Direct consequences are the financial valuation of the repair activities required to return the infrastructure object's structural performance to its original state (e.g. the financial valuation of removing the rockfall debris and repairing the roadway damage). Indirect consequences are the financial valuation of the losses and additional expenditures incurred from transport and societal related impacts of the infrastructure object's reduced functional performance (e.g. the financial valuation of detouring around the closed roadway).

The risk of failure of object *A* with respect to hazard *B* is the product of the failure probability of a object *A* with respect to hazard *B* multiplied by the consequences of object *A* failing due to hazard *B*, Equation (3.1).

$$Risk_A^B = P_{fA}^B \cdot consequences_A^B \tag{3.1}$$

Where:

$Risk_A^B$ = the risk of failure of object *A* with respect to hazard *B* [CHF]
P_{fA}^B = the failure probability of object A with respect to hazard *B* [ ]
$consequences_A^B$ = the consequences of object *A* failing due to hazard *B* [CHF]

A hazard (e.g. a flood) is quantified in terms of its respective hazard parameters (e.g. flood depth, discharge, velocity) and the value of a given hazard parameter is the hazard parameter intensity (e.g. the discharge rate). The risk of failure of a given infrastructure object, *i*, with respect to hazard parameter, *h*, (e.g. flood depth) is equal to the integral of the risk of failure of object *i* over all potential hazard parameter intensities (e.g. flood depth of 0.5m, 1m, 2m). As shown in Equation (3.2), this is in turn equal to the product of the failure probability of object *i* with respect to the hazard parameter intensity *x*, multiplied by the failure consequences of object *i* with respect to each respective hazard parameter intensity *x,* integrated across all potential hazard parameter intensities.

$$Risk_i^h = \int_0^\infty \left(Risk_i^x \right) dx = \int_0^\infty \left(P_{fi}^x \cdot consequences_i^x \right) dx \tag{3.2}$$

Where:

$Risk_i^h$ = the risk of failure of object *i* with respect to the hazard parameter *h* [CHF]
$Risk_i^x$ = the risk of failure of object *i* with respect to hazard parameter intensity *x* [CHF]
P_{fi}^x = the failure probability of object *i* with respect to the occurrence of the hazard parameter intensity *x* [ ]
$consequences_i^x$ = the consequences of the failure of object *i* with respect to hazard parameter intensity *x* [CHF]

As hazard events seldom affect a given infrastructure object and as infrastructure objects can fail in numerous different failure modes, Equation (3.2) is further refined to Equation (3.3) by assuming the different failure modes are mutually exclusive. Thus, the resulting total risk with respect to the given hazard parameter is a summation of the risk of failure of object *i* with respect to the hazard parameter intensity *x* within each failure mode m_n.

$$Risk_i^h = \sum_{n=0}^{N} \left[\int_0^\infty \left(v_i^x \cdot P_{fi,m_n}^x \cdot consequences_{i,m_n}^x \right) dx \right] \tag{3.3}$$

Where:

v_i^x = the probability of the hazard parameter intensity *x* affecting object *i* [ ]
$P_{fi,mn}^x$ = the failure probability of object *i* failing in mode m_n with respect to the hazard parameter intensity *x* [ ]
$consequences_{i,mn}^x$ = the consequences of object *i* failing in mode m_n to the hazard parameter intensity *x* [CHF]

3.1.2 Analytically quantifying vulnerability – a general perspective

Turning to analytically quantifying vulnerability, the vulnerability of a transportation infrastructure object with respect to a hazard parameter is herein defined as the consequences a hazard parameter of a given intensity can cause due to the failure of the infrastructure object.

The vulnerability of object *i* failing in mode m_n to a hazard parameter intensity *x*, Equation (3.4), is the probability of object i failing in mode m_n with respect to a given hazard parameter intensity *x*

multiplied by the sum of the direct and indirect consequences of object *i* failing in mode m_n with respect to the hazard parameter intensity *x*.

$$Vulnerability_{i,m_n}^{x} = P_{fi,m_n}^{x}(DC_{i,m_n}^{x} + IC_{i,m_n}^{x}) \tag{3.4}$$

Where:

$Vulnerability_{i,mn}^{x}$ = the vulnerability of object *i* failing in mode m_n with respect to a hazard parameter intensity *x* [CHF]

$DC_{i,mn}^{x}$ = the financial valuation of the repair activities required to return object *i*'s failure in mode m_n with respect to the hazard parameter intensity *x* to object *i*'s original state [CHF]

$IC_{i,mn}^{x}$ = the financial valuation of the incurred transport and societal losses and additional expenditures due to infrastructure object *i*'s reduced functional performance by failing in mode m_n [CHF]

The direct consequences of object *i* failing in mode m_n for a given hazard *h* and its parameter intensity *x*, Equation (3.5), are in turn dependent on object *i*'s structural capacity in the failure mode m_n and the financial valuation of the activities required to repair this level of structural damage.

$$if\left(x > R_{i,m_n}^{x}\right) \rightarrow F_{i,m_n}^{x} \rightarrow DC_{i,m_n}^{x} \tag{3.5}$$

Where:

$R_{i,mn}^{x}$ = object *i*'s structural capacity with respect to the failure mode m_n and the hazard parameter intensity *x*

$F_{i,mn}^{x}$ = the structural state of object *i* failing in mode m_n to the hazard parameter intensity *x*

The indirect consequences of object *i* failing in mode m_n due to the hazard parameter intensity *x*, Equation (3.6), is herein defined as a product of the time required to return infrastructure object *i* having failed in mode m_n to the original state (hereafter referred to as the service interruption duration) and the daily financial valuation of the transport and societal losses and additional expenditures due to infrastructure object *i*'s reduced functional performance by failing in mode m_n.

$$IC_{i,m_n}^{x} = SI_{i,m_n}^{x} \cdot IC_{I,daily} \tag{3.6}$$

Where:

$SI_{i,mn}^{x}$ = the time required to return infrastructure object *i* having failed in mode m_n to the hazard parameter intensity *x* to a fully functional state [days]

$IC_{I,daily}$ = the daily financial valuation of the losses and additional expenditures incurred from transport and societal related impacts of infrastructure link *I*'s reduced functional performance [CHF] [2]

Therefore using the definition of Equation (3.6), the risk of failure and vulnerability of object *i* to hazard parameter *h*, Equations (3.3) and (3.4), can be refined as Equations (3.7) and (3.8).

$$Risk_i^h = \sum_{n=0}^{N}\left[\int_0^{\infty}\left(v_i^x \cdot P_{fi,m_n}^{x}\left(DC_{i,m_n}^{x} + SI_{i,m_n}^{x} \cdot IC_{I,daily}\right)\right)dx\right] \tag{3.7}$$

$$Vulnerability_{i,m_n}^{x} = P_{fi,m_n}^{x}(DC_{i,m_n}^{x} + SI_{i,m_n}^{x} \cdot IC_{I,daily}) \tag{3.8}$$

[2] While it is realized that natural hazard events can seriously or fatally injure individuals, these indirect consequences are not considered by this work. Please refer to ASTRA's "Safety of the road transportation system and its structures" series for additional information concerning the assessment of these indirect consequences (ASTRA, 2008).

One can observe from Equations (3.7) and (3.8), that to quantify the risk and the vulnerability curve of a given object *i* due to a hazard parameter *h*, one must evaluate five different terms – the probability of each hazard intensity *x* acting on the object *i*, the probability of object *i* experiencing failure in mode m_n, the direct consequences of object *i* failing in mode m_n, the service interruption duration of object *i* failing in mode m_n and the daily indirect consequences of object *i*'s reduced functional performance.

The remaining part of this chapter presents methodologies for assessing the probability of each hazard parameter intensity *x* acting on object *i*, the probability object *i* failing in mode m_n, the direct consequences of object *i* failing in mode m_n and the service interruption duration related to object *i* failing in mode m_n. Methodologies for determining the financial valuation of the losses and additional expenditures incurred from transport and societal impacts of a given infrastructure object's reduced functional performance can be found within (Hajdin, Axhausen, Bell, Birdsall, & Erath, 2008).

For clarity purposes, these general definitions of vulnerability and risk are applied in Example 3-1 to assess the vulnerability and risk of failure of a roadway object to a rockfall hazard.

Example 3-1: Evaluate the annual risk of failure of a roadway object exposed to a rockfall hazard.

Take a rockfall hazard *R* which is assessed to act on a roadway object *i* once every 30 years. It is further estimated that if the rockfall occurs, it will result in 3m of rock uniformly covering a 100m length of roadway. Removing this quantity of rock and repairing the roadway is estimated to take 3.5 days at a cost of 75,000 CHF. The daily transport and societal losses and additional expenditures due to the roadway's functional failure are estimated at 20,000 CHF.

The roadway object has negligible resistance to a rockfall hazard and thus in case of a rockfall event, the roadway object is buried in rockfall debris (the failure mode). The key rockfall hazard parameter for a roadway failing in this mode is the depth of deposited debris. The hazard parameter intensity is a uniform deposited rockfall debris depth of 3m.

From the data provided above, one can extrapolate the following information:

v_i^x = 1/30 years = 0.03333 per year (rate of a rockfall intersecting the roadway)
x = 3 meters of rock (rockfall parameter intensity)
$R_{i,m0}^x$ = 0 meters of rock (roadway structural capacity with respect the given failure mode)
$P_{fi,m0}^x$ = 1.00 (roadway failure probability)
$DC_{i,m0}^x$ = 75,000 CHF (direct consequences, i.e. repair cost)
$SI_{i,m0}^x$ = 3.5 days (service interruption duration)
$IC_{I,daily}$ = 20,000 CHF (daily indirect consequences)

Thus, the direct consequences of the roadway object *i*'s structural failure is:

$$DC_{i,m_0}^x = 75{,}000 \text{ CHF}$$

The indirect consequences of the roadway object *i*'s functional failure is:

$$IC_{i,m_0}^x = SI_{i,m_0}^x \cdot IC_{I,daily}$$

$$IC_{i,m_0}^x = (3.5 \text{ days})(20{,}000 \text{ CHF/day})$$

$$IC_{i,m_0}^x = 70{,}000 \text{ CHF}$$

Thus the roadway object *i*'s vulnerability with respect to the rockfall deposited depth of 3m, following Equation (3.4), is:

$$Vulnerability_{i,m_0}^{x} = P_{fi,m_0}^{x}\left(DC_{i,m_0}^{x} + IC_{i,m_0}^{x}\right)$$

$$Vulnerability_{i,m_0}^{x} = (1.00)(75{,}000\ \text{CHF} + 70{,}000\ \text{CHF})$$

$$Vulnerability_{i,m_0}^{x} = 145{,}000\ \text{CHF}$$

The annual risk of failure of the roadway object *i* to this rockfall hazard parameter intensity, following Equation (3.3), is:

$$Risk_i^R = \sum_{n=0}^{N}\left[\int_0^{\infty}\left(\nu_i^x \cdot P_{fi,m_n}^{x} \cdot consequences_{i,m_n}^{x}\right)dx\right]$$

$$Risk_i^R = (0.0333\ 1/\text{yr})(1.00)(\ 75{,}000\ \text{CHF} + 70{,}000\ \text{CHF})$$

$$Risk_i^R = 4{,}829\ \text{CHF/year}$$

3.1.3 General framework

To quantify the vulnerability and risk of infrastructure objects and the risk of infrastructure links contained within a transportation network, it is necessary to assess each of the terms in Equation (3.3), as follows:

- the probability of the hazard parameter intensity *x* affecting object *i* (ν_i^x)
- the failure probability of object *i* failing in mode m_n with respect to the hazard parameter intensity *x* ($P_{fi,mn}^{x}$)
- the consequences of object *i* failing in mode m_n to the hazard parameter intensity *x* ($consequences_{i,mn}^{x}$)

To formulate this information, it is necessary to answer the following five questions:

1) Is object *i* exposed to the hazard and what are the expected local hazard parameter intensities?
2) Is object *i* affected by the possible hazard parameter intensities?
3) What expected levels of damage does the possible hazard parameter intensities cause upon the object *i*?
4) What are the expected direct and indirect consequences for each expected level of damage?
5) For a link comprised of multiple objects, what are the resulting object vulnerabilities and object and link risks? (Sections 3.6 to 3.8)

The first question is answered by using existing practices and data that is under development from the geographic information system (GIS) based natural hazard assessment and infrastructure documentation data sources, presented in Sections 2.6 to 2.7, to conduct a geographic coincident analysis between the various hazards and infrastructure objects. The products of this coincident analysis are an assessment object length over which the given hazard acts (the object exposure length) and the local hazard parameter intensities for each hazard taken at discrete return periods as shown schematically in Example 3-1.

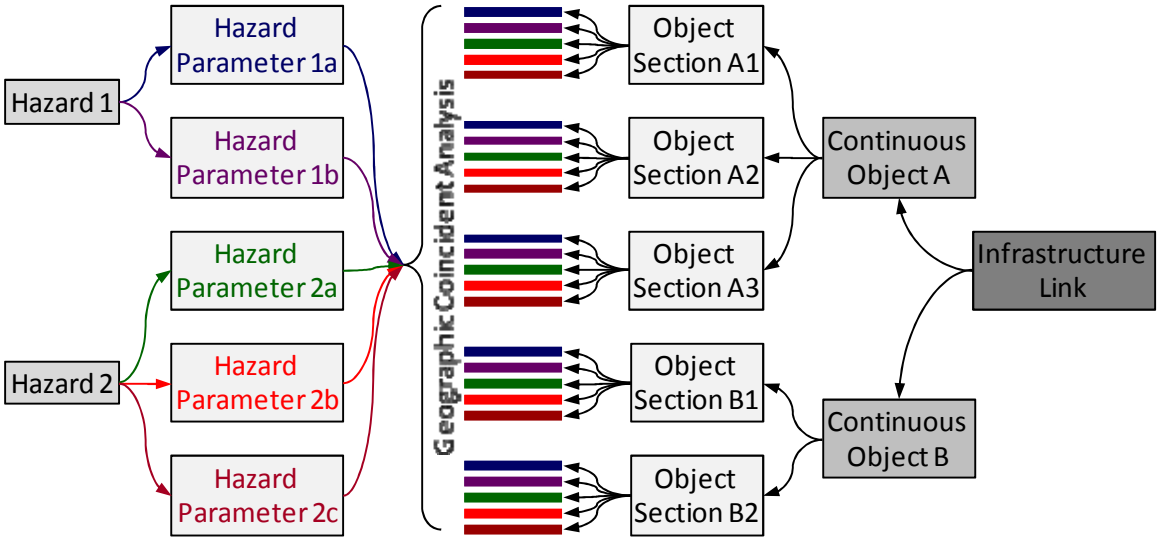

Figure 3-1: Schematic of a geographic coincident analysis between the hazard and infrastructure link data.

The second question is answered by assessing if an object is affected by a given hazard parameter intensity. This is accomplished by developing component specific failure assessment processes, Section 3.3 and Appendix A, which are employed to identify potential failure modes of each infrastructure object. The third and fourth questions are answered by using expert opinion and analyzes, Section 3.4, within the context of the possible hazard parameter intensity and the assessed failure mode, to estimate the levels of damage, the direct consequences (the structural repair costs), and the service interruption durations.

Lastly, the fifth and final question is answered by developing a comprehensive methodology for quantifying the failure vulnerability and risk of an object and the failure risk of a link with respect to a hazard or set of hazards. In Section 3.4, the discrete data collected and estimated in Sections 3.2 to 3.4 is extended to continuous functions by fitting a probability density function to the hazard parameter intensity data and by linearly interpolating and extrapolating functions to the exposed object length, the direct consequences and the service interruption durations. The vulnerability and risk of an object section is then quantified, Section 3.5.5 and 3.6, by considering an object responding in a single failure mode with respect to a hazard parameter and an object responding in multiple failure modes with respect to the same hazard parameter, schematically shown in Figure 3-2.

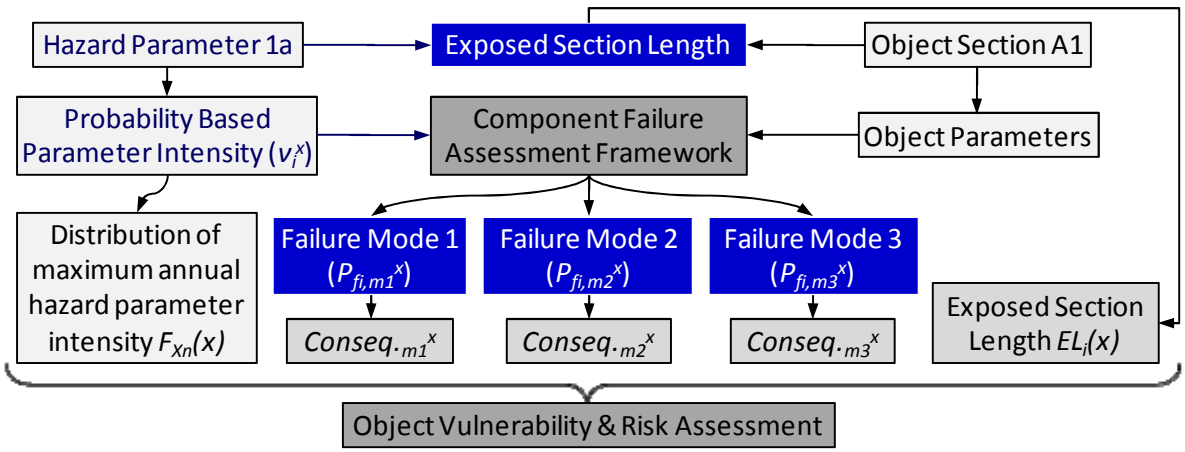

Figure 3-2: Schematic of the comprehensive object vulnerability and risk assessment methodology.

The analysis scope is then widened from an object section to a continuous object composed of a number of object sections. As a given hazard (e.g. a flood) has the potential to structurally and/or functionally damage numerous object sections within a given continuous object, and considering that as additional object sections are added the resulting direct consequences and service interruption times grow with at a less than purely linear rate. These structural repair and service interruption scale effects are considered by assessing an effective exposed object length – reduced total lengths which are a function of the considered hazard, Section 3.7. This effective exposed object length is then employed to assess the continuous object vulnerability and risk with respect to a single hazard and to multiple hazards.

The analysis scope is then widened further from the continuous object to a link composed of a number of continuous objects. The individual continuous object risks of failure with respect to specific hazards are then combined by considering the geographic-based correlation between the various hazards. The end result is an assessment of the risk of failure of a given infrastructure link with respect to multiple natural hazards. The influence of the employed temporal risk of failure assessment period (e.g. risk of failure over 5 years versus 50 years) is then assessed in Section 3.9.

This comprehensive vulnerability and risk assessment methodology is then applied, in Chapter 4, to analyze two different case studies – selected infrastructure objects within the Jaun Pass and within the Commune of Zofingen. The strengths, limitations and potential further applications of this comprehensive vulnerability and risk assessment method are then qualitatively assessed.

3.2 Identifying and quantifying object exposure to natural hazards

3.2.1 General Overview

The first step of the comprehensive vulnerability and risk assessment methodology is comprised of two stages. The first stage assesses if a given infrastructure object is exposed to the considered hazards and the second stage quantifies the expected local hazard parameter intensities at different event return periods.

During this first stage, a general geographic coincident analysis is conducted between the hazard parameter maximum event return period data and the infrastructure object data to determine if the given infrastructure objects are exposed to the considered hazards. Within Switzerland, the SilvaProtect hazard indication database and the maximum return period flood hazard identification map are respectively employed to document the maximum geographic reach of gravitational hazards (i.e. avalanche, landslide, rockfall and torrent) and the maximum geographic reach of the flood hazard. On the infrastructure object side, the Swiss Transportation Model (STM) and the KUBA infrastructure databases are used to geographically document the location of the various infrastructure objects. Objects not exposed to a given hazard are excluded from further analysis with respect to the given hazard.

The second stage, a detailed geographic coincident analysis is used to quantify the expected local hazard parameter intensities at different event return periods. To conduct this analysis, hazard parameter identification maps are employed to document the local hazard parameter intensities and the STM and KUBA infrastructure databases are used to determine the geographic location of the infrastructure objects. The end product of this second stage is a quantification of the local hazard

parameter intensities at discrete event return periods and the length of each object exposed to the various hazard parameter intensities.

An example geographic coincident analysis between a hazard and an infrastructure object is conducted within Section 3.2.2 to demonstrate the specific analysis stages and to assess the strengths, weaknesses and limitations of the current hazard and the infrastructure databases with respect to the evaluation of vulnerability and risk.

3.2.2 Example geographic coincident analysis

To demonstrate the stages of a geographic coincident analysis between a hazard and an infrastructure object, an example coincident analysis is conducted between the flood hazard data and the infrastructure object data for the transportation network connecting Brittnau to Zofingen, presented earlier in Section 0. Figure 3-3 presents the maximum possible flood hazard (EHQ), the STM infrastructure and the KUBA infrastructure data for the Brittnau-Zofingen roadway network.

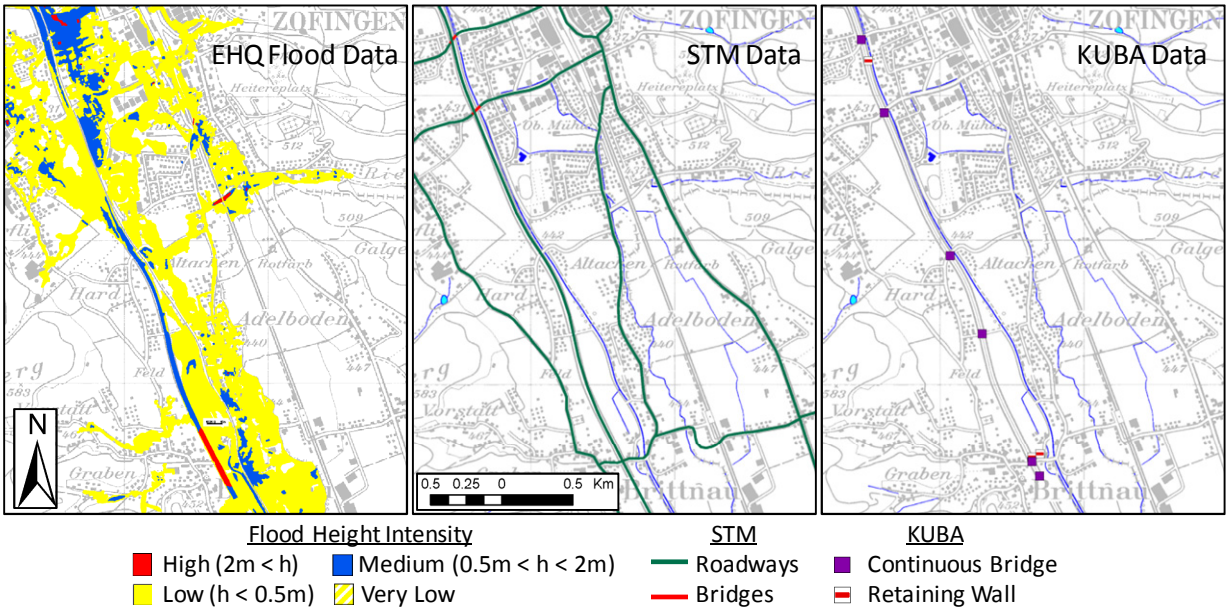

Figure 3-3: Flood hazard maximum return period and infrastructure data.

In Figure 3-3, one can observe the flood depth intensity ranges with the EHQ flood database, the roadways and bridges included in the Swiss Transportation Model and the national infrastructure objects specified within KUBA. From Figure 3-3, one can also observe what is not included, most strikingly, the limited number of infrastructure objects included in the KUBA data. This limited number of objects is a direct product of the limited scope employed by KUBA. Thus for given the region shown, KUBA can only provide information on infrastructure objects within the national highway system.

A geographic coincident analysis is then conducted between the flood hazard maximum return period and the infrastructure data to determine which infrastructure objects are and which infrastructure objects are not exposed to the flood hazard, Figure 3-4. From the coincident analysis presented in Figure 3-4, one can observe that a large number of the infrastructure objects are exposed to the maximum flood event.

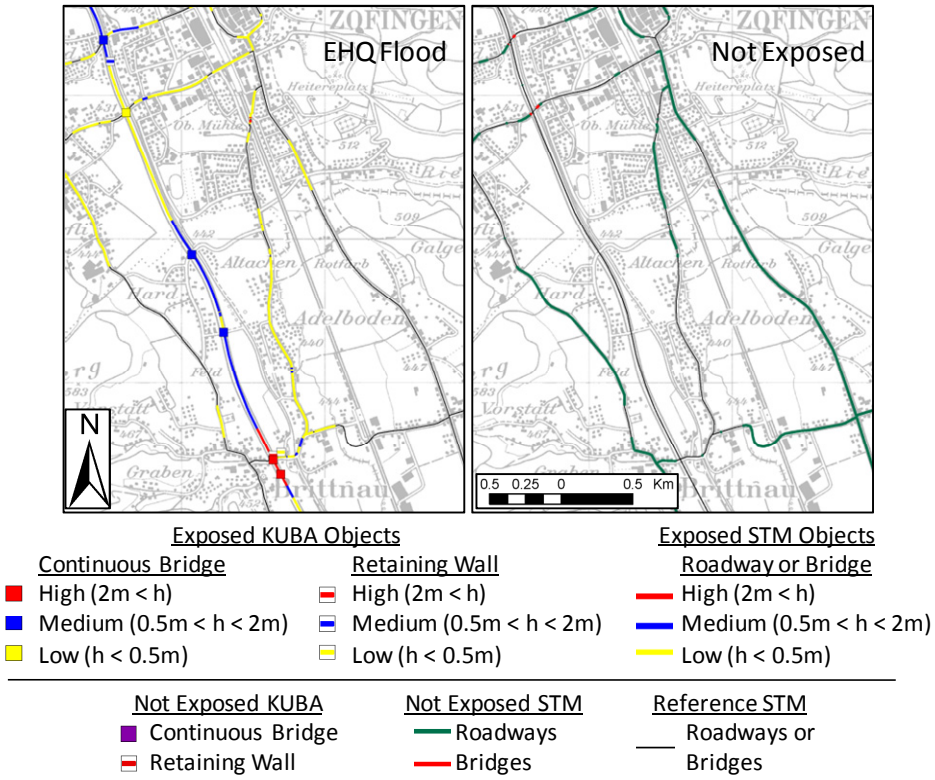

Figure 3-4: Coincident analysis: the maximum return period flood hazard data and the infrastructure data. [3]

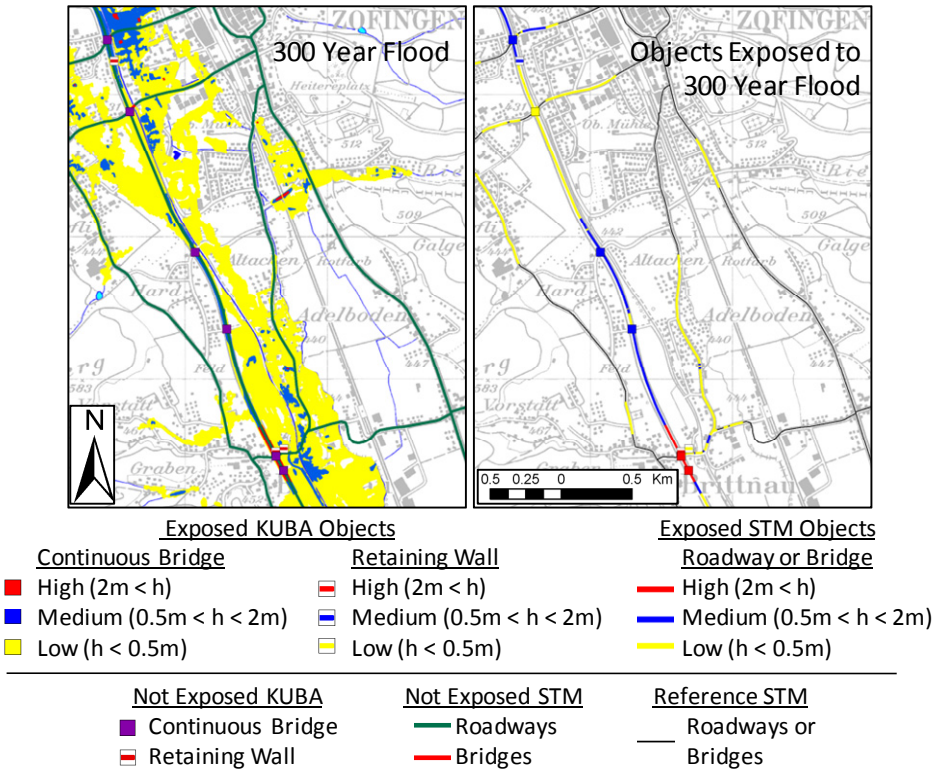

Figure 3-5: Coincident analysis between flood depth intensities for the 300 year return period event and the intrastructure objects.

[3] Every coincident analysis presented herein was conducted within the ArcMap user interface of ESRI's ArcInfo GIS program (ESRI, 2006).

In the second stage of the geographic coincident analysis, the objects exposed to the given hazard, in this case a flood hazard, are then further analyzed to determine the location specific hazard parameter intensities for specific return period events. Figure 3-5 presents such a coincident analysis between the 300 year return period flood event data developed by the Canton of Aargau in conjunction with the National Hazard Mapping Initiative and the STM and KUBA infrastructure data (Aargau, 2007).

From Figure 3-5, one can observe that the geographic coincident analysis yields not only the local hazard parameter intensity, in this case the local flood depth, but also the infrastructure object length over which these hazard parameter intensities are imposed. The detail of this geographic coincidence analysis can be presented in a map and in a table.

As this coincident analysis is conducted digitally within a GIS platform from individual hazard and infrastructure databases, the results visually presented above can also be quantitatively presented. Four specific infrastructure objects are identified in Figure 3-6 – 1) a portion of the A2 highway, 2) the most direct local road between Brittnau and Zofingen, 3) the bridge identified in Detail A, and 4) a retaining wall presented in Detail A.

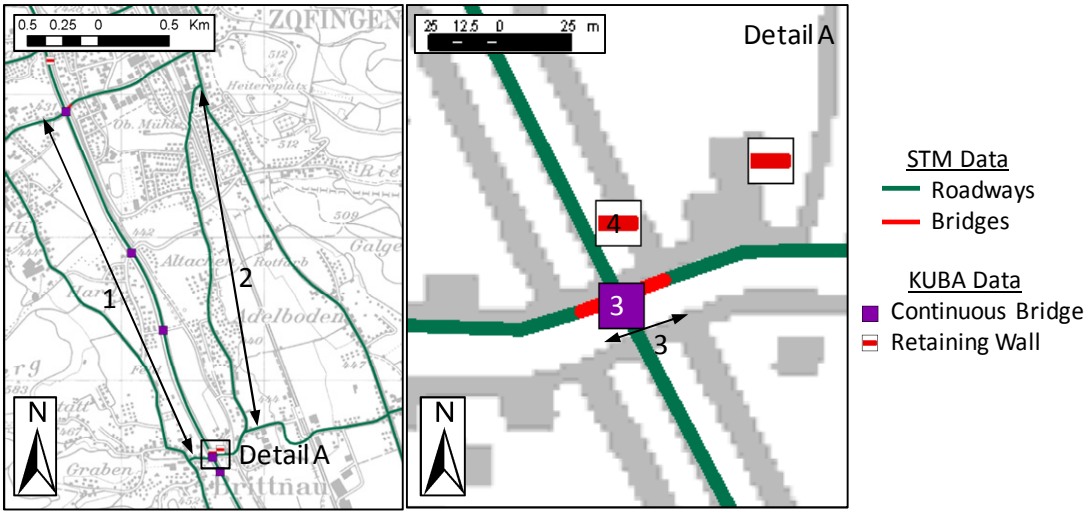

Figure 3-6: Detail presentation of specific infrastructure objects within the Zofingen roadway network.

The data included within the STM and KUBA databases for the selected objects is presented in Table 3-1. In reviewing this data, one can observe that the STM database focuses on transportation links providing information for infrastructure objects 1, 2 and 3 while KUBA focuses on structures and thus can provide information on the bridge and the retaining wall objects. Delving further into this data, the STM data specifies the infrastructure type, roadway class and length. The KUBA data details the infrastructure type, structural configuration, construction year, and key object properties and dimensions.

For each object contained within the STM database, the length of each object exposed to a specific event flood depth intensity range can be quantified and directly assigned. For example, 874 m of the 2246 m long Zofingenstrasse, connecting Brittnau to Zofingen, is exposed to flood depth of 0.5m or less during a 100 year flood event. As the objects in the KUBA are currently geographically represented as only single data points, one can only quantify if the object reference point is exposed to a given event flood depth intensity. Thus from the flood depth-KUBA coincident analysis, one can

determine that the bridge over the A2 has an expected flood depth intensity of 2m or deeper during a 300 year flood – a result consistent with the STM-flood depth coincident analysis.

Table 3-1: Quantitative results from the Zofingen detailed geographic coincident analysis.

	Reference	**1**			**2**			**3**			**4**		
	Name	A2 Highway			Zofingenstrasse			307 Bridge over A2			N2/108 Wall		
	STM	Yes			Yes			Yes			No		
	STM-Infra. Type	Road			Road			Bridge			-		
	STM-Class	Separated Highway			Class 2			Class 2			-		
	STM-Length(m)	2646			2246			32.6			-		
STM-Results	**Exp Length (m)**	H	M	L	H	M	L	H	M	L	H	M	L
	30 year Flood	0	0	0	0	0	0	0	0	0	-	-	-
	100 year Flood	0	0	127	0	0	874	0	0	1.8	-	-	-
	300 year Flood	244	1465	938	0	73	1275	28.5	0	4	-	-	-
	EHQ year Flood	244	148	922	20	24	1532	28.5	0	4	-	-	-
	KUBA	No			No			Yes			Yes		
	Infrastructure Type	-			-			Continuous Bridge			Retaining Wall		
	Construction Year	-			-			1976			1976		
	Number of Spans	-			-			2			-		
	Length (m)	-			-			29.9			128.8		
	Maximum Span (m)	-			-			14.4			-		
	Width (m)	-			-			11.6			-		
	Deck Surface (m^2)	-			-			347			-		
	Supports	-			-			Abutments			-		
	Height (m)	-			-			-			2m – 8m – 4m		
KUBA	30 year Flood	-			-			Not Exposed			Not Exposed		
	100 year Flood	-			-			Not Exposed			Not Exposed		
	300 year Flood	-			-			High Intensity			High Intensity		
	EHQ year Flood	-			-			High Intensity			High Intensity		

3.2.3 Critique of coincident analysis

From the example hazard-infrastructure object geographic coincident analysis presented above, one can observe that during the first stage the non-exposed objects are quickly identified and removed from further analysis. In the second stage, the detailed hazard parameter return period – infrastructure object geographic coincident analysis, the exposure length of each infrastructure object and the associated local hazard parameter intensities are quantified.

In studying the results from the detailed coincident analysis in a tabular format, it can be observed that the currently geographic representation of the KUBA data as single data points rather than as linear elements reduces the resulting analysis accuracy. On the hazard side, one can observe that the hazard parameter intensities (the flood depth) are represented as intensity ranges ($x < 0.5$m, $0.5 < x < 2$m and 2m $< x$). While such an abstraction is useful for limiting the overall database size, it significantly reduces the accuracy of the provided hazard parameter intensity information.

3.3 Component failure assessment process

3.3.1 General overview

With the exposed object lengths and local hazard parameter intensities identified, one must determine if the given objects are affected by the given hazard parameter intensities. To conduct this analysis, a failure assessment process has been developed for each considered infrastructure component (i.e. bridge, culvert, gallery, retaining wall, roadway and tunnel) and is designed to be applied to analyze the infrastructure objects within the given component. Each component failure assessment process employs key hazard parameter and infrastructure object data to systematically analyze the given object and identify the potential failure modes.

The component failure assessment process development is derived from the hazard-component failure scenarios. The most general set of failure scenarios has been developed by first identifying numerous situations in which a given hazard can cause the partial or complete failure of a given component. Common failure modes are identified for different failure scenarios. These individual failure modes have then been embedded into a structured assessment process and representative simple structural models have been formulated using the pertinent hazard and object data. These simple models are then employed to assess the potential of failure within each assessment step. These representative simple structural modes for each component are presented in Appendix A. Throughout this development, specific attention has been paid to directly using pre-existing hazard and component data when possible. A summary identifying the required hazard and component data, their respective availability and associated failure assessment steps is presented at the close of this section.

3.3.2 Hazard-component failure scenarios

To develop the component failure assessment process, the scenarios through which each hazard can impact each component are outlined. In identifying potential hazard-component failure scenarios, five different natural hazards (i.e. avalanche, flood, landslide, rockfall and torrent) and six different components (i.e. bridge, culvert, gallery, retaining wall, roadway tunnels) were considered. For example, in considering the scenarios in which an avalanche can cause partial or complete failure of a bridge, five unique failure scenarios can be identified – specifically:

1) An avalanche can come in contact with the bridge superstructure vertically overloading the bridge superstructure in shear or flexure.
2) An avalanche can come in contact with the bridge superstructure horizontally overloading the bearing connection between the superstructure and substructure causing the bridge to slide off its supports.
3) An avalanche can come in contact with the bridge superstructure horizontally overloading the bridge superstructure causing it to fail horizontally in shear or flexure.
4) An avalanche can come in contact with the bridge substructure overloading a pier in shear or flexure.
5) An avalanche can come in contact with the bridge superstructure and if the superstructure, the superstructure-substructure connection and the substructure ultimate strengths are not exceeded, the avalanche can bury the bridge running surface.

Table 3-2: Hazard-component failure scenarios.

		Hazard						
		Avalanche	**Flood**	**Landslide**	**Rockfall**	**Torrent**	**Total #**	**# Modes**
Component	**Bridge**	5	4	5	5	4	23	6
	Culvert	1	1	1	1	1	5	2
	Gallery	5	2	6	5	3	21	7
	Retaining wall	3	4	4	4	3	18	5
	Roadway	1	2	2	1	1	7	2
	Tunnel	0	2	0	0	2	4	2
	Total #	15	15	18	16	14	78	24

Therefore, as presented in Table 3-2, there are 5 different failure scenarios for the avalanche-bridge hazard-component combination.

In briefly looking through Table 3-2, one can observe that there are five or fewer different failure scenarios for the culvert and tunnel components while there are at least 18 different failure scenarios for the bridge, gallery and retaining wall components. The source of this difference is twofold. First, some of the components with a low number of failure scenarios are not exposed to all five hazards (i.e. a tunnel is assumed to not be exposed to avalanche, landslide or rockfall hazards). Secondly, in the cases where these components are exposed to a given hazard, the component resistance to the given hazard is limited or neglected (i.e. a culvert has limited resistance to being buried by an avalanche). Turning to the components with a high number of failure scenarios, bridge, gallery and retaining wall, this status is a direct result of the multiple levels of the given component's resistance as seen in formulating the Avalanche-Bridge failure scenarios presented above.

The remaining component, roadway, has an elevated number of failure scenarios, not only because it is exposed to all five hazards but also because a roadway object performance can be influenced by secondary supportive objects – specifically culvert and retaining wall objects. Thus a landslide can cause a roadway failure indirectly by damming a culvert passing underneath a roadway resulting in a localized flood which inundates the roadway.

In Section 3.3.3, the failure assessment process for the bridge component is presented. The detailed analysis procedures for the bridge and the failure assessment process and detailed analysis procedures for the five additional components have been included in Appendix A.

The included detailed analysis procedures are not intended to be exhaustive but are rather intended to show the analysis process and required data for an example component configuration.

3.3.3 The bridge failure assessment process

Bridges are elevated objects commonly constructed to carry the given transportation link over bodies of water, established transportation routes or locally uneven ground. Within this work, and as shown in Figure 3-7, a bridge is assumed to be composed of four key elements – foundation, piers and abutments, bearings and superstructure.

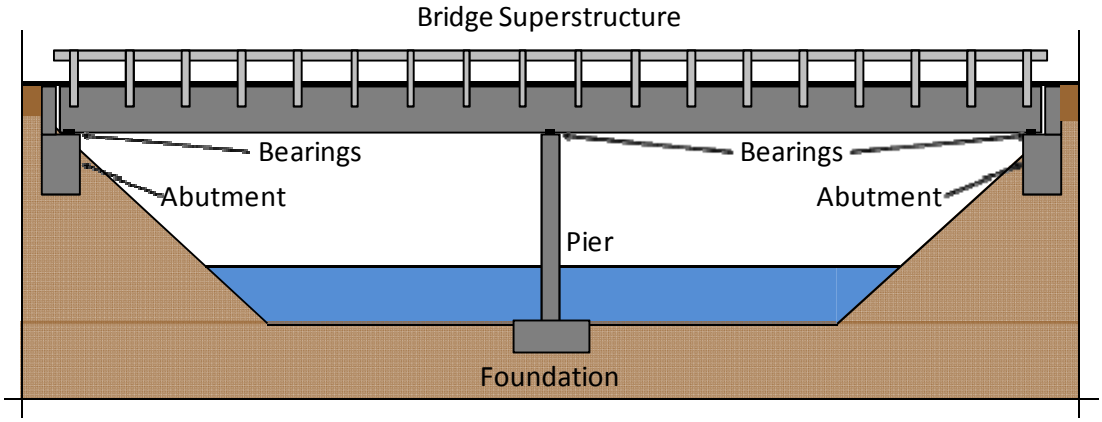

Figure 3-7: A typical bridge configuration.

In Table 3-3, one can observe that 23 different potential failure scenarios are considered in assessing the capacity of a bridge. When these failure scenarios are analyzed as a group, six failure modes are identified and arranged into the structured assessment process presented in Figure 3-8.

In Figure 3-8, one can observe that the first step, step A, requires a geographic coincident analysis be conducted between the given hazard and bridge object. If the bridge is found to be outside the geographic reach of the hazard, it is assumed the bridge is not affected by the given hazard and thus survives. But if the bridge is coincident with the hazard, one must assess if the bridge clearance is greater than the hazard running height, step B. If the hazard running height exceeds the bridge's clearance, the hazard will come in contact with the bridge superstructure, applying forces to the superstructure, the superstructure-substructure bearing connection, the pier and the material passing underneath the bridge superstructure. If the hazard does not exceed the bridge clearance, the hazard only comes in contact with the bridge foundation and piers.

The next step, step C, assesses if the hazard can undermine the pier foundation. In Table 3-3, one can observe that it has been assumed that only the flood and landslide hazards can undermine a bridge foundation, respectively through local induced scour or local rupture surface depth. Returning to Figure 3-8, one can observe that whether or not the hazard has come in contact with the bridge superstructure has an influence on the resulting flow (i.e. either non-pressurized flow or pressurized flow). In either situation, the resulting failure mode is identical, B1 – foundation is undermined.

Table 3-3: Bridge failure modes and associated hazards.

	Potential Hazards				
Failure mode	**Avalanche**	**Flood**	**Landslide**	**Rockfall**	**Torrent**
Foundation is undermined	-	x	x	-	-
Superstructure is overloaded vertically in shear or flexure	x	-	-	x	-
Superstructure is overloaded horizontally in shear or flexure	x	x	x	x	x
Bearings are overloaded horizontally or vertically	x	x	x	x	x
Bridge pier is overloaded horizontally in shear or flexure	x	-	x	x	x
Bridge surface submerged in liquid or debris	x	x	x	x	x

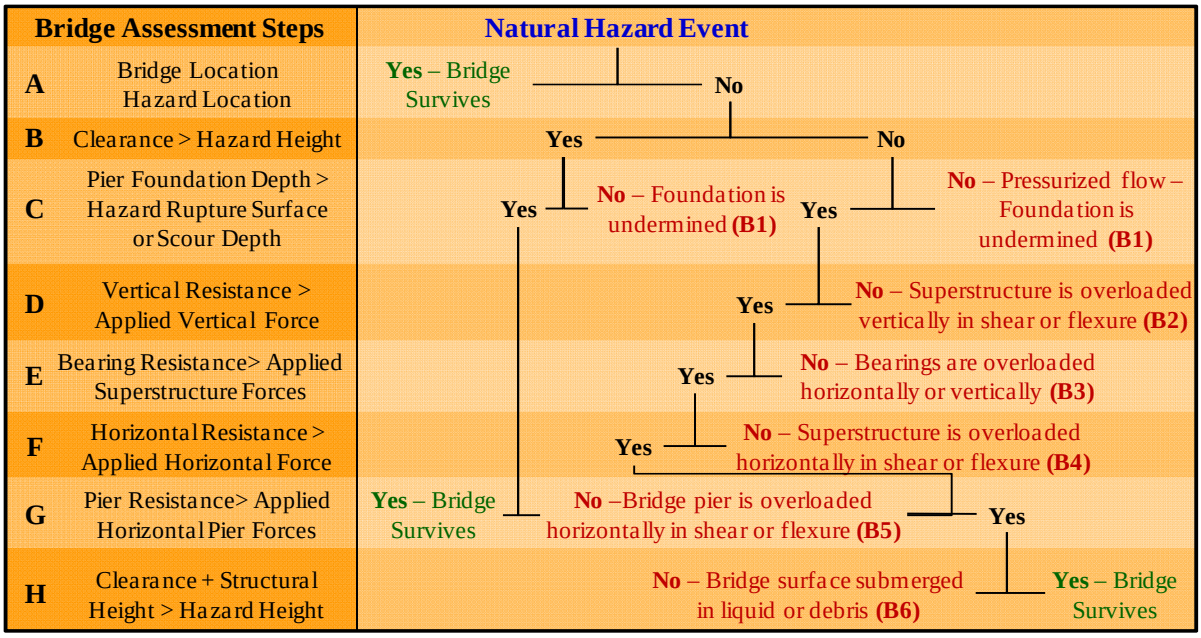

Figure 3-8: Bridge failure assessment process.

As mentioned earlier, the next analysis step, step D, is reached when the hazard has exceeded the bridge clearance. Taking the case where the hazard has exceeded the bridge clearance, analysis step D determines if the bridge superstructure vertical shear and flexural resistance is sufficient to withstand the applied hazard forces. In Table 3-3, one can observe that it has been assumed that only avalanche and rockfall hazards can cause a bridge superstructure to vertically fail. If the bridge superstructure has sufficient vertical capacity, one must then assess whether the bridge bearing system has sufficient horizontal and vertical capacity. In consulting the bridge detailed assessment procedures, Appendix A.2, one can observe that it has been assumed that only the flood and torrent hazard can cause a bridge bearing system to fail in vertical uplift, and any of the five hazards have the potential to horizontally overload the bridge bearing system. If the bridge bearings are overloaded, the bridge is assumed to fail in mode B3. If the bearing system does have sufficient capacity, one must continue the analysis process on to step F, assessing the horizontal shear and flexural capacity of the of the bridge superstructure. If the applied hazard force exceeds the bridge superstructure horizontal capacity, the bridge is assumed to fail in mode B4. If the bridge superstructure does have sufficient capacity, the analysis process then shifts to the pier resistance.

The hazard running height and whether the hazard exceeds the bridge clearance both have influence on the applied horizontal forces but in every case one must still assess if the pier(s) can withstand the applied horizontal pier(s) forces, step G. If the pier resistance is exceeded, it is assumed that the bridge will fail in mode B5. But if the pier does have sufficient capacity, the provided result is depended on whether or not the hazard running height exceeded the bridge clearance. If the hazard does not come in contact with the bridge superstructure, it is assumed that the bridge survives the event with this hazard intensity but if the hazard height has exceeded the bridge clearance, one must assess if the hazard height also exceeds the combined height of the bridge clearance and the bridge superstructure height, step H. If the hazard height does exceed this combined height, it is assumed that the bridge fails in mode B6 – bridge surface submerged in liquid or debris. If the hazard height does not exceed the combined bridge clearance and superstructure height, it is assumed the bridge survives exposure to this hazard intensity. Thus through applying the structured failure assessment

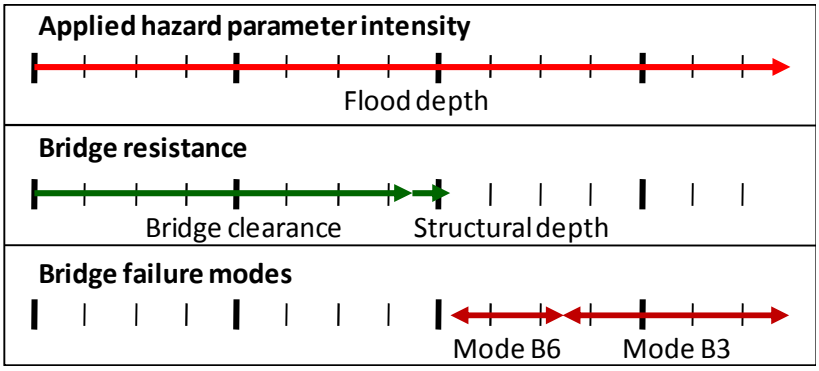

Figure 3-9: Example bridge multiple failure mode response.

process presented herein and within Appendix A.2, one can systematically qualitatively and quantitatively determine if a bridge is vulnerable to a given hazard intensity and if so, which failure mode controls for the given hazard intensity.

In consulting the failure assessment process for the culvert, gallery, retaining wall, roadway and tunnel components, respectively contained with Appendices A.3 to A.7, one can observe that while each component failure assessment process has been adapted to suit the structural configuration of each component, the assessment process is similar to the bridge assessment process presented above.

3.3.4 Intricacies of applying a component failure assessment process

As an object does have the potential to fail in multiple failure modes depending on the hazard intensity, Figure 3-9, the component failure assessment process must be applied not just at a single hazard parameter intensity but at multiple hazard parameter intensities, thereby identifying the range of each failure mode.

Additionally, if there are uncertainties of the hazard parameter intensities and/or the object parameter intensities (e.g. rockfall impact location or concrete compressive strength) one must iteratively conduct the failure assessment analysis with each analysis sampling the hazard and object parameter intensities as a function of their respective probability distributions. The end result of such an iterative analysis are not deterministic failure mode ranges as presented in Figure 3-9, but rather probability based failure mode ranges.

Lastly, in Figure 3-8, one can observe that the failure assessment process requires that multiple different parameter intensities must be obtained for a given hazard. Unfortunately, the reporting practice of hazard parameter intensities is to collect data for each parameter separately and not to correlate the individual parameters. Thus, without conducting a detailed onsite analysis, given the current practice, correlating individual hazard parameters is not considered herein.

3.3.5 Status of component and hazard data

In Section 3.3.3 and Appendix A, numerous hazard and component parameters were mentioned but, as presented in Sections 2.6 and 2.7, only a small number of these parameters are currently systematically collected and included within the natural hazard and infrastructure databases.

Table 3-4: Hazard parameter availability and applicable component failure modes (with x denoting required hazard parameter data and – denoting non-required hazard parameter data).

			Component Failure Mode																								
			Bridge							Culv		Gallery								Retain Wall					R	T
	Hazard Parameter	Available?	B	C	D	E	F	G	H	B	C	B	C	D	E	F	G	H	I	B	C	D	E	F	D	B
Avalanche	Running depth	No	x	-	x	x	x	x	x	-	-	-	x	x	x	x	x	x	-	-	-	x	x	x	-	-
	Horizontal pressure	Yes	-	-	x	x	x	x	-	-	-	-	x	x	-	x	x	x	-	-	-	x	x	-	-	-
	Angle of attack	No	-	-	x	x	-	x	-	-	-	-	-	-	-	x	x	x	-	-	-	-	-	-	-	-
	Deposited depth	No	-	-	-	-	-	-	x	x	-	-	-	-	-	x	x	x	-	-	-	-	-	-	x	-
Flood	Running depth	Yes	x	-	-	x	x	-	x	-	-	-	-	-	-	-	-	-	x	-	-	x	x	x	x	x
	Local scour depth	Partial	-	x	-	-	-	-	-	-	-	x	-	-	-	-	-	-	-	x	-	-	-	-	-	-
	Discharge	No	-	-	-	-	-	-	-	-	x	-	-	-	-	-	-	-	-	-	-	-	-	-	-	-
	Velocity	No	-	-	-	x	x	-	-	-	-	-	-	-	-	-	-	-	-	-	-	-	-	-	-	-
Landslide	Running depth	No	x	-	x	x	x	x	x	-	-	-	x	x	x	x	x	x	-	-	x	x	x	x	-	-
	Rupture surface depth	No	-	x	-	-	-	-	-	-	-	x	-	-	-	-	-	-	-	x	-	-	-	-	-	-
	Horizontal pressure	No	-	-	x	x	x	x	-	-	-	-	x	x	-	x	x	x	-	-	x	x	x	-	-	-
	Angle of attack	No	-	-	x	x	x	x	-	-	-	-	-	-	-	x	x	x	-	-	x	x	x	-	-	-
	Deposited depth	No	-	-	x	-	-	-	x	x	-	-	-	-	-	x	x	x	-	-	-	-	-	-	x	-
Rockfall	Running depth	No	x	-	x	x	x	x	x	-	-	-	x	x	x	x	x	x	-	-	x	x	x	x	-	-
	Rockfall energy	Yes	-	-	x	x	x	x	-	-	-	-	x	x	-	x	x	x	-	-	x	x	x	-	-	-
	Angle of attack	No	-	-	x	x	x	x	-	-	-	-	x	x	-	x	x	x	-	-	x	x	x	-	-	-
	Rockfall radius	No	-	-	x	x	x	x	-	-	-	-	x	x	-	x	x	x	-	-	x	x	x	-	-	-
	Deposited depth	No	-	-	x	-	-	-	x	x	-	-	-	-	-	x	x	x	-	-	-	-	-	-	-	-
Torrent	Running depth	Yes	x	-	-	x	x	x	x	-	-	-	-	-	x	-	-	-	x	-	-	x	x	x	-	-
	Velocity	Yes	-	-	-	x	x	x	-	-	-	-	-	-	-	-	-	-	-	-	-	x	x	-	-	-
	Deposited depth	No	-	-	-	-	-	-	x	x	-	-	-	-	-	x	x	-	-	-	-	-	-	-	x	x

Detailed summaries of both the cited hazard and component parameters are included below in Table 3-4 and Table 3-5.

In these tables, one can observe the current data availability and how these parameters are employed within each component assessment process. With such information it is hoped that practitioners and infrastructure managers might understand the importance of this data and include this required data set in future modeling and collection programs. To improve the data collection efficiency, it is important to remember that hazard and object parameters only need to be collected for objects which can fail in a mode which requires the given parameter data.

Good examples of this as needed basis and the implications it poses for the data collection process are the culvert height and the bridge superstructure width parameters. The culvert height parameter only needs to be collected for culverts located in regions exposed to gravitationally induced hazards (avalanche, landslide, rockfall and torrent). Likewise the bridge superstructure width parameter only needs to be collected for bridges exposed to avalanche and rockfall hazards. By employing similar data collection logic, the process of compiling this data can be significantly simplified.

3.3.6 Component failure assessment conclusion and critique

In this section, a comprehensive failure assessment process has been presented for one of the six considered infrastructure components – bridge, culvert, gallery, retaining wall, roadway and tunnel. For demonstrative purposes, the failure assessment process for the bridge component has been directly presented within this section and the failure assessment process for the additional five

Table 3-5: Component parameter availability and applicable hazards.

	Component Parameter	Available?	Avalanche	Flood	Landslide	Rockfall	Torrent
Bridge	Clearance	Yes	x	x	x	x	x
	Pier foundational depth	No	-	x	x	-	-
	Span length	Yes	x	x	x	x	x
	Superstructure width	Yes	x	-	-	x	-
	Superstructure vertical shear and flexural resistance	No	x	-	-	x	-
	Superstructure buoyancy	No	-	x	-	-	x
	Bearing horizontal & vert. capacity	No	x	x	x	x	x
	Superstructure height	No	x	x	x	x	x
	Superstructure project vertical area	No	x	x	x	x	x
	Superstructure horizontal shear and flexural resistance	No	x	x	x	x	x
	Pier resistance	No	x	-	x	x	x
Clvt	Culvert height	No	x	-	x	x	x
	Designed discharge	Yes	-	x	-	-	-
Gallery	Foundational depth	No	-	x	x	-	-
	Wall height	No	x	-	x	x	-
	Wall shear and flexural resistance	No	x	-	x	x	-
	Wall support shear and flexural resistance	No	x	-	x	x	-
	Wall support spacing	No	x	-	x	x	-
	Roof width	No	x	-	x	x	x
	Roof shear and flexural resistance	No	x	-	x	x	x
	Roof support shear and flexural resistance	No	x	-	x	x	x
	Roof support spacing	No	x	-	x	x	x
	Gallery frame lateral resistance	No	x	-	x	x	-
Retaining wall	Foundational depth	No	-	x	x	-	x
	Wall height	Yes	x	x	x	x	x
	Wall local shear resistance	No	-	-	-	x	-
	Wall global shear and flexural resistance	No	x	x	x	x	x
	Wall support spacing	No	x	x	x	x	x
	Foundational moment resistance	No	x	x	x	x	x
R	Supporting objects intact	No	x	x	x	x	x
Tun	Tunnel entrance location	Yes	-	x	-	-	x
	Tunnel utility elevation	No	-	x	-	-	x

components and the detailed quantitative assessment process for all six components are both included in Appendix A.

The component failure assessment process is intended to be employed not only at a single hazard intensity but rather at a number of potential hazard intensities. Through such an application process, one can identify not only the failure mode at each specific hazard intensity, but also the overall range of each failure mode. Additionally, if there are uncertainties concerning the hazard parameter and/or object parameter intensities, the component failure assessment process should be applied, with each analysis employing sampled probability based parameter data.

Lastly, the current natural hazard and infrastructure component parameter collection practices within Switzerland place two significant limitations on applying these component failure assessment processes.

First, current hazard and infrastructure data collection procedures are respectively the product of existing natural hazard assessment and the infrastructure management requirements. To apply these component failure assessment processes, a number of additional hazard and infrastructure parameter data need to be collected, but approaches exist for minimizing and streamlining the data collection process.

Secondly, the failure assessment process for the bridge, gallery and retaining wall components requires that multiple hazard parameter intensities be determined for a given hazard intensity. Currently, within Switzerland, the natural hazard parameter intensity data is reported separately for each individual hazard parameter. This hinders the process of interrelating different parameters for the same hazard. Thus it is strongly suggested that all hazard parameters for a given hazard be directly correlated or even integrated into a single overarching data set for the given hazard.

3.4 Estimating component failure mode direct consequences and service interruption durations

3.4.1 General Overview

In Section 3.3, a failure assessment process was developed for each infrastructure component. By employing this assessment process, one can identify the failure modes through which specific hazard parameter intensity ranges can cause the given infrastructure object to fail. With the hazard parameter intensity range and the failure mode identified, the next questions are – 'What expected levels of damage does the given hazard parameter intensities cause upon the object?` and 'What are the expected direct and indirect consequences for each expected level of damage?`

This section develops a structured process through which experienced practitioners can employ the component class, failure mode and hazard intensity information provided by applying the failure assessment process to estimate the incurred object direct consequences (i.e. the repair costs) and the service interruption durations, a key aspect to assessing the indirect consequences.

3.4.2 Developing a structured consequence estimation framework

In Section 2.8, a number of potential sources for quantifying an object's direct and indirect consequences resulting from an object failing due to a given hazard were presented. Some of the presented sources included local historical archives, public natural hazard event and infrastructure databases such as StorMe and KUBA, private and semi-private insurance databases such as Swiss-Re and the Swiss Cantonal Insurance Companies, and expert opinions. The source which shows the most promise for estimating direct consequences and service interruption durations of a failed transportation infrastructure object is expert opinion.

The structured estimation framework developed herein has been cut into five stages – the context, the input data, the consequence estimation, the visual presentation of the estimated consequences and the ancillary assumptions. In the first stage, the context stage, the component, hazard and the associated failure mode are all clearly stated. In the input data stage, the required natural hazard and

infrastructure object parameter data required to evaluate the given failure mode are clearly presented.

The third stage, the consequence estimation stage, is the core of this structured estimation framework and has been separated into three parts. In the first part, the infrastructure component is further specified by component classes based on infrastructure size and the unit present value original construction cost is quantified for each component class. The bridge, gallery, roadway and tunnel components, are segmented using the Vector25 component classes presented in Table 2-7, as the infrastructure object value and repair time is assumed to be a function of the object width and level of service. The culvert and retaining walls, whose dimensions are respectively a function of the designed discharge and design absorbable kinetic energy, are segmented discretely along these two design parameters. Thus the culvert component has been segmented into seven classes with the respective arbitrary threshold discharge values of 2.5, 10, 40, 160, 640 and 2560 m^3/s. The retaining wall component has been segmented into six classes by using the retaining wall height threshold value of 2 meters and the design kinetic energy threshold values of 30 and 300 KJ. With each component segmented into classes, the total original installation cost represented in 2008 values is calculated for a unit quantity of each component class. For the bridge, gallery, retaining wall, roadway and tunnel objects, a unit value of 100m length, or the maximum object length if it is less than 100m, and a unit value has been used for the culvert component.

In the second part of the consequence estimation stage, specific reference intensities are identified for each hazard parameter and will be employed to estimate the direct consequences and the service interruption durations. If reference intensities have already been identified for the given hazard parameter (i.e. flood depth intensities of 0.5 and 2 meters) they are employed, but if for hazard parameters not previously segmented, avalanche deposited depth, benchmark values are actively identified (i.e. avalanche deposited depth intensities of 2, 3 and 5 meters).

In the third part, experienced practitioners employ the defined failure mode context, infrastructure component class, and the benchmark hazard parameter intensities to estimate the resulting object direct consequences as a percentage of the total component class value and service interruption durations. These direct consequence and service interruption values are then visually presented in the fourth stage to aid the experienced practitioner in confirming that the provided estimations agree both in magnitude and in trend with their respective experience.

In the last stage of the structured estimation framework, all ancillary and supporting assumptions are definitively stated so that a future practitioner can fully understand any additional information and considerations made by the original experienced practitioner.

Example 3-2: Employ the structured consequence estimation framework to estimate the direct consequences and service interruption durations for a 100 meter length of a highway roadway object exposed to a flood hazard and fails in mode R2 – roadway buried in liquid or debris.

Context:

A highway class roadway object is exposed to a flood hazard and fails in mode R2 – roadway buried in liquid or debris.

Input data:

The natural hazard and infrastructure object data required to estimate the consequences of a highway roadway object failing in mode R2 to a flood hazard are respectively the local flood depth intensity and the geographic position of the roadway object. These two data sets can be respectively obtained from the Swiss Flood hazard identification maps, Section 2.6.3 and the Vector25 data, Section 2.7.1.

Consequence estimation:

Part one: The roadway object has already been identified as a highway component class. The total original construction cost of a 100 meter long highway roadway object is estimated at 300,000 CHF.

Part two: The Swiss National Hazard Mapping initiative has designated two threshold values for static flooding – 0.5 and 2 meters. These threshold values are herein employed as the reference hazard parameter intensities for the flood depth hazard parameter.

Part three: Employing the estimated infrastructure object class original construction cost and the reference hazard parameter intensity values, the hazard parameter intensity specific direct consequences (repair costs) and service interruption durations can be estimated. Such estimated values are presented in Table 3-6.

Table 3-6: Estimated direct consequences and service interruption durations for a highway class roadway object failing in mode R2 to a flood hazard.

Component Class	Intensity (m)	Unit Service Interruption Time (days/100m)	Original Construction Cost (CHF/100m)	% Loss	Unit Loss (CHF/100m)
Highway	0.5	4.00	300,000	5%	15,000
Highway	2	8.00	300,000	15%	45,000

Visual presentation of estimated consequences:

The estimated direct consequences and service interruption durations presented in Table 3-6 are then visually presented in Figure 3-10 to aid the expert practitioner in confirming both the magnitude and trend of the estimations.

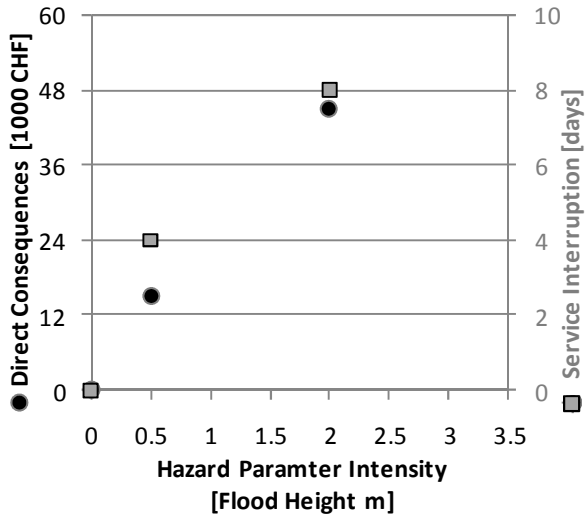

Figure 3-10: Estimated direct consequences and service interruption durations for a highway class roadway object failing in mode R2 to a flood hazard.

Ancillary assumptions:

The developed service interruption durations include the flood initiation, receding of water, debris collection and service restoration times.

3.4.3 Conclusions and critique

By specifying the component class, given hazard parameter intensities, and associated failure mode, experience practitioners have a defined context within which one can formulate general direct consequence and service interruption durations, as shown in Example 3-2. As shown in Sections 3.5.4 and 3.6, these discrete consequence estimations will be, transferred into continuous functions and subsequently employed to assess the vulnerability and risk of an infrastructure object section, continuous object and link.

3.5 Extrapolating from discrete data to continuous functions

3.5.1 General overview and motivation

In Sections 3.2 and 3.4 discrete values have been compiled identifying the local hazard parameter intensity as a function of event return period. Additionally, the exposed object lengths, the direct consequences and the service interruption durations have all been defined as a function of the hazard parameter intensity. To improve the vulnerability and risk calculation accuracy and to ensure that the local hazard parameter intensities directly match the exposed object length, direct consequence and service interruption duration values, continuous functions will be developed from each data set.

Sections 3.5.2 and 3.5.3 present methodologies for defining a probability density function based on the maximum hazard parameter intensity, respectively within a year and a specified time period, from the given discrete hazard parameter intensity data obtained from the geographic hazard parameter-infrastructure object analysis. Section 3.5.4 presents a methodology for employing linear interpolation and extrapolation to develop continuous functions from the discrete exposed object length, direct consequences and service interruption durations. As each methodology is presented, a descriptive example is included to physically demonstrate the proposed methodology.

3.5.2 Maximum hazard parameter intensity probability density function for infrequent events

The first step in transitioning from the discrete data to continuous functions is to represent the return period based hazard parameter intensities affecting the given object with a continuous function, thereby defining the distribution of the maximum annual intensity of hazard parameter *h*. One way to accomplish this is by fitting a probability density function to the return period based hazard data as shown in Example 3-3 (Ang & Tang, 1984).

Example 3-3: Develop the probability density of the maximum annual intensity of hazard parameter *h* by fitting a Gumbel Type I distribution to return period based hazard parameter intensity data.

One way to develop the probability density function specifying the maximum hazard parameter intensity in a given year is to fit a Gumbel Type I distribution to the return period based hazard parameter intensity data obtained from a hazard-object geographic coincident analysis. With such an approach, it is assumed that the hazard occurs infrequently enough that one can consider only the

maximum annual hazard intensity. Additionally, it is assumed that the object is immediately repaired to its current state following the hazard event, thereby conservatively removing changes in object resistance and temporally overlapping hazard events from consideration.

To fit a Gumbel Type I distribution to the return period based hazard parameter intensity data, these data points are first graphed on Gumbel Type I paper, Figure 3-11a. This horizontal logarithmic scale is then transferred from a logarithmic scale to a linear scale by calculating the Gumbel Type I standard extreme variate for each hazard parameter intensity return period, Equation (3.9) (Ang & Tang, 1984).

$$S_i = -\ln\left(-\ln\left(\frac{rp_i - 1}{rp_i}\right)\right) \tag{3.9}$$

Where:

S_i = the Gumbel Type I standard extreme variate for the given return period i [ ]

rp_i = the return period for hazard parameter intensity event i [ ]

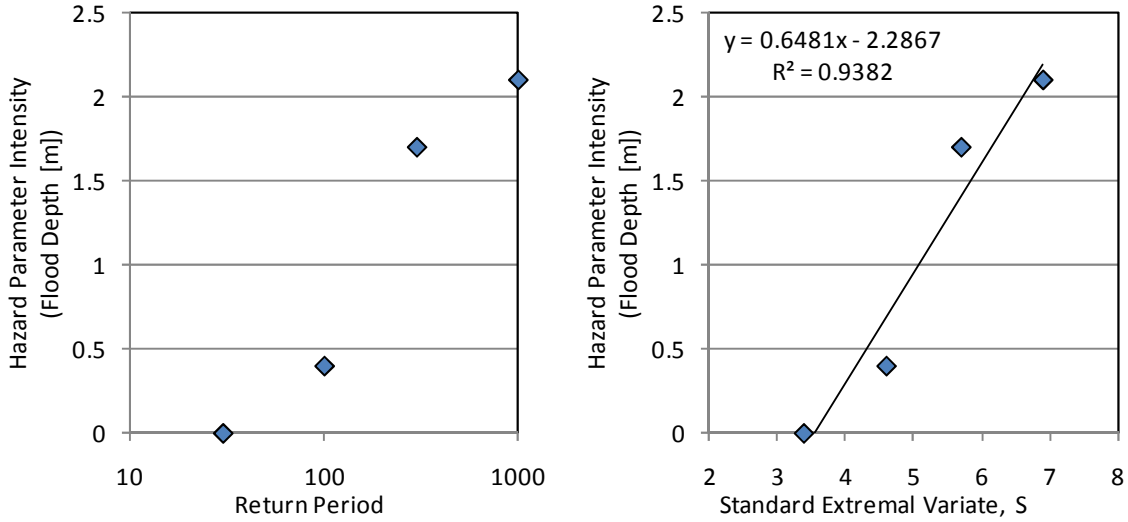

Figure 3-11: Fitting a Gumbel Type I distribution a) Hazard parameter intensity as a function of return period and b) hazard parameter intensity as a function of the standard extremal variate.

With both the axes arranged in a linear scale, Figure 3-11b, establishing a linear regression through the least-squares method, for example, becomes a relatively simple task. The linear equation, written in the format detailed in Equation (3.10), is then directly used to define the Gumbel Type I probability density function of the maximum annual hazard parameter intensity within a given year, following Equations (3.11) and (3.12) (Ang & Tang, 1984, p. 211).

$$f(S) = a \cdot S + b \tag{3.10}$$

$$\alpha_n = \frac{1}{a} \tag{3.11}$$

$$u_n = b \tag{3.12}$$

Where:

X_n = the maximum annual hazard parameter intensity [ ]

α_n = an inverse measure of the dispersion of X_n

u_n = the characteristic largest value of the initial variate X_n

Thus the annual probability density and cumulative distribution functions for the largest hazard parameter intensity in a single year, Equations (3.13) and (3.14), are thus presented in Figure 3-12 (Ang & Tang, 1984, p. 207).

$$f_{X_n}(x) = \alpha_n e^{-\alpha_n (x-u_n)} e^{-e^{-\alpha_n (x-u_n)}} \tag{3.13}$$

$$F_{X_n}(x) = e^{-e^{-\alpha_n (x-u_n)}} \tag{3.14}$$

Where:

$f_{Xn}(X)$ = the probability density function for the annual maximum hazard parameter intensity

$F_{Xn}(X)$ = the cumulative distribution function for the annual maximum hazard parameter intensity

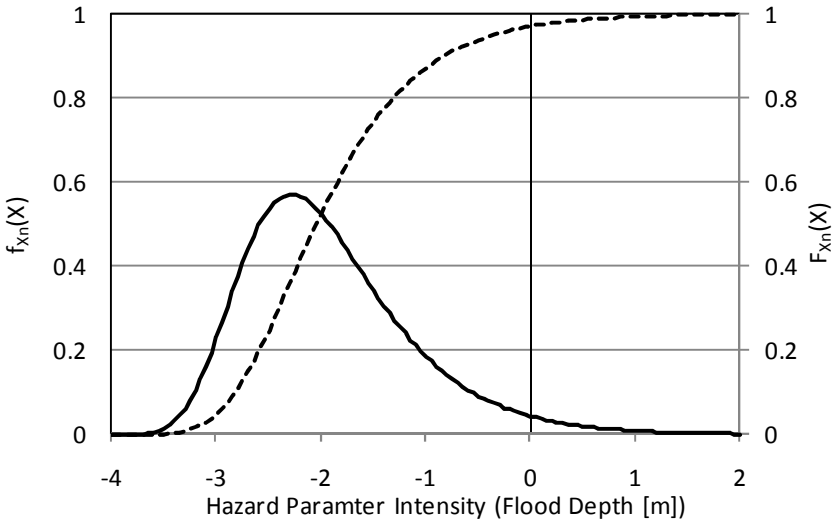

Figure 3-12: Probability density and cumulative distribution functions for the annual maximum hazard parameter intensity.

In Example 3-3, one can observe that the fitted probability density function details the probability of the various potential annual maximum hazard parameter intensities and a significant portion of these hazard parameter intensities have a negative magnitude. Within this work, negative hazard parameter intensities are treated as hazard events which do not occur. Thus it is only the portion of the probability density function to the right of the vertical axis which details the potential hazard parameter intensities.

It should be noted that other functions other than a Gumbel Type I distribution may fit the hazard parameter intensity data better, such as a Gumbel Type III distribution. In such cases, the more applicable function should be employed.

3.5.3 Maximum hazard parameter intensity probability density function for frequent events

The approach presented in Example 3-3, is only valid for infrequently occurring hazards. For hazards which occur more frequently than once every thirty years (i.e. one rock fall event occurring on average once every three years) the probability density function for the maximum hazard parameter intensity within a given year will fail to consider the probability density functions for smaller intensity hazard parameter events within the same year (i.e. the second largest and the third largest hazard

parameter intensities within a given year). To ensure that such data is not lost, the probability density function for shorter time periods should be developed, as is shown in Example 3-4.

Example 3-4: Develop the probability density function for the maximum hazard parameter intensity within a specified time period using Example 3-3 as a base.

Continuing with Example 3-3, the shape of the maximum hazard parameter intensity probability density and cumulative distribution functions for different time perspectives (i.e. the maximum event during one month or six months) for a Gumbel Type I distribution maintains an identical shape to the functions presented in Figure 3-12, but the definitions of the defining constants α and u change as a function of the considered time perspective. These defining constants are redefined with Equations (3.15) and (3.16) (Ang & Tang, 1984, p. 233).

$$\alpha_N = \alpha_n \tag{3.15}$$

$$u_N = u_n + \frac{\ln(N)}{\alpha_n} \tag{3.16}$$

Where:

N = the considered time perspective [years]
α_N = the Gumbel Type I inverse measure of the dispersion of X_N [ ]
u_N = the Gumbel Type I characteristic largest value of the initial variate X_N [ ]
X_N = the maximum hazard parameter intensity during the considered time perspective N [ ]

The probability density and cumulative distribution functions for the maximum expected hazard parameter intensity during a different time perspective (one month, six months) is estimated with Equations (3.17) and (3.18) (Ang & Tang, 1984, p. 232).

$$f_{X_N}(x) = \alpha_N e^{-\alpha_N (x-u_N)} e^{-e^{-\alpha_N (x-u_N)}} \tag{3.17}$$

$$F_{X_N}(x) = e^{-e^{-\alpha_N (x-u_N)}} \tag{3.18}$$

Where:

$f_{XN}(X)$ = the probability density function for the largest hazard parameter intensity during the time perspective N
$F_{XN}(X)$ = the cumulative distribution function for the largest hazard parameter intensity during the time perspective N

3.5.4 Exposed object section length, direct consequence, and service interruption continuous functions

The second step of obtaining continuous functions from discrete values is to fit continuous functions to the assessed exposed object section lengths, the estimated direct consequence and the estimated service interruption durations. The resulting continuous functions will take the general form of Equations (3.19), (3.20) and (3.21).

$$EL_i(x) = f(L_i^{hi}, hi, x) \tag{3.19}$$

$$DC_{m_n}(x) = f(DC_{m_n}^{HI}, HI, x) \tag{3.20}$$

$$SI_{m_n}(x) = g(SI_{m_n}^{HI}, HI, x) \tag{3.21}$$

Where:

$EL_i(x)$ = the exposed object section *i* length as a function of the hazard parameter intensity [m]

$DC_{mn}(x)$ = the direct consequence function fitted to the estimated direct consequences [CHF]

$SI_{mn}(x)$ = the service interruption duration function fitted to the estimated service interruption durations [days]

Example 3-5: Linearly interpolate and extrapolate the exposed object length, the estimated direct consequence and the estimated service interruption duration functions.

One way to develop these continuous functions is by interpolating and extrapolating linear functions between and beyond the determined exposed object section lengths, the estimated direct consequences and service interruption durations. This interpolation and extrapolation process can be conducted with Equations (3.22), (3.23) and (3.24) (Souders, 1966, p. 13).

$$EL_i(x) = \begin{cases} \dfrac{L_i^{hi_0} \cdot x}{hi_0} & x < hi_0 \\ L_i^{hi_0} + (x - hi_0) \cdot \dfrac{L_i^{hi_1} - L_i^{hi_0}}{hi_1 - hi_0} & hi_0 \le x < hi_1 \\ L_i^{hi_1} + (x - hi_1) \cdot \dfrac{L_i^{hi_2} - L_i^{hi_1}}{hi_2 - hi_1} & hi_1 \le x < hi_2 \\ L_i^{hi_2} + (x - hi_2) \cdot \dfrac{L_i^{hi_3} - L_i^{hi_2}}{hi_3 - hi_2} & hi_2 \le x < hi_3 \\ L_i^{hi_3} + K \cdot (x - hi_3) \cdot \dfrac{L_i^{hi_3} - L_i^{hi_2}}{hi_3 - hi_2} & hi_3 \le x_3 \\ L\max & L\max < EL_i(x) \end{cases} \tag{3.22}$$

$$DC_{m_n}(x) = \begin{cases} \dfrac{DC_{m_n}^{HI_0} \cdot x}{HI_0} & (x < HI_0) \\ DC_{m_n}^{HI_0} + (x - HI_0) \cdot \dfrac{DC_{m_n}^{HI_1} - DC_{m_n}^{HI_0}}{HI_1 - HI_0} & (HI_0 \le x < HI_1) \\ DC_{m_n}^{HI_1} + (x - HI_1) \cdot \dfrac{DC_{m_n}^{HI_2} - DC_{m_n}^{HI_1}}{HI_2 - HI_1} & (HI_1 \le x < HI_2) \\ DC_{m_n}^{HI_2} + (x - HI_2) \cdot \dfrac{DC_{m_n}^{HI_3} - DC_{m_n}^{HI_2}}{HI_3 - HI_2} & (HI_2 \le x < HI_3) \\ DC_{m_n}^{HI_3} + (x - HI_3) \cdot F \cdot \dfrac{DC_{m_n}^{HI_3} - DC_{m_n}^{HI_2}}{HI_3 - HI_2} & (x \ge HI_3) \end{cases} \tag{3.23}$$

$$SI_{m_n}(x) = \begin{cases} \dfrac{SI_{m_n}^{HI_0} \cdot x}{HI_0} & \left(x < HI_0\right) \\ SI_{m_n}^{HI_0} + (x - HI_0) \cdot \dfrac{SI_{m_n}^{HI_1} - SI_{m_n}^{HI_0}}{HI_1 - HI_0} & \left(HI_0 \le x < HI_1\right) \\ SI_{m_n}^{HI_1} + (x - HI_1) \cdot \dfrac{SI_{m_n}^{HI_2} - SI_{m_n}^{HI_1}}{HI_2 - HI_1} & \left(HI_1 \le x < HI_2\right) \\ SI_{m_n}^{HI_2} + (x - HI_2) \cdot \dfrac{SI_{m_n}^{HI_3} - SI_{m_n}^{HI_2}}{HI_3 - HI_2} & \left(HI_2 \le x < HI_3\right) \\ SI_{m_n}^{HI_3} + (x - HI_3) \cdot G \cdot \dfrac{SI_{m_n}^{HI_3} - SI_{m_n}^{HI_2}}{HI_3 - HI_2} & \left(x \ge HI_3\right) \end{cases} \quad (3.24)$$

Where:

hi_0, hi_1, hi_2, hi_3 = reference hazard parameter intensities employed within the geographic coincident analysis

HI_0, HI_1, HI_2, HI_3 = reference hazard parameter intensities employed in the consequence estimation

L_i^{hi0}, L_i^{hi1}, L_i^{hi2}, L_i^{hi3} = object section exposed lengths determined from the geographic coincident analysis [m]

L_{max} = the total length of the object section [m]

DC_{mn}^{HI0}, DC_{mn}^{HI1}, DC_{mn}^{HI2}, DC_{mn}^{HI3} = estimated direct consequences for the given component class and failure mode as a function of the hazard parameter intensity [CHF/100m]

SI_{mn}^{HI0}, SI_{mn}^{HI1}, SI_{mn}^{HI2}, SI_{mn}^{HI3} = estimated service interruption durations for the given component class and failure mode as a function of the hazard parameter intensity [days/100m]

K = exposed object section length extrapolation factor (typically 0.333) [ ]

F = estimated direct consequence extrapolation factor (typically 0.333) [ ]

G = estimated service interruption duration extrapolation factor (typically 0.333) [ ]

By extending these discrete values to continuous functions, these three data sets can be easily interrelated. Such a presentation of example estimated direct consequences, estimated service interruption durations and exposed object section lengths as a function of the hazard parameter intensity is made in Figure 3-13.

It is important to mention that this example assumes that the object section exposed lengths, the direct consequences and the service interruption durations follow a linear trend between each data point. As shown in Figure 3-14, variants to this assumption are by all means possible. As there are an infinite number of potential variants and to ensure a consistent approach is uniformly applied across all objects and hazards, within this work it has been assumed that the exposed object section length, direct consequence and service interruption duration continuous functions evolve linearly. Additionally it should be noted that to ensure the extrapolated data points are considered in the subsequent vulnerability and risk analysis but do not automatically dominate the resultant analysis, extrapolation factors significantly less than one (in these cases 0.333) or the maximum potential value are employed.

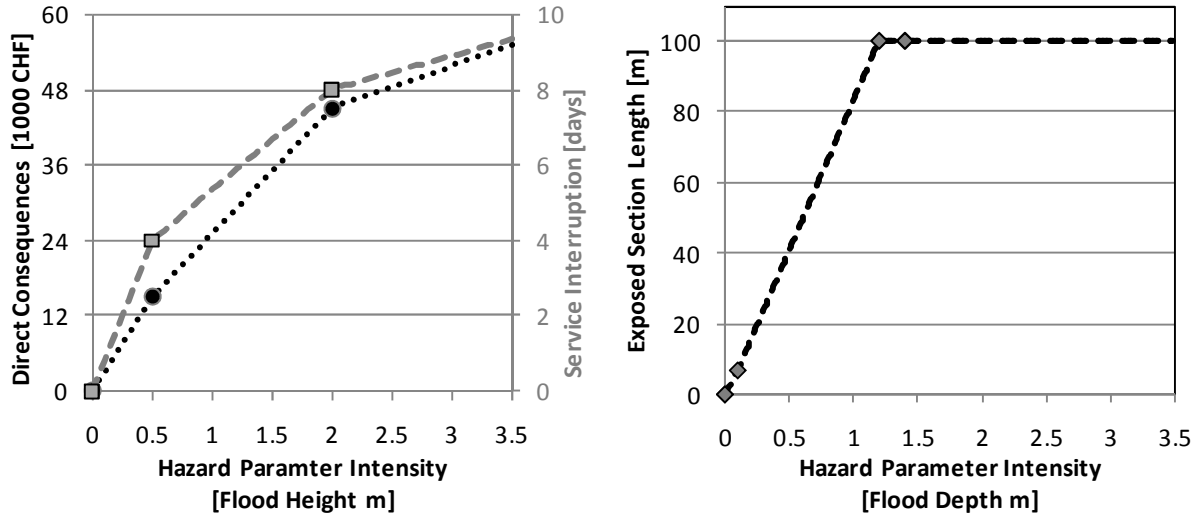

Figure 3-13: a) Linearly interpolated direct consequences and service interruption durations as a function of the hazard parameter intensity, b) Linear interpolated exposed object section length as a function of the hazard parameter intensity.

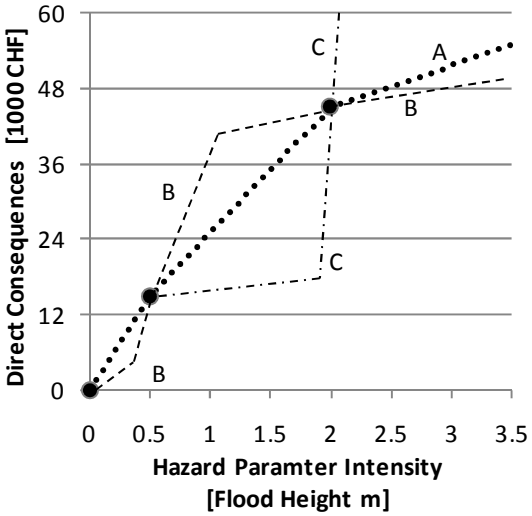

Figure 3-14: Other potential functions which also meet the estimated direct consequences.

3.5.5 Conclusion and critique

In this section, methodologies for developing continuous functions from the local hazard parameter intensity, exposed object section lengths, direct consequences and service interruption duration discrete data complied in Sections 3.2 and 3.3. While these methodologies do provide only a best fit continuous function and they do have a potential to under or over estimate the associated values, as is descriptively shown in Figure 3-14, and thus can add some uncertainty into the calculation process, these continuous functions make the resulting vulnerability and risk assessments possible by ensuring the exposed object section lengths, estimated direct consequences and estimated service interruption durations can all be quantified at the same hazard parameter intensities.

3.6 Quantifying object section vulnerability and risk

3.6.1 Overview

In Sections 3.2 to 3.4, the discrete local hazard parameter intensities, exposed object section lengths, infrastructure object failure mode(s), direct consequences and service interruption durations were all assessed. In Section 3.5, this data has been extrapolated from discrete values to continuous functions. In this section, these continuous functions will be used in conjunction with the general vulnerability and risk Equations (3.8) and (3.7) to assess the vulnerability and risk of an infrastructure object section with respect to a given hazard parameter.

3.6.2 Vulnerability and risk assessment considering a single failure mode

By employing the continuous functions developed within Section 3.5 to further specify the general vulnerability and risk equations introduced in Section 3.1, one arrives at Equations (3.25) and (3.26).

$$Vulnerability^{h}_{i,m_n}(x) = EL_i(x) \cdot (DC_{m_n}(x) + SI_{m_n}(x) \cdot IC_{I,daily}) \tag{3.25}$$

$$Risk^{h}_{i,m_n} = \int_0^{\infty} \left(f_{X_n,i}(x) \cdot EL_i(x) \cdot \left(DC_{m_n}(x) + SI_{m_n}(x) \cdot IC_{I,daily} \right) \right) dx \tag{3.26}$$

Where:

$f_{Xn,i}(X)$ = the probability density function for the largest annual hazard parameter intensity at the considered object section *i*

By distributing the terms in Equations (3.25) and (3.26), one can solve for the direct consequence and service interruption duration vulnerability and risk Equations, as presented in Equations (3.27) to (3.30).

$$Vulnerability^{h}_{i,m_n,DC}(x) = EL_i(x) \cdot DC_{m_n}(x) \tag{3.27}$$

$$Vulnerability^{h}_{i,m_n,SI}(x) = EL_i(x) \cdot SI_{m_n}(x) \tag{3.28}$$

$$Risk^{h}_{i,m_n,DC} = \int_0^{\infty} \left(f_{X_n,i}(x) \cdot EL_i(x) \cdot DC_{m_n}(x) \right) dx \tag{3.29}$$

$$Risk^{h}_{i,m_n,SI} = \int_0^{\infty} \left(f_{X_n,i}(x) \cdot EL_i(x) \cdot SI_{m_n}(x) \right) dx \tag{3.30}$$

Example 3-6: Compute the direct consequence and service interruption duration vulnerability curves and risks for an 100 meter long highway roadway object section given the hazard parameter probability distribution, exposed object section length, direct consequence and service interruption duration continuous functions detailed in Figure 3-12 and Figure 3-13.

Applying Equations (3.27) and (3.28) to assess the direct consequence and service interruption duration vulnerability curves for a 100 meter long highway roadway object section given the hazard and consequence continuous functions detailed in Figure 3-12 and Figure 3-13 yields the direct consequence and service interruption vulnerability functions presented in Figure 3-15.

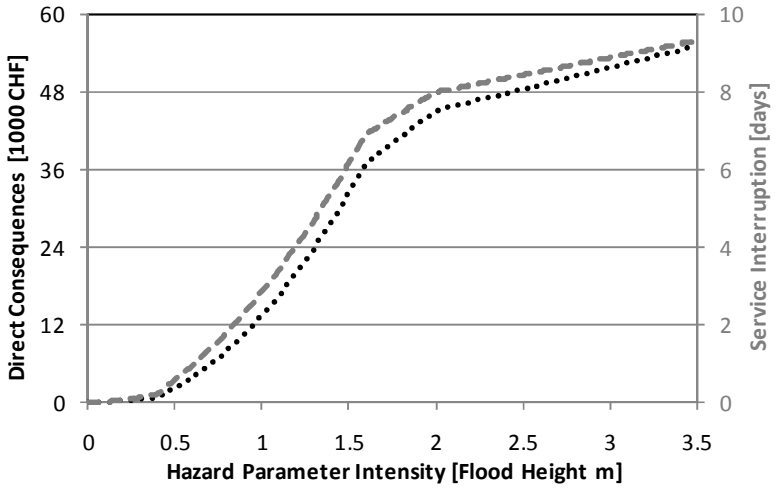

Figure 3-15: Object section direct consequence and service interruption duration vulnerability curves for a given hazard parameter.

Applying Equations (3.29) and (3.30) to assess the direct consequence and service interruption duration risks for a 100 meter long highway roadway object section given the hazard and consequence continuous functions detailed in Figure 3-12 and Figure 3-13 yields, respectively, the direct consequence and service interruption duration annual risks of 240.60 CHF and 0.047 days.

3.6.3 Vulnerability and risk assessment considering multiple failure modes

Section 3.6.2 presents a quantitative vulnerability and risk assessment procedure by assuming there is only one failure mode controlling the object's response to a given hazard across all hazard parameter intensities. Such an assumption is ubiquitously true for the culvert component but can be only potentially true for each of the other five components if given favorable object resistance and applied hazard parameter interactions.

If there are multiple active failure modes across the range of potential hazard parameter intensities or if there are multiple failure modes potentially active for a specific hazard parameter intensity or intensity range, such an assumption is invalid. For the former situation, take the example of a bridge which responds in failure mode B6 (bridge surface submerged in liquid) for medium intensity floods but responds in failure mode B1 (pier foundation is undermined) for high intensity floods. For the latter situation, take the example of a gallery exposed to a high intensity rockfall hazard which can potentially respond in failure modes G4, G5 or G6 as a function of the rockfall impact location.

To consider this first situation, one must first identify the failure modes which are active across a given hazard intensity range, define the intensity range across which each failure mode is dominate and confirm that only one failure mode is active for each potential hazard intensity. If the hazard parameters for the different failure modes are not all identical, one must also relate the individual hazard parameter intensities to the hazard intensity.

With such an assessment conducted, one can then employ the vulnerability and risk Equations (3.25) and (3.26) and the hazard parameter intensity ranges applicable to each failure mode to assess the vulnerability and risk for each individual failure mode. The independent failure mode vulnerabilities and risks are then combined resulting in a composite assessment which considers the influence of each active failure mode. Applying this approach to Equations (3.25) and (3.26) and considering three

failure modes (*p*, *q*, and *r*) with the respective hazard parameter intensity ranges (0 to *a*, *a* to *b* and *b* to *c*) results in Equation (3.31) and (3.32).

$$Vulnerability_i^H(x) = \begin{Bmatrix} EL_i(x)\cdot(DC_{m_p}(x) + SI_{m_p}(x)\cdot IC_{I,daily}) & (x < a) \\ EL_i(x)\cdot(DC_{m_q}(x) + SI_{m_q}(x)\cdot IC_{I,daily}) & (a \le x < b) \\ EL_i(x)\cdot(DC_{m_r}(x) + SI_{m_r}(x)\cdot IC_{I,daily}) & (c > x) \end{Bmatrix} \quad (3.31)$$

$$Risk_i^H = \begin{Bmatrix} \int_0^a \left(f_{X_n,i}(x)\cdot EL_i(x)\cdot\left(DC_{m_p}(x) + SI_{m_p}(x)\cdot IC_{I,daily}\right)\right)dx \\ +\int_a^b \left(f_{X_n,i}(x)\cdot EL_i(x)\cdot\left(DC_{m_q}(x) + SI_{m_q}(x)\cdot IC_{I,daily}\right)\right)dx \\ +\int_b^c \left(f_{X_n,i}(x)\cdot EL_i(x)\cdot\left(DC_{m_r}(x) + SI_{m_r}(x)\cdot IC_{I,daily}\right)\right)dx \end{Bmatrix} \quad (3.32)$$

Where:

Vulnerability$_i^H(x)$ = the vulnerability function of object section *i* with respect to hazard *H* by considering the active failure modes *p*, *q* and *r* [CHF]

Risk$_i^H$ = the risk of object section *i* with respect to hazard *H* by considering the active failure modes *p*, *q* and *r* [CHF]

The second multiple failure mode combination is commonly the result of varying hazard-object interaction geometry and object resistance. These influences can be assessed by iteratively analyzing the hazard and object with the failure assessment process by calling the hazard and object parameter intensities as a function of their respective probability distributions. From such an analysis, one can identify the failure modes which can potentially be active across the hazard parameter intensity range and determine the probability of each failure mode within each hazard parameter intensity range.

Applying this approach to Equations (3.25) and (3.26) and considering three failure modes (*j*, k and *l*) results in Equations (3.33) and (3.34).

$$Vulnerability_i^H(x) = \begin{Bmatrix} P_{i,m_j}^x \cdot EL_i(x)\cdot(DC_{m_j}(x) + SI_{m_j}(x)\cdot IC_{I,daily}) \\ +P_{i,m_k}^x\left(1 - P_{i,m_j}^x\right)\cdot EL_i(x)\cdot(DC_{m_k}(x) + SI_{m_k}(x)\cdot IC_{I,daily}) \\ +P_{i,m_l}^x\left(1 - P_{i,m_k}^x\right)\left(1 - P_{i,m_j}^x\right)\cdot EL_i(x)\cdot(DC_{m_l}(x) + SI_{m_l}(x)\cdot IC_{I,daily}) \end{Bmatrix} \quad (3.33)$$

$$Risk_i^H = \begin{Bmatrix} \int_0^\infty P_{i,m_j}^x \cdot f_{X_n}(x)_i^x \cdot EL_i(x)\cdot\left(DC_{m_j}(x) + SI_{m_j}(x)\cdot IC_{I,daily}\right)dx \\ +\int_0^\infty P_{i,m_k}^x\left(1 - P_{i,m_j}^x\right)\cdot f_{X_n}(x)_i^x \cdot EL_i(x)\cdot\left(DC_{m_k}(x) + SI_{m_k}(x)\cdot IC_{I,daily}\right)dx \\ +\int_0^\infty P_{i,m_l}^x\left(1 - P_{i,m_k}^x\right)\left(1 - P_{i,m_j}^x\right)\cdot f_{X_n}(x)_i^x \cdot EL_i(x)\cdot\left(DC_{m_l}(x) + SI_{m_l}(x)\cdot IC_{I,daily}\right)dx \end{Bmatrix} \quad (3.34)$$

3.6.4 Conclusion

In this section, the general vulnerability and risk Equations (3.8) and (3.7), presented in Section 3.1, have been applied in conjunction with the continuous local hazard parameter intensity probability distribution, exposed object section length, direct consequences and service interruption duration functions developed in Sections 3.2 to 3.4 to assess an object section's vulnerability and risk given a single or multiple failure modes.

3.7 Quantifying continuous object vulnerability and risk

3.7.1 Overview

In Section 3.6, a methodology was presented for employing the continuous functions for the local hazard parameter intensities, the exposed object section lengths, the infrastructure object section failure mode(s), the direct consequences and service interruption durations to assess the vulnerability and risk of an object section. This section presents a methodology for expanding the scope employed in Section 3.6 from the object section to the continuous object which is comprised of numerous object sections all of the same component. For example, Figure 3-16 presents a link which has been cut into continuous objects, labeled with numbers, and each continuous object has been cut into object segments, labeled with letters.

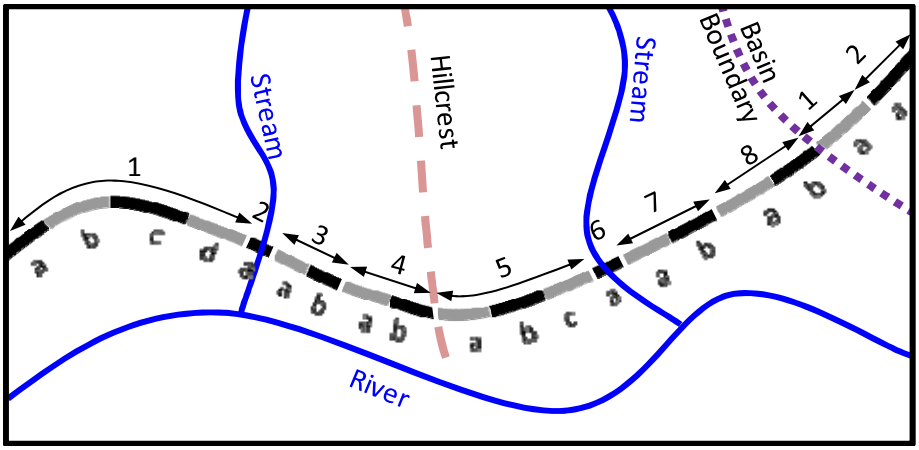

Figure 3-16: Defining continuous objects and object sections.

In widening this scope, there are reconstruction economies of scale and mutually inclusive direct consequences and service interruption durations. These scale effects are considered by developing a continuous object effective exposed length from the combined expose lengths of each object section which considers an infrastructure component and natural hazard specific attenuation factor. This effective exposed continuous object length is then employed in Sections 3.7.3 and 3.7.4 to quantify the continuous object direct consequence and service interruption duration vulnerabilities and risks considering that the continuous infrastructure object responds in a single or multiple failure modes.

3.7.2 Calculating the continuous object effective exposed length

To transition this assessment from the individual object section to the continuous object, one should consider the influence of reconstruction economies of scale and mutually inclusive direct consequences and service interruption durations. Herein, these scale factors are considered by

assessing the effective exposed object section length by formulating an effective exposed length function, the general form of which is presented in Equation (3.35).

$$aEL_i(x) = f(x, RES, EL_i(x), DC^x_{m_n}, SI^x_{m_n}) \tag{3.35}$$

Where:

$aEL_i(x)$ = the effective exposed length of object section *i* as a function of the hazard parameter intensity *x* [m]

RES = reconstruction economies of scale [ ]

Example 3-7: Develop the effective exposed object section length by considering repair economies of scale and mutually inclusive indirect consequences.

On way to assess the effective exposed object section length is to multiply the sum of the linearly interpolated or extrapolated object lengths exceeding 100 meters with an object length attenuation factor. Estimated object length attenuation factors are given in Table 3-7. This effective exposed object section length is then used in place of the exposed object section length in the vulnerability and risk calculations.

Table 3-7: Estimated component length natural hazard specific attenuation factors.

	Natural Hazards				
Components	**Avalanche**	**Flood**	**Landslide**	**Rockfall**	**Torrent**
Bridge	0.80	0.80	0.50	0.80	0.80
Culvert	0.10	0.30	0.30	0.10	0.30
Gallery	0.80	0.25	0.50	0.80	0.30
Retaining Wall	0.80	0.80	0.80	0.80	0.75
Roadway	0.80	0.10	0.50	0.80	0.80
Tunnel	- - -	0.30	- - -	- - -	0.30

To better understand the reasoning behind the component length attenuation factors, consider a 20 meter long roadway object exposed to each of the five hazards. The avalanche, rockfall and torrent hazards occur abruptly and therefore the majority of the service interruption duration is dedicated to repairing the affected object. Therefore, when the object length is extended from 20 meters to 200 meters, the direct consequences and service interruption times significantly increase at a close to proportional rate. Following this argument, component length attenuation factors of 0.80 are reasonable estimates for the avalanche, rockfall and torrent hazards.

The landslide hazard event is a comparatively longer duration event and therefore a larger portion of the service interruption duration is dedicated to the occurrence of the actually event. Additionally, repairing infrastructure objects affected by landslides commonly requires the availability of specialized equipment. Therefore as the effected roadway object length increases from 20 meters to 200 meters, the direct consequences and service interruption duration times are assumed to increase at a less than proportional rate. Thus, herein, the landslide roadway length attenuation factor has been estimated at 0.50.

In considering the last hazard, flood, the occurrence of the event constitutes the majority of the service interruption time and a roadway object affected by a static flood commonly requires only minor debris cleanup. Therefore as the effected object length increases from 20 meters to 200 meters, the direct consequences and service interruption times are herein assumed to only slightly

increase. Thus the flood roadway component effected length attenuation factor has been estimated at 0.10.

The effective exposed object section length calculation can therefore be conducted with Equation (3.36). In Equation (3.36) one can observe that the first 100m of the continuous object is non-attenuated. With each effective exposed object section length assessed, one can determine the effective exposed continuous object length by summing of the effective exposed object section lengths as shown in Equation (3.37).

$$aEL_i(x) = \begin{cases} EL_i(x) & \sum_{i=1}^{n} EL_i(x) \le 100 \\ EL_i(x) \cdot \left(\dfrac{J \cdot \left(\sum_{i=1}^{n} EL_i(x) - 100 \right) + 100}{\sum_{i=1}^{n} EL_i(x)} \right) & \sum_{i=1}^{n} EL_i(x) > 100 \end{cases} \quad (3.36)$$

Where:

J = the applicable component length natural hazard specific attenuation factor [ ]

n = the total number of object sections located within the continuous object *I* [ ]

$$aEL_I(x) = \sum_{i=1}^{n} aEL_i(x) \quad (3.37)$$

Where:

$aEL_I(x)$ = the effective exposed length of continuous object *I* as a function of the hazard parameter intensity [m]

To further contextualize Equation (3.36), consider the example of a 300 year static flood event inundating 4811 meters of a continuous highway object. As earlier introduced, the unit direct consequences and service interruption durations have been estimated for a unit length of 100 meters. Thus if one were to directly apply the exposed object length, the resulting direct consequences and service interruption durations for the flooded section of highway would be more than forty-eight times greater than the direct consequences and service interruption durations for a 100 meter length of roadway. Such a solution would significantly overestimate the direct consequences and service interruption durations by applying Equation (3.36) and summing the individual effective exposed object section lengths, one can assess the effective exposed continuous object length. As presented in Figure 3-17, the effective exposed continuous object length is 571 meters, an eighty-eight percent decrease from the exposed continuous object length but still more than five and a half times greater than the respective estimated indirect consequences for a 100m length of roadway.

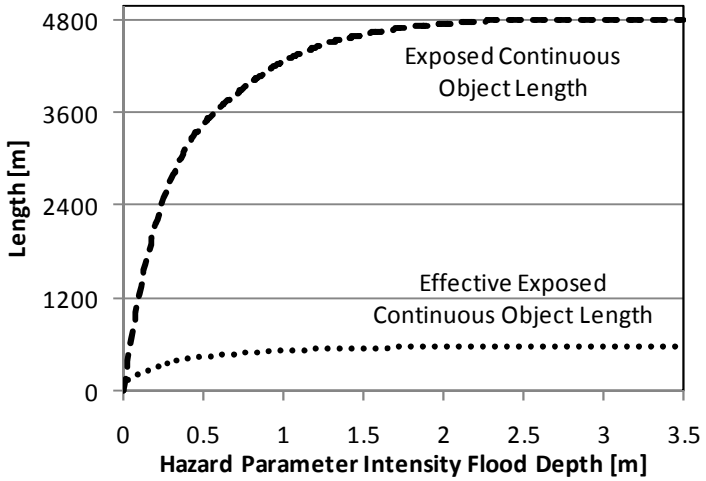

Figure 3-17: Exposed continuous object length and effective exposed continuous object length.

3.7.3 Calculating continuous object vulnerability and risk to a single hazard

The continuous object vulnerability to a given hazard *h*, assuming the entire continuous object responds in the same failure mode, is assessed in a similar manner to Equations (3.27) and (3.28) with the effective exposed continuous object length replacing the exposed object section length, as shown in Equations (3.38) and (3.39).

$$Vulnerability^{h}_{I,m_n,DC}(x) = aEL_I(x) \cdot DC_{m_n}(x) \tag{3.38}$$

$$Vulnerability^{h}_{I,m_n,SI}(x) = aEL_I(x) \cdot SI_{m_n}(x) \tag{3.39}$$

Where:

$Vulnerability_{I,DC,mn}{}^{h}$ = the continuous object *I* direct consequence vulnerability with respect to the hazard parameter *h* assuming each object section responds in the identical failure mode m_n [CHF]

$Vulnerability_{I,SI,mn}{}^{h}$ = the continuous object *I* service interruption duration vulnerability with respect to the hazard parameter *h* assuming each object section responds in the identical failure mode m_n [CHF]

The annualized continuous object risk to the given hazard over a specified reference period, assuming the continuous object is exposed to a single hazard, is assessed by summing the individual object section effective annualized risk. In the general sense, an object risk to a given hazard parameter can be computed with Equations (3.40) and (3.41).

$$Risk^{h}_{I,DC} = \sum_{i=0}^{n}\left[\int_{0}^{\infty} f_{X_n,i}(x) \cdot aEL_i(x) \cdot DC_{m_n} dx\right] \tag{3.40}$$

$$Risk^{h}_{I,SI} = \sum_{i=1}^{n}\left[\int_{0}^{\infty} f_{X_n,i}(x) \cdot aEL_i(x) \cdot SI_{m_n} dx\right] \tag{3.41}$$

Where:

$Risk_{I,DC}{}^{h}$ = the annual continuous object *I* direct consequence risk with respect to the hazard parameter *h* [CHF]

$Risk_{I,SI}^{h}$ = the annual continuous object *I* service interruption duration risk with respect to the hazard parameter *h* [days]

Example 3-8: Quantify the direct consequence and service interruption duration annualized risks given the data presented in Example 3-3 and Example 3-7.

From the information presented earlier in Example 3-3 and Example 3-7, one can employ Equations (3.40) and (3.41) to evaluate the annualized continuous object risk to given hazard parameter. In this example, the road object annualized direct consequence and service interruption duration risks to a static flood hazard are respectively 803 CHF/year and 0.181 days/year.

3.7.4 Calculating continuous object risk to multiple hazards

With the risks evaluated independently for a given continuous object exposed to multiple hazards, these individual hazard-continuous object risks are combined into a multi-hazard continuous object risk. The simplest approach is to just assume that all the hazards are mutually exclusive. With such an assumption, one can employ Equation (3.42) to assess the multi-hazard object risk.

$$Risk_I = \sum_{z=1}^{5} R_I^{H_z} \tag{3.42}$$

Where:

$Risk_I$ = the multi-hazard continuous object risk [CHF]
R_I^{Hz} = the individual hazard specific object risks [CHF]

While such an approach is simple and straightforward, it overestimates the continuous object's risk exposure by assuming that all hazards are mutually exclusive, for any temporally coinciding hazards would be counted twice. While such an assumption may be valid for the avalanche hazard, which is the only hazard to occur in the depths of winter, such an assumption is a gross simplification for correlated hazards like flood and torrent hazards. Hazard temporal coincidence is herein assumed to be predominately the result of one hazard triggering another hazard, such as a flood inducing a torrent, or both hazards being triggered by a tertiary instigator, such as a flood and landslide being triggered by excessive localized rainfall. To evaluate the resulting multi-hazard-object risk, a correlation-based calculation procedure has been developed.

Assuming the effects of each hazard on the respective continuous object have been completely captured in the object risk evaluation process, the avalanche hazard is not correlated to any of the other four hazards and the hazard correlation factors among the remaining five hazards can be estimated or evaluated, one can employ Equation (3.43) to estimate the total multi-hazard object risks.

$$\left\{\begin{array}{c} Risk_I = R_I^{H_1} + R_I^{H_i} + R_I^{H_j}\left(1-C_{i,j}\right) + R_I^{H_k}\left(1-C_{i,k}\right)\left(1-C_{j,k}\right) \\ +R_I^{H_l}\left(1-C_{i,l}\right)\left(1-C_{j,l}\right)\left(1-C_{k,l}\right) \end{array}\right\} \quad \left\{\begin{array}{c} R_I^{H_i} \geq R_I^{H_j} \\ \geq R_I^{H_k} \geq R_I^{H_l} \end{array}\right\} \tag{3.43}$$

Where:

R_I^{H1} = the continuous object *I*'s risk to avalanche hazards [CHF]
R_I^{Hi}, R_I^{Hj}, R_I^{Hk}, R_I^{Kl} = the continuous object *I*'s risk to the four hazards (flood, landslide rockfall, torrent) are called in decreasing risk magnitude [CHF]

$C_{A,B}$ = the correlation factor between the greater magnitude hazard risk *A* and the lesser magnitude hazard risk *B* [ ]

In developing Equation (3.43), it has been assumed that the magnitude of an object's risk to each of the four non-avalanche hazards can be used as a proxies for determining the causality chain position of the various hazards. While this may not be a correct assumption in all instances, it will ensure that the computed multi-hazard object risk is conservatively assessed.

Example 3-9: Develop an example object hazard correlation matrix.

A key element of Equation (3.43) are the hazard correlation factors. Herein the hazard correlation factors have been estimated and the resulting hazard correlation factors for a given pair of hazards are detailed in Table 3-8.

Table 3-8: Example component hazard correlation matrix.

	Avalanche	**Flood**	**Landslide**	**Rockfall**	**Torrent**
Avalanche	- - - -	0.00	0.00	0.00	0.00
Flood	0.00	- - - -	0.30	0.05	0.30
Landslide	0.00	0.30	- - - -	0.05	0.40
Rockfall	0.00	0.05	0.05	- - - -	0.05
Torrent	0.00	0.30	0.40	0.05	- - - -

The hazard correlation matrix, Table 3-8, estimates the probability of two hazards temporally coinciding with the instigator (larger magnitude risk) and instigated (lesser magnitude risk) hazards respectively as row and column titles. While the correlation factors presented in Table 3-8 have been purely estimated, the procedure detailed herein can be further adapted to the given component failure mode or environment by employing regional or even environmental-specific correlation factors.

In Table 3-8, one can observe that it has been assumed that there is no correlation between the avalanche hazard and the flood, landslide, rockfall and torrent hazards as it is assumed that the avalanche hazard is temporally mutually exclusive from the four other hazards. Furthermore, correlation factors between single hazard risks (avalanche hazard risk correlated with an additional avalanche hazard risk) have not been included in Table 3-8 as it has been assumed that the effects of each hazard on the respective object have been completely captured in the object section and continuous object risk evaluation process.

Applying this multi-hazard-object risk evaluation process to an abstract case of a continuous object exposed to the five hazards (avalanche, flood, landslide, rockfall and torrent) with respective direct consequence risk magnitudes of CHF 3,500, CHF 17,325, CHF 4,425, CHF 150 and CHF 24,350. It can be observed that of the four non-avalanche risks, the torrent risk is the largest risk followed by the flood, the landslide and the rockfall risks in descending order. Thus from Equation (3.43) and Table 3-8, the multi-hazard continuous object risk is computed following:

$$Risk_I = \begin{matrix} 3500 + 24350 + 17325(1-0.30) + 4425(1-0.40)(1-0.30) \\ +150(1-0.05)(1-0.05)(1-0.05) \end{matrix}$$

Thus the multi-hazard object direct consequence risk considering potential hazard correlations is CHF 41,965. If all hazards were assumed to be mutually exclusive following Equation (3.42), the resulting multi-hazard object risk would be CHF 49,750, an 18.5% overestimation.

3.7.5 Conclusion and critique

In this section, the scope of analysis is expanded from a single object section to a continuous object comprised of multiple object sections. In making this transition, post-failure reconstruction economies of scale and mutually inclusive direct consequences and service interruption durations are considered by assessing an effective exposed continuous object length. The effective exposed continuous object length is developed by multiplying the continuous object length exceeding 100 meters by a hazard specific attenuation factor. This effective exposed continuous object length is in turn employed to assess the direct consequence and service interruption vulnerability and risk of a continuous object responding in a single and in multiple failure modes to a given hazard. These risk values will in turn be employed in Section 3.8 to quantify the risk of a link composed of multiple continuous objects.

3.8 Quantifying link risk

3.8.1 Introduction and overview

In Sections 3.7.3 and 3.7.4 the methodology for assessing the risk of failure of a continuous object with respect to a single and to multiple hazards is formulated. In Section 3.8, the methodology for quantifying risk of failure of a link comprised of multiple continuous objects exposed to multiple hazards is developed by considering the fact that a functional failure of a continuous object or object section within a link is a functional failure of the entire link. Thus, link level service interruption duration risks are developed by considering the geographic-based correlation between continuous object service interruption duration risks.The developed methodology is used to quantify the total risk of failure of a given link with respect to multiple natural hazards.

3.8.2 Calculating multi-hazard, multiple continuous object link risk[4]

Expanding the risk assessment methodology from a single continuous object exposed to multiple hazards to a single link comprised of multiple continuous objects each exposed to multiple hazards introduces an additional aspect – geography-based hazard correlations. For direct cost risks, it is herein assumed that all hazard specific object risks are mutually exclusive and thus the link direct consequences risk can be assessed with Equation (3.44).

$$Link\_Risk_{DC} = \sum_{I=1}^{n} \sum_{H=0}^{5} Risk_{I,DC}^{H} \tag{3.44}$$

Where:

$Link\_Risk_{DC}$ = the link direct consequence risk due to all hazard continuous object risks [CHF]
$Risk_{I,DC}^{H}$ = continuous object *I*'s direct consequence risk exposure to hazard *H* [CHF]

For service interruption duration risks, a service interruption incurred by any object within the link is a service interruption incurred by the entire link. Therefore, when considering service interruption duration risks, one must consider geography-based hazard correlations. As shown in Figure 3-18, this process of considering geography-based hazard correlations begins by first assigning the continuous

[4] In this section, the service interruption risks of objects contained within a given geographic region (i.e. slope, gully, basin, link) are attributed directly to the respective region for notation simplification purposes.

objects within a given link along a three level hierarchical classifications – drainage basins, gullies and slopes.

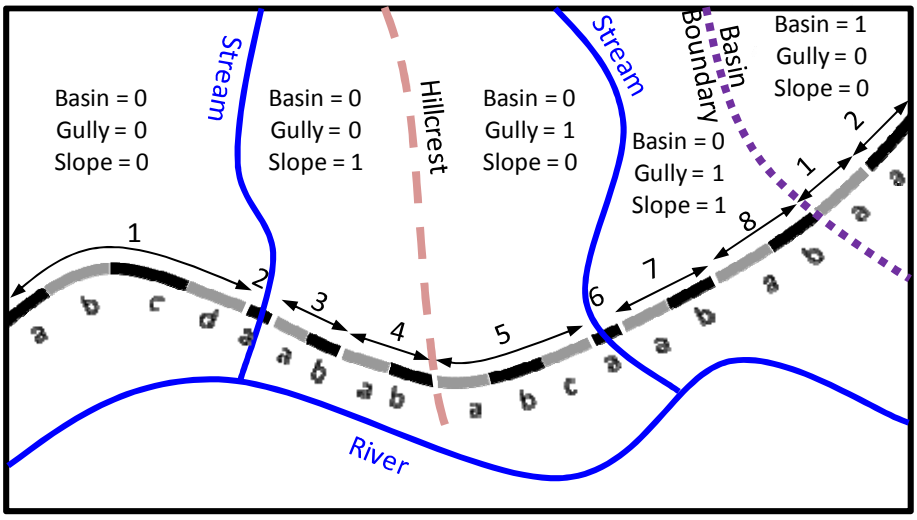

Figure 3-18: Geographically-based object classifications.

The correlation between hazards are either produced by two or more hazards occurring at the same time or by one hazard instigating an additional hazard(s) (e.g. a flood causing a torrent). The causality chain between a set of hazards is a product of the local hazard parameter intensities, topography, and geology. As the feasibility of developing causality chains and correlation matrices for each location is questionable, it is herein assumed that inter-hazard correlations are a product of the relative geographic level (slope, gully and drainage basins).

With objects geographically assigned, hazard correlation matrices for each geographic hierarchical level (slope, gully, basin and multi-basin) must be assessed or estimated. Once formulated, these correlation matrices can be employed in conjunction with Equation (3.45) to assess how the estimated hazard correlations between the inferior hierarchical level continuous objects' and object sections' hazard specific risks combine to formulate a superior hierarchical level continuous objects' and object section's hazard specific risk.

$$\left\{\begin{array}{l} R^{1}_{I,SI}=\sum_{i=1}^{n}\left[\left(R^{1}_{i,SI}\right)\left(1-LC^{1,1}\right)\right]+R^{1}_{j,SI}\cdot LC^{1,1} \\ R^{k}_{I,SI}=\sum_{i=1}^{n}\left[R^{k}_{i,SI}\left(1-LC^{k,k}\right)\right]+R^{k}_{q,SI}LC^{k,k} \\ R^{l}_{I,SI}=\left(\sum_{i=1}^{n}\left[R^{l}_{i,SI}\left(1-LC^{l,l}\right)\right]+R^{l}_{r,SI}LC^{l,l}\right)\left(1-LC^{k,l}\right) \\ R^{m}_{I,SI}=\left(\sum_{i=1}^{n}\left[R^{m}_{i,IN,SI}\left(1-LC^{m,m}\right)\right]+R^{m}_{s,SI}LC^{m,m}\right) \\ \qquad\times\left(1-LC^{k,m}\right)\left(1-LC^{l,m}\right) \\ R^{p}_{I,SI}=\left(\sum_{i=1}^{n}\left[R^{p}_{i,IN,SI}\left(1-LC^{p,p}\right)\right]+R^{p}_{t,SI}LC^{p,p}\right) \\ \qquad\times\left(1-LC^{k,p}\right)\left(1-LC^{l,p}\right)\left(1-LC^{m,p}\right) \end{array}\right\} \left\{\begin{array}{c} i\geq 2 \\ R^{1}_{j,SI}=\max\left\{R^{1}_{i,SI}\right\} \\ R^{k}_{q,SI}=\max\left\{R^{k}_{i,SI}\right\} \\ R^{l}_{r,SI}=\max\left\{R^{l}_{i,SI}\right\} \\ R^{m}_{s,SI}=\max\left\{R^{m}_{i,SI}\right\} \\ R^{p}_{t,SI}=\max\left\{R^{p}_{i,SI}\right\} \\ R^{k}_{q,SI}\geq R^{l}_{r,SI}\geq R^{m}_{s,SI}\geq R^{p}_{t,SI} \end{array}\right\} \qquad (3.45)$$

Where:

$R_{I,SI}^{1}$ = superior hierarchical level service interruption duration risk with respect to avalanche hazard [days]

$R_{I,SI}^{k}$ = superior hierarchical level service interruption duration risk with respect to hazard *k* [days]

$R_{i,SI}^{'1}$ = inferior hierarchical level continuous object and object section service interruption duration risk with respect to the avalanche hazard [days]

$R_{j,SI}^{'1}$ = maximum inferior hierarchical level continuous object and object section service interruption duration risk with respect to the avalanche hazard [days]

$R_{q,SI}^{'k}$ = maximum inferior hierarchical level continuous object and object section service interruption duration risk with respect to hazard *k* [days]

k, *l*, *m*, *p* = hazard reference variables

j, *q*, *r*, *s*, *t* = maximum inferior hierarchical level continuous object and object section service interruption duration risk reference variables with respect to each hazard

n = the number of continuous objects and object sections in the inferior hierarchical level

$LC^{A,B}$ = the correlation factor specifying the correlation between the initial hazard *A* and the secondary hazard *B*, both within the same inferior hierarchical level

If there is only one continuous object or object section within the inferior hierarchical level, the assessed continuous object or object section's hazard specific service interruption duration risks are transferred directly to the superior hierarchical level, as shown in Equation (3.46).

$$\left\{\begin{array}{l} R_{I,SI}^{1} = R_{i,SI}^{1} \\ R_{I,SI}^{2} = R_{i,SI}^{2} \\ R_{I,SI}^{3} = R_{i,SI}^{3} \\ R_{I,SI}^{4} = R_{i,SI}^{4} \\ R_{I,SI}^{5} = R_{i,SI}^{5} \end{array}\right\} \quad \{i = 1\} \tag{3.46}$$

With the service interruption duration risks transferred to the highest geographical hierarchical level, the link risk can be assessed by summing the individual hazard risks as is shown in Equation (3.47).

$$Link\_Risk_{SI} = \sum_{H=1}^{5} R_{SU,SI}^{H} \tag{3.47}$$

Where:

$Link\_Risk_{SI}$ = link risk level service interruption duration risk with respect to all five hazards [days]

The process of developing a hazard correlation matrix for each geographic hierarchical level is presented in Example 3-10 and in Example 3-11 these hazard correlation matrices are employed to assess the link service interruption duration risks from continuous object service interruption duration risks.

Example 3-10: Estimate the hazard correlation matrix for each geographic hierarchical level.

Slope risk correlation matrix

The first matrix, Table 3-9, details the estimated correlation between different hazard specific object service interruption duration risks located within the same slope, Figure 3-19. As in Table 3-8, the

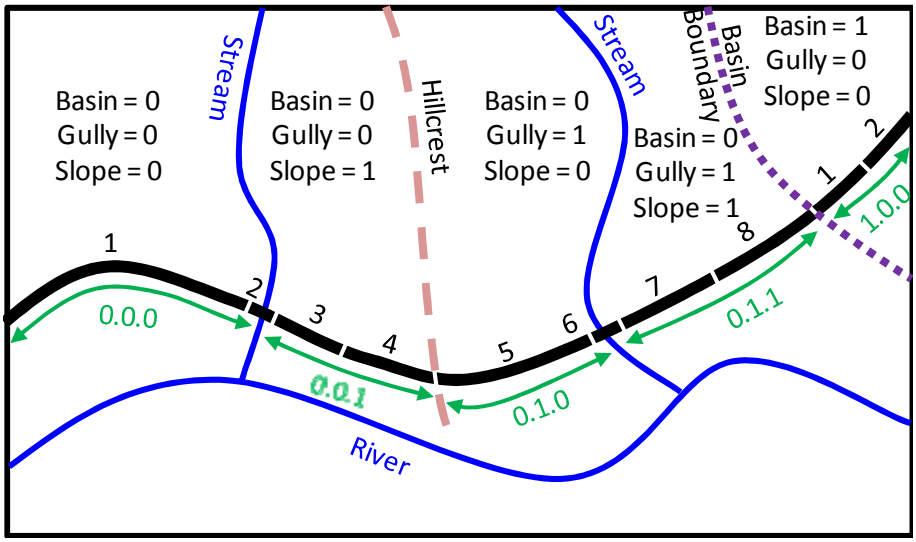

Figure 3-19: Geographically-based object assessment – hazard specific object service interruption duration risks located within the same slope.

Instigator (larger magnitude risk) hazard and the instigated (smaller magnitude risk) hazard are located along the rows and columns respectively. In comparing Table 3-9 to Table 3-8, one can observe that the two matrices are almost identical, but diagonal values dealing the estimated correlation between identical hazards (i.e. two flood hazards each affecting two different objects at the same time) have been added to Table 3-9.

Table 3-9: Example estimated correlation matrix for hazard specific object service interruption duration risks located within the same slope.

	Avalanche	Flood	Landslide	Rockfall	Torrent
Avalanche	0.90	0.00	0.00	0.00	0.00
Flood	0.00	1.00	0.30	0.05	0.30
Landslide	0.00	0.30	0.95	0.05	0.40
Rockfall	0.00	0.05	0.05	0.10	0.05
Torrent	0.00	0.30	0.40	0.05	0.90

Table 3-9 can then be employed to determine the hazard specific risks affecting each slope. As in determining the multi-hazard object risk, the sequence in which hazards are designated as instigator hazards has been assumed to be directly related to the maximum of each hazard specific object service interruption duration risk magnitude. Thus the risk of the objects located within a given slope with respect to each hazard can be evaluated from the hazard specific object risks by applying Equation (3.45) and the estimated correlation factors from Table 3-9.

Gully risk correlation matrix

With the hazard specific service interruption duration risk evaluated for each slope within the link, Figure 3-20, the focus then shifts to evaluating the hazard specific service interruption duration risk for each gully. To accomplish this, an estimated correlation matrix for the hazard specific slope service interruption duration risks within the same gully has been developed Table 3-10. In comparing Table 3-10 to Table 3-9, the object risk correlation matrix, it can be seen that the correlation factors for all the hazard specific risks in Table 3-10 are lower, with the landslide risk correlation factors being significantly lower. This significant reduction in the landslide risk correlation has been made to reflect the assumption that the landslide occurrence is the product of localized

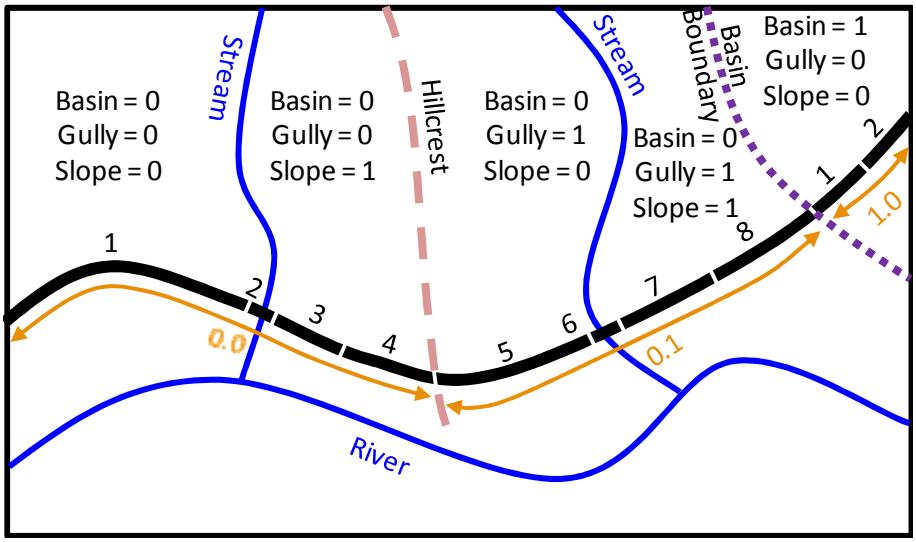

Figure 3-20: Geographically-based object assessment - hazard specific object service interruption duration risks located within the same gully.

parameters (e.g. local topography, geology, water concentration). With the slope risk correlation matrix estimated, the hazard specific risk exposure of a given gully can be evaluated with Equation (3.45) or Equation (3.46) by employing the slope as the inferior hierarchical level and the gully as the superior hierarchical level.

Table 3-10: Example estimated correlation matrix for hazard specific slope service interruption duration risks within the same gully.

	Avalanche	Flood	Landslide	Rockfall	Torrent
Avalanche	0.80	0.00	0.00	0.00	0.00
Flood	0.00	0.95	0.20	0.05	0.30
Landslide	0.00	0.20	0.40	0.00	0.25
Rockfall	0.00	0.05	0.00	0.05	0.02
Torrent	0.00	0.30	0.25	0.02	0.85

Basin risk correlation matrix

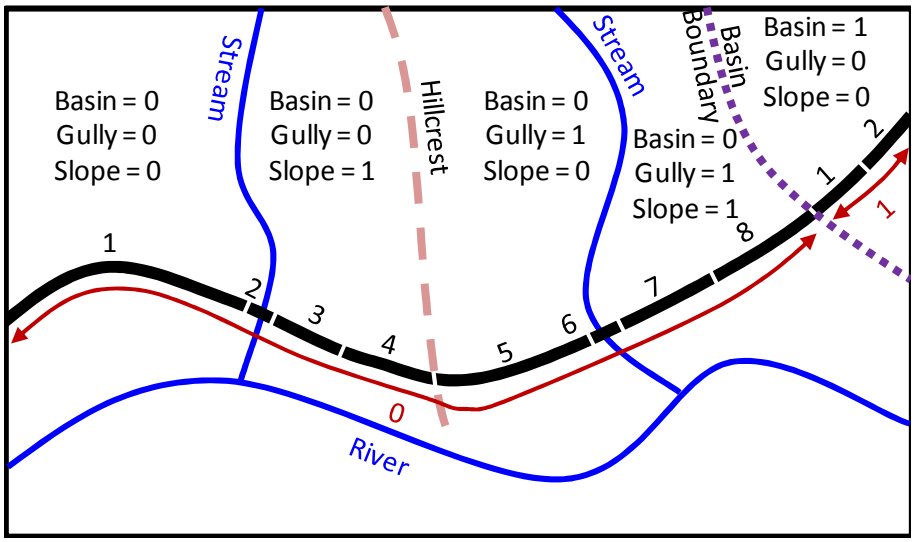

Figure 3-21: Geographically-based object assessment - hazard specific object service interruption duration risks located within the same basin.

With the hazard specific service interruption duration risks evaluated for each gully within the link, Figure 3-21, the focus then shifts to evaluating the hazard specific risks for each basin. This is accomplished by first estimating a correlation matrix for hazard specific gully risks located within the same basin, Table 3-11. In comparing the slope risk correlation and the object risk correlation matrices, Table 3-11 and Table 3-10, it can be seen that all of the hazard correlation factors are lower in Table 3-11, reflecting the increasing geographical distance between hazards, with the avalanche and torrent specific risk correlation factors significantly decreased. This reduction is due to the assumption that avalanche and torrent hazards are predominately instigated by intense localized precipitation and thus when one compares two different gullies, the occurrences of intense localized precipitation, inducing avalanche and torrent hazards will be only partially correlated.

Table 3-11: Example estimated correlation matrix for hazard specific gully service interruption duration risks within the same basin.

	Avalanche	Flood	Landslide	Rockfall	Torrent
Avalanche	0.30	0.00	0.00	0.00	0.00
Flood	0.00	0.60	0.05	0.00	0.10
Landslide	0.00	0.05	0.05	0.00	0.02
Rockfall	0.00	0.00	0.00	0.00	0.00
Torrent	0.00	0.10	0.02	0.00	0.20

With the gully service interruption duration risk correlation matrix formulated, one can calculate the hazard specific basin risks by employing Equations (3.45) or (3.46) and by defining the gully and the basin respectively as the inferior and superior hierarchical levels.

Multi-basin risk correlation matrix

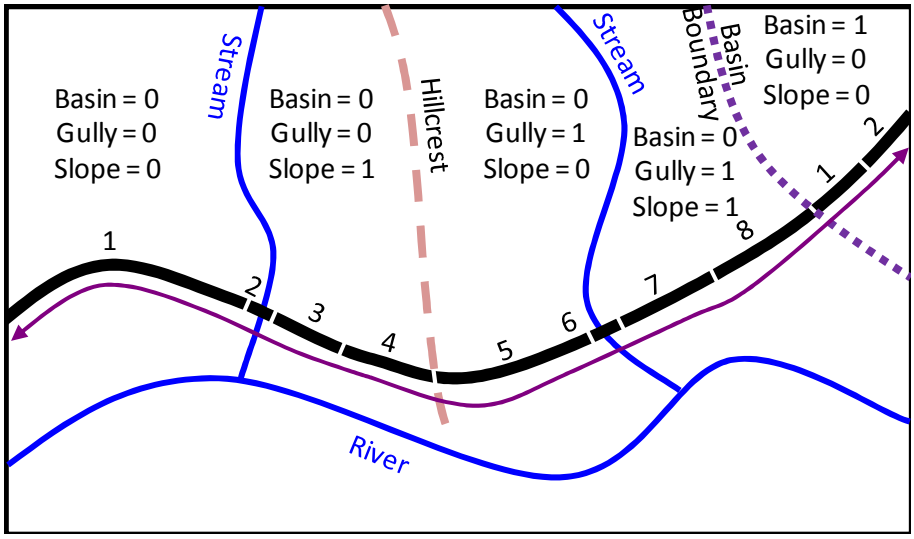

Figure 3-22: Geographically-based object assessment - hazard specific object service interruption duration risk located within the same link.

With the hazard specific service interruption duration risks evaluated for each basin within the link, Figure 3-22, the focus then shifts to evaluating the total hazard specific risks. To accomplish this, one must first estimate a correlation matrix for hazard specific service interruption duration risks located in different basins, Table 3-12. In comparing Table 3-12 to Table 3-11, respectively the basin and gully risk correlation matrices, one can observe that hazard specific risk correlation factors are further decreased to approaching or equal to zero. Most notably, the flood hazard risk correlation factor

which had maintained a rather high correlation factor for the gully correlation matrix, is assumed to be significantly reduced reflecting the assumption that floods in different drainage basins are only slightly correlated.

Table 3-12: Example estimated correlation matrix for hazard specific basin service interruption duration risks.

	Avalanche	Flood	Landslide	Rockfall	Torrent
Avalanche	0.10	0.00	0.00	0.00	0.00
Flood	0.00	0.15	0.00	0.00	0.02
Landslide	0.00	0.00	0.00	0.00	0.00
Rockfall	0.00	0.00	0.00	0.00	0.00
Torrent	0.00	0.02	0.00	0.00	0.05

With the hazard specific basin service interruption duration risk correlation matrix estimated, one can evaluate the total hazard specific link risk by employing Equation (3.45) or (3.46) and by defining the basin and the link respectively as the inferior and superior hierarchical levels.

Example 3-11: Calculate the link service interruption duration risks of a link composed of 10 continuous objects in a geographical configuration detailed in Figure 3-18 and having the assessed service interruption duration risks detailed in Table 3-13.

Table 3-13: Assessed hazard specific object service interruption risks.

	Link Segment	Avalanche	Flood	Landslide	Rockfall	Torrent
Continuous Objects	0.0.0.1	0.180	1.200	2.50	0.175	2.100
	0.0.0.2	0.000	1.750	0.000	0.000	3.285
	0.0.1.3	0.560	0.430	0.765	0.425	0.625
	0.0.1.4	1.500	0.135	2.250	1.185	0.295
	0.1.0.5	3.500	0.125	2.850	1.650	0.180
	0.1.0.6	0.000	1.950	0.195	0.000	3.765
	0.1.1.7	0.465	0.835	1.250	0.380	1.540
	0.1.1.8	2.255	0.245	1.855	0.715	0.445
	1.0.0.1	1.975	0.000	1.665	0.435	0.000
	1.0.0.2	0.495	0.255	0.065	0.185	0.365

In Figure 3-18, Example 3-10 and Table 3-14, one can observe that the process of calculating the link service interruption duration risk will have to pass through each geographic hierarchical level following the schematic presented in Figure 3-23.

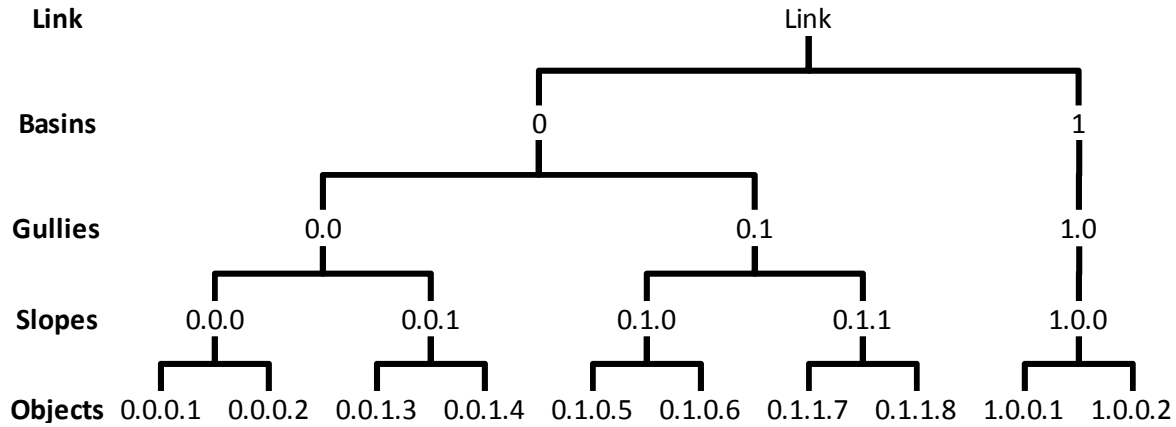

Figure 3-23: Schematic for assessing the link service interruption duration risk.

Conducting this assessment by employing Equation (3.45), Equation (3.46) and the correlation matrices detailed in Example 3-10 yields the results presented in Table 3-14.

Table 3-14: Hazard specific service interruption duration risks for each hierarchical level.

	Link Segment	Avalanche	Flood	Landslide	Rockfall	Torrent
Slopes	0.0.0	0.180	1.225	0.105	0.150	3.495
	0.0.1	1.556	0.200	2.288	1.489	0.373
	0.1.0	3.500	0.956	1.716	1.415	3.783
	0.1.1	2.302	0.409	1.918	0.906	0.951
	1.0.0	2.025	0.119	1.668	0.571	0.208
Gullies	0.0	1.592	0.657	1.763	1.599	3.551
	0.1	3.960	0.519	2.210	2.230	3.926
	1.0	2.025	0.119	1.668	0.571	0.208
Basins	0	5.075	0.739	3.808	3.829	6.766
	1	2.025	0.119	1.668	0.571	0.208
Link	- - - -	6.897	0.823	5.476	4.401	6.964

Thus, summing the hazard specific link service interruption duration risks yields a link service interruption duration risk of 24.6 days. If this calculation was conducted assuming that all of the hazard specific object service interruption duration risks were mutually exclusive, the resulting link service interruption duration risk would have been assessed as 46.8 days, an increase of 90.3%.

3.8.3 Computing link total equivalent financial link risk exposure

The last step in the risk calculation process is the quantification of the total equivalent financial link risk exposure. This is conducted by summing the direct consequence risk and the service interruption duration risk multiplied by the daily financial valuation of the losses and additional expenditures incurred from transport and societal related impacts of infrastructure link *l*'s reduced functional performance, Equation (3.48).

$$Link\_Risk = Link\_Risk_{DC} + Link\_Risk_{SI} \cdot IC_{I,daily} \tag{3.48}$$

Where:

Link_Risk = the financial equivalent link risk exposure considering direct and indirect consequences [CHF]

Example 3-12: Assess the total equivalent financial link risk exposure for the link detailed in Figure 3-18 with hazard specific direct consequence risks detailed in Table 3-15, hazard specific service

Table 3-15: Assessed hazard specific continuous object direct consequence risks.

	Link Segment	Avalanche	Flood	Landslide	Rockfall	Torrent
Continuous Objects	0.0.0.1	3,250	8,765	13,850	1,330	11,255
	0.0.0.2	0	7,230	0	0	14,965
	0.0.1.3	4,790	5,440	5,480	4,690	8,670
	0.0.1.4	10,395	1,855	11,870	8,550	3,955
	0.1.0.5	18,610	2,240	12,155	7,585	1,390
	0.1.0.6	0	10,405	2,015	0	16,485
	0.1.1.7	3,685	7,665	7,925	3,695	9,250
	0.1.1.8	13,270	2,335	9,350	7,725	4,560
	1.0.0.1	9,785	0	8,960	4,655	0
	1.0.0.2	4,365	2,640	935	1,860	1,125

interruption duration risks detailed in Table 3-13 and a daily indirect consequences resulting from the closure of the given link of 34,000 CHF/day.

Employing Equation (3.44) to calculate the total link direct consequence by considering all hazard specific continuous object direct consequence risks yields a total link direct consequence risk of 301,010 CHF. From Example 3-11, the total link service interruption duration risk is 24.6 days. By employing Equation (3.48), the resulting total financial equivalent link risk is 1,136,000 CHF.

3.8.4 Conclusion

Section 3.8.2 presents a methodology for quantifying the direct consequence and service interruption duration risks resulting from a link composed of multiple continuous objects each exposed multiple hazards. In particular, the direct consequence risks have been assumed to be series independent while the service interruption duration risks have been assumed to be series dependent. Thus to quantify the service interruption duration risks, hazard correlation matrices for each geographic hierarchical level (i.e. slopes, gullies, basins and intra-basins) are formulated and employed to determine the link service interruption duration risks. With both risk types quantified, in Section 3.8.3, the total link risk is assessed by multiplying the service interruption duration risk by the indirect consequences of closing the link for a given day. Therefore, by applying this methodology, one can quantify the total risk exposure of a link composed of multiple continous infrastructure objects each exposed to multiple hazards.

3.9 Calculate risks over multiple years

3.9.1 Overview

With the risk assessment methodologies for an infrastructure object section, a continuous infrastructure object and an infrastructure link each exposed to a single or to multiple hazards, the question now turns to how to assess these risks over an extended time period. This temporal aspect of risk is quantified by first assessing the number of events that can probabilistically occur within a given time period. This present value of these probabilistic events is then assessed to consider any potential inflation or depreciation rates. The resulting value is a present value quantification of the risk exposure with respect to the given hazard over multiple time periods.

3.9.2 Quantifying temporal effects on assessed risk

To broaden the risk assessment temporal horizon from one year to *T* years, one must consider the probability of the various failure events occurring over a temporal horizon extending beyond one year. The general form for the distribution of an event occurring at a given time *t* is quantified with the Poisson Process, Equation (3.49).

$$P(n,t) = \frac{(\nu \cdot t)^n}{n!} e^{-\nu \cdot t} \tag{3.49}$$

Where:

P(n,t) = the probability of *n* events in period *t*

n = the number of events

t = the considered time period [years]
v = the event occurrence rate [years]$^{-1}$

Further specifying the probability detailed in Equation (3.49) by including only events smaller in intensity than a given intensity yields Equation (3.50).

$$P\left(n, X \le x, t\right) = P(n, X \le x, i) \cdot \frac{\left(\nu \cdot t\right)^{i}}{i!} e^{-\nu \cdot t} \tag{3.50}$$

Where:

P(n, X ≤ x, t) = the probability of *n* events in period *t* that are less in intensity than or equal to a threshold intensity *x* [ ]
x = a threshold or reference intensity

Expanding Equation (3.50) yields Equation (3.51).

$$P\left(n, X \le x, t\right) = \sum_{i=0}^{\infty} \binom{i}{n} P\left(X \le x\right)^{n} \left(1 - P\left(X \le x\right)\right)^{i-n} \cdot \frac{\left(\nu t\right)^{i}}{i!} e^{-\nu \cdot t} \tag{3.51}$$

Equation (3.51) can be simplified to Equation (3.52).

$$P\left(n, X \le x, t\right) = \frac{\left(P\left(X \le x\right) \cdot \nu \cdot t\right)^{n}}{n!} e^{-P(X \le x) \cdot \nu \cdot t} \tag{3.52}$$

To determine the number of events that are less than or equal to a given threshold event *x,* an infinite sum is taken of Equation (3.52) resulting in Equation (3.53).

$$E\left(n, X \le x, t\right) = \sum_{n=0}^{\infty} \frac{\left(P\left(X \le x\right) \cdot \nu \cdot t\right)^{n}}{n!} e^{-P(X \le x) \cdot \nu \cdot t} \cdot n \tag{3.53}$$

Where:

E(n, X ≤ x ,t) = the number of events less than or equal to a given threshold event *x* occurring within time *t*

Through algebraic derivation, Equation (3.53) reduces to Equation (3.54).

$$E(n, X \le x, t) = P(X \le x) \cdot t \tag{3.54}$$

Applying this finding to the calculation of risk during a time horizon *T* years, assuming the failed objects are immediately returned to their original states and considering potential discount rates, the object direct consequence and service interruption duration risks for a given hazard parameter can be computed with Equations (3.55) and (3.56).

$$Risk_{DC,T}^{H} = \sum_{n=1}^{T} \left(e^{rate_{DC} \cdot n} \cdot Risk_{DC}^{H} \right) \tag{3.55}$$

$$Risk_{SI,T}^{H} = \sum_{n=1}^{T} \left(e^{rate_{SI} \cdot n} \cdot Risk_{SI,T}^{H} \right) \tag{3.56}$$

Where:

$rate_{DC}$ = the direct consequence discount rate [ ]
$rate_{SI}$ = the service interruption discount rate [ ]
T = the risk assessment temporal horizon [years]

$Risk_{DC,T}^{H}$ = the object direct consequence risk for a given hazard *H* over a time perspective of *T* years [CHF]
$Risk_{SI,T}^{H}$ = the object service interruption duration risk for a given hazard *H* over a temporal horizon of *T* years [days]

Example 3-13: Develop the equations quantifying an object's risk with respect to given hazard by considering the largest hazard parameter intensity during a defined time perspective *N*

Refining the risk assessment methodology further by considering the largest hazard parameter intensity during *N* years rather than considering just the largest hazard parameter intensity in a given year as defined by Equation (3.17), causes the object direct consequence and service interruption duration risk Equations (3.55) and (3.56) respectively evolve to Equations (3.57) and (3.58).

$$Risk_{DC,T,N}^{H} = \sum_{n=1}^{T\cdot\frac{1}{N}} \left(e^{rate\cdot N\cdot n} \cdot Risk_{DC,N}^{H} \right) \tag{3.57}$$

$$Risk_{SI,T,N}^{H} = \sum_{n=1}^{T\cdot\frac{1}{N}} \left(e^{rate\cdot N\cdot n} \cdot Risk_{DC,N}^{H} \right) \tag{3.58}$$

Where:

$Risk_{DC,T,N}^{H}$ = the object direct consequence risk for a given hazard *H* over a time perspective of *T* years considering the maximum hazard parameter intensity in *N* years [CHF]
$Risk_{SI,T,N}^{H}$ = the object service interruption duration risk for a given hazard *H* over a time perspective of *T* years considering the maximum hazard parameter intensity in *N* years [days]

Example 3-14: Using the approach presented in Example 3-13, evaluate the object direct consequence and service interruption duration risks to a given hazard for two different time perspectives (*N*) (one year and one month), two different discount rates (0 and 0.02) over five different temporal horizons (*T*) (1, 10, 25, 50 and 100 years).

To evaluate how the different variables, including the event time perspectives (*N*), the discount rate and the risk assessment temporal horizon (*T*) can influence the evaluated object direct consequence and service interruption duration risks to a given hazard parameter, these risks have been evaluated for the predefined two different event time perspectives using two different financial discount rates over five different time horizons, as shown in Table 3-16.

Table 3-16: Direct consequence and service interruption duration risks evaluated using two different time perspectives, two different discount rates over five different time horizons.

	One Potential Failure per Year (*N* = 1)			**One Potential Failure per Month (*N*=1/12)**		
	$Risk_{DC,T}^{H}$		$Risk_{SI,T}^{H}$	$Risk_{DC,T,N}^{H}$		$Risk_{SI,T,N}^{H}$
***T* [Years]**	**0.00**	**0.02**	**0.00**	**0.00**	**0.02**	**0.00**
1	1,670	1,704	0.338	1,678	1,696	0.339
10	16,704	18,677	3.377	16,779	18,590	3.394
25	41,760	54,724	8.444	41,947	54,469	8.486
50	83,519	144,950	16.887	83,894	144,274	16.971
100	167,039	538,964	33.774	167,788	536,451	33.943

In comparing the two vertically oriented halves of Table 3-16, one can quickly observe that the duration of the considered time perspective – the maximum hazard parameter intensity within a

given year or the maximum hazard parameter intensity within a given month – does not have a significant impact on these computed risks. This finding should stand as long as the shortest return period event (in this case 30 years) is significantly larger that the employed time perspective (1 year). Where such a relationship is not maintained, a time perspective shorter than 1 year should be employed, see Example 3-15.

Turning to the discount rates, it can be seen that for short risk assessment temporal horizons, the discount rate influence is limited, but as the assessment time horizon extends beyond 10 years, this influence becomes significant. Therefore, in calculating multi-year risks, one should specify and consistently employ a single discount rate.

In selecting a time horizon over which the various risks should be evaluated, one should consider how the calculated risks will be employed. If they are purely intended to be employed in comparing and contrasting the object and link risks, the employed time horizon will not influence the evaluation process as long as it is held consistent across all objects and links. If the evaluated risks are intended to be employed in assessing different design and retrofit options and implementation schedules, it is recommended to use a longer time horizon, such as 50 year time horizon, so that the magnitude of the long-term potential financial and temporal losses can be appropriately considered.

3.9.3 Conclusion and critique

In this section, a methodology for quantifying a risk extending over multiple considered time periods and considering the temporal valuation of money is presented. This valuation is formulated by summing the product of the infrastructure risk over a single time period and the compounding interest equation evaluated at each considered time period.

It is important to note that as this assessment methodology employs current hazard identification maps over an extended temporal horizon, by default, it is assumed the risk remains constant over the considered temporal horizon. Additionally it is assumed that if the infrastructure object does fail during the given time period, it is immediately reconstructed to its original state. Where reality strays from these assumptions, a more detailed approach which considers the varying hazard parameter intensity, varying infrastructure object resistance and post-failure reconstruction implications should be developed.

3.10 Conclusion

This chapter presents a comprehensive vulnerability and risk calculation methodology. This methodology is initiated by conducting a geographic coincident analysis between the considered hazards and infrastructure objects. For the coincident hazards and object sections, the exposed object section lengths and the hazard parameter intensities are recorded for specific return period events. Additionally all object data is obtained from the various databases and previous onsite inspections. The respective component failure assessment process is then employed to determine if the given object section is affected by the given range of hazard parameter intensities and if so, in which failure mode(s) the object section responds. With the potentially active failure modes identified, experienced practitioners are asked to develop unit estimates, given a set of predefined hazard parameter intensities, of the direct consequences and service interruption durations resulting from an object section of a given class responding in a specific failure mode. These discrete data sets are then employed to develop continuous probability distribution functions and linearly interpolated

and extrapolated functions. These functions and the identified failure mode(s) are then employed to quantify the direct consequence and service interruption duration risks of the given infrastructure object section.

The analysis scope is then extended from the individual infrastructure object section to the continuous object which is comprised of a number of object sections. In making this expansion, reconstruction economies of scale resulting from mutually inclusive direct consequences and service interruption durations are considered by assessing an effective exposed continuous object length. This effective exposed continuous object length is in turn employed to assess the continuous object vulnerability and risk due to object sections responding in a single or multiple failure modes.

With the continuous object single hazard risks assessed, the analysis scope is expanded further to the link level. At the link level, the focus is on assessing the link risk due to multiple continuous objects being exposed to multiple hazards. To conduct this assessment, both intra-hazard correlations and geographically based hazard correlations are considered. The resulting assessment provides a link direct consequence and service interruption duration risk assessment. These two values can then be combined by considering the daily indirect consequences incurred from transport and societal related impacts of a link's reduced functional performance.

These analyzed risks are then extended to multiple year risks by considering the probability of having a given event occur over the considered time period and the time valuation of money over the considered time period. The end result of the methodology presented in this chapter is an actionable comprehensive methodology for assessing the vulnerability and risk of infrastructure object sections, continuous objects and links to natural hazards. Additionally, by implementing this comprehensive methodology, it is believed an infrastructure manager can better quantify the risk exposure of a given infrastructure object and link, determine if increases in infrastructure resistance or in natural hazard protection measures are warranted, focus risk mitigation funding to the most risk prone regions of the infrastructure network and finally transparently quantify the financial risk exposure of an infrastructure network.

This methodology forms a foundational approach for conducting a system wide natural hazard risk assessment. When this methodology is integrated into an existing infrastructure management system, the infrastructure manager will be able to actively consider an infrastructure object's potential natural hazard failure risk in modeling the infrastructure deterioration and in developing optimal maintenance solutions. Furthermore, through implementing this methodology, the infrastructure manager will be able to determine the required annual funding which should be invested and made available for natural hazard prevent and failure response. The expected end result is reduced infrastructure object failure potential, improved natural hazard protection systems and a more stable funding and infrastructure management.

This vulnerability and risk assessment methodology is employed in Chapter 4 to assess the vulnerability and risk of selected infrastructure objects located along the Jaun Pass and the A2 highway as it transverses the towns of Zofingen and Brittnau.

4 Infrastructure vulnerability assessment case studies

4.1 Introduction

In this chapter, the comprehensive procedure for assessing vulnerability and risk of infrastructure developed in Chapter 3 is employed to analyze two different case studies. The first case study, Case Study A, focuses on analyzing a link of the A2 highway exposed to potential flood hazards. In the second case study, Case Study B, selected infrastructure objects from the Jaun Pass roadway link – specifically a gallery and tunnel infrastructure objects – are analyzed using the developed assessment methodology. These case studies will also be employed to demonstrate the feasibility of the developed vulnerability and risk assessment methodology and to highlight areas for additional development and improvement.

4.2 Case Study A: Vulnerability and risk assessment of the Zofingen A2 highway

Figure 4-1: a) Looking North at the A-2 highway located west of the Wigger River and b) Looking south at a portion of the levee separating the A-2 Highway from the Wigger River.

Zofingen, located in the Canton of Aargau, is a 10,500 person town situated within the Wigger Valley, a north facing river valley located in north-central Switzerland. The primary private transportation access route servicing the Wigger Valley is the A2 Highway, a four lane limited access highway situated on the eastern bank of the Wigger river. This case study analyzes the vulnerability and risk of a 6729m link of the A2 which runs between Oftringen interchange in the north and the Mehlsecken interchange in the south.

Table 4-1: Zofingen A2 highway continuous infrastructure objects, presented in a north to south sequence.

Ref	Infra. Type	Infra. Class	Length [m]
1	Road	Highway	546
2	Bridge	Highway	36
3	Road	Highway	357
4	Bridge	Highway	40
5	Road	Highway	5750

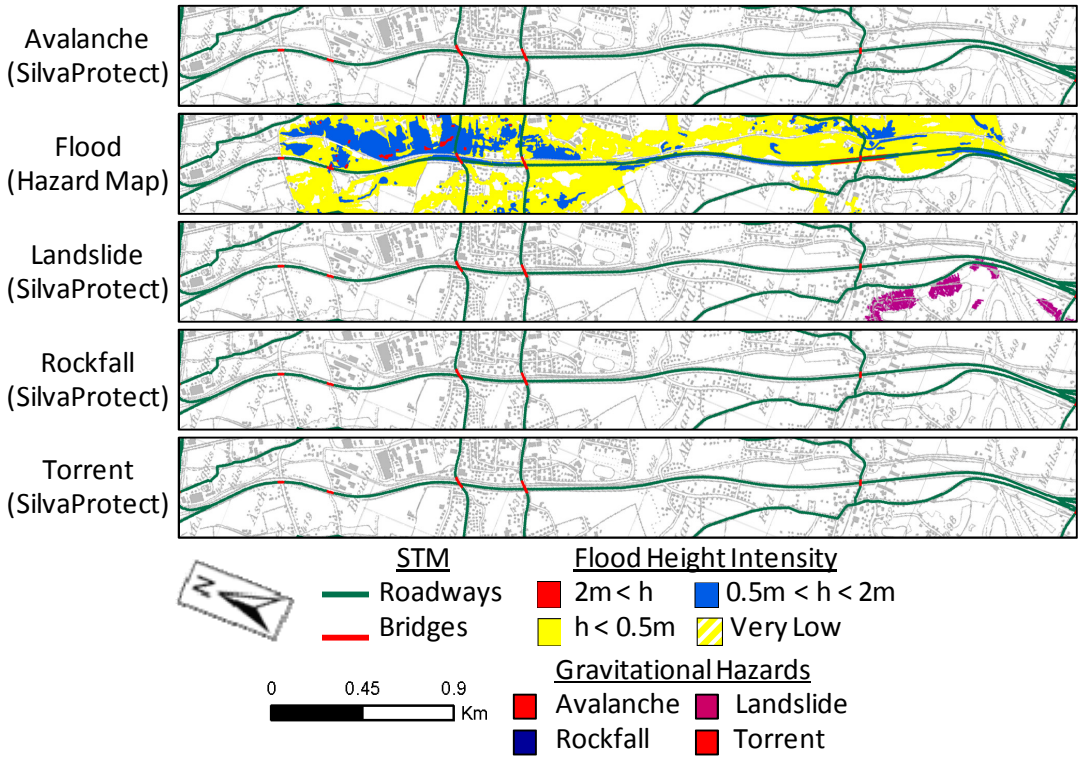

Figure 4-2: Coincident analysis between the considered hazards and the A2 highway link.[5]

hazard, the flood hazard, and secondly only the latter two continuous infrastructure objects, infrastructure objects 4 and 5 presented in Table 4-1, are the only continuous objects exposed to the flood hazard.

These two continuous infrastructure objects were then cut into 100 meter long object sections resulting in one 40m long object section from the exposed A2 bridge and fifty-seven 100m long and

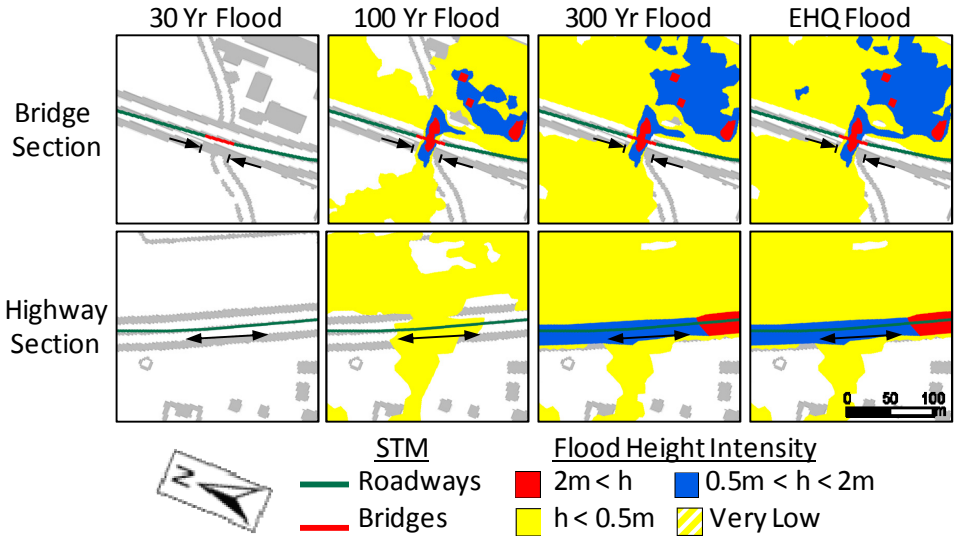

Figure 4-3: Selected bridge and highway infrastructure object section exposure to flood hazard.

[5] The contribution of the levee protect system bordering the Wigger River was actively considered in the development of the Zofingen flood hazard identification maps and thus any additional contribution from the levee is not directly considered within this work.

Table 4-2: Zofingen A2 selected exposed bridge and highway object section discrete data.

Object Section:	Bridge Section				Highway Section			
Hazards:	Flood				Flood			
Return period:	30	100	300	1000	30	100	300	1000
Hazard parameter intensity (m depth)	0	2.5	2.8	3.0	0	0.1	1.2	1.4
Object exposed length (m)	0	22	24	24.5	0	100	100	100

one 50m long object sections from the exposed A2 highway. A detailed coincident analysis was then conducted between each object section and the available flood parameter data, the flood depth identification maps, for each return period event. A visual presentation of this coincident analysis is made in Figure 4-3 and a tabular presentation is made in Table 4-2.

It should be noted that the specific hazard parameter intensity data presented in Table 4-2 has been estimated from the hazard-object coincident analysis as the hazard data is presented purely as hazard parameter ranges rather than specific parameter intensities.

With the exposure of the bridge and highway objects confirmed and the hazard parameter intensities quantified, the next step is to apply the respective component failure assessment process presented in Section 3.3 and Appendix A.6 to identify if these hazard parameter intensities can cause the concerned object section to fail.

Figure 4-4: Eastern elevation of the exposed A2 bridge.

The bridge component failure assessment process was applied to analyze exposure of the A2 highway bridge, shown in Figure 4-4, to the flood depth intensities presented in Table 4-2, yielding the results shown in Table 4-3. Specifically, in applying the bridge component failure assessment process, one can observe that the bridge is exposed only to the flood hazard (thus step A for the flood hazard is negative). Furthermore, the flood depth does not exceed the bridge clearance nor is the bridge foundation susceptible to scour. Thus the bridge does not experience failure to any of the expected flood depth intensities.

The roadway component failure assessment process was then applied to analyze the exposure of the A2 highway section, shown in Figure 4-1a, to the flood depth intensities presented in Figure 4-2, yielding the results shown in Figure 4-4. As mentioned earlier, the resistance of the supporting objects – specifically the levees lining the Wigger River have been considered in the development of

Table 4-3: Zofingen exposed A2 bridge failure assessment steps and hazard scenario identification.

	Bridge Assessment Steps	Avalanche	Flooding	Landslide	Rockfall	Torrent
A	Bridge location Hazard location	Yes	No	Yes	Yes	Yes
B	Clearance > Hazard Height	-	Yes	-	-	-
C	Pier Foundation Depth > Hazard Rupture Surface or Scour Depth	-	Yes	-	-	-
D	Vertical Resistance > Applied Vertical Force	-	-	-	-	-
E	Bearing Resistance > Applied Superstructure Forces	-	-	-	-	-
F	Horizontal Resistance > Applied Horizontal Force	-	-	-	-	-
G	Pier Resistance > Applied Horizontal Pier Forces	-	-	-	-	-
H	Clearance + Structural Height > Hazard Height	-	Yes	-	-	-
	Failure Scenario	**-**	**-**	**-**	**-**	**-**

flood depth intensity maps. Thus, in applying the roadway component failure assessment process, no additional supporting objects were considered. Thus, for the flood hazard, assessment step A is negative and steps B and C are non-applicable. Additionally, as the expected flood induced scour depth is negligible, assessment step D is positive, resulting in failure scenario R2-F – roadway is inundated with liquid. Furthermore, as the roadway object has no resistance to a flood depth intensity, the roadway section is assumed to experience failure in mode R2-F as soon as the flood depth exceeds 0m.

Table 4-4: Zofingen A2 highway object section failure assessment steps and hazard scenario identification.

	Roadway Assessment Steps	Avalanche	Flooding	Landslide	Rockfall	Torrent
A	Roadway location Hazard location	Yes	No	Yes	Yes	Yes
B	Supporting Object Location ≠ Hazard Location	-	-	-	-	-
C	Supporting Objects Intact?	-	-	-	-	-
D	Hazard Rupture Surface or Scour Depth = 0	-	Yes	-	-	-
	Failure Scenario	**-**	**R2-F**	**-**	**-**	**-**

With the roadway failure mode identified as R2-F, one can estimate the direct consequences and service interruption durations for a highway class roadway object failing in mode R2 to a flood hazard. These values were previously presented in Table 3-6.

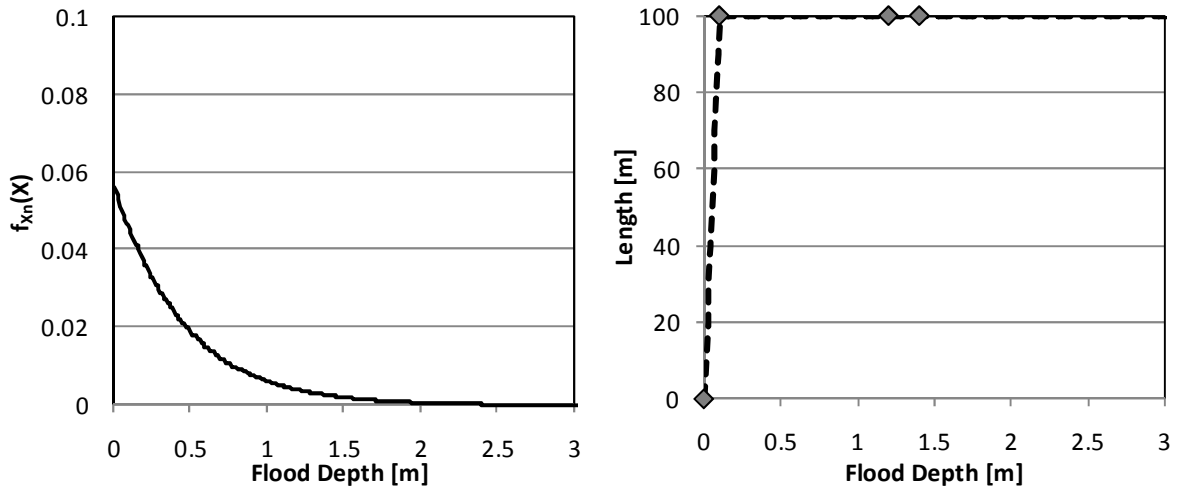

Figure 4-5: a) Gumbel Type I distribution fitted to the local flood depth intensities and the exposed object section length as a function of the flood depth intensity.

With the discrete data sets identifying the local hazard parameter intensity as a function of return period, the exposed object lengths, the direct consequences and the service interruption durations determined, employing the procedure presented in Section 3.5, continuous functions are fitted to these discrete data sets. A Gumbel Type I distribution has been fitted to the expected local hazard parameter intensities and interpolating and extrapolating linear functions to the selected exposed object section length are presented in Figure 4-5. The interpolated and extrapolated linear functions to the direct consequences and service interruption times are presented in Figure 3-13.

The procedures presented in Section 3.6, and Equations (3.27) to (3.30) were then employed to quantify the direct consequence and service interruption vulnerability curves and the risk of the each exposed highway object section. The direct consequence and service interruption duration vulnerability curves for the considered highway object section is presented in Figure 4-6a. Furthermore, the direct consequence and service interruption duration annual risks for the considered highway object section are respectively 305.90 CHF/year and 0.0715 days/year.

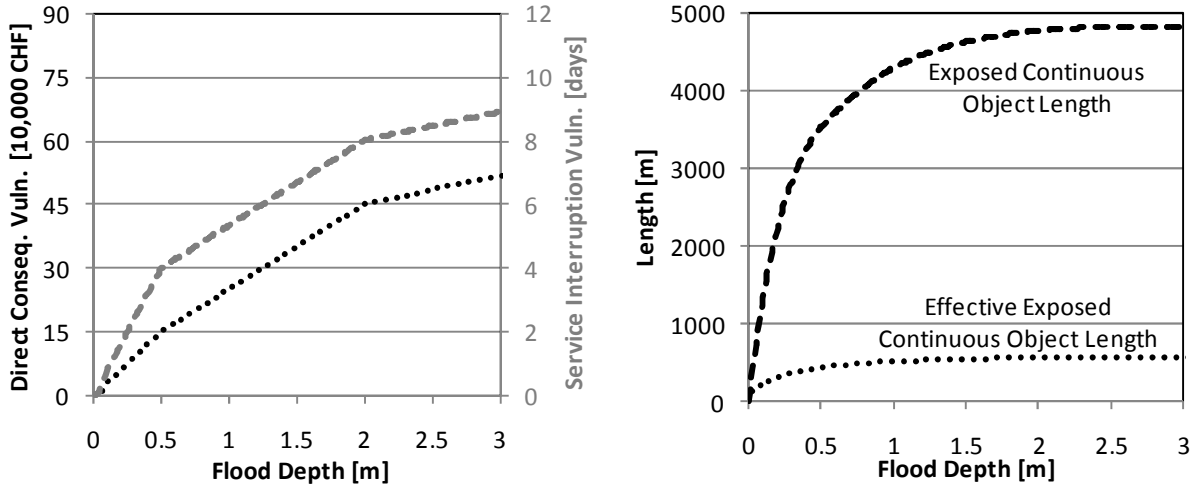

Figure 4-6: a) Direct consequence and service interruption vulnerabiliy curves as a function of the flood depth intensity and b) The exposed continuous object length and the effective exposed continuous object length as a function of the flood depth intensity.

Expanding the analysis from the selected object section to the continuous A2 highway continuous object, the procedure presented in Section 3.7 was employed to assess the continuous object effective exposed length. This was conducted by employing the estimated object length flood specific attenuation factor for a roadway component detailed in Table 3-7 and Equation (3.36). The continuous object exposed length and the continuous object effective exposed length for the A2 highway continuous object are presented in Figure 4-6b. Furthermore, the direct consequence and service interruption annualized risks for the A2 continuous object were assessed by employing Equations (3.40) to (3.41). The annualized direct consequence and service interruption risks to the flood depth are 816.14 CHF/year and 0.184 days/year. As this is the only exposed continuous object within the studied A2 link, per the procedure presented in Section 3.8, these effective continuous object annualized risks are equivalent to the link annualized direct consequence and service interruption risks.

Equations (3.55) and (3.56) were then employed to expand the direct consequence and service interruption risks time horizon from one year to 50 years by uniformly using a discount rate of 0.02, resulting in direct consequence and service interruption risks of 70,822 CHF and 15.97 days.

Considering the daily financial valuation of the losses and additional expenditures incurred from transport related impacts of closing this A2 highway link is 64,740 CHF per day (Hajdin, Axhausen, Bell, Birdsall, & Erath, 2008), the total financial equivalent link risk exposure considering direct and indirect consequences, following Equation (3.48), is 1,104,600 CHF/50 years.

By analyzing this section of the Zofingen A2 highway link with the developed vulnerability and risk assessment methodology, one can quantify the annual and multi-year risks facing this given roadway link. With this information, an infrastructure manager can analyze the viability of potential mitigative actions including strengthening the levee system separating the Wigger River from the A2 highway, identifying potential detour roadway links which can be employed in the case of the flooding of the A2 highway, and informing the local government administration and community of these potential risks. Through this informed decision making process, infrastructure managers can efficiently reduce the potential and consequences of future natural hazard induced infrastructure failures.

4.3 Case Study B: Vulnerability and risk assessment of selected objects within the Jaun Pass

The Jaun Pass is a class 1 east-west oriented high mountain roadway pass linking the Fribourg Cantonal town of Charmey to the Bern Cantonal towns of Boltigen, Reichenbach and eventually Spiez. This case study focuses on objects located along a 7.8 km section of the Jaun Pass extending from the La Jogne river eastward to the Fribourg-Berne cantonal boarder. In addition to the Class 1 roadway objects, this section also includes numerous retaining walls, six bridges, six culverts, one gallery and one tunnel. Even though the retaining wall, bridge, culvert and roadway objects are exposed to numerous avalanche, rockfall, landslide and torrent hazards, as this is the only case study containing gallery and tunnel objects, this case study will focus on these two objects.

4.3.1 The Jaun Pass gallery

Figure 4-7: Looking east at Jaun Pass gallery.

The 371 m long gallery, shown in Figure 4-7 and detailed in Figure 4-9, was constructed in 1974 and is located immediately east of the La Jogne bridge on the western side of the case study. Structurally, the gallery roof is composed of a continuous 80 cm thick reinforced concrete slab spanning 8 meters across the roadway. On the uphill side, the gallery roof is supported by a continuous 4 meter high reinforced concrete retaining wall and the top of the gallery roof is flush with the in situ soil. On the downhill side, the gallery roof is supported by 50 cm by 50 cm reinforced concrete columns spaced at

3.5 meters on center. Contextually, the gallery is situated at the foot of a 1000m high avalanche and torrent shoot which during normal rain events contains water which is conveyed over the gallery in a dedicated open conduit. The uphill slope has a 20% grade and the downhill slope gently slopes away from the gallery at a 2% grade[6].

In conducting a geographic coincident analysis between the SilvaProtect natural hazard indication maps, the Fribourg Cantonal natural hazard identification maps and the STM specified gallery location, Figure 4-8, it can be seen that the gallery, the orange line transversing each image, is exposed to avalanche, torrent and flooding hazards and not exposed to rockfall and landslide hazards.

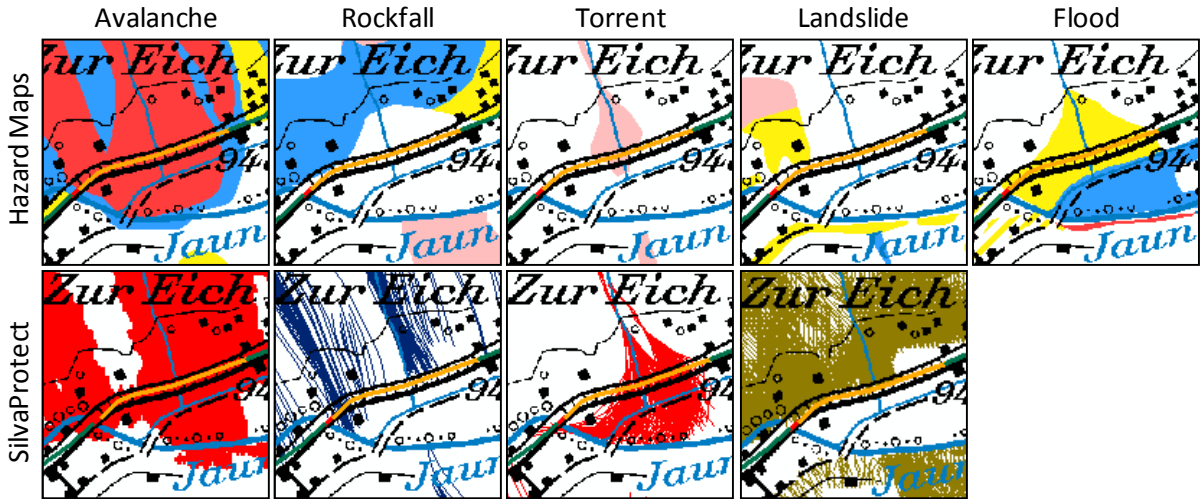

Figure 4-8: Jaun Pass gallery - Natural hazard indication and identification maps.

To facilitate the analysis of the Jaun Pass gallery, the gallery continuous object is cut into four object sections with respective lengths of 85, 100, 100 and 86m. Applying the gallery component failure assessment process, Figure A-18, it can be seen that as the Jaun Pass gallery foundations are well embedded in the hill side and the top of the uphill gallery wall is flush with the in situ soil, thus the assessment steps B to D are all positive and step E is negative, Table 4-5.

Furthermore, it can be seen that while both the flood and torrent hazards pass over the gallery, it is believed that the hazards will not apply a significant horizontal or vertical force to the gallery roof – thus assessment steps F to H are all positive. Additionally, even though the gallery wall incorporates an open-air culvert to guide water across the gallery, it is believed that during torrent and flood hazard events, the roadway passing through the gallery will also be flooded with water and debris. Therefore step I is negative for both the flooding and torrent hazards and the respective failure scenarios are G7-T (gallery flooded with torrent debris) and G7-F (gallery flooded with water).

[6] These dimensions have been estimated from the onsite visual site assessment.

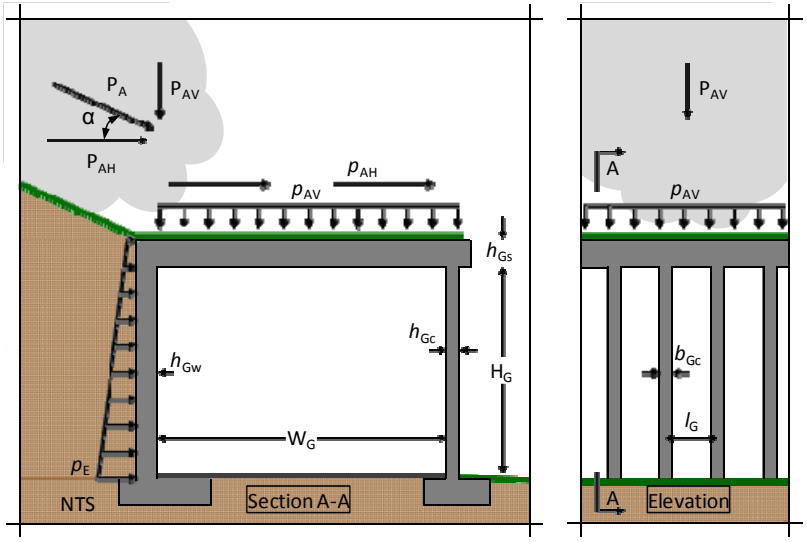

Figure 4-9: Jaun Pass structural analysis schematic in a) cross section and b) elevation.

Turning to the avalanche hazard, one must assess if the gallery wall, gallery roof and frame structural resistance to the static earth pressure and a high intensity avalanche hazard (P_A = 30kN/m^2). Ideally this would be accomplished by quantifying the gallery resistance in terms of the expected avalanche pressure intensities. As the gallery's structural resistance or even a generalized structural rating has not been included in a centralized database, it was decided to employ a finite element program to quantify the structural resistance of a 3.5 meter wide strip of the gallery wall and roof centered around one of the gallery column. This analysis, focusing on the gallery assessment steps F, G and H, found that the gallery has more than sufficient strength to resist the combined forces of the high intensity avalanche hazard, the static soil pressure, and the gallery members' self weight. Thus, even though high intensity avalanches can and do occur at this location, the gallery has been designed to withstand these forces – thereby ensuring that this hazard does not pose any additional risk to this section of the roadway link. Thus, as shown in Table 4-5, for the avalanche hazard, assessment steps A and E are negative and steps B-D and F-I are all positive.

Table 4-5: Jaun Pass gallery failure assessment steps and failure scenario identification.

Gallery Assessment Steps		Avalanche	Flood	Landslide	Rockfall	Torrent
A	Gallery location Hazard location	No	No	Yes	Yes	No
B	Gallery foundational depth > Hazard rupture surface or scour depth	Yes	Yes	-	-	Yes
C	Gallery wall resistance > Applied horizontal force	Yes	Yes	-	-	Yes
D	Wall column resistance > Applied horizontal force	Yes	Yes	-	-	Yes
E	Gallery wall height > Hazard height	No	No	-	-	No
F	Gallery roof resistance > Applied vertical force	Yes	Yes	-	-	Yes
G	Roof support resistance > Applied vertical forces	Yes	Yes	-	-	Yes
H	Gallery frame resistance > Combined horizontal & vertical forces	Yes	Yes	-	-	Yes
I	Is hazard Flood or torrent	Yes	No	-	-	No
	Hazard Scenario	**-**	**G7-F**	**-**	**-**	**G7-T**

4.3.2 Jaun Pass gallery discrete data

The natural hazard data for this area is currently limited to only hazard parameter identification maps which segment the hazard data into four color coded zones by considering both hazard parameter intensity and hazard parameter probability. Thus, for the flood and torrent hazards, one is unable to determine where within each return period (30, 100, 300 and 1000 years) the given natural hazard intensity rests and the geographic extents of these respective events. In face of these limitations, it has been assumed, as shown in Figure 4-8, that the yellow flooding and red torrent zones represents respectively 0, 0.3, 0.6 and 1.4m water depth and 0, 0.6, 1.1 and 1.4m deposited depth for each of the four reference return periods (30, 100, 300 and 1000). Furthermore, from the hazard map information shown in Figure 4-8, it can be determined that the maximum length of the flooding and torrent zones are respectively 354m and 88m. As with the hazard intensity data, one must also assume the gallery length exposed to each hazard given the predefined return periods (30, 100, 300 and 1000). Thus it has been assumed that 0, 85 215 and 354m of the Jaun Pass gallery is exposed to the flood hazard and 0, 40, 80 and 88m of the gallery is exposed to the torrent hazard, both respectively taken at 30, 100, 300 and 1000 return periods.

Table 4-6: Jaun Pass gallery discrete continuous object data.

Failure mode	**G7-T**				**G7-F**			
Return period	**30**	**100**	**300**	**1000**	**30**	**100**	**300**	**1000**
Hazard parameter intensity (m depth)	0	0.6	1.1	1.4	0	0.3	0.6	1.4
Object exposed length (m)	0	40	80	88	0	85	215	354
Hazard intensity (m depth)	**0**	**0.5**	**1**	**2**	**0**	**0.5**		**2**
Unit direct consequences (CHF/100m)	0	24000	48000	72000	0	14400		38400
Unit Service interruption (days/100m)	0	6	8	10	0	2		4

The last pieces of information needed to compute the total direct consequences and service interruptions resulting from each hazard exposure, are the estimated unit direct consequences and service interruptions for the predefined hazard intensities. As presented in Figure 4-8, for a flood water depth of 0, 0.5 and 2m, the unit direct consequences for a 100m length of class 1 gallery have been estimated at 0, 14400 and 38400 CHF and the unit service interruption durations have been estimated at 0, 2 and 4 days. Likewise, for a torrent deposited depth of 0, 0.5, 1 and 2, the unit direct consequences have been estimated at 0, 24000, 48000 and 72000 CHF and the unit service interruption durations have been estimated at 0, 6, 8 and 10 days.

4.3.3 Assessing an example object section – fitting continuous functions

Taking one of the two middle object sections and assuming the hazard location is symmetrically applied to each object section results in the discrete data presented in Table 4-7. One can then apply the procedure presented in Section 3.5 to transition the discrete data to continuous functions. First a

Table 4-7: Jaun Pass galley section discrete data.

Object Section	**Section 2 & 3**								**Section 1 & 4**							
Failure Modes	**G7-T**				**G7-F**				**G7-T**				**G7-F**			
Return period	**30**	**100**	**300**	**1000**	**30**	**100**	**300**	**1000**	**30**	**100**	**300**	**1000**	**30**	**100**	**300**	**1000**
Hazard parameter intensity (m depth)	0	0.6	1.1	1.4	0	0.3	0.6	1.4	0	0	0	0	0	0	0.6	1.4
Object exposed length (m)	0	20	40	44	0	42.5	100	100	0	0	0	0	0	0	7.5	77

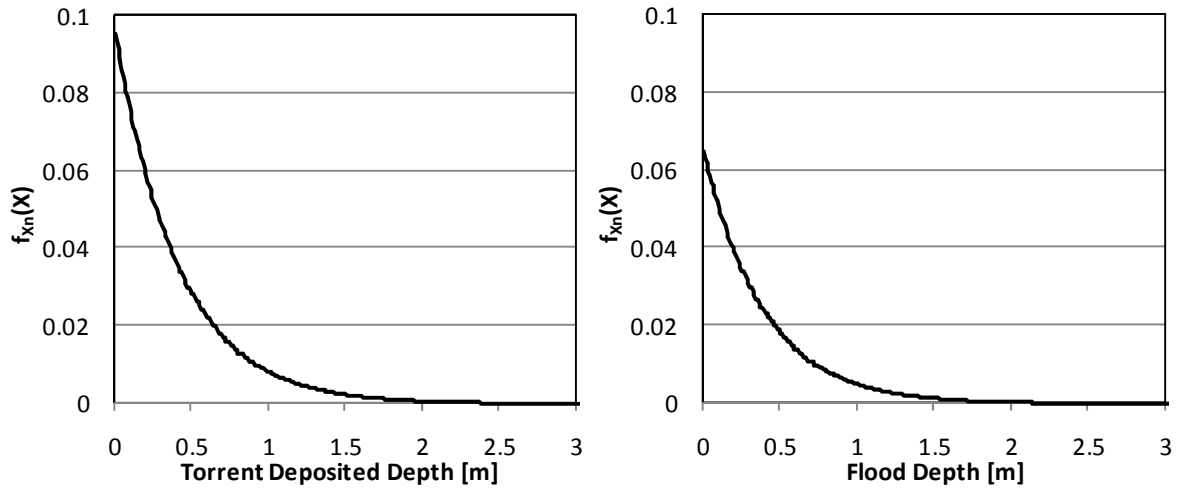

Figure 4-10: Gumbel Type I distribution fitted to the Jaun Pass gallery: a) Torrent hazard and b) Flood hazard.

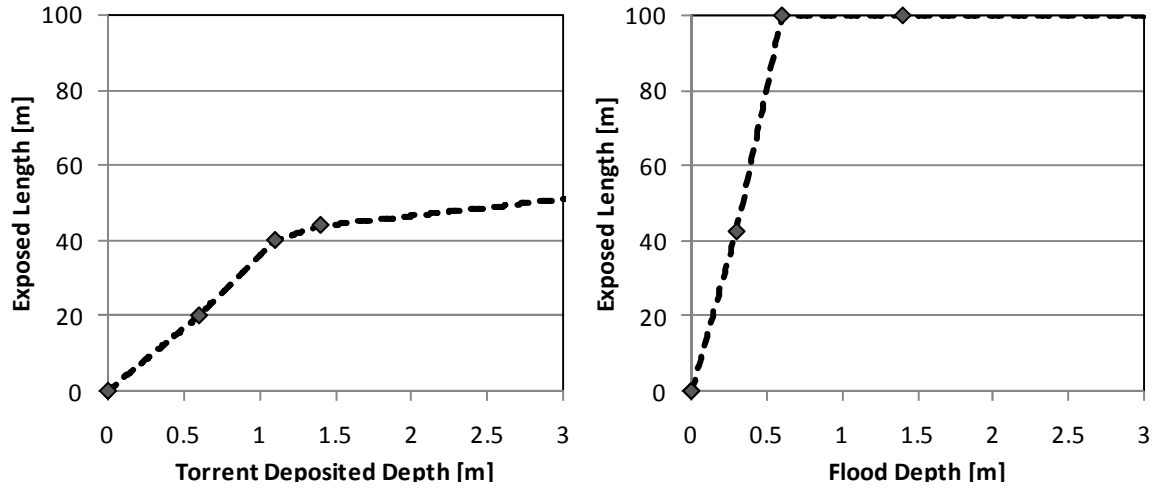

Figure 4-11: Jaun Pass gallery section exposed length for: a) Torrent hazard, b) Flood hazard.

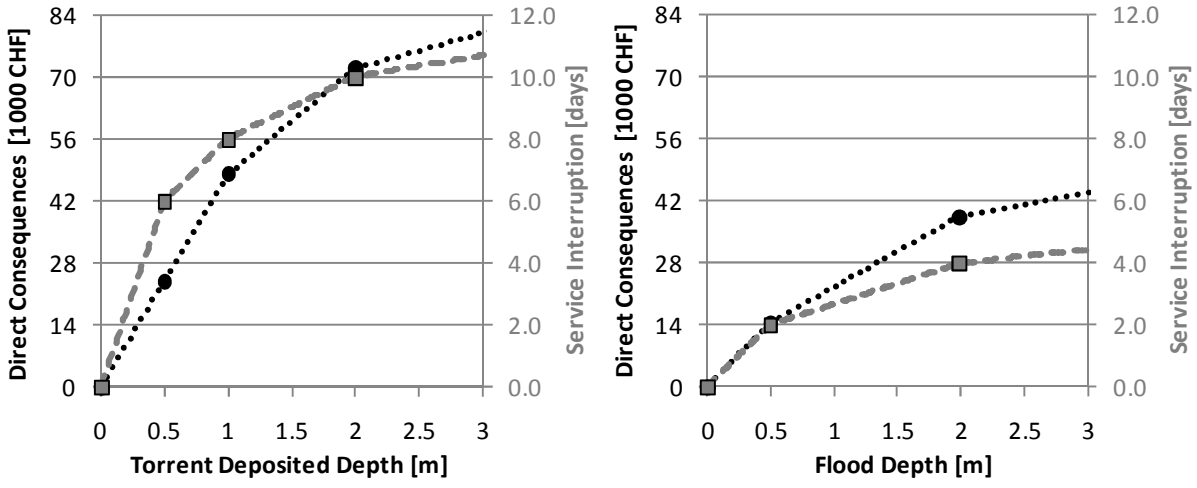

Figure 4-12: Jaun Pass gallery direct consequences and service interruption times estimated for: a) Torrent induced failure modes G7-T, b) Flood induced failure mode G7-F.

Gumbel Type I distribution is fit to the return period based hazard parameter data, Figure 4-10. Equations (3.22), (3.23) and (3.24) are then employed to develop continuous functions from the

discrete exposed section length, direct consequences and service interruption hazard parameter intensity linked data, Figure 4-11 and Figure 4-12.

In these six figures presented above, one can observe that the torrent hazard has a higher probability of occurring, Figure 4-10, but the flood hazard effects a larger portion of the object segment, Figure 4-11. Lastly, the torrent hazard unit direct consequence and service interruption durations are significantly higher than the flood hazard direct consequences and service interruption durations, Figure 4-12.

4.3.4 Object segment vulnerability and risk

With these continuous functions developed, one can calculate the vulnerability curves and risks for this object section. The vulnerability curves are developed by applying Equations (3.27) and (3.28) to the exposed length, unit direct consequences and unit service interruption duration functions presented above results in the vulnerability functions shown in Figure 4-13.

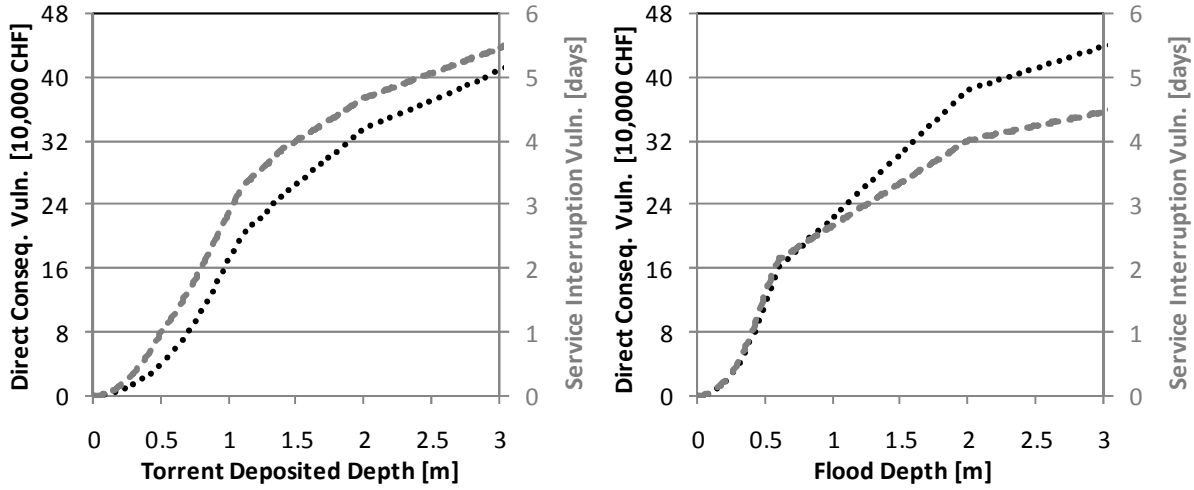

Figure 4-13: Jaun Pass gallery segment direct consequence and service interruption duration vulnerability curves for: a) Torrent, b) Flood hazard.

From the vulnerability functions presented above, one can observe that the vulnerability functions are within the same order of magnitude. The gallery-flood vulnerability curves initially outpace the gallery-torrent vulnerability curves. At higher hazard parameter intensities, the torrent service interruption duration vulnerability curve exceeds the flood service interruption duration vulnerability curve and the flood direct consequence vulnerability curve exceeds the torrent direct consequence vulnerability curve.

Equations (3.27) and (3.28) are respectively employed to calculate the direct consequence and service interruption duration risks from the probability density functions and vulnerability curves presented above. The resulting object section risks are presented in Figure 4-14.

Figure 4-14: Jaun Pass gallery direct consequence and service interruption duration risks with respect to the flood and torrent hazards.

Object Section	Section 2 & 3		Section 1 & 4	
Failure Mode	**G7-T**	**G7-F**	**G7-T**	**G7-F**
Direct consequence risk	176.20	229.04	0	47.66
Service interruption risk	0.0330000	0.023778	0	0.005954

4.3.5 Continuous object effective exposed length, vulnerability and risk

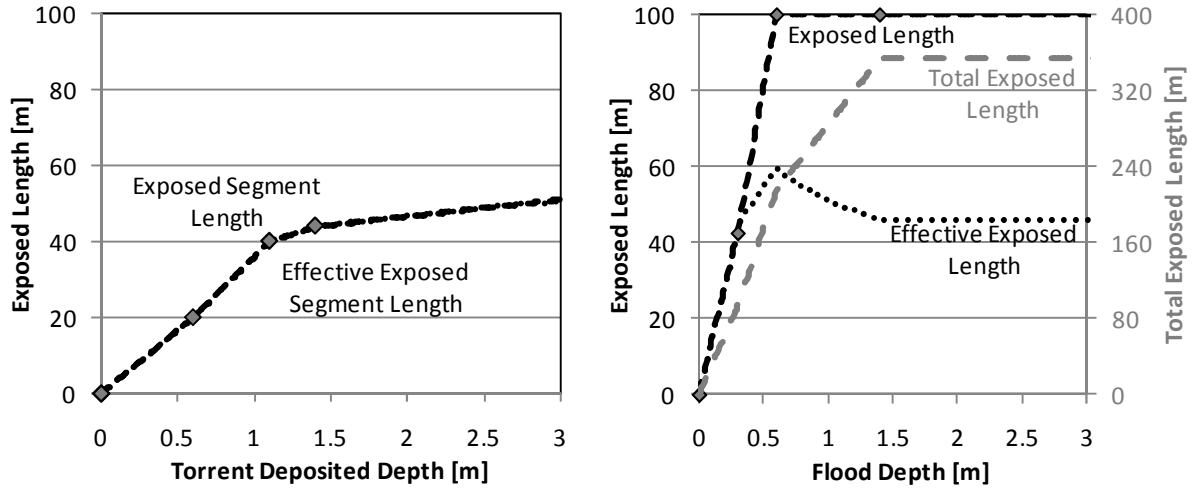

Figure 4-15: Exposed and effective exposed continuous object section lengths of the Jaun Pass gallery to: a) Torrent hazard, b) Flood hazard.

The Jaun Pass gallery direct consequences and service interruption duration vulnerability curves are then assessed from the effective exposed gallery continuous object lengths, estimated direct consequences and estimated service interruptions duration using Equations (3.38) and (3.39). From the vulnerability curves presented in Figure 4-16, one can observe that the gallery direct consequence vulnerability to both the torrent and flood hazards are fairly equivalent but the gallery service interruption vulnerability is noticeably different, with the torrent hazard incurring a more than 25% increased service interruption duration when compared to the flood hazard vulnerability.

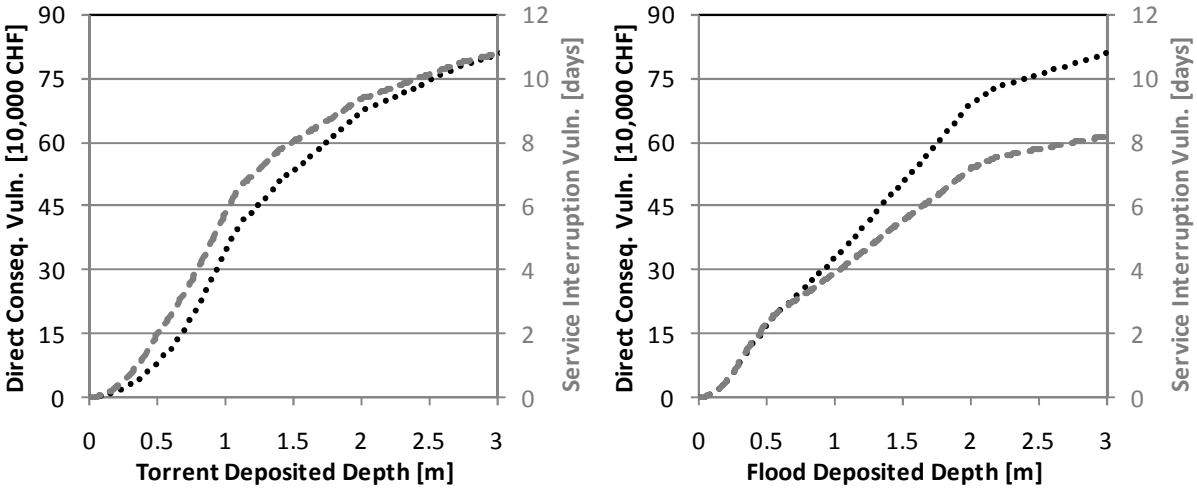

Figure 4-16: Juan pass gallery vulnerability to the: a) Torrent hazard and b) Flood hazard.

Turning to Table 4-8, one can observe that the foundational discrete data is presented in the first half of this table. In particular, one can observe the differences between the torrent and flood hazard exposed gallery continuous object lengths and the unit direct consequences. The annualized direct consequence and service interruption duration risks, assessed with Equations (3.40) and (3.41), are presented in the central section of Table 4-8. From the annualized risks, one can observe that the torrent hazard which has a significantly smaller geographical reach, incurs a more than 22% greater

direct consequences and more than 75% longer service interruption times as compared to the flood hazard incurred direct consequences and service interruption times. By considering the unit indirect costs of the additional driving time and distance induced by closing the Jaun Pass for one day (15260 CHF/day) (Hajdin, Axhausen, Bell, Birdsall, & Erath, 2008), one can determine the financial equivalent annualized indirect risk incurred by each hazard. When these incurred indirect risks are compared against the direct consequence annualized risks, one can observe that the indirect risks for the torrent and flood hazards are respectively more than 280% and 190% greater than the annualized direct consequence risks.

Table 4-8: Jaun Pass Gallery analyzed risk considering hazard scenarios G7-T and G7-F

Failure mode	**G7-T**				**G7-F**			
Return period	**30**	**100**	**300**	**1000**	**30**	**100**	**300**	**1000**
Hazard parameter intensity (m depth)	0	0.6	1.1	1.4	0	0.3	0.6	1.4
Object exposed length (m)	0	40	80	88	0	85	215	354
Hazard intensity (m depth)	**0**	**0.5**	**1**	**2**	**0**	**0.5**		**2**
Unit direct consequences (CHF/100m)	0	24000	48000	72000	0	14400		38400
Unit Service interruption (days/100m)	0	6	8	10	0	2		4
Equivalent length factor	0.3				0.25			
Annualized direct conseq. risk (CHF/yr)	352.32				287.63			
Annualized service interruption (days/yr)	0.0650				0.0362			
Unit indirect consequences (CHF/day)	15260 CHF/day							
Annualized indirect risk (CHF/yr)	992.43				551.95			
Annualized hazard risk (CHF/yr)	**1,344.75 CHF/yr**				**839.58 CHF/yr**			
Hazard risk over 50 yrs (CHF/50 yr)	**116,691.99 CHF/50 yrs**				**72,764.49 CHF/50 yrs**			
Inter-hazard correlation factor	0.30				0.25			
Annualized object risk (CHF/yr)	**1932.46 CHF/yr & 0.0903 days/yr**							
Object risk over 50 yrs (CHF/50 yrs)	**167,627.13 CHF/50 yrs & 4.518 days/50 yrs**							

The annualized object risk for the Jaun Pass gallery was then assessed using Equation (3.43) and Table 3-8. This assessment has found that annually more than 1900 CHF are at risk due to the torrent and flood hazards. The gallery financial equivalent and service interruption risks over a 50 year reference period respectively considering discount rates of 0.02 and 0.00 were then quantified with Equations (3.55) and (3.56). This assessment found that the over a 50 year reference period, the gallery equivalent financial risk is 167,600 CHF and the total expected service interruption risk is 4.5 days.

Thus through applying this vulnerability and risk assessment methodology to the Jaun Pass Gallery, one can quantify the gallery's annualized risk exposure to each hazard – a key tool for assessing the gallery's level of risk exposure. With this quantified risk, an infrastructure manager can start to assess the viability and the appropriateness of various environmental, contextual, object and transportation network risk mitigation actions. In the case of the Jaun Pass gallery, such mitigation activities could include: increasing the capacity of the open-air conduit transversing the gallery or constructing retention basins and check dams to diminish the torrent intensity and occurrence probability.

4.3.6 Jaun Pass tunnel

Figure 4-17: Jaun Pass tunnel - Looking west through tunnel.

The 170m long naturally-ventilated cut tunnel, shown in Figure 4-17, is located 580 meters west of the Fribourg-Berne Cantonal boarder. The tunnel, constructed in 1993, provides a bypass through a portion of the hillside thereby adverting landslide hazards that had previously plagued the roadway. The only utilities inside the tunnel is the tunnel lighting which is suspended from the tunnel roof.

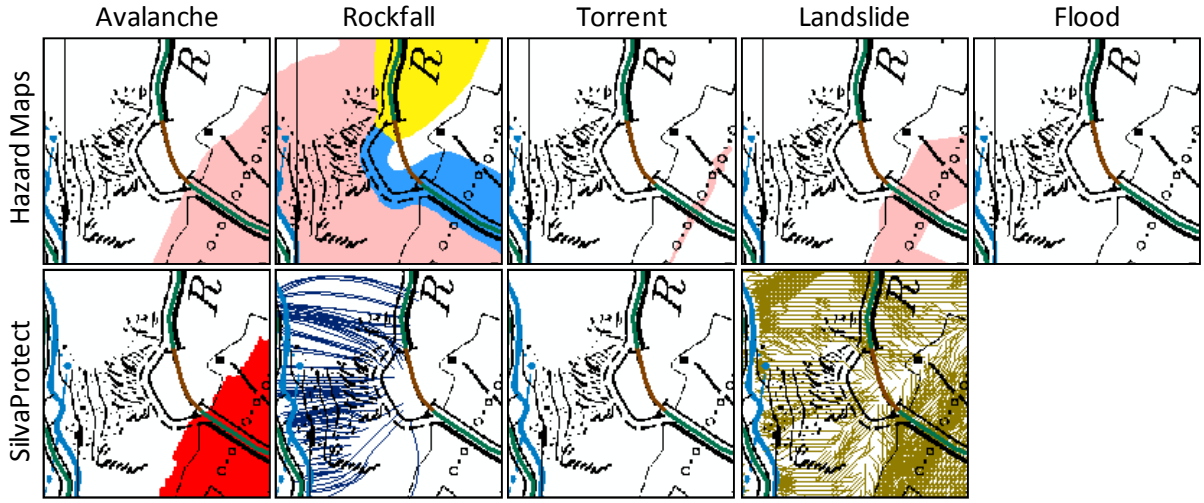

Figure 4-18: Jaun Pass tunnel - Natural hazard indication and identification maps.

In Figure 4-18, one can observe the previous and now closed roadway, shown in double dashed lines, the Jaun Pass tunnel, shown in brown, the SilvaProtect natural hazard indication maps and the Fribourg Cantonal natural hazard identification maps. In this figure, one can observe that the tunnel is not exposed to either landslide or flooding hazards – the only two hazards for which a tunnel is assumed to be vulnerable. Thus, as shown in Table 4-9, the tunnel is not exposed to either hazard and does not experience a failure due to any natural hazards.

Table 4-9: Juan Pass tunnel assessment steps and hazard scenario identification.

Tunnel Assessment Steps		Avalanche	Rockfall	Torrent	Landslide	Flooding
A	Tunnel entrance location Hazard location	-	-	Yes	-	Yes
B	Tunnel utility elevation > Hazard height	-	-	-	-	-
	Failure Mode	-	-	-	-	-

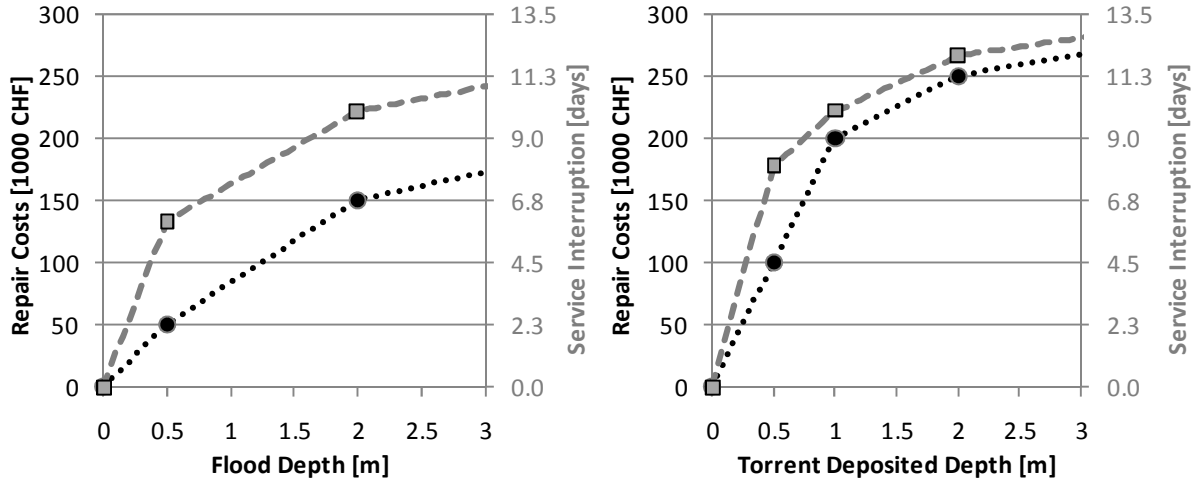

Figure 4-19: Jaun Pass tunnel unit direct consequences and service interruption times estimated for: a) Torrent hazard, b) Flood hazard.

For the sake of consistency, unit direct consequences and service interruption times have been estimated for a 100m length of a class 1 tunnel exposed to torrent and flood hazards, Figure 4-19. In conducing these estimates, it has been assumed that as the tunnel utilities are suspended from the tunnel roof, the tunnel could only experience failure in failure modes T1-F and T1-T, tunnel 'flooded' with liquid or debris.

In Table 4-10, one can observe that the tunnel hazard parameters and object exposed lengths are both zero for all considered return period events (30, 100, 300 and 1000). Therefore the object vulnerability, annualized risk and risk over a 50 year reference period are all negligible. This assessment therefore confirms that this tunnel built in 1993 is well designed and does not warrant any modifications or additions.

Table 4-10: Jaun Pass tunnel analyzed risk considering hazard scenarios T1-F and T1-T.

Failure mode	**T1-F**				**T1-T**			
Return period	**30**	**100**	**300**	**1000**	**30**	**100**	**300**	**1000**
Hazard parameter intensity (m depth)	0	0	0	0	0	0	0	0
Object exposed length (m)	0	0	0	0	0	0	0	0
Hazard intensity (m depth)	**0**	**0.5**		**2**	**0**	**0.5**	**1**	**2**
Unit direct consequences (CHF/100m)	0	50,000		150,000	0	100,000	200,000	250,000
Unit Service interruption (days/100m)	0	6		10	0	8	10	12
Equivalent length factor	0.3				0.25			
Annualized direct risk (CHF/yr)	0				0			
Annualized service interruption (days/yr)	0				0			
Unit indirect consequences (CHF/day)	15260 CHF/day							
Annualized indirect risk (CHF/yr)	0				0			
Annualized hazard risk (CHF/yr)	**0 CHF/yr**				**0 CHF/yr**			
Hazard risk over 50 yrs (CHF/50 yr)	**0 CHF/50 yrs**				**0 CHF/50 yrs**			
Inter-hazard correlation factor	0.30				0.30			
Annualized object risk (CHF/yr)	**0 CHF/yr & 0 days/yr**							
Object risk over 50 yrs (CHF/50 yrs)	**0 CHF/50 yrs & 0 days/50 yrs**							

4.4 Conclusion and critique

In this chapter, the infrastructure vulnerability and risk assessment methodology developed in Chapter 3 has been employed to quantify the natural hazard risks potentially affecting a number of infrastructure objects. These case studies confirm that it is feasible to apply this methodology to conduct a detailed comprehensive assessment of the natural hazard risks affecting the built transportation infrastructure. Furthermore, through quantifying the natural hazard risks affecting each infrastructure link, an infrastructure manager can determine the potential losses facing each infrastructure object and transparently focus the limited funds and time to address the most critical risks. In reviewing these case studies in detail, one can observe that there are three main areas for additional improvement – natural hazard intensity data reporting, direct consequence and service interruption estimation and inter-hazard correlation estimation.

The current methods of reporting the natural hazard parameter intensities, reporting hazard intensity ranges for each event return period (Case Study A) or reporting general hazard risk-based regions (Case Study B), are both too abstract to be directly employed in this assessment methodology without making additional onsite assessments or general estimations. The interesting fact is that in process of developing either of these two reporting formats, much more detailed data is modeled and formulated, but unfortunately this level of data is not included in the final reported data. Thus it is proposed that the natural hazard data reporting practices be expanded so that two different sets of data be reported, one set similar to the current reporting format which is intended to be distributed on printed hazard identification maps and one set identifying the local hazard parameters intensities which is intended to be digitally distributed. Without such an improvement, additional onsite assessments will need to be conducted for each exposed infrastructure object to acquire the needed natural hazard data.

Turning to the second area for additional improvement, the direct consequence and service interruption duration estimation, one can see from these case studies that the direct consequence and service interruption duration values for each hazard parameter intensity threshold has been roughly estimated. With such estimations, one can gain a ballpark estimate of the order of magnitude of the given risk affecting a given infrastructure object but one is unable to directly compare and contrast different hazard risks affecting different infrastructure object types. Thus it is proposed to formulate a group of experienced practitioners who can use their experience to further refine these direct consequence and service interruption duration estimates.

The last main area for additional improvement, intra-hazard and inter-hazard correlation estimation, is currently addressed by developing estimated intra-hazard and geographically-based inter-hazard correlation factors. While such estimates employed within this work are a beginning, further assessment accuracy can be achieved by modeling the intra-hazard and inter-hazard correlation for each of the three main topographic regions of Switzerland – the mountainous region, the valley region and the plain region. Through such additional work, one would be able to clarify and validate the intra-hazard and inter-hazard correlation estimates currently employed in this vulnerability and risk assessment methodology.

While the comprehensive vulnerability and risk assessment methodology developed in Chapter 3 and applied to analyze two different case studies in Chapter 4 does require additional industry and research activities before it is employed in a large-scale implementation, it does form, for the first time, a solid and comprehensive methodology for quantifying the risks affecting the built

transportation infrastructure. With this quantified risk, risk managers can start to address the most pressing issues, but the long-term implementation of analytically optimal maintenance solutions address sudden or gradual failure modes are still exposed to financial funding support failures due to incongruent evaluation of the provided level of performance between the infrastructure manager's nominal evaluation measures and the experiencing society.

These exposures are addressed in the second half of this work. Chapter 5 identifies the infrastructure object parameters the public personality interacts with. It then specifies a process for modeling how the performance differences between subsequent interactions can be evaluated using two case studies to illustrate how an individual's experience-based assessments evolve in time as the individual interacts with a changing infrastructure system. Next in Chapter 6, the work formulates an approach for incorporating additional experiences into the individual's evaluative norms. The affective assessment approach is then employed to analyze two cases to better understand the implications an experience-based evaluation approach can have on the evaluations of a set of interactions (Case Study E and Case Study F). These case studies examine the implications an experience-based evaluation perspective has for individuals with different experience histories and within environments with different deterioration rates. Lastly, the feasibility of applying such an experience-based evaluation approach is assessed in Chapter 7 by conducting a pilot study (Case Study G). In this study, it is determined that conducting a calibration study was not feasible within this work, but should be pursued in the immediate future. The work comes back to the Comprehensive Natural Hazard Risk Assessment Methodology in Chapter 8, the conclusion.

5 Social experienced-based with an infrastructure system's condition

5.1 Introduction

Operating and maintaining an infrastructure system is a union of two dichotomous entities: the analytical civil engineer and the experiencing public. In a perfect society, the concerns of the former would be actively and completely supported by the latter, but in practice, this support can be less than incomplete. This chapter presents two descriptive case studies to demonstrate how the public's experience-based assessments can fluctuate in time, to highlight core elements central to quantifying the dynamic social experience-based assessment of risk, and to conjecture the potential ramifications of divergence between these two dichotomous entities. The first case study analyzes the changing social assessments following a fatal motor vehicle-pedestrian accident in the center of Lausanne, Switzerland. The second case study focuses on an individual's theoretical interaction with the Brooklyn Bridge and investigates how an individual's experience-based assessments may evolve as they interact with a given infrastructure object. This chapter closes by descriptively exploring the potential implications such fluctuating social experience-based assessed performance observed in these two cases may have on the management of infrastructure systems.

5.1.1 Incongruent evaluation methods

Civil engineers employ codes and guidelines developed from laws, jurisprudence and industry practices to maintain the built civil engineering systems. Often civil engineers find that their analytically optimal maintenance solutions fail to be fully realized because societal funding or approval is left unfulfilled (ASCE, 2005) (The Economist, 1999) (The Economist, 2005). It is this human and social influence that can be a failure source of the analytically optimal maintenance plans (The Economist, 1998). To better understand this dynamic process and to develop truly sustainable solutions, civil engineers must personally understand and actively consider how society's experience-based evaluation of an infrastructure system dynamically evolves in time.

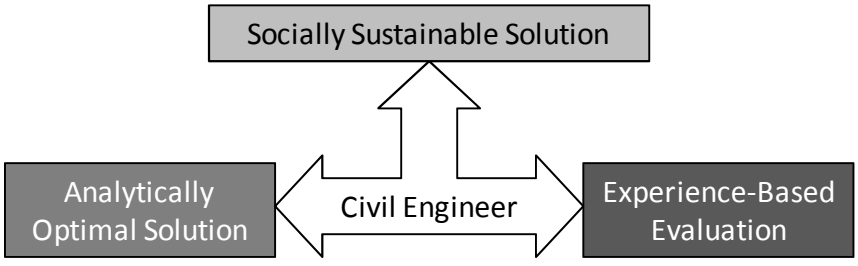

Figure 5-1: Civil engineer's role in developing sustainable solutions.

5.1.2 Engineer's vs. society's evaluation

To become a civil engineer, a person conducts extensive training over a number of years to learn how to quantify forces, stresses, strains, deflections and eventually failure probabilities. As a result of this training, when a civil engineer views a bridge, he no longer sees just an elevated roadway connecting two separate landmasses, he instead sees stresses and moments, cracks and corrosion. Civil engineers, individually and as a community, have employed this analytical viewpoint to develop

observation-based inspection and assessment methods to detail the current level of performance, model future performance levels, and estimate the funds required to achieve given levels of future performance (Hartle, Thomas, Mann, Danovich, Sosko, & Bouscher, 2002). This inspection and assessment process has been automated and streamlined through the development and implementation of bridge management systems.

Like a civil engineer, each person in society has also conducted extensive training, but rather than studying problem analysis and analytical assessments, this training relies on personal interactions and experiences. This training starts soon after birth and continually develops and evolves with each additional interaction within the bounds of the person's mental and physical capacities (Simon, 1957). To evaluate each new interaction and to determine and select the desired response, each person employs their previous experiences to form evaluation benchmarks or norms. An evaluation norm is herein defined as the perceived summary of the set of all previous interactions with a specific parameter and is employed to evaluate future interactions with the given parameter. Following each interaction, the interaction's result and ramifications are assessed against the individual's norm and this assessment is subsequently incorporated into the existing evaluation norm which in turn is employed by the individual to assess the next interaction (Kahneman & Miller, 2002). A detailed presentation of the specific steps of an evolving evaluation process is detailed in Chapter 6.

To demonstrate one approach currently employed by civil engineers, consider the Life Quality Index (LQI) an approach employed to evaluate the loss of a human life.[7] The LQI is a financial evaluation of the maximum optimal life-saving investment that should be employed to save a life given the local country's annual production, life expectancy and work to leisure ratio. The developers of the life quality index propose that engineers should analyze potential life-saving investments within a cost-benefit framework and employ the LQI as an upper bound on the value of a human life. Through implementing this approach, the LQI developers envision that civil engineers can equally distribute risk reduction funds, that risk management decisions can be transparently conducted, and that once the assessment process is known and accepted, this approach can remove the day-to-day risk decisions from the public arena, where in the LQI developers' opinion, it does not belong (Nathwani, Lind, & Pandey, 1997).

Unfortunately, when civil engineers conduct such an analysis they are only considering the life saving investment of their particular project – a minute section of the environment. From this analysis, risk reduction measures which are assessed as too financially prohibitive are prevented from being implemented and thus, in principle, funds can be allocated to more pressing risks. An example posed by the LQI developers is the potential investments of chloroform reduction at 70 pulp and paper mills (an investment of $19.3 million/life saved) verses the investment in reducing developing world diarrheal diseases (an investment of $1.03/life saved). They argue, admirably so, that such risk reduction funds should be reduced from prohibitive investments like chloroform reduction and increased for advantageous investments like diarrheal disease reduction programs (Nathwani, Lind, & Pandey, 1997).

Unfortunately, the LQI developers have failed to recognize the lack of a mechanism to transfer these saved risk reduction funds to these more worthy causes. Rather such saved risk reduction funds are commonly split between internal profit for the owner (the pulp and paper mill owners) and external

[7] A detailed analysis of the Life Quality Index is included in Appendix B.

cost savings for the customer (the paper product customer). The end result of implementing such an approach is that a nominal evaluative measure of the maximum life-saving investment is publically stated, no mechanism is specified for shifting these saved funds to more pressing needs and by removing the decision process from the public realm, decision makers are exposing themselves and their decisions to potential evaluation gaps between their nominal evaluative measure and the societal experience-based evaluation of a potential life saving investment.

Rather than blindly employing such nominal values or attempting to construct a regulatory framework to administer the redirection of saved risk reduction funds to more worthy causes, it is proposed that civil engineers must establish a better understanding and actively consider how society's experience based evaluations are formed and dynamically evolve in time.

5.2 Case Study C: Changing perceptions in a post-intentional action environment[8]

5.2.1 Case Study Overview

Managing civil infrastructure, particularly in a post-intentional action environment, is a complex process and potential risk mitigation structural modifications often can jeopardize the financial sustainability of a given civil infrastructure. This case study presents the social and infrastructure management ramifications resulting from a non-ideologically motivated intentional fatal motor vehicle accident on a major bridge in the center of Lausanne. The public exposure to the intentional action, the civil infrastructure management following the intentional action, the media coverage and the subsequent criminal investigation are qualitatively analyzed.

This analysis shows that the post-intentional action criminal investigation and public usage of the operating civil infrastructure object can substantially reframe and attenuate the potential social experience-based assessed risk. Furthermore, infrastructure managers can, once the object has been deemed safe by structural engineers, attenuate social assessed risk by returning the object to full public use following an intentional action. Thereafter, the civil engineer can focus on primarily technical aspects in reviewing and developing potential long-term risk mitigation structural modifications.

5.2.2 Grand-Pont: A Lausanne transportation link

The Grand-Pont was built in 1844 to span the Flon river valley which, at the time, separated Lausanne from Lake Geneva and the vineyards to the south and east. The Grand-Pont was built as a 175 m long, 10 m wide and 25 m high masonry arch bridge comprised of six inferior and 19 superior arches, Figure 5-2a. The bridge has since undergone four major modifications to raise the surrounding earth to the top of the inferior arches (1874), to widen the roadway by adding cantilever pedestrian walkways and replacing the pedestrian railings (1892), to further widen the bridge to the current width of 15.3m by increasing the length of the cantilevered pedestrian walkways (1934), and to refurbish the masonry arch pillars (2001) (Rapport du Jury, 2005), Figure 5-2b. Since the 1840s, the City of Lausanne has extended southward and the Grand-Pont has become the key transportation link connecting Lausanne's commercial, governmental and religious centers with the judicial and

[8] Portions of this case study are based upon (Birdsall & Brühwiler, 2006a).

transportation centers. The geographic position held by the Grand-Pont can be seen in Figure 5-3 in which the roads in the Flon river valley are shaded black and the pedestrian-only roadways are shaded gray. As a result of its position, in the year 2003, the Grand-Pont experienced an average daily vehicular traffic of 15,600 vehicles.

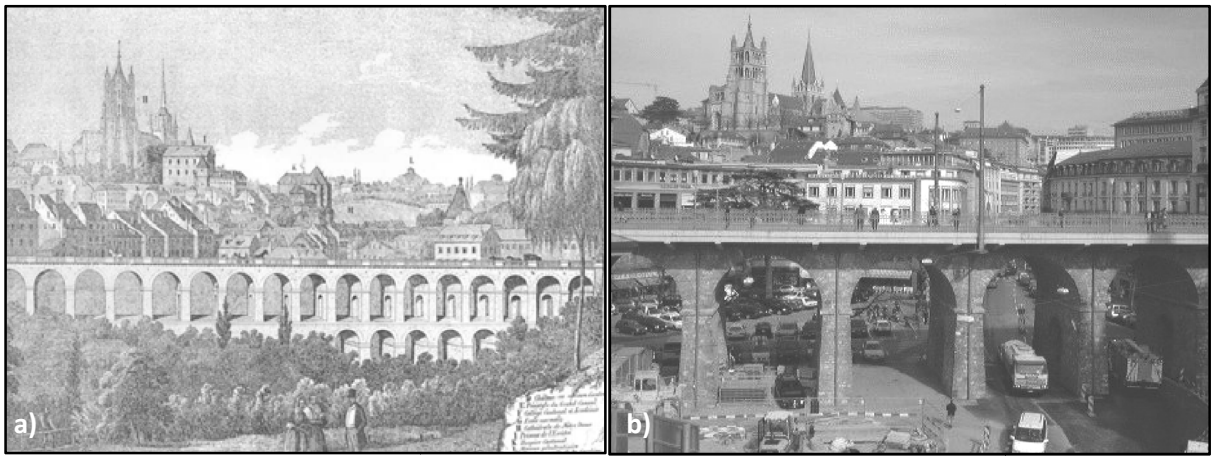

Figure 5-2: a) Grand-Pont engraving shortly after completion 1844, b) The Grand-Pont elevation in 2004.

5.2.3 Lausanne demographics and mortality data

Lausanne is a city of 125,000 composed of 63% Swiss and 37% foreign residents situated on the northern shores of Lake Geneva. Lausanne's average mortality and accident data, and annual personal event experience and exposure for the two years preceding 2003 are presented in Table 5-1. The occurrence of death and traffic injuries is relatively common during a given year, but the occurrence and direct exposure to vehicular deaths and homicides is relatively rare. This is the environment of experience in which the Grand-Pont accident occurred.

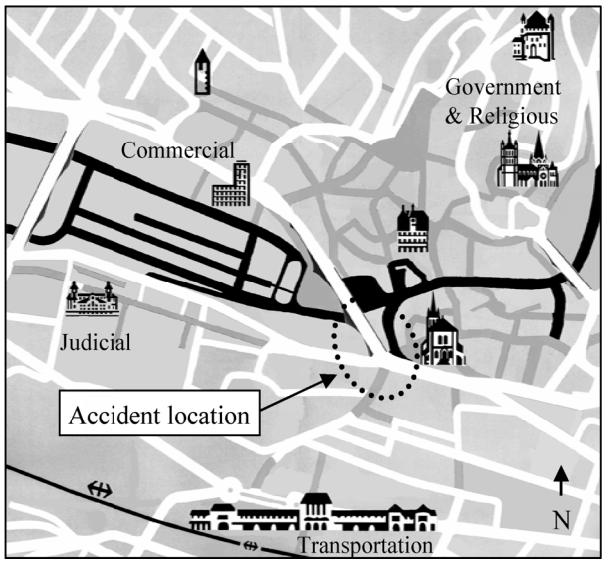

Figure 5-3: Lausanne traffic network (Lausanne Tourisme, 2003).

5.2.4 The Grand-Pont Accident details

On July 8, 2003, at the height of the mid-day lunch hour, a car approaching the Grand-Pont left the roadway, drove down the bridge's eastern pedestrian walkway, through the pedestrian railing and off the bridge – landing on a roadway 11 meters below. The Opel Vectra was traveling at 50

Table 5-1: Average yearly Lausanne mortality and traffic statistics (2001-2002) (Canton de Vaud, 2006).

Item	μ	Experience*	Exposure**
Total deaths	1142	1 in 111	1 in 1.11
Vehicular deaths	8.5	1 in 14,919	1 in 149
Homicides	1	1 in 126,814	1 in 1,268
Suicides	23.5	1 in 5,396	1 in 54
All violent deaths	61.5	1 in 2,062	1 in 20.6
Traffic accidents	1929	1 in 66	1 in 0.66
Traffic injuries	491	1 in 258	1 in 2.58
Pedestrian accidents	101.5	1 in 1,249	1 in 12.5

* Chance of personally experienced during an average year. ** Chance of being exposed during an average year (based on an assumed average exposure radius of 100 people per given event).

kilometers per hour when it entered the sidewalk at the Rue du Grand-Pont pedestrian crosswalk, Figure 5-4 (Antonoff, 2003). As the car drove down the sidewalk, between the road and the building, it came in contact with ten pedestrians, leaving six people injured on the sidewalk and sweeping another four off the walkway on its hood – crushing and killing three of the four on the roadway below (Le Matin Online, 2003a). The deceased included three women aged 22 to 40, one of whom was 21 weeks pregnant. The injured included three men, three women and a child aged 2 whose pregnant mother was killed in the accident. The driver of the car suffered minor injuries in the accident and was detained for questioning (Combremont, 2003).

The first responders to the injured were the adjacent witnesses and local police officers. One officer immediately drove the injured 2-year-old to Lausanne's hospital even before the emergency crews arrived. Within two minutes of the accident, emergency ambulances and fire crews started to arrive at the accident scene, in all nine ambulances and 22 medical emergency personnel responded to the accident (Zingg, Le Matin, 2003a). The affected individuals were assessed and stabilized or recovered onsite before being transported to the local hospital, Figure 5-5a and Figure 5-5b. The accident was observed by pedestrians walking across the Grand-Pont, patrons eating lunch in neighboring restaurants, and employees and clients standing in the adjacent businesses (Antonoff, 2003). As the emergency response mounted, pedestrians congregated on the eastern Grand-Pont walkway to watch the on-going emergency rescue, Figure 5-5c. Rescue personnel employed blankets to shield the public's view during the recovery operation and the Grand-Pont vehicular traffic was halted in both directions during the rescue effort to facilitate access to the accident site (Le Journal, 2003a) (Le Journal, 2003b).

In the days following the Grand-Pont accident, there was an out-pouring of public mourning for the injured and deceased, and disbelief and anger directed against the driver. The accident location became a make-shift shrine where members from the public congregated to lay flowers and pay their respects to the injured and deceased. One mourner even experienced a subsequently fatal heart attack at the accident site (Zingg, 2003b). The public reaction became more complex two days after

Figure 5-4: Vehicular accident location and trajectory

Figure 5-5: a) Emergency personnel tending to pedestrians on the Grand-Pont walkway (Genevay, 2003), b) Personnel respectfully recovering the deceased who were crushed by the falling car (Genevay, 2003), c) Pedestrians watching the rescue and recovery efforts (Le Journal, 2003a).

the accident when one of Lausanne's two principle newspapers ran the phrase "Suicidaire et meurtrier" (Suicidal murder) as its front page title, provided the driver's name and reported the driver's previous attempt to commit suicide (24 Heures, 2003).

Even though the accident did transpire on private property, the Lausanne municipal town council representative for public works, Olivier Français, a practicing professional civil engineer, gave a public statement from the accident site on the evening of the accident. He stated that the occurrence of a car driving fifty meters down a pedestrian sidewalk, hitting a railing that was located in a vehicle-

restricted zone and breaking through this railing which was design purely for pedestrian loading was completely unforeseen, but he assured the public that Lausanne's bridges and pedestrian railings met the Swiss building codes (Le Journal, 2003a). In the days following the accident, the private owner of the pedestrian railing replaced the original railing with a similar strength railing, citing the original railing did meet pedestrian loading requirements and was located in a vehicle-restricted zone (Rime, 2004).

On the evening of the first accident, the driver was questioned by the police. He stated that as he was turning onto the Grand-Pont, his attention was distracted as he adjusted the station on his radio. As an unintended result, he reported, his car deviated and when he lifted his eyes from the radio, he noticed he was on the sidewalk and there was someone in front of him. Thereafter, he lost control of his car. The driver remembered hearing screams but did not remember hitting and running over pedestrians, driving through the pedestrian railing, or driving off the bridge. The next memory the driver did have was unbuckling his seatbelt, extracting himself from the car, and waiting beside his overturned car for medical attention.

On July 22, 2003, the driver was charged with first degree murder, attempted second degree murder, intention to cause serious and minor bodily harm, endangering the life of others, and reckless driving (Bédat, 2003). The driver's lawyer requested the judge to issue a complete review of the Grand-Pont, the pedestrian sidewalk, the driver's car, and the driver's physical and mental states at the time of the accident (Co, 2004). This request was granted and the subsequent multi-faceted review extended from the fall of 2003 until July 2005 (Passer & Bédat, 2005). The Lausanne Judicial Tribunal examined this review and judged the driver mentally sound at the time of the accident and therefore able to stand trial. A criminal trial was convened in November 2005 and the driver was found guilty and received a 10-year sentence (Le Temps, 2005).

5.2.5 The second Grand-Pont accident

At 1:30am on October 18, 2003, four months after the first Grand-Pont accident, a second man attempted to commit suicide by driving off the Grand-Pont. Contrary to the previous incident, this individual made his attempt in the middle of the night rather than in the middle of the day and obliquely engaged the pedestrian railing at the center of the bridge rather than perpendicularly engaging it on the Grand-Pont approach. These modifications, combined with the fact the driver also intercepted one of the lamp posts that lines the Grand-Pont, prevented his car from leaving the bridge surface. The vehicle impact did dislodge a 4 meter section of pedestrian railing and the adjacent lamp post from the bridge which fell and crushed two cars parked underneath the Grand-Pont.

No one was hurt during this incident, but this second incident reinforced the potential lack of safety provided by the Grand-Pont railings, particularly in the face of this new risk source. Furthermore, the second accident occurred in a location where the City of Lausanne had complete legal responsibility.

The Lausanne public works response following this second accident was to immediately strengthen the existing railing by connecting each individual railing section together with two steel wire ropes threaded through the cast iron railing elements at two different elevations.

Additionally, the Lausanne civil engineering office initiated a long-term railing design selection process and public design competition to determine a location-specific architecturally-appropriate permanent method to separate the roadway from the walkway (Muhieddine, 2003). A permanent

design was selected in November 2005, Figure 5-6, which employed intermittently spaced concrete and metal bollards to visually and physically separate the roadway from the walkway and a walkway railing designed to withstand standard pedestrian loads. This conceptual design was selected because it minimized the visual and logistical impact on the Grand-Pont while physically separating the vehicular and pedestrian traffic. With this design selected, the fiscal and construction phases are

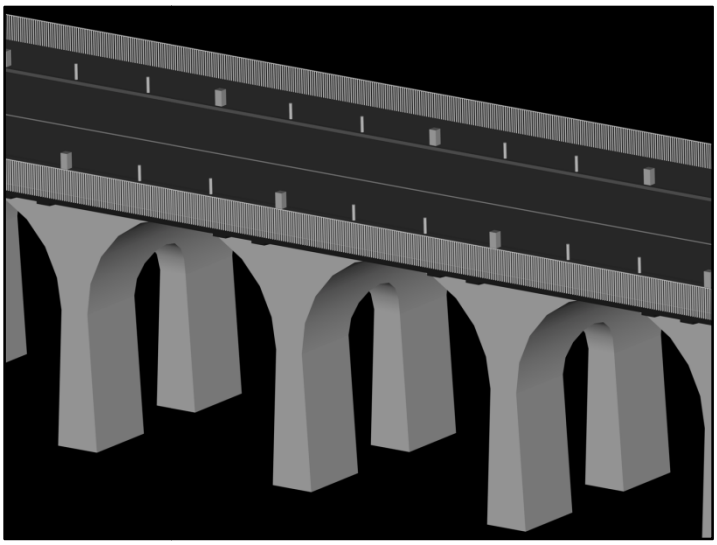

Figure 5-6: Selected permanent vehicular and pedestrian restraint design (Rapport du Jury, 2005).

in process (Prin, 2005) but as of the fall of 2008 this conceptual design has not been further developed.

5.2.6 Lausanne's experiences in time

The Swiss form of LexisNexis®, Swissdox, was employed to obtain topic specific news articles published during the time period studied to develop an event timeline and to determine the media content exposure for each population region. Swissdox is a web-based printed media archiving service that facilitates complete article text querying of 61 swiss-german, 21 swiss-french and 1 swiss-italian printed media sources by key-word and time period. For a given search, Swissdox provides the article text, the first three lines of text, the title of the originating media source, the publication date, the total number of words, and the option to download a copy of the original text (Swissdox, 2006).

Linguistically universal key-terms "Lausanne" and "Grand-Pont" were employed to ensure the conducted search included media sources from all three languages. A primary search was conducted using the time period July 1, 2003 to March 1, 2006 and netted 1758 potential articles. This set of potential articles was then reviewed for relevancy to the Grand-Pont accident, the public reaction, or the resulting criminal trial by using the title and the first three lines of text. Instances where a media source printed a given article in multiple editions of the same media source were counted only once to ensure each article was not doubly counted. Through hand sorting, the original set of 1758 articles was reduced to a final data set of 198 articles. This set was then sub-sorted by date, geographic audience and topic.

The article set's temporal distribution by month is presented in Figure 5-7 and is overlaid by key events and periods for reference. It can be observed that while there was initially strong media presence following the accident, this presence quickly diminished. Additional media attention surges were registered when the second Grand-Pont accident, the first railing modification, and the Grand-Pont accident first anniversary occurred. Otherwise between August 2003 and June 2005, while the complete review of the Grand-Pont, the car and the driver were in process, the media attention directed at the Grand-Pont accident was relatively light. The media attention returned to the Grand-

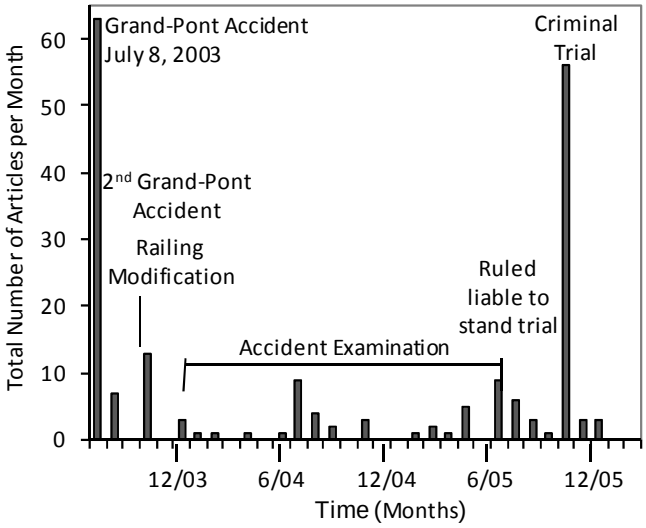

Figure 5-7: Article temporal distribution by month.

Pont accident when the driver was ruled liable to stand trial and reached a heightened apex during the criminal trial.

The geographic reach of each event was investigated by sorting the article data set into three groups by geographic target audience (Lausanne, Geneva and the Swiss-German region of Switzerland). The number of articles published in each geographic region per month is plotted in Figure 5-8. One can

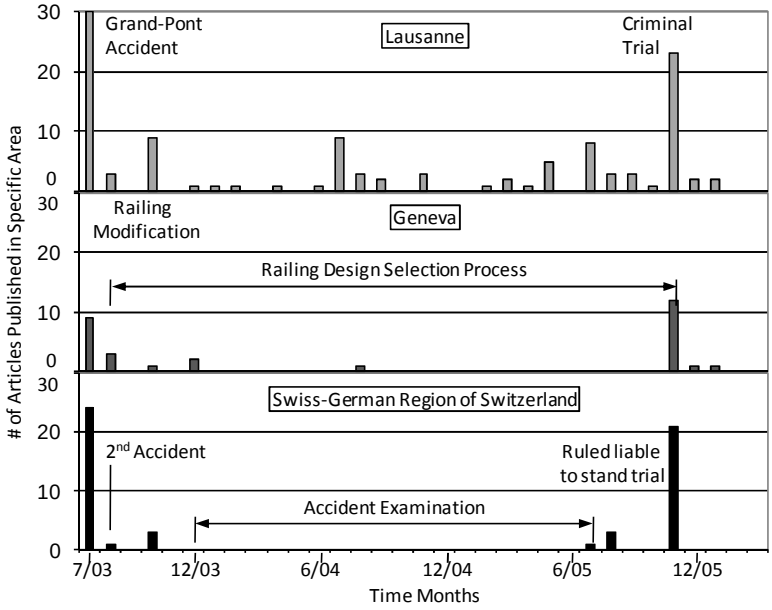

Figure 5-8: Number of articles published within the Lausanne, Geneva, and Swiss-German regions of Switzerland per month.

observe that the Grand-Pont accident and the initial investigation reporting spanned all three geographic areas. The coverage of the 2nd accident likewise extended to all three areas but at a reduced magnitude. Thereafter, between January 2004 and June 2005, during which the accident review and the long-term structural modification selection process transpired, only the Lausanne media sources published articles. The Grand-Pont accident articles did once again span all three regions once the criminal trial began.

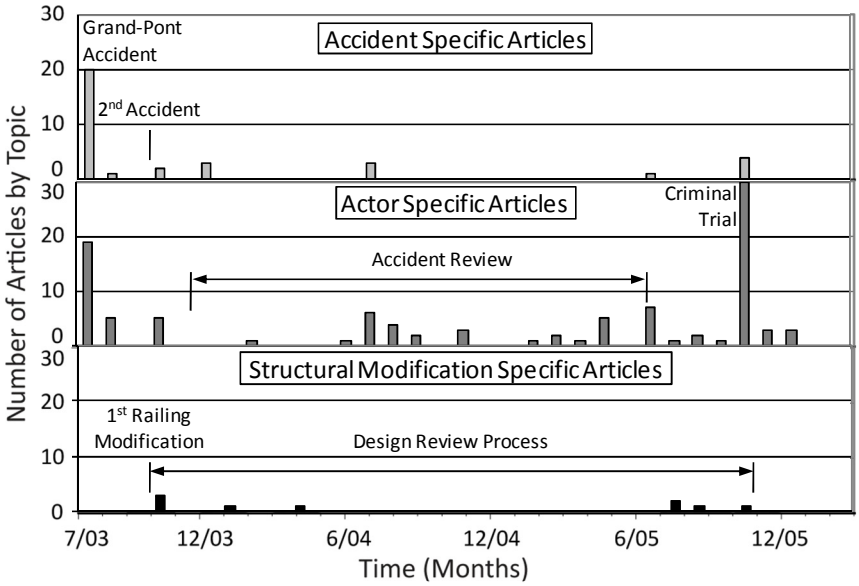

Figure 5-9: Accident, actor, and structural modification article topic comparison.

The geographic article data for Lausanne and Geneva were then sub-sorted by primary topic into accident specific articles, actor specific articles and structural modification specific articles by reviewing the title and the first three lines of text of each article. The topic temporal distribution is presented in Figure 5-9. One can observe the accident specific articles were focused around the time period immediately following the accident, the second Grand-Pont accident, the accident's first year anniversary and the criminal trial. Juxtaposed, the actor specific articles were also initially focused around the accident, but were thereafter distributed between June 2004 and October 2005 as the Grand-Pont accident complete review was being conducted. Additionally, this media attention was almost purely focused to the Lausanne region. The actor specific media coverage then reached an apex during the criminal trial in November 2005.

While the accident specific and actor specific articles were actively published during the time period studied, a surprisingly few number of structural modification specific articles were published. The structural modification articles started at a diminutive apex during October 2003 following the second Grand-Pont accident. Thereafter, between the emergency retrofit in October 2003 and the selection of a conceptual permanent design in November 2005, very few structural modification focused articles were published.

The Swiss residents, and the Lausanne residents in particular, were also exposed to an indiscernible risk education source – their personal usage and interaction with the operating Grand-Pont. As mentioned earlier, the Grand-Pont carries an average daily vehicular traffic of 15,600 vehicles. Without even considering the active pedestrian or public transport traffic, this vehicular volume is equivalent to 8% of Lausanne's population crossing the Grand-Pont twice each day. Through this

personal exposure, a large portion of Lausanne's population had the opportunity to personally experience and reconfirm the safe operation of the Grand-Pont.

5.2.7 Reframing and attenuating experience-based assessed risk

The individuals present at the first Grand-Pont accident and emergency response were exposed to a high intensity experience through personally viewing the accident and emergency response. The broader Lausanne community was also exposed to the accident through the subsequent intense media coverage. But the duration of these first and second hand personal experiences were temporally limited as the Grand-Pont returned to operation within hours of the accident and the media attention dissipated in the month following the accident.

Four months after the first accident, there was an additional intentional action directed against the Grand-Pont pedestrian railings, but the Lausanne public was shielded from this event by the occurrence time (1:30am) and the limited media exposure. But the Lausanne community was not shielded from their personal usage of the Grand-Pont in their necessary daily activities, the long-duration criminal investigation and the criminal trial actively detailed in the media.

It is argued that these additional events significantly reframed and attenuated the experience-based safety risk assessment impression made by the Grand-Pont accident. This attenuated perceived risk can be observed in the fact that only 9 articles, 4.5% of the total 198 Grand-Pont articles addressed the safety, the emergency structural retrofit or the long-term structural modifications as its primary topic. This attenuated social experience-based risk assessment afforded Lausanne's civil engineering community the professional freedom to respond to the events as they unfolded from a primarily technical standpoint – first by rationalizing the low potential for additional intentional acts, then by quickly responding by implementing a limited-term emergency retrofit and initiating a systematic conceptual permanent design selection process.

5.3 Case Study D: Experiencing an evolving evaluation[9]

5.3.1 Case Study Overview

Managing and mitigating civil infrastructure gradual deterioration comprises the bulk of an infrastructure manager's maintenance focus. Furthermore, the glacial rate at which infrastructure objects deteriorate can present management difficulties in their own right. This case study presents a descriptive theoretical set of interactions and the associated induced assessments an individual has with a specific object. These interactions and assessments are then analyzed to identify what elements are within the scope of civil engineers, what ramifications such experience-based assessments pose to the management of infrastructure systems and potential management solutions.

5.3.2 An evolving normative evaluation

To detail an evolving normative evaluation, please join the author on a mental pilgrimage to the Brooklyn Bridge. To set the stage, assume the reason for the pilgrimage is because you have been

[9] Portions of this case study are based upon (Birdsall & Brühwiler, 2006b).

transferred to your company's office in downtown Manhattan and they have arranged an apartment for you in Brooklyn on the opposite side of the East River from Manhattan.

After spending two days in New York City meeting with your future co-workers and taking a cab over the Brooklyn bridge to see your apartment, you decide to spend your last free afternoon before you leave walking across the Brooklyn Bridge along your future commuting path. As you walk across the Brooklyn Bridge, you notice that the walkway you are on is above the traffic which is rushing past by below. Then you start to notice the bridge's late 19th century architectural detail and as you approach the western tower, you start to notice the intricate web of stay and suspender steel wires descending from the tower top and from the main cable. As you approach mid-span you turn to look south, into the sun, and from there you can see Governor's Island and the New York Bay in the distance and you think to yourself, I can make this move.

The first morning

Your next interaction with the Brooklyn Bridge is four weeks later on the morning of your first day in the New York Office. The preceding weekend you had just moved into your apartment and now is the time for the work week to begin. As you walk across the Brooklyn Bridge you notice that there are many more people walking and biking over the bridge. Many just like you are dressed in business clothes and are heading off to work, others are out for some early morning exercise. The walkway you are walking on is divided down the middle like a street with each direction taking a side. As you work your way across the bridge you find yourself passing slower walkers and moving quickly towards the railing to avoid bicyclists that rush past you. As you continue toward work, even though you and the people around you are walking in the same direction, there is no personal exchange amongst you, no head nods, no smiles, not even a good morning. Walking with, past and around these people feels like walking through a row of thin concrete colonnades for the people surrounding you are warm and as friendly as concrete. You had heard New Yorkers could be cold and curt, well now you've started to experience it firsthand.

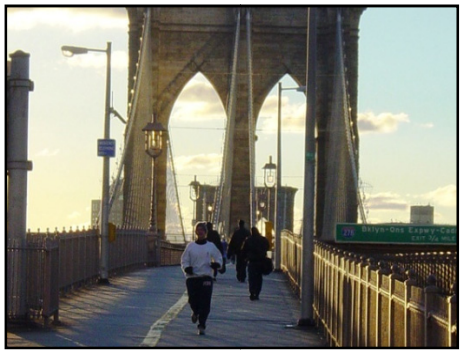

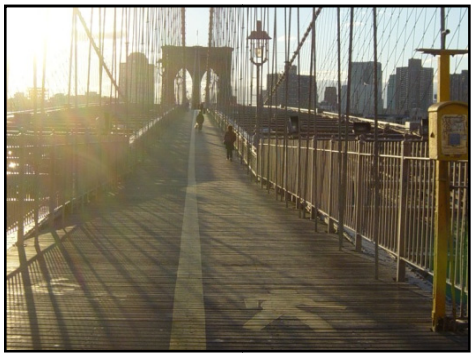

The return trip home

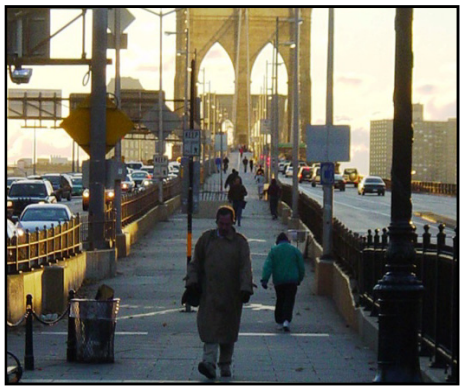

On your return trip home after spending your first day filling out paperwork, you notice blisters forming on the backs of your heals. You guess the combination of fairly new shoes and a noticeable increase in your amount of daily walking is not the best combination. As you reach toward mid-span your concentration becomes focused on the orange and red sunset accents filling the sky. On your way off the bridge and toward your apartment you can feel the chill of the fall starting to set in and you know that it will soon be a bit harder walk.

Third week of work

By now you have purchased more comfortable walking shoes and a large vented umbrella and you find that you have gotten used to the daily commute or rat-race as some might call it. Now that you've grown accustomed to the commute, you are no longer taken back by the curtness of the people (some of your friends might even say that you've grown a bit more curt yourself) or by the views and sights from the bridge – granted you still do stop and watch the last few moments of sunlight on particularly clear days. Now you find yourself noticing the large semi-tractor trailers that pass on the roadway below and their exhaust that wafts onto the walkway. You also notice the amount and arrangement of trash and litter on the walkway and how it varies with the wind, the time of day and the cleaning cycle of the garbage men. What you have also started to notice is the small variations in the localized deterioration of the main cable paint and wire wrapping, the walkway's wooden boards, and the chain-link fencing boarding the walkway.

Six months later

By the end of February you've amassed quite a range of "commuting" clothing including a thick down parka, wind proof hat and gloves, heavy-duty hiking boots for those mornings when the New York area is blanketed in snow, and of course a hand-knit wool scarf. Your co-workers were not surprised to see you walking to and from work during the warmer months of September and October but now in the depths of February they give you strange and inquisitive looks when you arrive to the office red-faced and foggy-glassed. Additionally, now that you've grown accustomed to your environment, you now only notice particularly out of the "ordinary" things like tourists walking and gawking as they

cross the bridge in the morning, or damage left behind by some individual who had too much "fun" the preceding night. It is only the items presenting a significant environmental change from day to day that draws your attention now, not the views, not the traffic, not the curt people, not the long walk, and not the cold air – only the items that significantly change.

5.3.3 Analyzing personal evaluation evolution

From the descriptive example included above, it can be observed that when an individual interacts with and evaluates his environment, the evaluation process is limited to parameters personally experienced. For a civil engineering object such as the Brooklyn Bridge this set of evaluation parameters include such items as the architectural appeal, the traffic volume, the surrounding views, the walkway surface and the general cleanliness. A further interesting observation is that the bridge's current condition is not directly employed in the evaluation process, for a number without a benchmark is valueless. Rather it is the structure's changing performance with respect to the individual's evaluation norm, formed from the individual's interactions with the given bridge and similar bridges. In formulating the norm for a given parameter, a given person mentally references each previous interaction they have had with the given parameter and weights each interaction by the relative variance the said interaction has in reference to the respective norm (Slovic, Finucane, Peters, & MacGregor, 2002).

One can also see that during the first few interactions the individual responds like a tourist. The individual's attention is initially drawn to the parameters in the environment exhibiting the most significant change to his previous interactions – the architecture, the view from midspan, the number of commuters, the demeanor of the people. After a number of interactions, the person's physical adaptation (the purchasing of activity appropriate gear) and the experience-based evaluation norm adaptation starts with the parameters exhibiting the largest amount of change taking the lead. Over time, this evaluation norm shifts thereby reducing the impact these parameters have on the individual and allowing other parameters to draw the individual's attention such as the truck exhaust, the amount and location of litter, and localized deterioration. Following a large number of interactions, the person completes the physical and evaluation norm adaptation to the "new" environment resulting in the individual noticing only the items which change within this "new" environment.

5.4 Parameters influencing social experience-based assessments

To identify parameters influencing social experience-based assessments, one must observe that society's interaction with an object is influenced by the structural and system parameters, the individual user parameters and the temporal frequency of these parameters. Parameter classification and examples from the Brooklyn Bridge series interactions are presented in Table 5-2. From Table 5-2 it can be seen that a majority of parameters are beyond the influence of the civil engineering field and there are only a few parameters such as the use of the structure, the structural condition and

Table 5-2: Parameter source, temporal nature and examples

Parameter source	Temporal nature	Examples
Component/system	Continually evolving	Pedestrian traffic, weather, structural condition
Component/system	Discrete event	Localized trash and damage
Individual user	Continual evolution	Adaptable to social and physical environment
Individual user	Discrete event	Blisters, commuting clothing

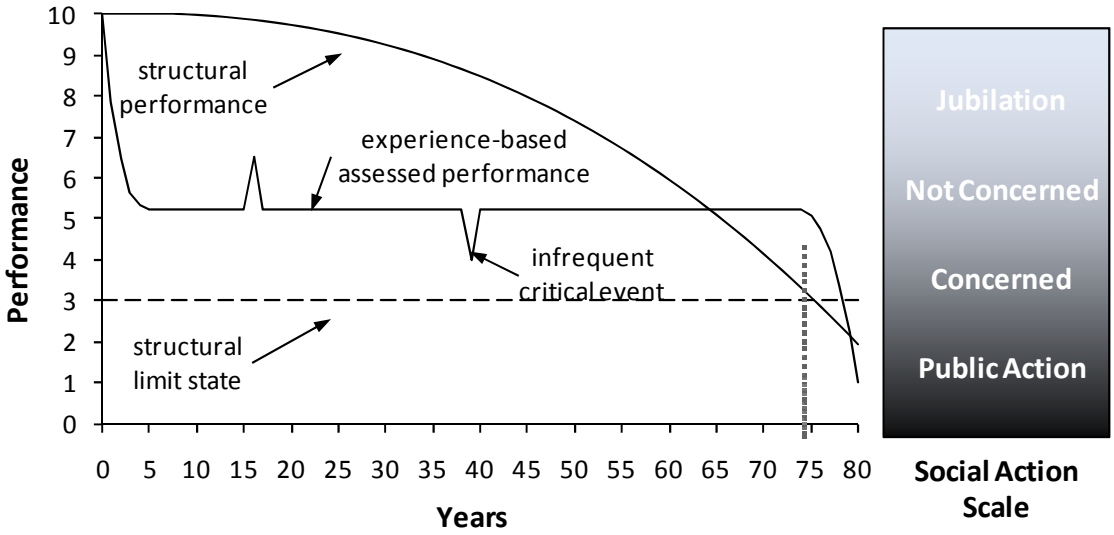

Figure 5-10: Experience-based assessed performance as a function of structural performance in time.

the localized damage level within a civil engineer's realm.

To hypothesize about the potential ramifications of evolving societal evaluation one must recognize the incongruent evolutionary rates of a bridge's deteriorating condition and society's adaptation to this changing environment. Bridges are commonly designed with life-spans of 80 or additional yearsas shown in Figure 5-10, but as seen in the Brooklyn Bridge case example, an individual is able to adapt to and with the changing environment in a matter of weeks or months. *Therefore, as an infrastructure object slowly ages and starts to deteriorate, society is unable to recognize this deterioration for they are evolving with the changing environment.*

As is presented in Figure 5-10, society only recognizes and considers the condition of a bridge when:

1) The object is newly built
2) Distinguishing positive and negative events occur
3) The object reaches a critical deteriorated state

Therefore as an object deteriorates, currently within the realm of a bridge's condition, it is only the occurrence of infrequent critical events and when the bridge reaches a limit state (safety, serviceability, durability) that can induce society to recognize the deteriorated condition of a bridge.

This phenomenon was also observed and very well documented in Graham and Thrift's assessment of societal aspects of repair and maintenance.

5.5 Communicating to society

Civil engineers currently communicate to society by employing their expertise to advise society of potential dangerous situations (ASCE, 2005) and by employing their responsibility as wards of the society's wellbeing to limit the use of or close infrastructure objects in critical condition (Hartle, Thomas, Mann, Danovich, Sosko, & Bouscher, 2002). It is suggested that civil engineers currently fail to even consider estimating the potential impact analytically optimal management solutions may have on the society's experience-based assessment of performance and what constraints this evolving assessed performance may impose on funding and implementing the analytically optimal management solution.

For instance, as shown in Figure 5-11, a focused, high quality but incomplete maintenance action implemented to change elements society regularly interacts with has the potential to provide society with an evaluation benchmark thereby facilitating each individual in personally experiencing the level of service provided. Such evaluation benchmarks are particularly poignant for assessing structural deterioration. When taken one step further, such focused actions when implemented as the given object is approaching an increased deterioration state have the potential to aid society in identifying structural deficiencies and funding needs.

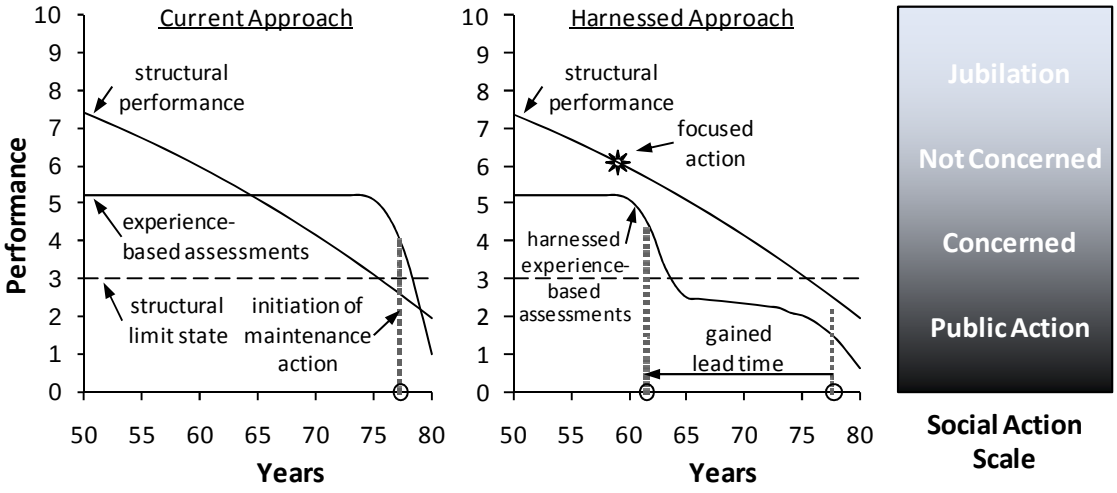

Figure 5-11: Gained maintenance lead time by employing a focused incomplete action.

In the Brooklyn Bridge example, locally replacing the walkway boards or repainting only a part of the railing are examples of focused, high quality but incomplete maintenance actions which are the core of the "Harnessed Approach." While such focused and incomplete actions are, on the face value, individually logistically and economically inefficient, they have the potential to reduce the implementation risks of otherwise optimal management solutions.

5.6 Reflecting backwards – moving forward

To develop and implement sustainable management solutions, an infrastructure manager must have not only an analytically optimal management solution, but also have the long-term political and financial support to fully implement the optimal management solution. Without this support, the implementation of such analytically optimal solutions commonly fail to be realized and in their wake leave a situation which is far from optimal.

The two case studies presented in this chapter detail two different types of situations which must commonly be weathered during the implementation of analytically optimal solutions – a severe discrete event and an individual's evolving evaluative norm.

In Case Study C, it was shown that while the severe discrete event can induce significant responses within the general and civil engineering communities, these induced experience-based assessed risks can be quickly attenuated as the public reinteracts with the operating affected object during their required daily activities and as the public attention shifts to alternative issues. This attenuated experience-based assessed risk can provide the civil engineering community the opportunity to systematically evaluate and respond to such emerging risk sources.

In Case Study D, a descriptive set of interactions were presented to demonstrate how an individual's evaluative measures and thus what they consciously experience shifts as an individual's range and depth of experience grows and evolves. While this ability to adapt is one of the most significant strengths of each individual, it poses significant challenges for the civil engineering community, for as infrastructure objects deteriorate, society unconsciously adapts to this degrading performance. Additionally, an individual's experience-based assessment of the provided infrastructure performance is limited to the elements he personally interacts with – the structure's architectural appeal, the weather, localized damage and personal contextual events. This limited range of parameters poses additional challenges for an infrastructure manager, for it is commonly only the significant structural elements, the bridge girders, expansion joints and decks, which are the primary focus of infrastructure management systems. As it has been theorized in this second case study, an infrastructure manager can transform these socially significant parameters into a communication tool to bring general awareness to the deteriorated state of specific components by implementing focused, high quality but incomplete maintenance actions.

To assess the potential implementation risks induced by evolving societal experience-based assessed risk and thus to select and effectively implement an analytically optimal management solution, methodologies, models and procedures have to be identified and developed for quantitatively assessing societal experience-based assessed risk. These tasks are further developed in Chapters 6 and 7. In particular, existing findings and methodologies for assessing and quantifying perceived risk from numerous different fields are presented in the first quarter of Chapter 6. The elements of a quantitative model for assessing this evolving socially assessed risk, the affective assessment approach, is presented in the middle half of Chapter 6. The affective assessment approach is then applied in two different examples in the last quarter of Chapter 6 to show both the breath of the model and the different influences personal experience, exposure frequency and magnitude of parameter change can have on an individual's induced risk assessments and the individual's evaluative norm. A potential procedure for implementing the affective assessment approach to assess an individual's experience-based risk assessments in an existing infrastructure system is then developed in Chapter 7.

6 Affective assessment approach: Quantifying experience-based evaluations

6.1 Introduction

Infrastructure managers are charged with developing and implementing analytically optimal and financially efficient management solutions to fulfill society's needs. During the past thirty years, infrastructure managers have turned to infrastructure management systems to aid in the development of optimal management solutions. Unfortunately infrastructure management systems determine society's needs by estimating the value of intangibles with nominal measures. While this approach does simplify the solution development process, it actively ignores the potential for societal sensitivity to amplify or attenuate the value of the given intangible.

This chapter develops the affective assessment approach from key psychology tenets to quantify how an individual constructs and refines his experience-based evaluation measures as they are exposed to a sequence of interactions. This affective assessment approach is then employed in three different case studies to show how an individual's affective responses can shift in time. The first case study demonstrates the steps employed by the affective assessment approach to quantify an individual's experience and to reformate his assessed range of experience. To better understand the dynamic trends and local intricacies of societal sensitivity to varying levels of preexisting assessed experience and provided levels of performance, the second case study analyzes three different individuals exposed to seven different levels of performance to highlight how personal experience, frequency of exposure and interaction intensity can influence an individual's induced affect. The third case study analyzes an individual's response to a three-week theoretical construction traffic modification to explore how the induced affect can be integrated directly into the quantification of user costs.

The findings from these three case studies are then employed to assess the feasibility of three potential management philosophies – analytically developed maintenance decisions, socially developed maintenance decisions, and analytically developed socially sensitized decisions.

6.1.1 Experience-based risk assessment – foundations of the affective assessment approach

Infrastructure maintenance is driven by the interaction of three key elements: the infrastructure's deterioration state, the available maintenance funding, and the public's experience-based evaluation of the provided assessment, Figure 6-1. Civil engineers are commonly asked to take a leading role in formulating optimal maintenance plans. Their engineering training and professional experience has provided each civil engineer with the skills to calculate a given infrastructure's deterioration state, to formulate potential short and long-term maintenance methods, and to estimate the relative cost of each potential method. But when it comes to the third aspect, quantifying the public's assessment of the provided performance, civil engineers find themselves beyond their domain of experience. Civil engineers therefore commonly revert to either 1) ignoring societal issues by actively limiting the scope of their work to purely technical issues, 2) employing the precautionary principle and overdesigning the given infrastructure element in question or 3) attempt to include societal issues in

their technical decisions by employing nominal intangible evaluation measures like the Life Quality Index or similar assessment approaches. Unfortunately each of these different approaches circumvent the key issue – society's evaluations are the product of their given interactions with the given infrastructure object evaluated against their continually evolving range of experience which is constructed from all previous interactions and further tempered by all subsequent interactions. This chapter takes an essential step along this path by applying key findings from the field of psychology to develop an experience-based assessment approach to quantify an infrastructure user's assessed interactions.

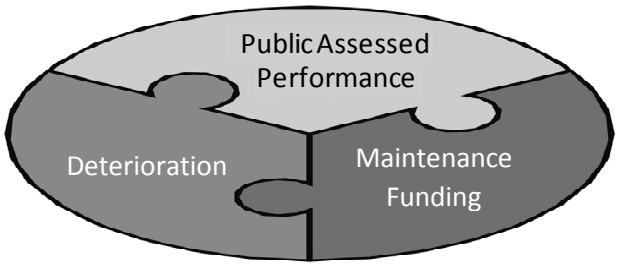

Figure 6-1: Infrastructure maintenance – three key elements.

6.2 The general mechanisms of an evolving evaluation process

6.2.1 Early quantification of an experience-based decision process

Even as early as 1738, it was recognized by researchers in economic theory that not all individuals equally value the same good. In particular, Daniel Bernoulli wrote in his *Exposition of a New Theory on the Measurement of Risk* that the "utility of an item may change with circumstances" and "(t)he man who is emotionally less affected by a gain will support a loss with greater patience" (Bernoulli, 1954, pp. 24, 26). To quantify this phenomenon, Bernoulli proposed equation (6.1):

$$BP = (AC^m \cdot AD^n \cdot AE^p \cdot AF^q \cdot \cdots)^{\frac{1}{m+n+p+q+\cdots}} - AB \tag{6.1}$$

where:

BP = the value of the potential action
AB = the initial value of goods
AC, *AD*, *AE*, *AF*,…. = the future potential value of the goods (sequentially increasing)
m, *n*, *p*, *q*,… = the number of ways the respective action can be achieved

From this equation it can be seen that as the value of the individual's initial value of goods increases, the value of the potential action decreases. Thus a decision that a rather financially limited individual may view as highly valuable, a non-financially limited individual may view with lesser value or even complete indifference. Thus the valuation assigned to a given good, tangible or intangible, is as much a factor of the given good as it is the individual context in which the valuation is made.

6.2.2 Laying the foundation for a contextually based decision processes

The general psychological theory on how individuals define, conceptualize and evaluate their reality – the psychology of personal constructs – was formulated by George Kelly and who first published his theory in 1955 (Kelly G. A., 1955). In working with farmers and other general citizens of the mid-west

United States during the 1930s, Dr. Kelly observed that his patients showed the most psychological improvement when he was able to assist his patients in ordering and understanding the confusion they currently found themselves in (Boeree, 1997). From these observations and experiences Dr. Kelly formulated his fundamental postulate that "A person's processes are psychologically channelized by the ways in which he anticipates events." (Kelly G. A., 1963, p. 46). This fundamental postulate was further supported by 11 corollaries, or conjectures, presented in Appendix C.

The fundamental postulate and the corollaries of the psychology of personal constructs directly links a person's actions to how he anticipates his respective interactions. These anticipations are based on the individual's constructs – the individual's discrete mental concepts of his experienced reality. Each construct addresses a limited range of the individual's experienced reality and an individual's mental concept of reality is comprised of a limited number of total constructs. An individual's constructs are formulated from the individual's previous interactions. As an individual is exposed to additional interactions, he unconsciously modifies, further structures, formulates additional or discards his constructs as needed. When an individual's interactions extend beyond his pre-existing scope of experienced reality, he employs fragments of multiple, and potentially contradictory, constructs to anticipate this "new" interaction. As the scope of an individual's experienced reality increases, the individual's ability to adapt is limited by his ability to adapt each of his various constructs (Kelly G. A., 1963).

In analyzing how this theory influences general societal interaction, one can observe that each individual constructs his experienced reality differently, but the similarity of two individuals is determined by the similarity of their respective personal constructs. Lastly, if a person can understand the construction process of another individual, he can actively play a role in helping this individual in exploring or even modifying his personal constructs.

6.2.3 General concepts defining the shape and details of an experience-based decision process

Numerous researchers have worked to further explore and document how an individual mentally constructs his experienced reality and how these constructions influence the individual's sensitivities to future interactions. This work has particularly focused on the construction, experience and modulation corollaries.

While George Kelly was formulating his theory on the psychology of personal constructs, Herbert Simon, an economist by training, was attempting to simulate the human decision making processes with computers. Dr. Simon observed that individuals did not closely follow the classical concepts of rationality in which each potential alternative is actively considered, modeled, and evaluated. Rather an individual's finite computation and predictive abilities caused the individual to limit the number of alternatives considered. By considering only a segment of reality, the given individual's range of potential options was reduced thereby significantly altering the resulting decision. Dr. Simon coined this form of decision making where an individual's finite faculties limits the range of reality considered, *bounded rationality* (Simon, 1957).

This limited number of alternatives considered can also be influenced by the range of an individual's experience or the amount of information available to the individual. Amos Tversky and Daniel Kahneman employed numerous interview-based experiments to study how an individual's limited information can influence the individual's future expectations and decisions. In particular, they

observed that an individual will employ his experience, in this case limited to the provided information, as an evaluation anchor or norm from which they will make intuitive adjustments in the formulation of various assessments, future expectations and decisions. In most cases, this process of anchoring and adjustment results in an extremely efficient decision process. Unfortunately, under certain circumstances, the approach of anchoring and adjustment causes individuals to exhibit biases towards the norm, show a limited imagination of potential additional options or consequences, overestimate the validity of an assessment, and ignore issues of probability (Tversky & Kahneman, 1974).

Interaction evaluation mechanism:

With the range of considered alternatives defined and future expectations formulated, the individual then employs his senses – sight, sound, touch and smell – to observe his experienced portion of reality (Mahoney, 2003). The individual unconsciously and/or consciously compares these observations against his pre-existing expectations to identify the elements of his experienced reality that has deviated from his pre-existing expectations. It is these positive or negative deviations and how they relate to the pre-existing expectations, and not the current state of the observation, that the individual then employs in the evaluation of the given interaction (Kahneman & Tversky, 1979). Thus, an individual quantifies the interaction with the contextual evaluation or affect – the "positive or negative quality" of the interaction and not the current state of the observed interaction (Slovic, Finucane, Peters, & MacGregor, 2002, p. 397).

In valuating interactions, Dr. Kahneman and Dr. Tversky observed in studying individuals' responses to games of chance that they exhibited heightened valuation sensitivities to probabilities that approach zero and absolute probability (Kahneman & Tversky, 1979). It is proposed that this theory can be extended to normative evaluations with the bounds of the norm being analogous to the zero and absolute probability. This hypothesis can be applied to a normative valuation process by observing that as an additional interaction approaches and extends beyond the limits of the person's experience, the limits of his norm, a heightened valuation can be observed (Kelly G. A., 1955) (Slovic, Finucane, Peters, & MacGregor, 2002).

With the given interaction valuated, the individual is then faced with the task of forming a decision from this valuation. Rather than striving for a maximum condition state in the process of formulating decisions, individuals commonly employ a *satisfying* approach in which the observations are assessed on a satisfactory or unsatisfactory scale. While this approach significantly reduces the required assessment faculties and is relatively quick, it causes the individual to settle for satisfactory condition states rather than striving for maximum condition states (Simon, 1957).

Post-interaction norm reformation:

Once the individual has observed, assessed and evaluated each additional interaction, he then employs this additional observed interaction to refine, temper or even reformulate his evaluation norm. In studying this evaluation and reformation process in patients undergoing semi-invasive medical treatments by having the patients evaluating the current interaction (the experienced affect) on a scale from 0 to 10, Daniel Kahneman observed that retrospective evaluations conducted at the completion of the treatment were equivalent to the average of the peak and end evaluations (Kahneman, 2000). As this retrospective experience-based assessment is influenced by the individual's most extreme and most recent interactions, his evaluation norms can shift as his affective evaluation of his interactions shift. Thus, an individual's evaluation norm is a function of the

intensity and sequence of his previous interactions, and can in turn frame and alter his resulting evaluation of a future interaction (Kahneman, 2003) (Frederick & Loewenstein, 2003).

The influence of gradual evaluation norm reformation and the sequence of an individual's interactions can have over a given evaluation is well described in Brickman and Campbell's identification of the "hedonic treadmill." Brickman and Campbell observed that "[a]s the environment becomes more pleasurable, subjective standards for gauging pleasurableness will rise, centering the neutral point of the pleasure-pain, success-failure continuum at a new level such that once again as many inputs are experienced as painful as are pleasurable." (Brickman & Campbell, 1971, p. 287) Thus as the individual's subjective standards rise, an interaction that was once evaluated as pleasurable can be later viewed as painful.

This experience-based evaluation process has three key implications, 1) each individual has unique evaluation norms which are the product of the intensity, range and sequence of his respective environmental interactions, 2) evaluation norms of different individuals vary as much as their respective intensity, range and sequence of interactions differ and 3) an individual's evaluation norms can be significantly altered by a small number of very high intensity interactions or a large number of relatively low intensity interactions (von Glasersfeld, 1996).

6.3 Quantifying experience-based affective evaluation

In light of the dynamic evaluation findings presented above, it is proposed to employ an affect-based evaluation approach and the human temporal sensitivity documented by (Brehmer, 1970) to quantify the impact of a sequence of interactions. This affect-based evaluation approach differs in three key aspects from previous works – the affective assessment is a direct function of the range of previous experience, both the perceived standard deviation and the perceived mean are weighted with the temporal depreciation factor, and the stimuli measurement is conducted as a function of the parameter performance units (i.e. speed in km/hr). This affect-based approach is applied in Sections 6.4 and 6.5 to quantify the user sensitivity to varying levels of service and to identify more representative methods for assessing user assessments of an operating infrastructure system.

The affective assessment approach focuses on the evaluation of the current interaction against the individual's previous perceived experience. This approach can be broken down into three key phases: an initial interaction, a second interaction, and subsequent interactions.

6.3.1 The initial interaction

This assessment process begins with an individual experiencing a new interaction for the first time. As shown in Figure 6-2a, this initial interaction has, for demonstrative purposes, an intensity (S_1) of 50 on a range of 0 to 100. As this is the individual's first interaction with the given environment, the initial interaction's induced affect (its induced emotion) is equal to 1. Following the findings of Tversky and Kahneman (1974), the individual uses this initial interaction as an anchor (hereafter referred to as the initial perceived mean experience, $p\mu_1$) and an adjustment (hereafter referred to as the initial perceived standard deviation experience, $p\sigma_1$) to form a distributed perceived range of experience.[10] As this is the individual's first interaction, the initial perceived mean experience ($p\mu_1$) is equal to the intensity of the initial interaction (S_1). Additionally, a minimum intensity value is

[10] Throughout this work, all perceived ranges of experiences are assumed to be normally distributed.

specified for the perceived standard deviation experience ($p\sigma_{min}$) to ensure that the perceived standard deviation does not become too small - thereby creating a hypersensitive individual. In this example, a minimum intensity value of 10 is employed.

Prior to a second interaction, the individual unconsciously employs this initial perceived range of experience to formulate his emotional sensitivity, his potential affect, to a second interaction. The individual's potential affect following this initial interaction is computed using Equation (6.2) and is graphed in Figure 6-2b.

$$AS_i = AF^{\left|\frac{S_i - p\mu_{i-1}}{p\sigma_{i-1}}\right|} \tag{6.2}$$

Where:

AS_i = the potential induced affect for interaction i given the interaction intensity, the perceived mean and the perceived standard deviation of experience of all previous interactions.

AF = the affective assessment factor which is in this and all other examples set to a value of 2 in agreement with the findings of Brehmer (1970).

S_i = the measured intensity of the current interaction i.

$p\mu_{i-1}$ = the perceived mean experience for all previous interactions (1 to i-1).

$p\sigma_{i-1}$ = the perceived standard deviation of experience for the previous interactions (1 to i-1).

Thus the individual's potential induced affect for a second interaction given the initial interaction is presented in Equation (6.3).

$$AS_2 = 2^{\left|\frac{S_2 - p\mu_{2-1}}{p\sigma_{2-1}}\right|} = 2^{\left|\frac{S_2 - 50}{10}\right|} \tag{6.3}$$

In Equation (6.3) and in Figure 6-2b, one can observe that as the offset between the initial perceived mean experience and the second interaction intensity increases, the resulting induced affect increases by a multiple of 2 for every additional perceived standard deviation.

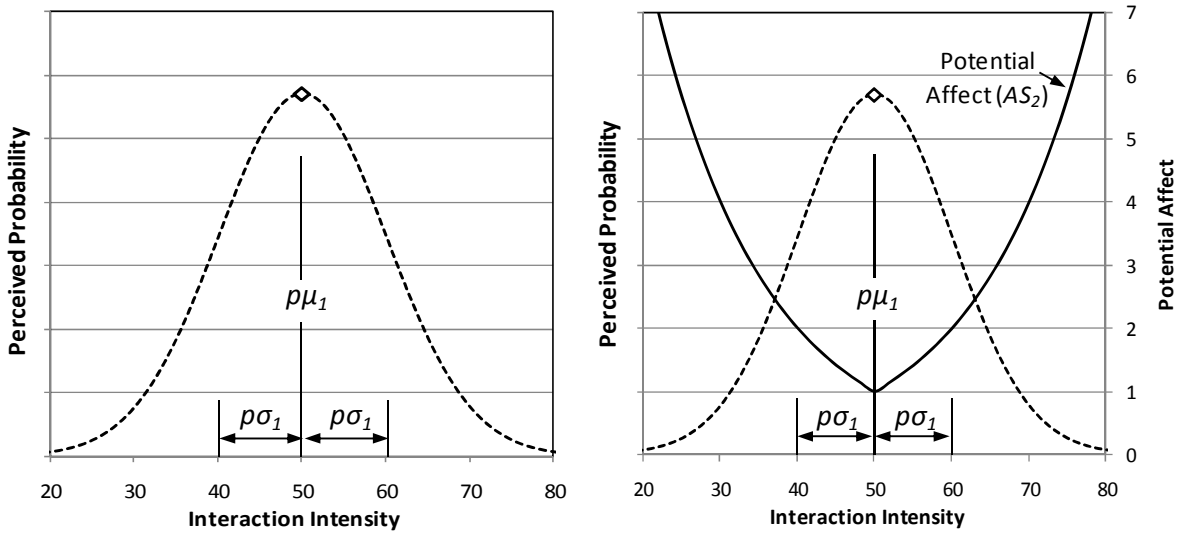

Figure 6-2: a) Range of perceived experience following the initial interaction, b) Potential induced affect for the second interaction.

6.3.2 The second interaction

The individual then experiences his second interaction. As presented above, the previous perceived range of experience of the initial interaction is employed to determine the individual's induced affect. Taking the assumption that the intensity of the second interaction is equal to a value of 34 on a range of 0 to 100, the associated induced affect is:

$$AS_2 = 2^{\left|\frac{34-50}{10}\right|} = 3.03$$

Following this second interaction, the individual must reformulate his perceived range of experience and thus reformulate his perceived mean and perceived standard deviation of experience. This reformation process, as observed by Kahneman (2000), is influenced by the induced affect and the memory depreciation for all previous interactions. The induced affect, as noted above, for the first and second interactions are respectively 1 and 3.03. Memory depreciation is incorporated into the affective-assessment approach by employing a depreciation factor (D_j) introduced in Equation (6.4) and plotted in Figure 6-3b.

$$D_j = \begin{cases} 1 & (j \le A) \\ \left(\frac{1}{n}\right)^{j-A} & (j > A) \end{cases} \qquad (6.4)$$

Where:

D_j = the memory depreciation factor for the considered interaction j [ ]

j = the number of interactions between the considered interaction and the current interaction [ ]

A = the number of non-depreciated interactions (currently set to 2) [ ]

n = the memory depreciation rate (currently set at 1.06) [ ]

Thus the memory depreciation of the initial and the second interactions are both equal to 1.

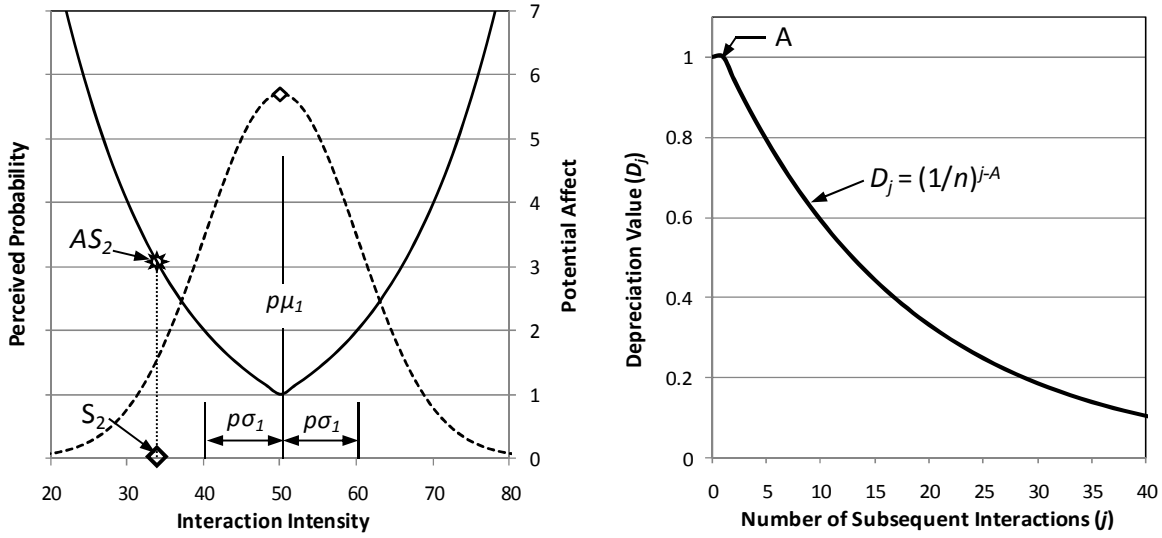

Figure 6-3: a) Second interaction and associated induced affect, b) Memory depreciation as a function of number of subsequent interactions.

The individual then reconstructs his perceived mean and perceived standard deviation experience by weighting each interaction intensity with its respective induced affect and memory depreciation as shown in Equations (6.5) and (6.6).

$$p\mu_i = \frac{\sum_{k=1}^{i} S_k AS_k D_{i-k}}{\sum_{k=1}^{i} AS_k D_{i-k}} \tag{6.5}$$

$$p\sigma_i = \begin{Bmatrix} p\sigma_{\min} & \left(\sqrt{\frac{1}{i}\sum_{k=1}^{i}(S_k - p\mu_k)^2} \le p\sigma_{\min}\right) \\ \sqrt{\frac{1}{i}\sum_{k=1}^{i}(S_k - p\mu_k)^2} & \left(\sqrt{\frac{1}{i}\sum_{k=1}^{i}(S_k - p\mu_k)^2} > p\sigma_{\min}\right) \end{Bmatrix} \tag{6.6}$$

Where:

$p\sigma_{min}$ = the minimum perceived standard deviation of experience [ ]

Thus the perceived mean and the perceived standard deviation following the second interaction are:

$$p\mu_2 = \frac{\sum_{k=1}^{2} S_k AS_k D_{i-k}}{\sum_{k=1}^{2} AS_k D_{i-k}} = \frac{(34)(3.03)(1)+(50)(1)(1)}{(3.03)(1)+(1)(1)} = 37.97$$

$$p\sigma_2 = \sqrt{\frac{1}{2}\sum_{k=1}^{2}(S_k - p\mu_k)^2} = \sqrt{\frac{(50-50)^2+(34-37.97)^2}{2}} = 2.81 \le p\sigma_{\min}$$

$$p\sigma_2 = p\sigma_{\min} = 10$$

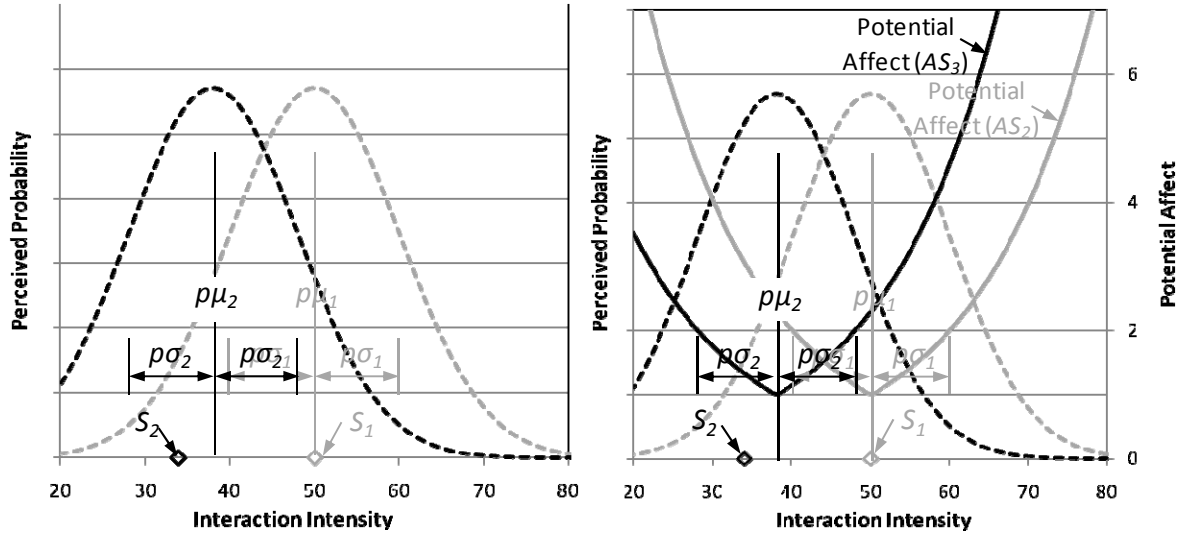

Figure 6-4: a) Shift in perceived range of experience, b) Shift and dilation in potential affect.

With the perceived range of experience reconstructed, the individual then recomputes his potential induced affect for the subsequent interaction following Equation (6.2).

$$AS_3 = 2^{\left|\frac{S_3 - p\mu_2}{p\sigma_2}\right|} = 2^{\left|\frac{S_3 - 37.97}{10}\right|}$$

The evolutionary experience of transitioning from the initial interaction to the second interaction is shown in Figure 6-4. During this transition, the individual reconstructs his previous perceived range of experience, shown in gray, by including the affective valuation of the second interaction, denoted AS_2, for the measured intensity S_2. The inclusion of the affective and memory depreciation values causes the individual's perceived mean experience to shift and has the potential to cause the perceived standard deviation of experience to dilate or contract. Furthermore, in comparing the individual's potential induced affect for a third interaction against the second interaction, one can observe that the individual's sensitivity for all intensities above the value $(p\mu_1+p\mu_2)/2$ has increased and the individual's sensitivity for values below this point has decreased.

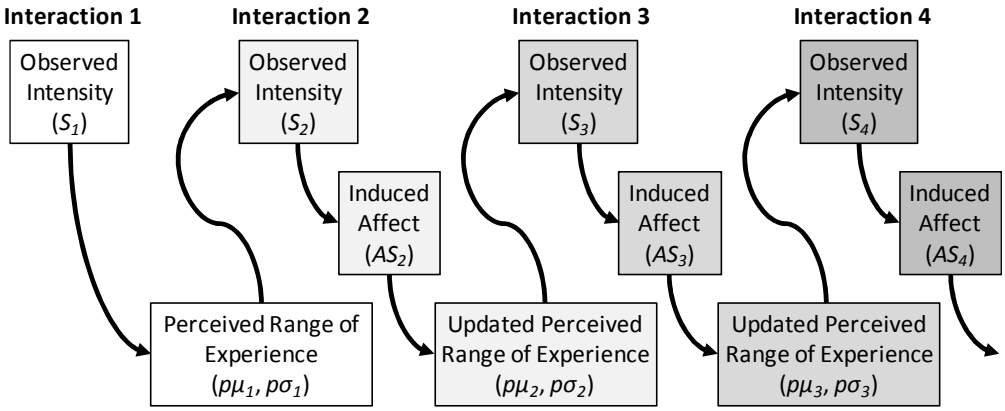

Figure 6-5: Schematic of the process of assessing the induced affective response.

Table 6-1: Interaction intensity, perceived mean experience, perceived standard deviation of experience, and induced affect.

Interaction (i)	Intensity (S_i)	Perceived Mean ($p\mu_{i-1}$)	Perceived Deviation ($p\sigma_{i-1}$)	Induced Affect (AS_i)
1	50	-	-	1.00
2	34	50.0	10.0	3.03
3	56	37.9	10.0	3.49
4	42	46.3	10.0	1.35
5	35	46.1	10.0	2.16
6	57	44.1	10.0	2.44
7	46	47.0	10.0	1.07
8	38	47.5	10.0	1.92
9	29	46.5	11.6	3.36
10	42	43.0	10.0	1.06

6.3.3 The subsequent interactions

With foundation for the individual's experience-base evaluative norm formulated during the first two interactions, consider the potential induced responses of the same individual being exposed to an additional eight interactions. The process of assessing the induced affective response for each additional interaction given the respective previous perceived range of experience and recalculating the perceived range of experience is identical to the process presented in Section 6.3.2 and is schematically presented in Figure 6-5.

The interaction intensity, perceived range of experience and induced affect for the total set of ten interactions are presented in Table 6-1 and plotted in Figure 6-6. The intensity for these eight interactions have a maximum intensity of 57 and a minimum of 29. In Table 6-1, one can also observe that rather than including the perceived range of experience values for each interaction (the perceived mean and perceived standard deviation), the values for the previous interaction (*i*-1) are employed. The previous perceived range of experience values are listed, because these are the values upon which the current interaction's induced affect is computed.

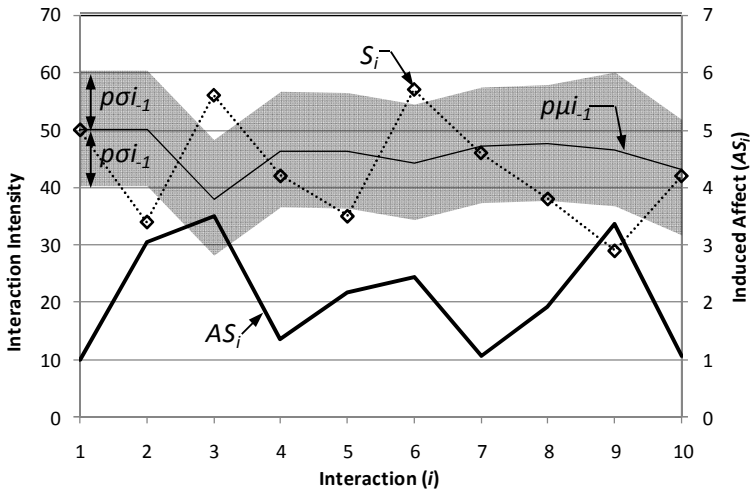

Figure 6-6: Interaction intensity, perceived range of experience and induced affect.

In Figure 6-6, one can observe that the intensity (S_i), the previous perceived mean for each interaction ($p\mu_{i-1}$), the breath of the previous perceived first standard deviation ($p\sigma_{i-1}$), and the associated induced affect are clearly presented. Across this set of interactions, one can observe that initially the individual's perceived range of experience is very sensitivity to each additional interaction. This can be seen in perceived range of experience shift between interactions 3 and 4 where an interaction intensity deviating 19.1 units from the previous perceived mean experience causes the perceived mean to shift by 9.6 units. By interaction 9, the perceived range of experience is much less sensitive to an additional interaction with an interaction intensity deviating 17.5 units from the previous perceived mean causing the perceived mean to shift by only 3.5 units. This solidification of the individual's perceived range of experience is a direct product of the individual's increasing level of experience with the given entity. In interaction 3, the individual (who has experienced only two other interactions) responds to the positive interaction by significantly raising his expectations for interaction 4. While in interaction 9, the individual responds to the negative interaction by only slightly adjusting his expectations but for the most part just enduring this negative interaction.

6.4 Case Study E: Experience-based assessment of a roadway performance

From the affect-based assessment approach presented in Section 6.3, one can observe an individual's potential induced affect is significantly influenced by his previous perceived range of experience, the intensities of the subsequent interactions and the frequency in which an individual interacts with the given risk source. This case study explores how sensitive an individual's induced affect is to varying levels of previous perceived range of experience, subsequent interaction intensities and risk source exposure frequencies. These findings are then placed into four different contexts and conditions commonly encountered by the practicing civil engineer including gradually

deteriorating roadways, traffic accident induced congestion, construction induced lane closures and traffic volume induced congestion.

6.4.1 Individual preexisting range of experience

Consider three individuals – a local, a foreigner and a new driver – all commuting to work each morning along a given roadway during a four month period (60 total interactions). The breadth and depth of the three individuals' previous range of experienced speeds with the given or similar roadways are presented in Table 6-2. The specific interaction performance values for each individual were randomly generated assuming the roadway speed is normally distributed with the following mean (μ) and standard deviation (σ) values:

Table 6-2: Individual preexisting range of experience.

Ref	Individual	Duration	μ [km/h]	σ [km/h]	# Interactions
1	Local	15 years	90	10	3600
2	Foreigner	5 years	62	10	1200
3	New driver	3 months	90	10	45

6.4.2 Roadway case study conditions

To better understand the dynamic trends and local complexity of subjective interaction evaluation, seven different roadway conditions, presented in Table 6-2, are considered. The first condition – no deterioration – assumes the roadway performance remains consistent with the local's previous experience (μ = 90 km/hr and σ = 10 km/hr). Condition B, minor deterioration, assumes the roadway average performance decreases linearly from 90 km/h to 80 km/h during the course of the case study – a performance modification commonly the result of minor roadway surface quality deterioration. The major deterioration condition, which is indicative of significant reduction in roadway capacity associated with a lane closure, assumes the average roadway performance decreases uniformly by 60 km/h for the duration of the case study. The additional four conditions – frequent and infrequent, minor and major deterioration – assume the individual is randomly exposed to either the minor or major deteriorated roadway conditions on average once a week or once every two months, respectively. These additional four conditions are included to model the potential impact of frequent and infrequent events such as higher than normal vehicle volume (minor deterioration) and traffic accidents or lane closures (major deterioration).

Table 6-3: Roadway condition parameters and associated representative conditions.

Ref	Condition	μ [km/h]	σ [km/h]	# Interactions	Representative condition
A	No deterioration	90	10	60 out of 60	'Perfectly' maintained roadway
B	Minor deterioration	90-80	10	60 out of 60	Roadway surface deterioration
C	Major deterioration	30	10	60 out of 60	Land closures
FB	Frequent – minor	90-80	10	12 out of 60	Vehicle demand ~ road capacity
FC	Frequent – major	30	10	12 out of 60	Weather events & accidents
IB	Infrequent – minor	90-80	10	2 out of 60	Vehicle demand ~ road capacity
IC	Infrequent – major	30	10	2 out of 60	Traffic accidents

6.4.3 Presentation of case study results

The affective assessment approach introduced in Section 6.3 was employed to model the induced subjective evaluation for the three individuals experiencing each of the seven roadway conditions.

The total number of negative interactions (herein defined as an interaction value which is less than the respective preexisting perceived mean), the summation of the total induced negative affect across all 60 case study interactions and the maximum interaction negative affect for each individual – roadway combination are presented in Table 6-4.

Additionally, the breath of the first perceived standard deviation (representative of an individual's preexisting perceived experience), the interaction performance values and the induced affect for all three individuals under the no deterioration, minor deterioration, major deterioration, frequent minor deterioration, frequent major deterioration and infrequent major deterioration states are presented in Figure 6-7a to Figure 6-7f.

No deterioration

For the first roadway condition, no deterioration, the total and maximum negative induced affect (Table 6-4) is near or at a minimum for each individual. In Figure 6-7a, the foreigner's pre-case study first perceived standard deviation, representative of the foreigner's perceived range of experience, initially induces a positive affect but this affect quickly dissipates as the foreigner adapts to the higher performance. Within this deterioration state, the only individual who would observe a change of performance would be the foreigner during his initial ten interactions with his new environment.

Constant minor deterioration

In the second roadway condition, constant minor deterioration, one can observe that the total and maximum negative induced affect is higher than the no deterioration condition, but this increase is, across the board, less than thirty percent (Table 6-4). Additionally, as seen in Figure 6-7b, the foreigner's pre-case study first perceived standard deviation, representative of the foreigner's perceived range of experience, initially induces a positive affect but quickly dissipates as the foreigner adapts to the higher yet slowly deteriorating condition. Additionally, as the performance gradually deteriorates, each individual's perceived range of experience also gradually deteriorates preventing them from observing this deterioration.

Constant major deterioration

The constant major deterioration roadway condition, the third condition, induces the second largest total and maximum negative induced affect. Furthermore, the foreigner's pre-case study lower expected performance causes the foreigner to have a smaller induced negative affect as compared to the local or new driver. These initial induced affect variances converge within the first five case study interactions resulting in all three individual's converging on similar, and a markedly reduced affect. Thus, even though each individual experiences a massive concentrated induced affect as they shift

Table 6-4: Number, total and max negative induced affect for all individual-condition combinations.

		Induced affect								
		Local			Foreigner			New Driver		
Ref	Road Condition	#	Sum	Max	#	Sum	Max	#	Sum	Max
A	No deterioration	35	69	5.3	30	56	5.2	35	69	5.3
B	Minor deterioration	39	88	6.7	31	70	6.7	39	88	6.7
C	Major deterioration	42	175	58.0	44	118	8.4	42	168	57.7
FB	Frequent – minor	31	78	15.9	25	64	15.7	31	78	15.9
FC	Frequent – major	36	325	94.0	30	276	69.3	36	128	38.0
IB	Infrequent – minor	15	70	5.0	17	56	5.0	15	70	5.0
IC	Infrequent – major	23	113	50.5	22	88	30.9	21	97	50.3

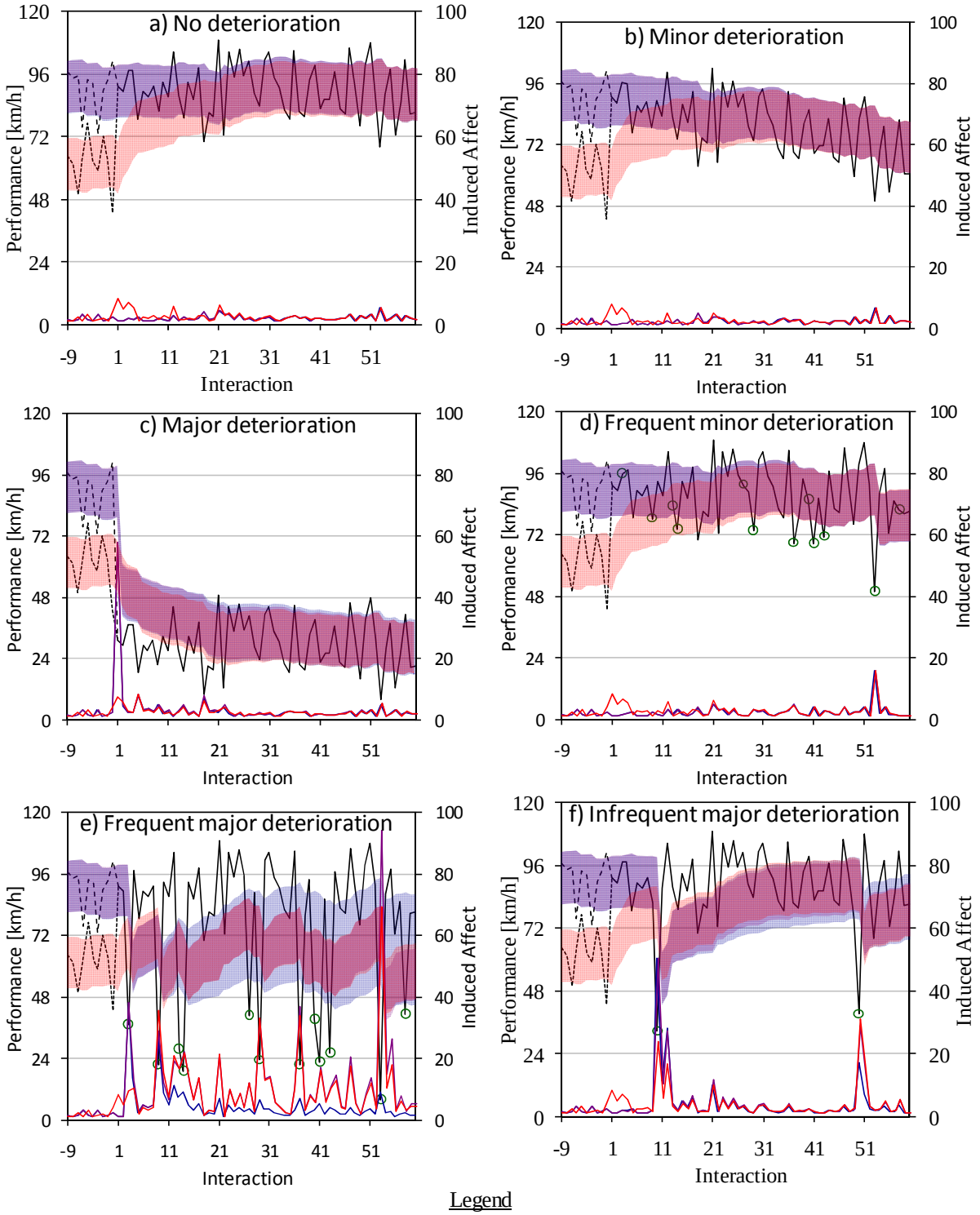

Figure 6-7: Interaction values, perceived range of experience and induced affect for a) no deterioration, b) minor deterioration, c) major deterioration, d) frequent minor deterioration, e) frequent major deterioration and f) infrequent major deterioration.

into the constant deterioration state, they adapt to this deteriorated state surprisingly quickly. Therefore, it is expected that these individuals would only observe a change of performance during and following the performance shift, but as they adapt to this constant deteriorated state their ability to ascertain this deteriorated performance decreases.

Frequent minor deterioration

Within the frequently experienced minor deterioration roadway condition, each individual randomly experiences a minor deteriorated roadway on average once a week – with these deteriorated performance interactions denoted by the green circles in Figure 6-7d. As with the previous three cases, the foreigner's adaptation to these higher, yet deteriorating, performance is clearly present. Interestingly, the individuals' reduced interaction with the deteriorating roadway prevents the perceived range of experience from gradually shifting. Rather the perceived range of experience adaptation process is much more abrupt and accompanied with amplified induced negative affects. Thus, within such an environment, the individuals will be able to observe the minor deterioration and their perceived range of experience is much less likely to shift with the deteriorating performance as is the case for the constant minor deterioration state.

Frequent major deterioration

The fifth roadway condition, frequently experienced major roadway deterioration, Figure 6-7e, peppers all three individuals with a barrage of major deterioration events – on average once a week. The magnitude, frequency and uncertainty of these events creates the highest induced total and maximum negative affect of all seven cases. The performance uncertainty of this condition causes the perceived range of experience to continuously shift in all three individuals. Additionally, this performance uncertainty specifically causes the new driver, who has just 3 months of previous driving experience, to broaden his perceived range of experience, thereby adapting to this extremely uncertain state of service. While it is expected that each individual will significantly observe all of these major deterioration events, as they interact with this environment, their perceived range of experience will expand as they adapt to and eventually become significantly less sensitive to this deteriorated and an erratic level of performance.

Infrequent minor deterioration

Within the second to last condition, infrequent minor deterioration, the exposure frequency and interaction performance deterioration are too small to induce either a noticeable negative affect or a shift of the perceived range of experience. Thus it is expected that the individuals will not observe these deteriorated states nor will their perceived range of experience significantly shift.

Infrequent major deterioration

In the last condition, infrequent major deterioration, the magnitude of each deteriorated interaction is large enough to significantly shift the perceived range of experience but the events are spaced far enough apart to facilitate the individual's readaptation to the non-deteriorated condition. This readaptation in turn further resensitizes the individual to potential subsequent major deterioration interactions. Thus within such environment, not only will each individual significantly observe each deteriorated state but their perceived range of experience will have time to recalibrate towards the non-deteriorated conditions.

6.4.4 Implications for infrastructure managers

In assessing the implications these findings have for the infrastructure management field, the two key questions that should be asked are: 1) what is the source of the deteriorated performance (structural deterioration or construction projects) and 2) does the manager want to stimulate or suppress the individual's ability to observe these deteriorated states.

If the deteriorated performance is caused by structural deterioration, to help support the eventual implementation of a maintenance action, it would be best for society to be able to observe this deteriorated performance but sustain a high expectation of infrastructure performance. From this study, it is expected that an environment similar to either the frequent minor deterioration or the infrequent major deterioration would help to aid the public in observing these deteriorated states and in sustaining a high expectation of performance – two motivators for supporting maintenance actions.

If the deteriorated performance is a product of the infrastructure manager's implemented construction project, it would be best for society's ability to observe this deterioration to be limited. From this study, it is expected that constant environments similar to the no deterioration, minor deterioration or major deterioration states would help to aid the public in adapting to these deteriorated performance states.

This analytical approach of simulating the expected infrastructure performance, modeling the perceived range of experience and induced affect for each major group of citizens and selecting the management approach which provides the desired response (either heightening or suppressing the public's observation abilities) is proposed to be actively employed by infrastructure managers as a tool to help select an analytically optimal maintenance solution from the set of potential maintenance solutions which has a high potential of inducing a socially sustainable environment.

6.4.5 Reviewing case study findings

From this case study, one can observe an individual's versatility in adapting to changing environments ranging from gradual minor deterioration to abrupt major deterioration shifts. Unfortunately, this strength can also be a limitation for it reduces and eventually suppresses potential induced affective responses which are normally completely considered within standard civil engineering analytical assessments of intangibles.

Table 6-5: Individual ability to observe the change and the duration of this observation window for each individual-condition combination.

		Observation ability			Observation window	Simulated Represented Roadway Condition
Ref	**Road Condition**	**Local**	**Foreigner**	**New Driver**		
A	No deterioration	Very Low	Very Low	Very Low	Non existent	'Perfectly' maintained roadway
B	Minor deterioration	Low	Very Low	Low	Non existent	Roadway surface deterioration
C	Major deterioration	High	Moderate-High	High	Present after shift	Lane closures
FB	Frequent – minor	Low	Very Low	Low	Ever present	Vehicle volume ~ road capacity
FC	Frequent – major	Very High	Very High	High	Present-limited	Vehicle volume >> road capacity
IB	Infrequent – minor	Very Low	Very Low	Very Low	Non existent	Vehicle volume ~ road capacity
IC	Infrequent – major	Moderate	Low-Moderate	Moderate	Present after each event	Traffic accidents

This ability to adapt and the associated sensitivity suppression are apparent in the minor deterioration, frequent minor deterioration, infrequent minor deterioration and major deterioration condition states. Unfortunately, an individual's versatility can also be a limitation by heightening an individual's sensitivity as seen in the frequent and infrequent major deterioration conditions. Thus in Table 6-5, a general summary of an individual's potential observation ability and observation window for each individual-condition combination is presented. With this information, infrastructure managers can work to select analytically optimal maintenance solutions which either help to heighten or suppress the public's ability to observe the deteriorated condition states. Through aiding the public in observing or adapting to deteriorated condition states, an infrastructure manager can work towards creating an environment supportive of the long-term implementation of an analytically optimal maintenance solution.

6.5 Case Study F: Affective redistribution of user costs[11]

6.5.1 Case study overview

The following case study focuses on eastbound US interstate I-26, the inbound Northwest highway access route for Charleston, South Carolina, at the US-52 and Ashley Phosphate Road junction, mile marker 209. This highway link is shown in Figure 6-8a and b and is denoted with small black arrows. The data employed herein was obtained from traffic monitoring site 0071-1 of the South Carolina Traffic and Polling and Analysis System and was collected by an automatic traffic recorder (SCDOT, 2008). This study addresses the hourly traffic data for the 42 working-day period between November 9, 2005 and January 10, 2006. It is assumed, the studied individual commutes along this section of highway each work day between the morning hours of 7:00 and 8:00 on all non-national holidays.

In Figure 6-9a, the average speed and volume for this section of roadway is presented. It can be observed that the volume peaks at 7:00, the beginning of the morning commute, and then exceeds the highway's capacity resulting in a drop of the average speed. The 7:00 traffic speed and volume

Figure 6-8: a) Charleston metro area, b) Eastbound I-26 at the US-52 and Ashley Phospahte Road junction (Google, 2006).

[11] Portions of this case study are based upon (Birdsall & Brühwiler, 2006).

for the studied 42-day period is presented in Figure 6-9b. From Figure 6-9b, it can be seen that the speed and volume are relatively inversely correlated, with the speed reaching a maxima when the volume is at a minimum and vice versa. Of particular interest are days 30 to 36 which are the working days between December 22 and January 2, the Christmas and New Year holiday time. It is during this period that the traffic volume drops and the traffic speed achieves free-flow conditions.

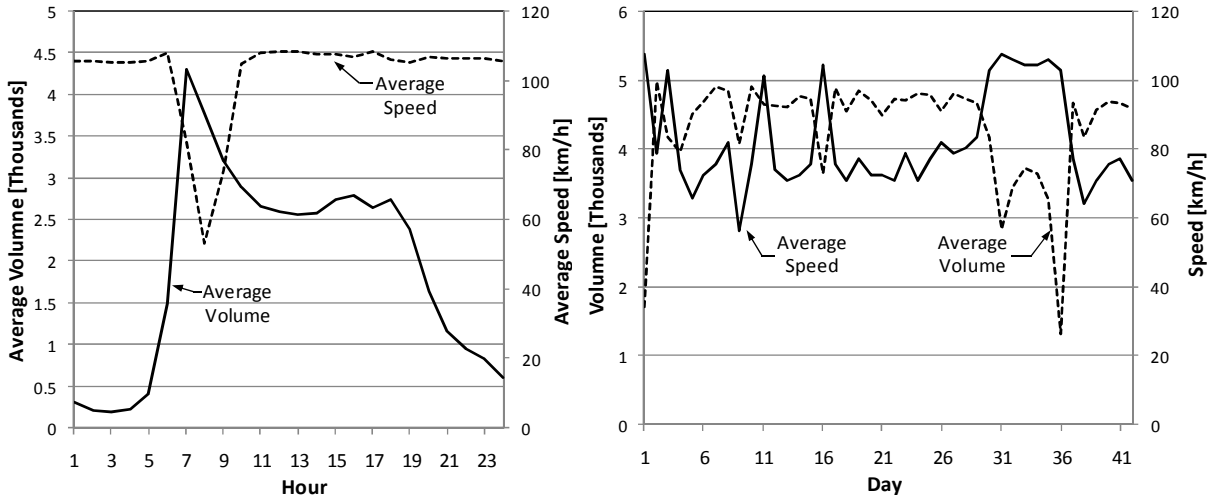

Figure 6-9: a) Average hourly speed and volume, b) 7:00 traffic speed and volume.

6.5.2 Affective assessment of traffic data

The traffic speed data was analyzed with the affective assessment approach introduced in Section 6.3 and the results for the 7:00 traffic data are presented in Figure 6-10. This analysis employs the average traffic speed, shown as a solid line, to sequentially define the perceived mean and perceived standard deviation, shown with the shaded region, are in turn employed to evaluate the induced affective assessment of the subsequent commuting speeds, shown in bold. In this analysis, it is assumed that the given individual's experience is limited to this study, therefore the interaction on day 2 is completely framed by the interaction on day 1. This framing results in a large affective response, for the interaction on day 2 is significantly beyond the individual's previous experience. This experience shift induces the individual to redefine and reconstruct his previous perceived

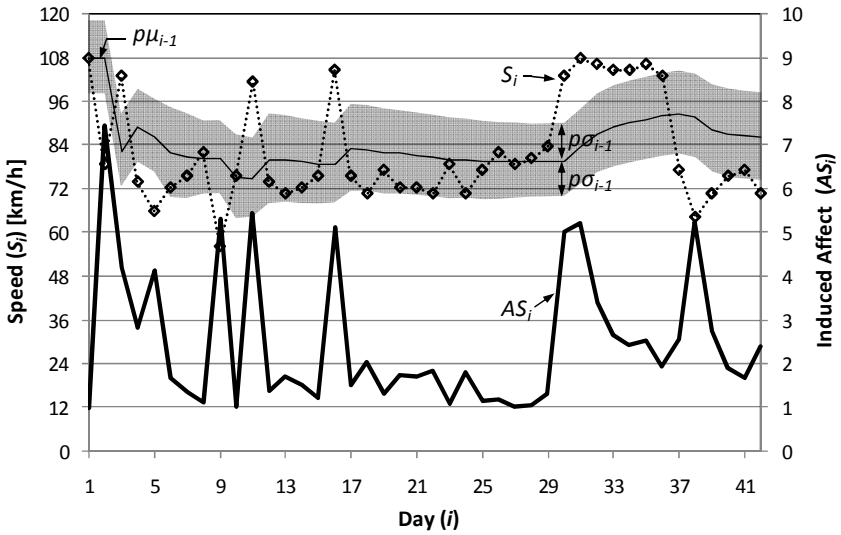

Figure 6-10: Affective analysis of 7:00 traffic speed.

experience (his perceived mean and perceived standard deviation). As the individual's interactions transpire, his evaluation measures respond and evolve, sometimes at a slow rate as on days 13 and 21, sometimes at a rapid rate as on days 9, 11 and 16. This analytical process, as in the psychological process, results in a dynamic experience-based evaluative measure.

What is of particular interest is the individual's Christmas holiday commuting interactions, days 30 to 36. It is during this time that the individual experiences free-flow traffic conditions for an extended period of time. Initially this traffic change has a significant affect, for the individual is accustomed to the constrained traffic conditions. As the individual's experience with the free-flow traffic conditions broadens, the novelty and the induced affect diminish, for the individual's perceived range of experience has evolved to accept and even anticipate these free-flow conditions. As a direct result, when the individual once again experiences constrained traffic conditions, on days 37 and 38, the affect of these standard and sub-standard traffic conditions is amplified.

6.5.3 Affective analysis applied to user cost distribution

With this insight into the dynamic nature of an individual's affective valuation, it is only natural for it to be applied to the standard analytical quantification of traffic speed, the driving speed user costs. For an example case study, the Interstate I-26 traffic speed data is extended for an additional three weeks to include a theoretical 15-day construction period to accommodate the theoretical rehabilitation of an overpass. The traffic data for the additional three weeks is developed by assuming the construction traffic speed directly corresponds to the three week period between days 12 and 26 but is uniformly reduced by a speed of 20 km/hr.

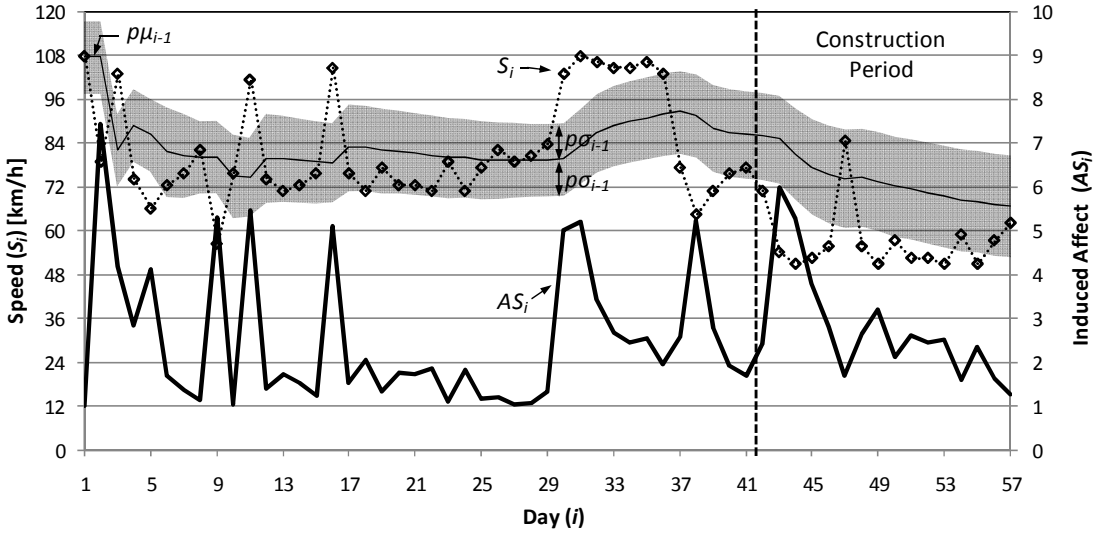

Figure 6-11: Affective analysis of 7:00 construction traffic speed.

The original 42-day traffic data and the additional 15-day construction traffic data for all 24 hours were then analyzed with the affective analysis approach. The results for hour 7:00 are presented in Figure 6-11. It can be observed that the initial 42 days of data frames this three-week construction period, providing a pre-established evaluative measure. Therefore when the 20 km/hr speed reduction is introduced, the response is initially significant, but as the individual experiences this speed reduction, his evaluative measures adjust to this new condition and the induced affective valuation reduces. By day 57, the end of the 3-week construction period, the individual's evaluative

measures have adjusted to and compensated for the construction conditions and therefore the induced affective valuation is substantially reduced.

When this affective assessment is applied to weight and redistribute, in a net zero sum, the standard traffic delay user costs, the result is apparent. The affect-weighted individual user costs per day for the 7:00 to 8:00 traffic period are presented against the standard user costs in Figure 6-12. The standard user costs were calculated by multiplying the additional time delay for each day introduced by the 20 km/hr construction speed reduction, by the number of users considered, one, and the user constant time valuation factor, x. The affect-weighted user costs were calculated by multiplying the affective valuations presented in Figure 6-11 by the respective standard user costs and the total 15-day user costs and dividing by the 15-day affective valuation and user cost summations.[12] In Figure 6-12, one can observe that by affectively weighting the user costs, 16% of the total user costs are redistributed over the first three days, the first 20% of the construction period. These aligned and redistributed construction user costs more-closely model the dynamic and evolutionary nature of user valuation as compared to the standard nominal user cost assessment approach and can thus help an infrastructure manager in identifying the high 'cost' periods of a construction project.

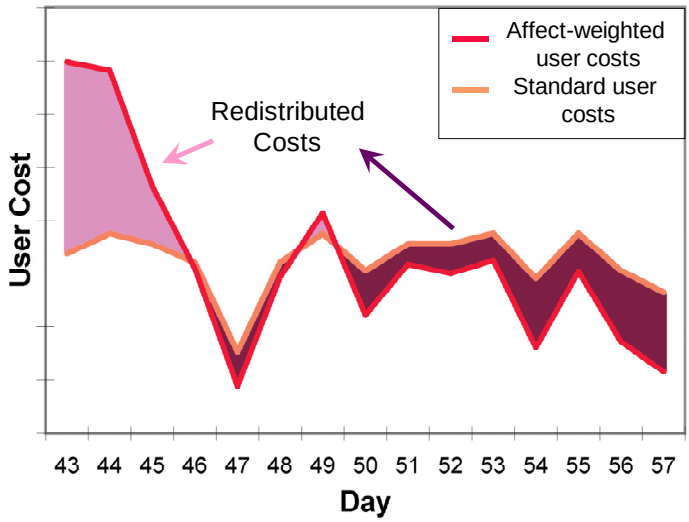

Figure 6-12: Standard and affect-weighted user costs during the construction period.

6.6 Implications for infrastructure management

Case Study E and Case Study F presented above demonstrate how societal sensitivity can adapt, shift or even remain constant under varying levels of service. The question that still remains is what implications does a dynamically changing societal sensitivity have in store for infrastructure management. This question can be investigated by considering the long-term feasibility of three different management approaches – analytically developed and implemented decisions, socially developed and implemented decisions and a analytically-developed socially-sensitized decision process.

[12] For non-hindsight calculations it is proposed to employ previous construction zone traffic performance data in parallel with statistical construction traffic modeling to calculate the future traffic performance, the standard user costs, and the associated affective assessment.

Analytically developed and implemented decisions

When an infrastructure manager develops and implements decisions by considering purely technical issues, the manager focuses on providing or achieving specified short and long-term technical and financial constraints, such as preventing major deterioration on all structures or minimizing the total user incurred costs, at the lowest invested cost. As the considered time perspective of these management programs commonly extends into multiple years or even decades, it is not uncommon for societal sensitivity to adjust or even drastically change during the implementation of such management solutions. When societal sensitivity changes in time, an interest gap can develop between the analytically and financially optimal infrastructure manager's maintenance plan and society's interests and concerns. As this analytical-social experience-based gap widens, society's political and financial support of the infrastructure manager's maintenance plans can be placed into jeopardy. Thus, even though an analytically developed infrastructure management solution may appear to be the optimal decision on paper, potential analytical-social gaps can compromise an infrastructure manager's well laid plans by undermining political or financial support.

Socially developed and implemented decisions

One approach to circumvent potential analytical-social gaps is to pass the majority of the decision development and implementation tasks directly onto society. The functionality of purely socially formulated and implemented decisions is highly influenced by the given stakeholders' previous assessed experience and range of interactions as seen in the case studies presented in Sections 6.4 and 6.5. This said, the frequency with which individuals interact with infrastructure systems – particularly transportation infrastructure systems – helps to ensure that the induced affective assessments and the range of perceived experience quickly converges across all individual groups, even for individual's with different preexisting perceived experiences as seen in Figure 6-6.

Unfortunately, while society may reach a consensus on a particular decision, the analytical validity of this decision can be significantly paced into question. As seen in the case studies presented above, individuals can become desensitized to interactions with static or linearly-constant performance deterioration values and can conversely become sensitized to interactions with uncertain performance values. Thus commonly it is the uncertain or rapidly changing performance issues such as traffic accidents, natural hazard induced failures or the frequent vehicular congestion that are addressed in highly socially influenced decision processes while static or linearly changing performance issues including roadway surface deterioration and other forms of gradual deterioration remain unaddressed or even unnoticed. Thus, while purely socially developed and implemented decisions may, on the surface, appear to be addressing the key problems at hand, they can be potentially unfit for addressing static or linearly changing performance issues.

Analytically founded, socially sensitized decision process

Returning to the public responsibility of the infrastructure manager, to develop and implement analytically efficient solutions which fulfill the needs and concerns of society, a feasibility way forward is for infrastructure managers to formulate a set of analytically optimal maintenance decisions and then to model the potential societal sensitivity in time for each potential solution as has been conducted in Sections 6.3 and 6.4. With a societal sensitivity perspective, an infrastructure manager can then select the maintenance solution which develops enough societal sensitivity to ensure the required funding is provided (i.e. the infrequent-major deterioration combination) but prevents social sensitivity from reaching levels which start to undermine society's faith in the

infrastructure manager (i.e. the frequent-major deterioration combination) – thereby bridging the analytical-social experience-based gap.

Preliminary studies have shown that societal sensitivity to both minor and major deterioration events can be actively managed. Societal sensitivity to minor deterioration events can be amplified by introducing performance evaluation benchmarks and societal sensitivity following major deterioration events can be attenuated by assisting society in personally interacting with and revalidating the performance of the built infrastructure as has been observed in Sections 6.3 and 6.4. As these societal sensitivity management tools are still in their infancy, infrastructure managers are encouraged to select analytically optimal maintenance solutions which are projected to maintain the desired level of societal sensitivity and to only consider potential active societal sensitivity management tools in focused as needed cases.

6.7 Conclusions

Infrastructure managers are charged with fulfilling society's needs by effectively and efficiently managing the built infrastructure. During the past thirty years, infrastructure managers have increasingly turned to infrastructure management systems to develop analytically optimal management solutions. Unfortunately, these management systems assess society's valuation of intangibles with nominal valuation measures negating the possibility of considering contextual issues which can potentially amplify or attenuate society's experience-based evaluation of the given intangible.

To better understand the dynamic nature of societal sensitivity, the affective assessment approach has been developed from key psychology and behavioral economics findings and employed to analyze society's sensitivity in different demonstrative case studies. This approach focuses on modeling the process by which an individual's assessed range of experience is constructed, how his interaction induced affective responses are assessed and the processes by which these affective responses are employed to refine or even redefine his assessed range of experience.

In Case Study E, three theoretical individuals – a local, a foreigner and a new driver – are exposed to seven different levels of roadway performance. From these case study results, one can observe that individuals can adapt to almost any level of performance so long as the performance level is constant. Unfortunately this adaptation results in the attenuation of societal sensitivity to constant or gradually changing levels of performance and in the amplification of societal sensitivity to rapidly changing levels of performance. Thus if society is left to its own accords, only rapidly changing condition states (i.e. traffic accidents or natural hazards) will most likely be addressed while constant and gradually changing condition states (i.e. roadway surface deterioration, lane closures, and roadway capacity limitations) will most likely be not addressed or even go unnoticed.

In Case Study F, the potential affective responses induced by documented highway traffic speeds under non-construction and construction periods is analyzed. The individual's construction period affective responses are then employed as a benchmark against which the standard nominal user costs are aligned and redistributed. While the total sum of the user costs remains constant, the affective response user cost redistribution more closely models the individual's perceived costs by capturing the dynamic and evolutionary nature of this affective user cost evaluation.

To ensure the built infrastructure is maintained in an analytically optimal fashion, infrastructure managers must take the lead in developing potential analytically optimal management plans. But the

infrastructure manager's work does not end here for he still must assess the potential societal sensitivity to each potential management plan. The analytically and socially optimal management plan is thus the analytically optimal plan which ensures a background societal sensitivity level is maintained while preventing societal sensitivity from reaching levels which can undermine society's faith in the infrastructure manager. By implementing the analytically-optimal socially-sustainable management solution, the infrastructure manager can optimally address the technical infrastructure issues while working to confirm that the implemented activities are supported over the long-term by the respective society.

In Chapter 7, this approach is applied through a pilot case study using GPS documentation and semi-structured qualitative surveys to assess the feasibility and applicability of this method.

7 Methods for documenting an experience-based assessment of risk[13]

7.1 Introduction

7.1.1 Context

When an infrastructure manager conducts a risk assessment, he employs the level of acceptable risk within the respective industry to determine the required safety and operational changes to ensure the range of risk sources operate in an `acceptable' manner. A citizen from the risk source's community forms an experience-based assessment of the given risk from his interactions with the risk manager's `acceptably' operating risk sources. From this personal experience-based assessment of risk, the general citizen forms his own acceptable level of risk. The resulting key question is: How does the risk manager's `acceptable' level of risk compare to the general citizen's `acceptable' level of risk and what tools can the risk manager use to induce different levels of acceptable risk (Figure 7-1)?

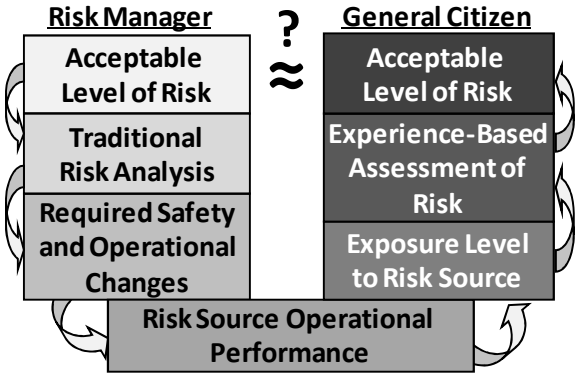

Figure 7-1: Acceptable level of risk: Relating the risk manger's usage and the general citizen's experience-based assessment.

If the risk manager's acceptable level of risk is more conservative than the general public's acceptable level or risk, a lack of public support and funding for the risk manager's decisions can be the result. On the other hand, when the public's acceptable level of risk is more conservative than the risk manager's acceptable level of risk, the public's safety expectations can be left unfulfilled by the risk manger – potentially jeopardizing the public's trust in the risk manager. Finally, when the risk manager's acceptable level of risk is in close agreement with the public's acceptable level of risk, a publicly-supportive environment can be produced.

To improve the probability of achieving a close agreement between the risk manager's and the public's acceptable level of risk, one should monitor representative citizens' personal experience-based assessments of risk to determine how their various interactions cause their acceptable level of risk to be refined or even redefined. Thus, when variations between the risk manager's and the public's acceptable level of risk are observed, a risk manager can evaluate both potential technical management changes, modifying the risk manager's definition of the acceptable level of risk, and

[13] Portions of this chapter are based upon (Birdsall & Brühwiler, 2007).

operational management changes that can induce changes in the general citizen's definition of the acceptable level of risk.

Documenting the continually refining and redefining process of an individual's experience-based assessment of risk is logistically intensive if not altogether impossible. Logistically feasible risk source exposure documentation methodologies must be identified if such risk assessment monitoring activities are to enter general risk management. This identification process is initiated by assessing existing agent-system documentation methods within the transportation fields, testing the most promising method, evaluating approaches for quantifying and contextualizing data, detailing how these methods can be applied within the context of infrastructure management and proposing key elements of an experience-based assessment of risk monitoring program.

Normative evaluation

From the field of psychology, one can observe an individual employs their senses (sight, sound, touch and smell) to assess their environment interactions (Mahoney, 2003). From these assessments, the individual forms mental constructs – discrete relative mental concepts of their environment (Kelly G. A., 1955). The individual then employs these existing constructs to frame and evaluate their future experiences (Kahneman, 2003). Where environmental changes are either unconsciously or consciously observed, the individual is spurred to determine if the change correlates with a previous construct, whether the change is positive or negative and if any reaction is required (Bargh & Chartand, 1999) (Slovic, Finucane, Peters, & MacGregor, 2002). The individual then employs these future interactions to refine or redefine, where warranted, their personal constructs to ensure they reflect their experienced reality (Kahneman, 2000) (Kelly G. A., 1955). The end result is a unique experienced reality for each individual. This experienced reality is a product of the intensity, range, and sequence of the individual's environmental interactions (von Glasersfeld, 1996).

From these observations, an individual's experience-based assessment of risk is defined as a function of the individual's uncertainty with a risk source and how the individual's risk source interactions vary with respect to his pre-established norms. Therefore, to reformulate the individual's experience-based assessment of risk, one must document in detail an individual's actual and perceived temporal interactions with a given risk source. Thus, potential participant environmental documentation approaches must be identified and evaluated.

A risk environment, in this case a public transport system, is selected with which the participant is required to frequently interact with during the course of their daily activities. This risk environment was chosen for it has been documented to produce a cognitive risk assessment process which is predominately an unconscious and automated decision process rather than an active and pensive decision process (Brehmer, 1970). This test environment will assist in evaluating potential participant experience-based assessment of risk research methodologies.

7.2 Participant-system interaction documentation methodologies

To reconstruct an individual's experience-based assessment of risk, one must first document the individual's daily interactions with the risk source and the individual's resulting induced affect. Within a public transportation system, this documentation process includes recording time, location, performance and induced affective parameters. Interaction is defined as the direct personal usage of a public transportation system. All secondary and tertiary exposure venues (learning about public transportation risk issues from the media or from talking with colleagues) are actively ignored for it is

assumed the individual's frequent and personal usage of the system will outweigh external influences. Through consulting the field of transportation engineering, it can be seen there are already a number of time, location and performance documentation methodologies, Table 7-1, including: (1) self administered travel surveys, (2) human-system interaction documentation, (3) passive cellular signal tracking, (4) active cellular signal tracking, and (5) global position system (GPS) tracking.

Table 7-1: Participant-system documentation methodologies.

Method	Aspects	Limitations
Travel survey	Manually record date, start & end locations	Incorrect documentation common
Human-system interaction	Automatically records time at start, end & other key waypoints	System requirements, data of insufficient detail
Passive cellular signal	Movements through cellular network	Anonymously recorded
Active cellular signal	GPS receiver in cell phone broadcasts location	USA only
GPS tracking	GPS receiver documents location & time multiple instances a minute	Limited battery & data storage

Self-administered travel survey

Self-administered travel surveys are the most basic of the location documentation approaches. In this approach, respondents are asked to document the date and the start and end locations of their daily trips taken within a transportation system. Providing this information is relatively simple and non-time intensive task for a participant and it can therefore be easily applied to longitudinal studies involving a large number of respondents. From each study, one can ascertain the frequency and range of the participant's travels (Axhausen, Zimmermann, Schönfelder, Rindsfüser, & Haupt, 2002).

While this methodology documents the location and date of the various interactions, it fails to document the individual's micro (how long a station stop lasted) or even global temporal experienced performances (how long the entire trip took). Furthermore, as this methodology asks participants to document their daily trips, short trips and multiple location trips are commonly either non-recorded or recorded incorrectly (Wolf, 2004).

Human-system interaction documentation

In the human-system interaction documentation approach, a participant's interaction with a system is recorded at key points, commonly at entry, exit and waypoints. This methodology is commonly integrated within the given system and such systems have been used to establish customer preferences, to document participant movements and even to rate a participant's likelihood to commit a crime (Cho, Kim, & Kim, 2002) (Landfried, 2006).

The completely integrated nature of this approach has the potential to be ethically questionable as was recently the case in the United States (AP, 2006), and therefore it is essential to actively obtain and document a participant's permission to use such collected information. Furthermore, as this method only documents the individual's interactions at key points, the individual's experiences at intermediate points may not be able to be determined. As an individual's risk construction is a continuously refining and redefining process, this discrete documentation methodology does not adequately document an individual's interactions.

Passive agent cellular signal tracking

Passive agent cellular signal tracking is essentially an adaptive human-system interaction documentation methodology in which cell phone towers serve as waypoints. The methodology is as follows: take a person carrying a cell phone, at any point in time the cell phone is connected to one or more cell towers. As the cell phone moves through a cellular network, the cell phone's signature is passed from one cell phone tower to the next. Through signal analysis and triangulation, a cellular service provider can determine the location and speed of a cell phone carrier. This methodology has already been tested in a number of countries to anonymously monitor traffic speeds (Smith, Zhang, Fontaine, & Green, 2003) (Ygnance, Remy, Bosseboeuf, & Da Fonseca, 2000).

To effectively implement such a documentation approach, one needs to actively engage the cell phone service providers and to address the cell phone customer privacy issues. The current approach employed by cell phone providers is to 1) issue limited term access to cell phone signature data (extending from a few days to many months) and 2) remove all identifying customer data prior to releasing the cleansed data to a third party (Fontaine & Smith, 2004). The anonymous nature of passive cellular tracking negates its applicability to documenting an individual's set of experiences for one is unable to match an individual with their respective interactions.

Global positioning system (GPS) tracking

The global positioning system (GPS), established in 1993, is a system of 24 geostationary satellites. Each satellite, uses an atomic clock for reference, continuously broadcasts its location and time. These broadcasts are received by a GPS receiver which computes the distance to each satellite from the delay between sent and receipt times. The GPS receiver then employs triangulation to determine its location to an accuracy of 10 meters (Garmin, 2006). GPS receivers have been applied in many different civilian settings including navigation, trip documentation, and physical training (Wikipedia, 2007). To employ a GPS receiver to document movement, one must first turn on the unit, permit the unit to calibrate its position (an approximately 30 second process) and finally manually start data acquisition. While this is a rather lengthy process, it is believed that by requiring the participant to manually initiate data acquisition, the researcher can ensure a participant has active control over and full knowledge of the collection of their personal data. During active data acquisition, the GPS receiver automatically records time, location and speed data approximately every five seconds.

While GPS tracking currently offers the most promise in documenting a participant's interactions within a transportation network, the limited battery life and data storage capability (both under 30 hours) requires the participant to daily charge and upload the recorded data. These additional tasks can potentially compromise the feasibility of this documentation methodology.

Active agent cellular signal tracking

In 1999, the United States Federal Communications Commission (FCC) started a phased implementation of requiring cell phones providers to be able to provide a cell phone's location in the event an emergency phone call (911) was placed (FCC, 2007). The required accuracy has resulted in most service providers building a global positioning system (GPS) receiver into each new cell phone. In the event of an emergency, the service provider can query this GPS receiver (Charles, 2006).

Currently within the United States of America there are approximately 100 million GPS capable phones in operation but only one company, Nextel, permits customers to have direct access to this usually encrypted capability. With this access and an inexpensive program, Nextel users can

broadcast their location and speed every 15 seconds to a server or website (Mologogo, 2007). While this capability is readily available in the United States, to the author's knowledge, such capabilities and access have not yet been introduced in Europe.

While this documentation approach is ideal for documenting an individual's experience within a transportation system, given the requisite permission, it has not yet been introduced into the European market. Therefore other documentation methods will have to be employed until this capability arrives.

In the absence of the active agent cellular signal tracking, GPS tracking, with a 10 meter accuracy and full-day experience documentation capability, is currently the most promising participant-system documentation approach for a public transportation system.

7.3 Case Study G: GPS-based interaction documentation case study

7.3.1 Case study overview

To further explore the feasibility of documenting the experience-based assessment of risk, a four month case study was launched. In this study, the participant documented their daily interactions within a public transportation system with a Garmin Forerunner 205 GPS receiver, a wrist-mounted GPS unit originally designed for triathlon training. To improve the accuracy of the collected data, the participant was encouraged to turn on and calibrate the GPS unit prior to each use.

Additionally, the participant was asked to complete an 8-question semi-focused survey each day. This 8-question survey asked the participant to list three positive and three negative events that occurred during their day and to rate the intensity, between 10 and 0 and -10 and 0 respectively. Additionally, the participant was asked to list two events that occurred during their day's travels and to rate the events' intensities between -10 and 10. While it is fully understood that intensity ratings can be extremely contextually sensitive, even to the extremely minor events (Schwarz, 1987), the participant is asked to list and rate events from their daily interactions to document what the individual is focused on and perceives as changing in their daily lives. To improve survey response frequency, the participant was encouraged to fill in the survey at the same time each day. The GPS and survey data were digitally submitted by the participant each day.

7.3.2 Raw GPS documentation

During the case study, over one-hundred thousand data points detailing the individual's location, speed and acquisition time were collected. These data points detailed 220 distinct trips. This data was then classified into different trip types, 25 in all, using the starting point, end point and general location. An example trip and the associated experienced speeds as a function of distance are presented in Table 7-2a and b respectively. From these figures, one can observe the GPS location and speed measurement detail. From the Table 7-2b), one can also observe the calibration induced error immediately adjacent to distance 0, the significant speed differences between walking and riding the metro and even the two intermediate stops on the metro.

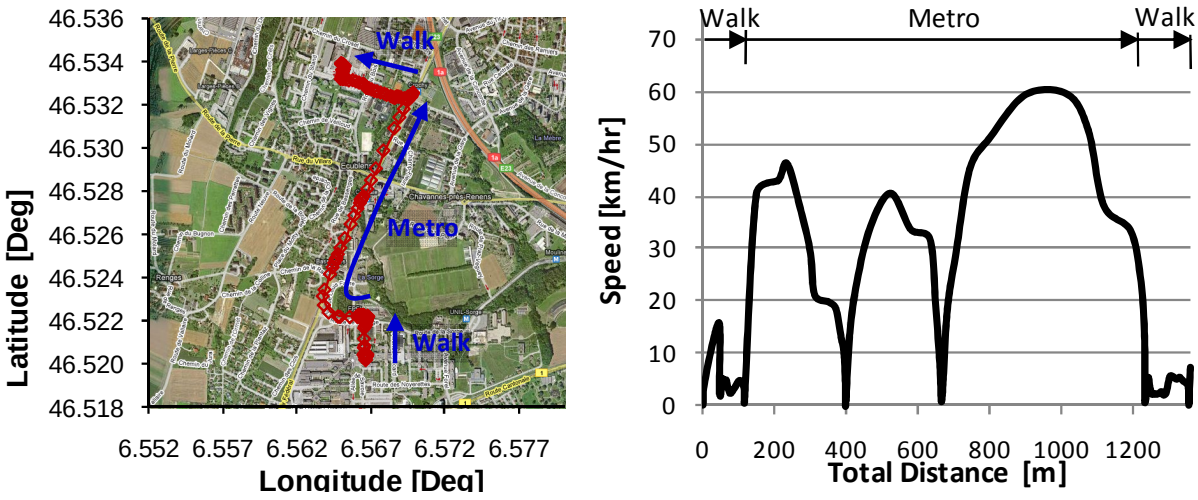

Table 7-2: a) An example trip - EPFL to a local shopping center, b) Trip speed as a function of trip distance.

In the detail presentation of this GPS documentation, Figure 7-2, the location of each data point is represented by a diamond. At higher speeds, such as when the participant is riding the metro, the data points are more spread out, but when the participant moves at slower speeds the data points are more closely spaced providing a detailed automated documentation of the individual's activities.

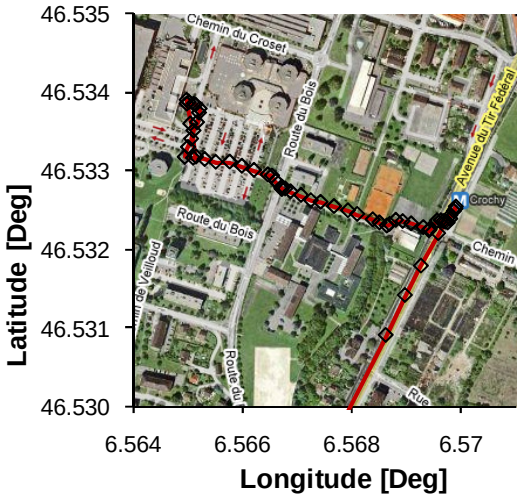

Figure 7-2: Detailed presentation of GPS documentation.

7.3.3 Analyzing the GPS documentation

The experience of additional trips along the same path can be relatively assessed by comparing the obtained GPS data for each subsequent trip. One such method is conducted by overlaying a subsequent trip on top of a previous trip and computing the time required to exceed a predefined range of movement.

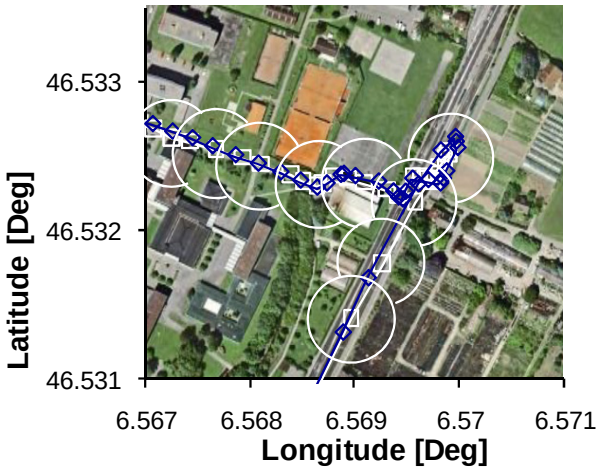

Figure 7-3: Contextual analysis using influence circles.

Figure 7-3 presents such an analysis. In this figure, one can observe that a subsequent trip is overlaid on the trip presented in Figure 7-2. 80 meter diameter influence circles, defining the referenced range of movement, are then sequentially added to the initial trip data points. The center of each circle coincides with a data point not contained with a preexisting influence circle. The time required for the individual to move from the center of a given circle to its perimeter is then calculated. The process of assigning unbounded data points to the preexisting influence circles is then repeated for the subsequent trip and the time required to extend beyond the respective influence circle's perimeter is calculated. These computed perimeter crossing times are then compared to determine how the individual's interactions have changed between the two trips.

The impact of this relative experienced change is modeled for demonstrative purposes using the affect-based assessment approach, presented in Section 6.3. In this approach, the induced affect of an interaction is defined as a function of the offset the current interaction varies from the preexisting perceived mean experience.

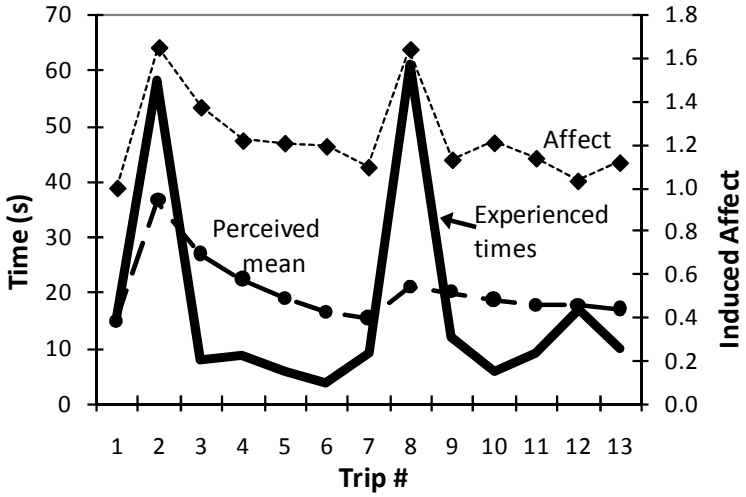

Figure 7-4: Affect-based assessment - An example analysis.

The affect-based assessment for an influence circle within the participant's commute path between home and work is presented in Figure 7-4. In this figure, one can observe that the individual passes through this influence circle on thirteen different trips during the studied period. Furthermore, the individual's experienced times varied from a minimum of 4 seconds to a maximum of 60 seconds.

The modeled induced affect for each subsequent experience and the resulting perceived mean are presented.

While this affect-based assessment approach can indicate how a given experienced time varies from a previous set of experienced times and how the average perceived experienced time evolves from one trip to the next, it is unable to indicate the motive or instigators behind this modified experienced time. Such increased times, as experienced during trips 2 and 8 presented in Figure 7-4, may be the product of a negative experience, such as increased traffic slowing the participant down, or a positive experience, such as stopping briefly to talk with a friend. Both events would induce a different affective response but both would produce an identical GPS history.

7.3.4 Semi-focused survey analysis and results

During the case study, the participant also submitted the semi-focused surveys by email at the end of each day. At the end of the case study, this set of surveys were analyzed and coded in bulk. The three positive and three negative daily event questions were coded into 13 classifications and the two daily travel event questions were initially coded into 18 classifications and then sub-coded into 5 comprehensive classifications. The 5 comprehensive classifications and examples of their represented events are presented in Table 7-3.

Table 7-3: Travel event classification.

Classification	Example represented events
Weather-time change	Shortening of the length of the day, changing weather conditions
Personal factors	Personal health and schedule events, work requirements
GPS documentable events	Missing a bus or train, changing of a train schedule
Travel environment	Number of passengers on train/bus, reading newspapers on the train
General environmental changes	Metro station construction, opening of an additional building entrance

The distribution and the average rating for each comprehensive classification are presented in Figure 7-5. One can observe that while the GPS documentable events classification is the largest comprehensive classification, it still accounts for only 40% of the documented travel events. Furthermore, from the intensity rating responses introduced in Section 7.3.1, the two most extreme average rating comprehensive categories, weather-time change and environmental changes, are not considered by the GPS documentation approach.

From these survey results, one can observe that while the GPS documentation does account for a significant portion of the noted events, these are still numerous additional sources contributing to the individual's experience-based assessment of risk other than those documented by GPS tracking.

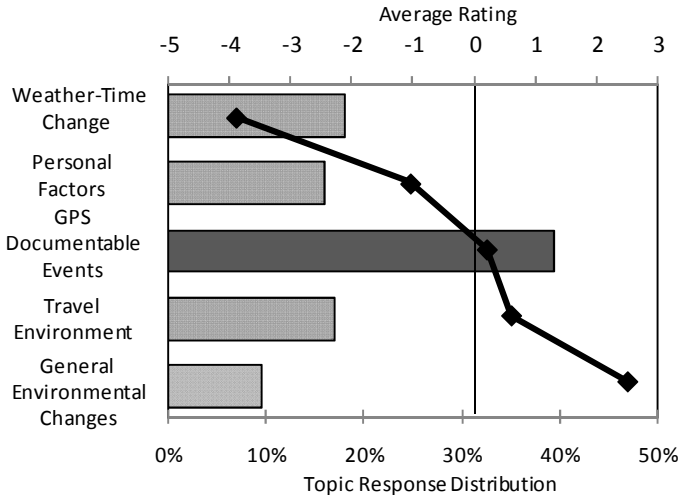

Figure 7-5: Travel event classification: Response distribution and average rating.

7.3.5 Case study summation

From this case study, one can observe that the GPS tracking approach provides an adequate automated documentation of the individual's movements and location-linked interactions within an individual's environments. Likewise, the semi-focused survey provides an insight into what the individual views as a significant event and introduces a perspective of the event topic coverage offered by the GPS tracking.

What is missing from the approaches employed during this case study is a confirmation of the psychological context and perspective of the interactions an individual has with their environment. Without this perspective, a researcher cannot differentiate between positive and negative experiences producing identical GPS histories.

7.4 Additional participant survey methods

To further complement and contextualize the GPS tracking approach, the feasibility of applying three different qualitative survey research methodologies, presented in Table 7-4, originally developed within the field of hedonic psychology – "the study of what makes experiences pleasant or unpleasant" – are evaluated (Kahneman, Diener, & Schwarz, Preface, 1999).

Table 7-4: Participant survey methods.

Method	Aspects	Limitations
Experience sampling method (ESM)	Portable timer indicates survey time; Avoids hindsight bias, multiple surveys per day	Potential for survey fatigue
Ecological momentary assessment (EMA)	Timer indicated survey, survey data complemented with quantitative data	Requires intensive analysis
Day reconstruction method (DRM)	Multi-phased event diary, reconstruct pervious day	Participant time intensive 45-75 minutes

Experience sampling method (ESM)

In the experience sampling method, developed by Csikszentmihalyi et al., participants employ a portable timer, such as a wrist watch or beeper, to indicate when they should manually or digitally complete a short predefined survey (Csikszentmihalyi, Larson, & Prescott, 1977). This process is replicated multiple times during a day and through this approach, researchers are able to collect a

detailed real-time documentation of an individual's experiences while minimizing hind-sight bias. Early studies employed a wrist alarm watch and paper forms. More recently, studies have evolved to using personal digital assistants (PDAs) for both notification and data collection. Furthermore, ESM has been employed to collect an upwards of fifty survey periods per participant within a given week (Csikszentmihalyi & Hunter, 2003). The experience sampling method has been used in the psychology, hedonic psychology and human system-interaction research fields (Intille, Rondoni, Kukla, Ancona, & Bao, 2003).

Ecological momentary assessment (EMA)

The ecological momentary assessment (EMA) approach is an extension of the ESM where the range of collected data is broadened to include environmental, social, psychological and biological states (Stone, Shiffman, & DeVries, 1999). In EMA, the participants are signaled by a timer to manually or digitally fill out a survey detailing their current state and recent previous events. This survey data is then complemented with environmental or participant quantitative data such as documenting participant medical vital signs (Smyth & Stone, 2003). By including environmental events, researchers have the potential to study the relationship between various environmental conditions and the resulting impact on the respondent in natural settings. The significant drawback of this research approach is the quantity of collected temporally dependent data. For a researcher or research team to process and analyze this volume of information can be a daunting task but the results are commonly worth the investment.

Day reconstruction method (DRM)

The day reconstruction method (DRM), developed in 2004, is a relatively recent systematic reconstruction documentation methodology (Kahneman, Krueger, Schkade, Schwarz, & Stone, 2006). In DRM, the study focus is the reconstruction of the individual's previous day. In the first of three phases, respondents are first asked to provide general background information on emotional, financial and life perspective topics. In the second phase, respondents are asked to write a confidential detailed event-based diary of their previous day's activities. This diary is intended only to assist the respondent in reconstructing the previous day's activities and is not submitted. In the last phase, respondents are asked to employ a provided response form to detail each event in their event-base diary. In particular, the response form addresses topics such as when, what, where, with whom, and how they felt during each episode. Respondents normally invest between 45 and 75 minutes to complete all three phases of the DRM. Thus far, DRM has been employed in the hedonic psychology and medical research fields (Kahneman, Krueger, Schkade, Schwarz, & Stone, 2006) (Spiegel, Knutson, Leproult, Tasali, & Van, 2005).

Participant survey method critique

The ESM and EMA participant survey methods offer the ability to gather real-time participant data. Unfortunately moving through a transportation system requires a number of the individual's faculties limiting the feasibility of taking real-time measurements. Furthermore, as the experience-based risk assessment reformation process continues for a period after using a transportation system, real-time measurements may miss this post-exposure risk assessment reformation.

The DRM offers an extremely detailed analysis of an individual's day. Unfortunately, this approach is extremely time intensive limiting the potential survey application frequency. Therefore this

approach, at the most, can be applied once or twice monthly to gain snapshot pictures of the individual's interactions and experience-based risk assessments.

7.5 Formulating a fused contextual and affective documentation method

It is believed, the contextual and affective quantification of recorded GPS and environmental data could best be achieved by having the participant's previous day's GPS and environmental data analyzed immediately each morning upon submission and the five most significant event variations presented to the participant in a survey format. This survey would ask the participant if they remembered anything specific from each of the five documented event variations. If the participant responds in the negative, no further questions would be asked, but the participant responds in the positive, further qualifying and contextualizing questions would be asked. These survey responses would be used to determine which environmentally documented events were consciously observed by the participant and what relative affective impact they induced.

While this questioning approach does by definition pose potentially leading questions which may increase the participant's likelihood of responding in the positive or in the negative, it significantly condenses the survey administration time and format. Additionally, less structured and more open-ended survey structures are not suggested for they would result in an increased the length of survey administration times.

It is hoped that a broader survey perspective touching upon more general aspects of the participants' transportation activities and their general hedonic states can be achieved by additionally administering the day reconstruction method (DRM) survey twice each month. Early in a research program, these DRM surveys would provide an insight into the participants' allocation of time, general hedonic states and interaction evaluation. This information would also provide the researcher with a base context within which the participant's environmental documentation data can be analyzed. As the research program unfolds, additional DRM surveys would provide insights into how the individual's activities, hedonic states and values vary in time. The collected environmental data can then be compared against these longitudinal qualitative insights to test potential causal linkages between environmental changes and induced affective responses.

7.6 Selecting case study environments

Selecting case study environments that are representative of the risk sources in question, finding participants who are interested in participating in an experience-based risk assessment monitoring program and developing a participant compensation package are elements essential to the success of a monitoring research program. In the example of a public transportation system, an initial 90 day case study focusing on further investigating the experience-based assessment of risk reformation processes would be the most appropriate next step. The controlling factor in the design of this initial case is the selection of 20 to 30 participants who are interested in participating in the research program, and not the specific environment. It is proposed that such individuals can be located through publicizing at local research institutions and within the given public transportation systems.

As this monitoring program requires daily participant action, it is suggested to have financial compensation as a key element of the participant compensation package. To ensure that the financial compensation can address issues including encouraging initial involvement in the monitoring program, giving the participants a sign of appreciation for providing daily environmental

and survey data and thanking the participants for completing the study, a multi-staged release of the financial compensation is proposed. Institutions are also encouraged to rely upon the strength of personal contacts and to pool the available limited resources into a limited number of prizes awarded at random to participants who complete the monitoring program.

Once this control case study is completed, secondary and tertiary cases investigating citizen experience-based assessment of risk reformation within public transportation systems actively under construction and undergoing varying levels temporal and quality performance is encouraged. Within these focused cases, the environment (the public transportation line under construction) is a significant constraint in selecting the case and a group of participants who normally interact with this environment should be located. As this initial condition significantly reduces the potential participant pool, it is proposed to directly publicize for interested individuals directly within the given transportation lines.

7.7 Key elements of an experience-based assessment of risk monitoring program

In developing an experience-based assessment of risk monitoring program, a manager must develop responses to the following questions:

- How does the general citizen interact with the given system?
- What interaction documentation methodologies can be applied to document the representative citizens' interactions with the given system?
- What is the relative applicability and effectiveness of these various interaction documentation methodologies?
- Through what avenues can the documented interactions be contextualized with qualitative methods?
- What specific environments would be most applicable in addressing the given experience-based assessment of risk questions?

In the example presented above, the key elements of a research program to monitor a citizen's experience-based assessment of a public transportation system related risk were highlighted. The direct personal usage of a public transport system by the general citizen is so frequent that all secondary and tertiary exposure venues were actively ignored. The relative applicability and effectiveness of potential personal usage documentation methods including travel surveys, human-system interaction documentation, passive cellular signal analysis, active cellular signal monitoring and GPS tracking were evaluated. Given the risk source of a public transport system, it was found that GPS tracking provided the most feasible location and time documentation approach.

In selecting applicable qualitative methods for contextualizing the environmental documentation data, the participant's limited faculties while using a public transport system, the time delay associated with the experience-based risk assessment reformation process and potential participant survey fatigue issues limited the qualitative methods to a daily focused survey and the semi-monthly Day Reconstruction Method survey. The focused survey is intended to be administered each morning and to investigate the individual's experience-based assessments of the previous day's five most significant documented event variations. The DRM survey is proposed to be administered twice each month to initially provide an insight into the individual's allocation of time, hedonic states and

valuation of interactions and over the long-term provide insights into how the individual's activities, hedonic states and values vary in time.

It is proposed to initially apply the developed monitoring program within a 90 day, 20-30 participant control case to further investigating the experience-based risk assessment reformation processes. Following this initial case, additional focused cases investigating citizen experience-based risk assessment reformation within public transportation systems under construction and undergoing varying levels temporal and quality performance is encouraged.

7.8 Conclusion

This chapter has focused on developing a procedure to document an individual's continually refining and redefining evaluation process. A case study was conducted employing a wrist mounted GPS unit to document the movements of the participant and an eight-question semi-focused daily survey to document what the individual is focused on and perceived as changing during his daily travels. This case study has found that while the GPS documentation methodology documents the physical movement of the participant, it failed to record additional parameters observed by the individual including weather, travel environment and general environmental changes parameters. Additionally, this case study failed to document the individual's psychological context and perspective during his interactions and thus one is unable to determine if a given interaction has neutral, negative or positive affect on the individual.

To work towards further complementing and contextualizing the GPS tracking approach three hedonic psychology participant survey methods were evaluated. This review found that while the experience sampling and the ecological momentary assessment methods showed potential to document an individual's interactions in real time, but as moving through a transportation system requires a number of faculties, the feasibility of employing such methods in union with a GPS documentation approach is viewed as low feasibility. The day reconstruction method provides a detailed analysis of an individual's day. Thus it is believed that employing a directed survey conducted each morning to explore previous day's activities which differed most significantly from the individual's previous interactions in conjunction with semi-monthly administered day reconstruction method would provide a good balance between detail and longitudinal qualitative insights

It is envisioned that the knowledge gained from these citizen experience-based assessment of risk monitoring programs will aid risk managers in better understanding the influence operational management changes can have on the general citizen's experience-based assessment of risk, calibration of the affective assessment approach and definition of acceptable level of risk.

8 Conclusion

This work focused on identifying and rectifying two analytical limitations of current infrastructure management systems: a) unforeseen natural hazard induced technical failures and b) political-financial funding support failures due to incongruent evaluation of the level of performance between infrastructure manager's nominal evaluation and the experiencing society. To address these limitations, the current work employed a two part approach – first by developing a methodology for quantifying the long-term natural hazard risks to the built infrastructure and secondly by formulating an approach for simulating an individual's experience-based evaluation of the provided level of infrastructure performance. The implementation of these approaches across an transportation infrastructure system by an infrastructure manager enables that manager to: a) improve performance simulation of potential natural hazard risks, thus actively considering an infrastructure object's natural hazard risk in modeling the infrastructure deterioration and in developing optimal maintenance solutions, b) determine the annual funding that should be invested and made available for natural hazards, and c) study how proposed technically optimal solutions may be socially received and can thus select those solutions which best maintain societal support throughout the duration of the maintenance solution. These tools form a technically optimal, socially sustainable infrastructure management model with implications for the subfield of infrastructure management and the entire civil engineering field, but first the development process must be summarized, the approaches detailed, and the findings discussed.

8.1 Component Failure Assessment Procedure

To quantify the long-term natural hazard risks to the built infrastructure, this work first had to develop an assessment procedure for systematically examining the simplified failure modes of each transportation infrastructure component (i.e. bridge, gallery, retaining wall, roadway, and tunnel), as the current natural hazard assessment methods and infrastructure management models lack a procedure for analyzing component failure modes.

The component failure assessment process development was derived from hazard-component failure scenarios. The most general set of failure scenarios was developed by first identifying numerous situations in which a given hazard can cause the partial or complete failure of a given component. Common failure modes were identified for different failure scenarios. These individual failure modes were then embedded into a structured assessment process and representative simple structural models, using the pertinent hazard and object data. These simple models, presented in Appendix A, were then employed to assess the potential of failure within each assessment step.

Findings, Implications, and Applications

Thus, one can systematically qualitatively and quantitatively determine if an infrastructure object is vulnerable to a given hazard intensity and if so, which failure mode controls for the given hazard intensity. Furthermore, this component failure assessment procedure forms a key linkage within the comprehensive natural hazard risk assessment methodology, connecting the hazard and infrastructure object data to the failure mode and consequence data. This linkage eliminates the need to assume an average level of consequences resulting from an infrastructure object's failure and replaces it with a vulnerability curve.

The component failure assessment procedure has four application implications for the subfield of infrastructure management and the field of civil engineering. First, an infrastructure manager can move towards integrating natural hazard risk assessments directly into existing infrastructure management systems. Second, the procedure facilitates the comprehensive natural hazard risk assessment methodology. Third, while more infrastructure and hazard data is required for the procedure, this required data is specifically identified aiding in the efficiency of the overall infrastructure data collection process. Lastly, the component failure assessment process is intended to be employed not only at a single hazard intensity but rather at a number of potential hazard intensities. Through such an application process, one can identify not only the failure mode at each specific hazard intensity, but also the overall range of each failure mode. Additionally, if there are uncertainties concerning the hazard parameter and/or object parameter intensities, the component failure assessment process should be applied, with each analysis employing sampled probability based parameter data. However, the procedure is not without limitations, notably, one must iteratively conduct the failure assessment analysis with each analysis sampling the hazard and object parameter intensities as a function of their respective probability distributions.

The current natural hazard and infrastructure component parameter collection practices within Switzerland place two significant limitations on applying these component failure assessment processes. First, current hazard and infrastructure data collection procedures are respectively the product of existing natural hazard assessment and the infrastructure management requirements. To apply these component failure assessment processes, a number of additional hazard and infrastructure parameter data needs to be collected, but approaches exist for minimizing and streamlining the data collection process. Secondly, the failure assessment process for the bridge, gallery and retaining wall components requires that multiple hazard parameter intensities be determined for a given hazard intensity. Currently, within Switzerland, the natural hazard parameter intensity data is reported separately for each individual hazard parameter. This hinders the process of interrelating different parameters for the same hazard. Thus it is strongly suggested that all hazard parameters for a given hazard be directly correlated or even integrated into a single overarching data set for the given hazard.

8.2 Comprehensive Natural Hazard Risk Assessment Methodology

The Comprehensive Natural Hazard Risk Assessment Methodology was formulated (in Chapter 3) and applied (in Chapter 4) following a review of the existing vulnerability assessment methodologies (in Chapter 2) which revealed that a comprehensive risk assessment platform for assessing natural hazard risks to the built transportation infrastructure does not currently exist.

To develop the comprehensive natural hazard risk assessment methodology, this work first developed the component failure assessment procedure discussed above. This component failure assessment procedure forms a key linkage within the comprehensive natural hazard risk assessment methodology, connecting the hazard and infrastructure object data to the failure mode and consequence data. This linkage eliminates the need to assume an average level of consequences resulting from an infrastructure object's failure and replaces it with a vulnerability curve. Next, data constraints were identified, notably, hazard intensity, failure consequences, and object expose lengths were found to be discrete data points requiring the development of continuous functions fitted to these datasets. From this data, one can calculate the object section vulnerability and risk with respect to the local hazards.

The scope was then expanded to continuous object analysis requiring the development of natural hazard attenuation factors to reduce the continuous object length thereby considering the influence of reconstruction economies of scale and mutually inclusive direct consequences and service interruption durations. This facilitated the assessment of continuous object vulnerability and risk. The scope of analysis was expanded further to transportation infrastructure link level by assessing the link risk due to multiple continuous objects being exposed to multiple hazards. This process required the development of geographically based natural hazard correlation matrices for each geographic feature (level). Next, the work assessed failure risks over time by considering the probability of having a given event occur over the considered time period and the time valuation of money.

To complete the methodology, the approach was employed in Chapter 4 to analyze the vulnerability and risk of selected infrastructure objects within two different roadway links. This analysis illustrated the feasibility of the methodology being applied to existing infrastructure systems and its potential to be used to relatively quantify different risks.

Findings, Implications, and Applications

The author identified three findings associated with this methodology. First, it allows infrastructure mangers to better quantify the risk exposure of a given infrastructure object and link, determine if increases in infrastructure resistance or in natural hazard protection measures are warranted, focus risk mitigation funding to most risk prone regions of the infrastructure network, and finally transparently quantify the financial risk exposure of an infrastructure network. Second, the methodology integrates a natural hazard risk assessment platform into the existing infrastructure management systems. Third, the approach requires additional component and natural hazard data to be collected, but methods to streamline this process have been identified (in Chapter 3) thus enabling existing data collection systems to easily adapt to these additional requirements.

The application of the methodology to the case studies (in Chapter 4) show not only that it is feasible to conduct a detailed comprehensive assessment of the natural hazards affecting the built infrastructure, but that there are three main areas for additional improvement in the methodology: a) natural hazard intensity data reporting, b) direct consequences and service interruption estimation and c) inter-hazard correlation estimation.

The current methods of reporting the natural hazard parameter intensities, reporting hazard intensity ranges for each event return period (Case Study A) or reporting general hazard risk-based regions (Case Study B), are both too abstract to be directly employed in this assessment methodology without making additional onsite assessments or general estimations. It is proposed that the natural hazard data reporting practices be expanded so that two different sets of data be reported, one set similar to the current reporting format which is intended to be distributed on printed hazard identification maps and one set identifying the local hazard parameters intensities which is intended to be digitally distributed. Without such an improvement, additional onsite assessments will need to be conducted for each exposed infrastructure object to acquire the needed natural hazard data.

Turning to the second area for additional improvement, the direct consequence and service interruption duration estimation, one can see from these case studies that the direct consequence and service interruption duration values for each hazard parameter intensity threshold has been roughly estimated. With such estimations, one can assess the order of magnitude of the given risk

affecting a given infrastructure object but one is unable to directly compare and contrast different hazard risks affecting different infrastructure object types. Thus it is proposed to formulate a group of experienced practitioners who can use their experience to further refine these direct consequence and service interruption duration estimates.

The last main area for additional improvement, intra-hazard and inter-hazard correlation estimation, is currently addressed by developing estimated intra-hazard and geographically-based inter-hazard correlation factors. While such estimates employed within this work are a beginning, further assessment accuracy can be achieved by modeling the intra-hazard and inter-hazard correlation for each of the three main topographic regions of Switzerland – the mountainous region, the valley region and the plain region. Through such additional work, one would be able to clarify and validate the intra-hazard and inter-hazard correlation estimates currently employed in this vulnerability and risk assessment methodology.

Overall, however, this methodology forms a foundation for conducting a system wide natural hazard risk assessment. When applied across an entire transportation infrastructure system, the infrastructure manager can actively consider an infrastructure object's potential natural hazard failure risk exposure in modeling the infrastructure deterioration and in developing optimal maintenance solutions. He can also determine the annual funding which should be invested and made available for natural hazard prevention and failure response. This is important because, currently, natural hazard induced failure responses are not directly funded or considered by infrastructure management systems. The expected end result is reduced infrastructure object failure potential, improved natural hazard protection systems, and a more stable funding and infrastructure management.

8.3 Affective Assessment Approach

To address the second limitation of infrastructure management systems, political-financial funding support failures due to incongruent evaluation of the level of performance between an infrastructure manager's nominal evaluation and the experiencing society, this work formulated an approach for simulating an individual's experience-based evaluation of the provided level of infrastructure performance—the affective assessment approach.

The affective assessment approach was developed from findings within the behavioral economics and psychology fields (in Chapter 6) and the realization that existing intangible evaluation approaches do not address the incongruities between an infrastructure manager's nominal evaluation and the experiencing society (Appendix B). A critical review of the Life Quality Index, an approach for assessing the maximum value of a life (Appendix A), accentuates these incongruities by showing the good intentioned proposal of developing a unified rationale for evaluating life-saving investments so that these decisions might be removed from the public arena actively exposes the risk manager and his decisions to potential differences between the analytically-based performance evaluation and societal experience-based performance evaluations, thus, forming the foundational need for the Affective Assessment Approach.

This approach first identified the infrastructure object parameters the public personality interacts with. It then specified a process for modeling how the performance differences between subsequent interactions can be evaluated using two case studies to illustrate how an individual's experience-based assessments evolve in time as the individual interacts with a changing infrastructure system.

Next in Chapter 6, an approach for incorporating additional experiences into the individual's evaluative norms was formulated. The affective assessment approach was then employed to analyze two cases to better understand the implications an experience-based evaluation approach can have on the evaluations of a set of interactions (Case Study E and Case Study F). These case studies examined the implications an experience-based evaluation perspective has for individuals with different experience histories and within environments with different deterioration rates. Lastly, the feasibility of applying such an experience-based evaluation approach was assessed in Chapter 7 by conducting a pilot study (Case Study G). In this study, it was determined that conducting a documentation and calibration study was not feasible within this work, but should be pursued in the immediate future.

Findings, Implications, and Applications

The work identified four key implications of this approach. First, it challenges infrastructure managers to step beyond their current purely analytical decision models and actively consider how potential management decisions may be received by the general public. Second, it proposes an approach for assessing how an individual's previous experience, interaction sequence and interaction intensity can cause the evaluation of an infrastructure performance to change. Third, through implementing the approach, an infrastructure manager can work to determine how analytically optimal solutions may be socially received and which solution can a) help the general public in observing or in ignoring infrastructure deterioration and b) prevent the provided performance from undermining or diluting society's level of expected performance. Such social dynamics can assist in ensuring the maintenance solution is fully implemented and funded. The funding connection has not yet been confirmed but the link is strongly suspected to exist especially in direct democracy funding situations as are found in Switzerland. Fourth, the functional performance of an infrastructure object is a primary medium for the infrastructure manager to communicate the current structural state of the object.

While, the potential applications of this approach have been demonstrated in Chapter 6, this model has not been calibrated to a given person or situation. The following aspects should be calibrated: a) the affective assessment factor, b) the memory depreciation factor, and c) the number of non-depreciated interactions. Additionally, the affective assessment approach has been applied to simulate the potential induced affect of single individual experiencing a single parameter, the experienced speed. This approach should be broadened by segmenting the experienced speed into subclassifications by considering the environment in which the speed is experienced (e.g. predominate times, weather conditions or trip purposes) and generalized by aggregating the individuals of society into social groups (e.g. business commuters, leisure drivers, professional drivers).

Through calibrating these parameters and by broadening and aggregating the application of the affective assessment approach, would facilitate an infrastructure manager to more effectively predict an individual's sensitivities to changing environments, enabling the manager to more accurately choose the technically optimal socially-sustainable management solution.

8.4 Fusing the Approaches

Returning to the chart Figure 1-3 introduced in the introduction, one can see that while the above approaches appear distinctly separate on one level, on another level, they come together to form a two prong technically optimal, socially sustainable infrastructure management model. These approaches when implemented into an existing infrastructural management system improve the system on both a limited level and a broader level. On the limited level, these approaches address the analytical limitations of current infrastructure management systems enabling infrastructure managers to:

- Improve performance simulation of potential natural hazard risks, thus actively considering an infrastructure object's natural hazard risk in modeling the infrastructure deterioration and in developing optimal maintenance solutions
- Improve annual funding assessments
- Study how proposed technically optimal solutions may be socially received and work to select solutions which best maintain their social support throughout the duration of the maintenance solution.

On a broader level, this model enables infrastructure managers to close two key engineering gaps:

- Appropriately quantifying and preventing natural hazard induced infrastructure failures
- Appropriately quantifying and effectively communicating infrastructure maintenance and funding needs to politicians and the general public

This should result in improved infrastructure management systems, built infrastructure, and fewer incongruities in communicating with the serviced population.

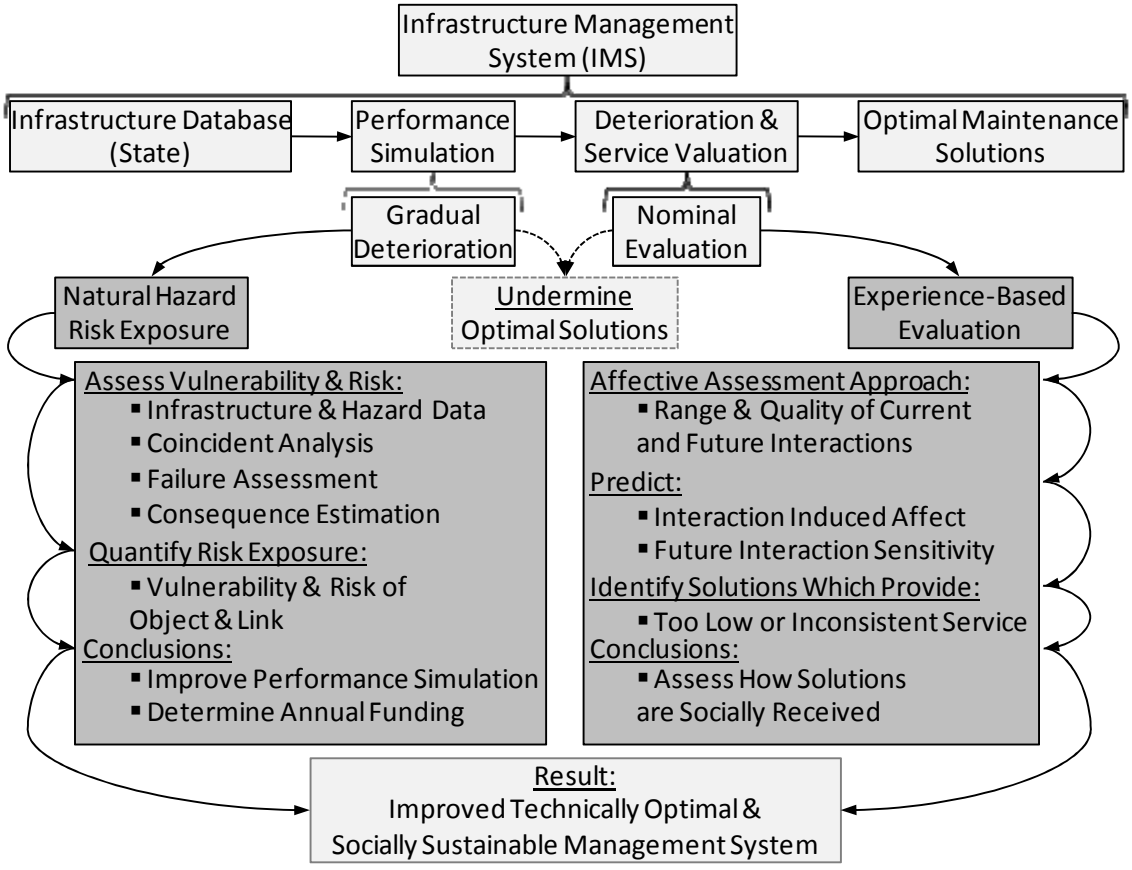

Figure 8-1: A technically optimal, socially sustainable management system.

Further Study

Once, the Component Failure Assessment Procedure has been automated, the recommended natural hazard and infrastructure object data has been collected, the Affective Assessment Approach has been calibrated, and these approaches have been integrated into an existing infrastructure management system, it is essential to conduct a joint implementation and monitoring study to examine to impact of this approach. Such a study should assess the ease of implementation and the medium term costs and benefits of each approach.

8.5 Overall Conclusions

Current infrastructure management systems are not technically optimal or social sustainable as they overlook potential sudden failure modes and potential incongruities between the analytically assessed and socially experience-based evaluated provided infrastructure performance. Therefore, this work developed the Component Failure Assessment Procedure, the Comprehensive Natural Hazard Risk Assessment Method, and the Affective Assessment Approach to form a technically optimal, socially sustainable infrastructure management model with implications for the subfield of infrastructure management and the wider civil engineering community.

Implications for Infrastructure Management

There are implications for the subfield of infrastructure management if the technically optimal socially-sustainable decision model is integrated into existing infrastructure management systems on two levels: the infrastructure manager level and the subfield level. On the infrastructure manager level, this model enables managers to:

- Improve the technical performance by assessing and quantifying risks posed by natural hazards and strengthening social sustainability by identifying and selecting infrastructure management solutions which help the serviced public in personally experiencing the current level of structural performance.
- Identify analytically optimal solutions which will result in the undermining or dilution of the society's expected performance so they can be removed from consideration.
- Minimize the natural hazard induced sudden failures and start to consider how to manage the built infrastructure in such a way that it can be used as a tool to communicate with the serviced public.

On the subfield level, this model enables researchers to:

- Realize that the transportation infrastructure systems they research are not isolated systems as the current infrastructure management models assume by default.
- Look beyond the purely analytical aspects of infrastructure systems and actively consider how the provided levels of performance will be socially framed and received.
- Explore avenues for cross disciplinary work with natural hazard assessment, emergency management, behavioral economics, and psychology decision-making domains.

Implications for Civil Engineering

On the wider civil engineering field level, this model enables practitioners to:

- Look beyond their analytical approaches and consider analytical scopes respective of their field's title, engineering the civil society.

- Begin to remove one of remaining technical stumbling blocks of civil engineering in the public's eye – appropriately quantifying and preventing natural hazard induced infrastructure failures.
- Begins to remove on the remaining implementation stumbling blocks of civil engineering – appropriately quantifying and effectively communicating infrastructure maintenance and funding needs to politicians and the general public.

Finally, in an age when infrastructure managers are starting to observe the strengths and weaknesses of infrastructure management systems, this work introduces and proposes a two prong integrated socially-sustainable technically-optimal decision model addressing two key gaps in current infrastructure management and civil engineering: a) appropriately quantifying and preventing natural hazard induced infrastructure failures and b) appropriately quantifying and effectively communicating infrastructure maintenance and funding needs to politicians and the general public. While this model has limitations, with further development and implementation, it should improve existing infrastructure management systems, built infrastructure, and remove the evaluation incongruities currently limiting infrastructure management and civil engineering.

A Failure assessment procedure

A.1 Element resistance assessment equations

The ultimate strength punching shear, direct shear and flexural strength Equations (A.1), (A.2) and (A.3) were developed by the United States government through extensive experimental testing to assess the plastic response of reinforced concrete member response to high magnitude forces. These equations were chosen for it is believed that they will accurately assess the reinforced concrete member's response to natural hazard high intensity loading.

The punching shear capacity of a doubly reinforced rectangular concrete member can be assessed with Equation (A.1). It should be noted that Equation (A.1) intentionally does not consider the contribution of shear reinforcement (US Army, 1990, p. 4.40).

$$v_c = 4\sqrt{f'_{dc}} \tag{A.1}$$

Where:

v_c = the punching shear stress capacity [N/mm^2]

f'_{dc} = the dynamic ultimate compressive strength of concrete [N/mm^2]

Likewise the direct shear capacity of a doubly reinforced rectangular concrete member can be assessed with Equation (A.2) (US Army, 1990, p. 4.39).

$$V_d = 0.18 f'_{dc}\, b \cdot d \tag{A.2}$$

Where:

V_d = the ultimate direct shear capacity [N]

b = width of the concrete compression face [mm]

d = the distance from the extreme compression fiber to the centroid of the tensile reinforcement [mm]

Additionally, the ultimate moment resistance of a doubly reinforced rectangular concrete member can be assessed with Equation (A.3) (US Army, 1990, p. 4.34).

$$M_u = \frac{A'_s \cdot f_{ds}}{b} \cdot \left(d - \frac{\left(A_s - A'_s\right) f_{ds}}{2 \cdot 0.85 \cdot b \cdot f'_{dc}} \right) + \frac{A'_s\, f_{ds}}{b} \cdot (d - d') \tag{A.3}$$

Where:

M_u = the ultimate moment resistance [Nmm]

A_s = the area of the tensile reinforcement within the width b [mm^2]

A_s' = the area of the compression reinforcement within the width b [mm^2]

d' = the distance from the extreme compression fiber to the centroid of the compression reinforcement [mm]

f_{ds} = dynamic design stress for reinforcement [N/mm^2]

A.2 Bridge failure assessment procedure

Bridges are elevated objects constructed to carry the given roadway or railway over bodies of water, established transportation routes over uneven ground. Within this work and as shown in Figure 3-7,

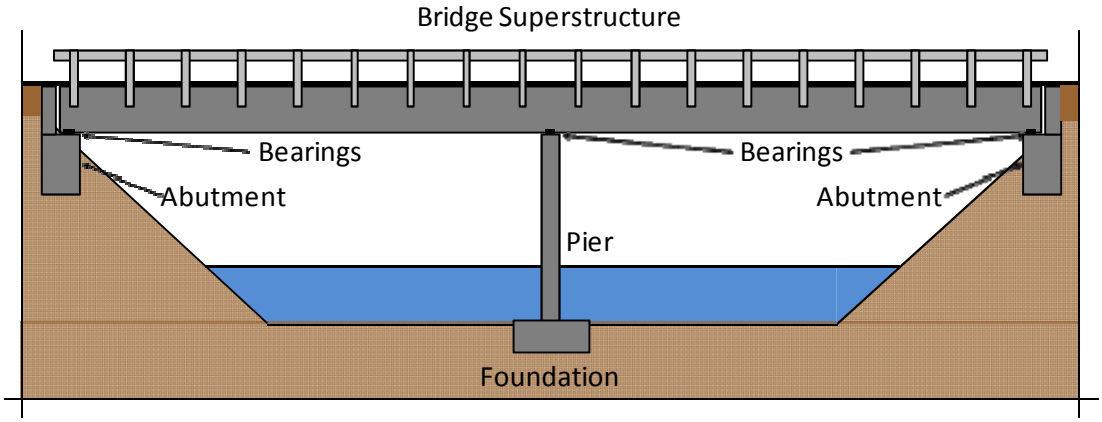

Figure A-1: A typical bridge configuration.

a bridge object is assumed to be composed of four key elements – foundation, piers and abutments, bearings and superstructure. In Table 3-3, 23 different potential hazard scenarios are considered in assessing the capacity of a bridge object. When these hazard scenarios are analyzed as a group, six failure modes can be identified and can be arranged into the structured assessment process presented in Figure 3-8.

Table A-1: Bridge failure modes and associated hazards.

	Potential Hazards				
Failure mode	**Avalanche**	**Flood**	**Landslide**	**Rockfall**	**Torrent**
Foundation is undermined	-	x	x	-	-
Superstructure is overloaded vertically in shear or flexure	x	-	-	x	-
Superstructure is overloaded horizontally in shear or flexure	x	x	x	x	x
Bearings are overloaded horizontally or vertically	x	x	x	x	x
Bridge pier is overloaded horizontally in shear or flexure	x	-	x	x	x
Bridge surface submerged in liquid or debris	x	x	x	x	x

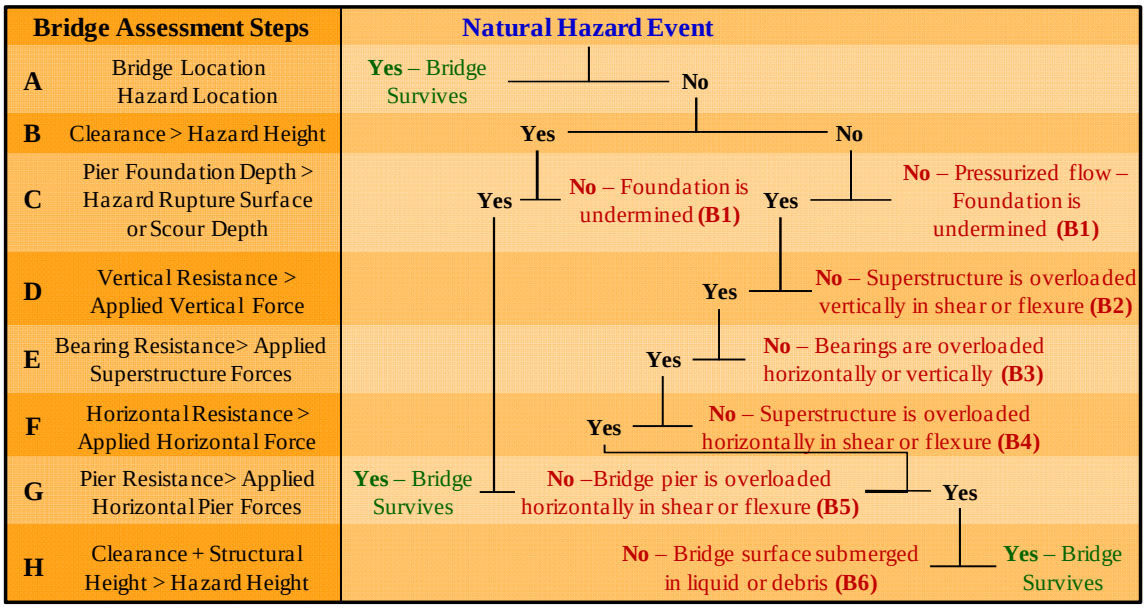

Figure A-2: Bridge component failure assessment process.

Bridge component failure assessment step A

The first step of the bridge failure assessment procedure, step A: bridge location ≠ hazard location, requires one to conduct a geographic coincident analysis between the location of the given bridge and the geographic reach of the five potential hazards. If a given hazard is not coincident with the given bridge, it is assumed that the bridge will not be affected by the given hazard. If the given hazard and bridge are coincident, one must assess the potential failures for the complete range of applicable hazard intensities.

Bridge component failure assessment step B

The second assessment step, step B: clearance > hazard running height, assesses if the given hazard height surpasses the bridge's clearance. The definition of bridge clearance and hazard running height are detailed in Figure A-3 and analytical defined in Equation (A.4).

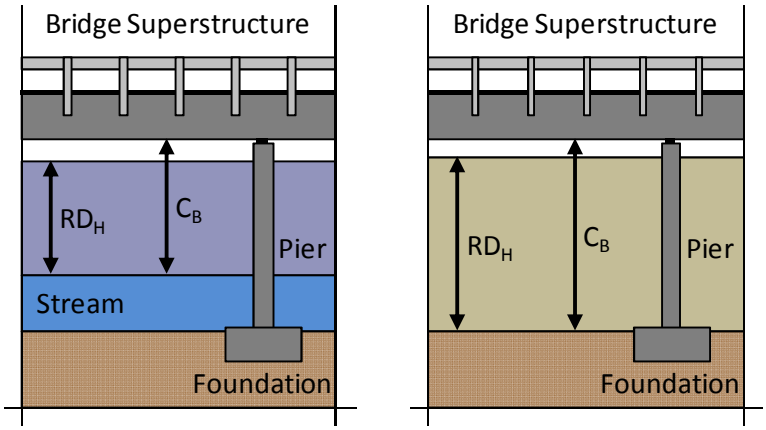

Figure A-3: Assessing if hazard running height surpasses bridge clearance for a) a bridge crossing a stream and b) a bridge crossing uneven ground.

$$RD_H > C_B \quad \{RD_H = RD_A \vee H_F \vee RD_L \vee RD_R \vee H_T\} \tag{A.4}$$

Where:

C_B = bridge clearance measured between the bottom of the superstructure and the average water level or surrounding earth [m]
RD_H = hazard running depth [m]
RD_A = avalanche running depth [m]
H_F = flood height [m]
RD_L = landslide running depth [m]
RD_R = rockfall running depth [m]
H_T = torrent height [m]

If the hazard running depth does not exceed the bridge clearance, it is assumed the hazard does not come in contact with the bridge superstructure and therefore one only needs to assess the capacity of the bridge pier and bridge foundations (assessment steps C and G), but hazard running depth does exceed the bridge clearance then one needs to conduct a complete assessment of the bridge superstructure, bearings, piers and foundations.

Bridge component failure assessment step C

The third step of the bridge component failure assessment process is: step C: pier foundation depth >

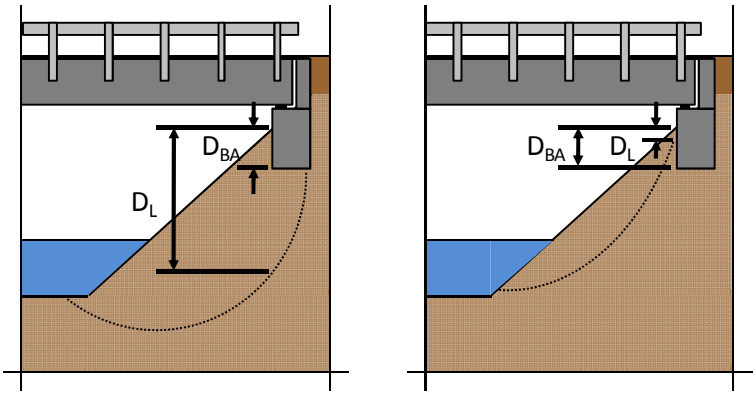

Figure A-4: Assessing if landslide depth exceeds abutment depth for a) a deep landslide or b) a shallow landslide.

hazard rupture surface or scour depth, and assesses the hazard intensity load affect on the bridge foundation.

It has been assumed that only two hazards, flood and landslide, can potentially undermine a bridge's foundations. The former hazard, landslide, is particularly applicable to the bridge abutments as is shown in Figure A-4. To assess a bridge abutments' vulnerability to landslides, one needs to verify that the abutment depth is deeper than the landslide fracture surface depth at the abutment location, as is presented in Equation (A.5).

$$D_{BA} > D_L \tag{A.5}$$

Where:

D_{BA} = abutment or pier depth measured from the ground surface at the downhill side of the abutment[m]

D_L = landslide rupture surface depth measured from the ground surface at the downhill side of the abutment [m]

In Figure A-4a, while a landslide does destabilize the embankment, the depth of the landslide at the abutment does not exceed the abutment depth, Equation (A.5), and thus the abutment is assumed to not fail. In Figure A-4b, a deep landslide destabilizes the embankment and the landslide rupture surface depth at the abutment location does exceed the abutment depth – thereby causing the expected failure of the abutment. The landslide rupture surface depth hazard should be assessed by an experienced geologist. While this assessment is typically general in nature, i.e. shallow or deep, such information can help to identify if the bridge abutment foundations are exposed to a potential landside hazard.

In assessing the flood hazard impact on the bridge foundations, whether or not the flood exceeds the bridge clearance has significant influence on the resulting flood induced scour depth, as shown schematically in Figure A-5. When flood water flows around a bridge's foundations, the local increased water speed created by the resulting vortices removes soil and stones from around each foundation, Figure A-5b. If the flood water height exceeds the bridge clearance, the water flow shifts from a non-pressurized flow to a pressurized flow, significantly increasing the general and localized water speeds. This increased water velocity not only causes the local pier scour to increase but also causes general scour of the stream floor, Figure A-5c.

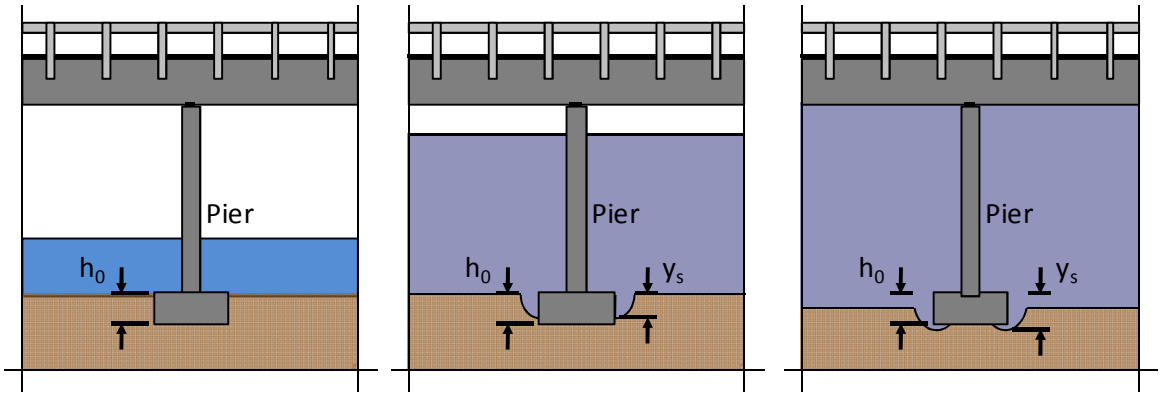

Figure A-5: Schematics detailing a) original pre-scour condition, b) a non-pressurized scour, c) pressurized scour.

Stream induced scour of bridge foundations – abutments and piers – can be evaluated following the approaches presented in *Evaluating Scour at Bridges* (Richardson & Davis, 2001). The process of identifying a scour depth assessment procedure of a bridge pier place on a spread footing is presented in Example A-1.

Example A-1: Identify an approach for evaluating the scour depth adjacent to a bridge pier placed on a spread footing foundation under non-pressurized and pressurized flow conditions.

This example focuses on identifying an approach for assessing the vulnerability of a bridge pier placed on a spread footing to non-pressurized and pressurized scour as spread footings are one most scour vulnerable bridge foundation types. As seen in Equations (A.6) and (A.7), the non-pressurized scour of a bridge pier is influenced by the pier geometry, the stream's hydraulic conditions during the flood, the stream bed conditions and the interaction between the pier and the footing. In particular, Equation (A.6) assesses how the presence of the footing works to shield the pier from scour and Equation (A.7) quantifies the total resulting scour induced by the presence of the pier (Richardson & Davis, 2001, pp. 6.10, 6.27).

$$K_{hpier} = \left(0.4075 - 0.0669\frac{f}{a}\right) - \left(0.4271 - 0.0778\frac{f}{a}\right)\frac{h_0 + T}{a} + \left(0.1615 - 0.0455\frac{f}{a}\right)\left(\frac{h_0 + T}{a}\right) - \left(0.0269 - 0.012\frac{f}{a}\right)\left(\frac{h_0 + T}{a}\right)^3 \quad \text{(A.6)}$$

Where:

K_{hpier} = footing shielding of pier coefficient [ ]
f = lateral footing extension measured from edge of pier [m]
a = pier width [m]
h_0 = elevation of bottom of footing measured from stream bed [m]
T = footing thickness [m]

$$y_{spier} = y_1 \cdot K_{hpier} \cdot 2 \cdot PK_1 PK_2 PK_3 PK_4 \left(\frac{a}{y_1}\right)^{0.65} \left(\frac{V_1}{\sqrt{y_1 g}}\right)^{0.43} \quad \text{(A.7)}$$

Where:

y_{spier} = local scour depth induced by the pier geometry [m]
y_1 = average upstream main channel depth prior to contraction scour [m]

V_1 = average flow velocity immediate upstream of the pier [m/s]
g = 9.807 gravitation acceleration [m/s^2]
PK_1 = pier nose shape correction factor [ ]
PK_2 = angle of flow attack correction factor [ ]
PK_3 = bed condition scour depth correction factor [ ]
PK_4 = pier armoring scour depth correction factor [ ]

To determine the localized scour induced by the presence of the footing, one must determine how the pier induced scour changes the stream's hydraulic condition, Equations (A.8) and (A.9), how the footing geometry modifies the stream's hydraulic patterns, Equations (A.10), (A.11) and (A.12), and the resulting scour induced by the footing considering the general footing geometry, the stream hydraulic state and the stream bed conditions, Equation (A.13) (Richardson & Davis, 2001).

$$y_2 = y_1 + \frac{y_{spier}}{2} \tag{A.8}$$

$$V_2 = \frac{V_1 y_1}{y_2} \tag{A.9}$$

Where:

y_2 = adjusted flow depth for spread footing induced scour calculations [m]
V_2 = adjusted flow velocity for spread footing induced scour calculations [m/s]

$$K_w = \begin{cases} 2.58\left(\frac{y_1}{a}\right)^{0.34}\left(\frac{V_1}{\sqrt{y_1 g}}\right)^{0.65} & \left\{ y_2 < 0.8a_f \wedge \frac{V_2}{\sqrt{y_2 g}} < 1 \wedge a_f > 50D_{50} \wedge \frac{V}{V_{50}} < 1 \right\} \\ \left(\frac{y_1}{a}\right)^{0.13}\left(\frac{V_1}{\sqrt{y_1 g}}\right)^{0.25} & \left\{ y_2 < 0.8a_f \wedge \frac{V_2}{\sqrt{y_2 g}} < 1 \wedge a_f > 50D_{50} \wedge \frac{V}{V_{50}} > 1 \right\} \\ 1 & \left\{ y_2 \geq 0.8a_f \vee \frac{V_2}{\sqrt{y_2 g}} \geq 1 \vee a_f \leq 50D_{50} \right\} \end{cases} \tag{A.10}$$

$$y_f = h_0 + T + \frac{y_{spier}}{2} \tag{A.11}$$

$$V_f = \frac{V_2 \ln\left(\frac{10.93 y_f}{D_{84}}\right)}{\ln\left(\frac{10.93 y_2}{D_{84}+1}\right)} \tag{A.12}$$

Where:

K_w = wide pier in shallow flow correction factor [ ]
a_f = spread footing width [m]
D_{50} = median diameter of bed material [m]
V_{50} = critical velocity of D_{50} sized material [m/s]
y_f = elevation bottom of footing measured from stream bed [m]
V_F = average flow velocity below top of footing [m/s]

D_{84} = diameter of 84% bed material is smaller [m]

$$y_{sfooting} = 2y_f FK_1 FK_2 FK_3 FK_4 K_w \left(\frac{a_f}{y_f}\right)^{0.65} \left(\frac{V_f}{\sqrt{y_f g}}\right)^{0.43} \quad \text{(A.13)}$$

Where:

$y_{sfooting}$ = local scour depth induced by the footing geometry [m]
FK_1 = footing nose shape correction factor [ ]
FK_2 = angle of flow attack correction factor [ ]
FK_3 = bed condition scour depth correction factor [ ]
FK_4 = footing armoring scour depth correction factor [ ]

The resulting combined total pier and footing scour is purely the sum of the two independent scour depths, as presented in Equation (A.14) (Richardson & Davis, 2001, p. 6.37).

$$y_{stotal} = y_{spier} + y_{sfooting} \quad \text{(A.14)}$$

Where:

y_{stotal} = total scour depth adjacent to the pier measured from the non-scoured stream bed [m]

If the water has come in contact with the bridge superstructure, the superstructure will further restrain the flow of water. This future restraint causes the flow of the stream to shift from non-pressurized flow to pressurized flow, significantly increasing the stream flow velocity. This increased flow rate in turn causes additional bed material to be uniformly scoured out from underneath the bridge. This uniform scour depth, considering the clearance under the bridge and the bed material, can be quantified with Equation (A.15) (Richardson & Davis, 2001, p. 6.22).

$$y_{spressure} = y_1 \left(-5.08 + 1.27\left(\frac{y_1}{H_b}\right) + 4.44\left(\frac{H_b}{y_1}\right) + 0.19\left(\frac{V_a}{V_{50}}\right)\right) \quad \text{(A.15)}$$

Where:

$y_{spressure}$ = depth of vertical contraction scour measured from the non-scoured stream bed [m]
H_b = clearance between the lowest superstructure point and the non-scoured stream bed [m]
V_a = average flow velocity of D_{50} bed material before scour [m/s]

The resulting total scour, considering the influence of the pier, footing and superstructure clearance, is likewise the sum of the individually assessed scour depths, Equation (A.16) (Richardson & Davis, 2001, p. 6.33).

$$y_{stotal} = y_{spier} + y_{sfooting} + y_{spressure} \quad \text{(A.16)}$$

These resulting total scour depths for each hydraulic condition are then compared against the depth of the pier footing, Equation (A.17)

$$h_0 > y_{stotal} \quad \text{(A.17)}$$

If this failure assessment confirms Equation (A.17) is false, it is assumed that the pier has failed due to scour.

Bridge component failure assessment step D

The fourth failure assessment step, step D vertical resistance > applied vertical force, focuses on evaluating the vertical resistance of the bridge superstructure and the applied vertical hazard force. In Table 3-3, one can observe that it has been assumed that only two hazards – avalanche and rockfall hazards – can induce a bridge superstructure to fail vertically.

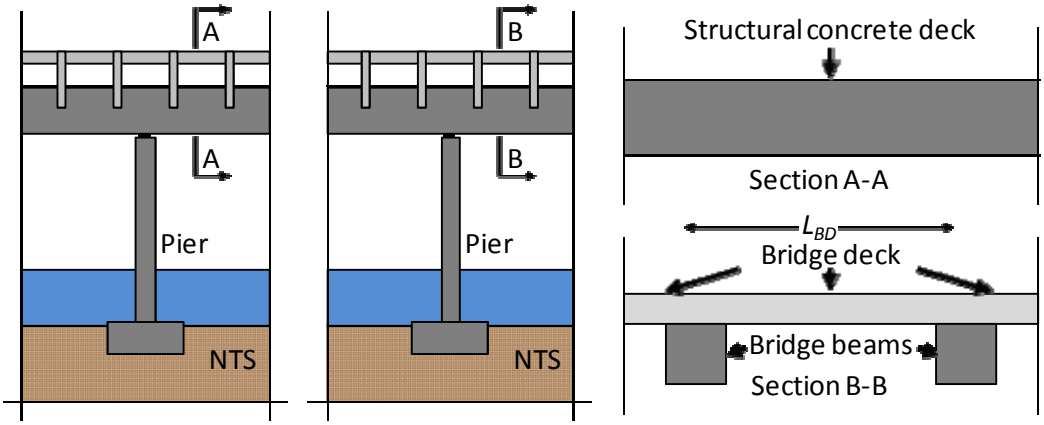

Figure A-6: Bridge superstructure configuration a) a structural concrete deck, b) a bridge deck supported by concrete beams.

Assuming the bridge superstructure follows one of two structure configures, either the bridge superstructure is composed of a structural concrete deck or is composed of longitudinal beams supporting a concrete deck, Figure A-6a and Figure A-6b, respectively.

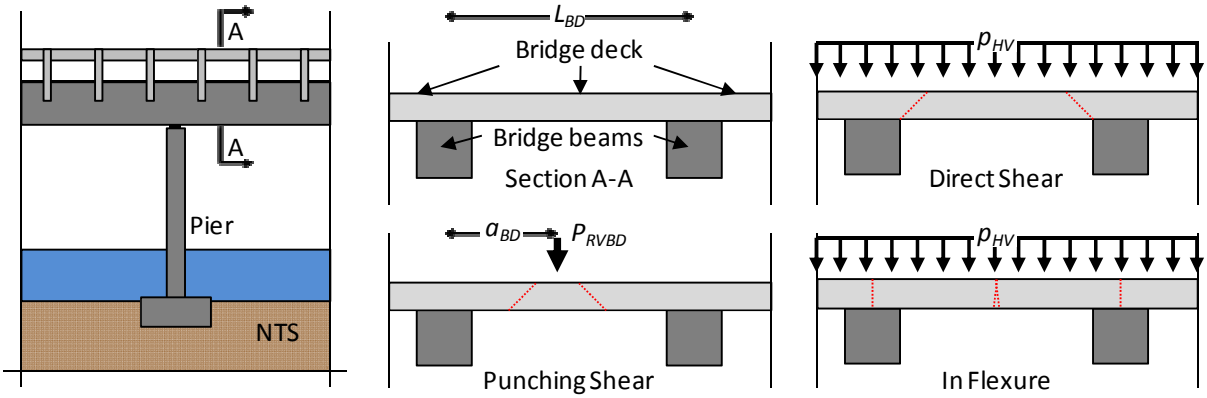

Figure A-7: Bridge deck overloaded in shear or flexure.

Considering the first bridge superstructure configuration, the punching shear strength can be determined with Equation (A.18) and considering the second bridge superstructure configuration and assuming the bridge deck is a doubly reinforced concrete member, Figure A-7, the punching shear, direct shear and moment capacity can be respectively computed with Equations (A.19), (A.20) and (A.21).

$$v_{cBS} = 4\sqrt{f'_{dcBS}} \tag{A.18}$$

$$v_{cBD} = 4\sqrt{f'_{dcBD}} \tag{A.19}$$

$$V_{dBD} = 0.18 f'_{dcBD} b_{BD} d_{BD} \tag{A.20}$$

$$M_{uBD} = \frac{A'_{sBD}\ f_{dsBD}}{b_{BD}} \cdot \left(d_{BD} - \frac{\left(A_{sBD} - A'_{sBD}\right) f_{dsBD}}{2 \cdot 0.85 \cdot b_{BD} f'_{dcBD}} \right) + \frac{A'_{sBD}\ f_{dsBD}}{b_{BD}} \cdot (d_{BD} - d'_{BD}) \qquad \text{(A.21)}$$

Where:

v_{cBS} = the punching shear stress capacity of the bridge structural deck [N/mm^2]
f'_{dcBS} = the dynamic ultimate compressive strength of the bridge structural deck [N/mm^2]
v_{cBD} = the punching shear stress capacity of the bridge deck [N/mm^2]
f'_{dcBD} = the dynamic ultimate compressive strength of concrete in the bridge deck [N/mm^2]
V_{dBD} = the ultimate direct shear capacity of the concrete deck [N]
b_{BD} = width of the concrete compression face of the concrete deck [mm]
d_{BD} = the distance from the extreme compression fiber to the centroid of the tensile reinforcement of the bridge deck [mm]
M_{uBD} = the ultimate moment resistance of the bridge deck [Nmm]
A_{sBD} = tensile reinforcement area within the width b_{BD} of the bridge deck [mm^2]
$A_s'_{BD}$ = compression reinforcement area within the width b_{BD} of the bridge deck [mm^2]
d'_{BD} = the distance from the extreme compression fiber to the compression reinforcement centroid of the bridge deck [mm]
f_{dsBD} = dynamic design stress for reinforcement of the bridge deck [N/mm^2]

For the avalanche hazard it can be assumed that the applied force is uniformly distributed and thus it can be assumed that the bridge deck will not fail in punching shear. Additionally, assuming the bridge deck performs as fixed-fixed beams, the induced maximum shear and moment forces can be computed with Equations (A.22) and (A.23) (AISC, 1998, p. 4.195).

$$V_{HBD} = \frac{p_{HV} b_{BD} L_{BD}}{2} \qquad \text{(A.22)}$$

$$M_{HBD} = \frac{p_{HV} b_{BD} {L_{BD}}^2}{12} \qquad \text{(A.23)}$$

Where:

V_{HBD} = the maximum hazard induced shear force within the bridge deck [N]
M_{HBD} = the maximum hazard induced moment force within the bridge deck [Nmm]
p_{HV} = the hazard vertical pressure [N/mm^2]
b_{BD} = the horizontal spacing of the bridge superstructure beams [mm]

For the avalanche hazard, the hazard vertical pressure can be computed from the avalanche horizontal pressures by considering the uphill slope as is shown in Equations (A.24).

$$p_{AV} = p_{AH} \tan\left(\alpha_B\right) \qquad \text{(A.24)}$$

Where:

p_{AV} = the avalanche vertical pressure [N/mm^2]
α_B = the bridge uphill slope [rad]

Turning to the rockfall hazard and assuming the bridge deck has a negligible cushion, the vertical force imposed on the bridge deck can be computed with Equation (A.25) (Chikatamarla, 2007, pp. 11-12).

$$P_{RVBD} = 2.8 {r_R}^{0.7} {E_{BD}}^{0.4} {E_R}^{0.6} \sin(\alpha_R) \qquad \text{(A.25)}$$

Where:

P_{RVBD} = the rockfall vertical force applied to the bridge deck [kN]
r_R = the radius of the boulder at the contact point [mm]
E_{BD} = the bridge deck modulus of elasticity [N/mm^2]
α_R = the rockfall angle of attack measured from the vertical

Thus, the respective induced punching shear, direct shear and moment forces are a function of the location of the rockfall impact point and can be calculated with Equations (A.26), (A.27), and (A.28) (Chikatamarla, 2007, pp. 11-12).

$$v_{RBD} = \frac{P_{RVBD}}{2\pi d_{cBD}\left(r_R + \frac{d_{BD}}{2}\right)} \tag{A.26}$$

$$V_{RBD} = \frac{P_{RVBD}\left(L_{BD} - a_{BD}\right)}{L_{BD}} \tag{A.27}$$

$$M_{RBD} = \frac{P_{RVBD}\left(L_{BD} - a_{BD}\right)a_{BD}}{L_{BD}} \tag{A.28}$$

Where:

v_{RBD} = the bridge deck ultimate rockfall induced punching shear [N/mm^2]
V_{RBD} = the bridge deck maximum rockfall induced direct shear [N]
M_{RBD} = the bridge deck maximum rockfall induced moment [Nmm]
a_{BD} = the horizontal position of the rockfall impact point measured from the closest bridge superstructure beam [mm]

These potentially induced hazard forces are then combined with the standard self, dead and live forces normally carried by the bridge to assess if the bridge deck capacity is exceeded.

With the assessment process for the local vertical failure of the bridge superstructure formulated, one must now analyze the potential of the bridge superstructure to globally fail in the vertical direction. This requires one to assess if the applicable hazards – avalanche or rockfall – can exceed the shear or flexural strength of the bridge structural deck or the bridge deck beams, for bridge deck configurations A and B respectively. For the first and second gallery configurations, assuming the bridge structural deck and the bridge beams, respectively, are doubly reinforced concrete members, each member's shear and flexural capacity can be determined using Equations (A.2) and (A.3) resulting in Equations (A.29) and (A.30). Please note the alternative definitions of the second bridge superstructure configuration width and depth variables detailed in Figure A-8.

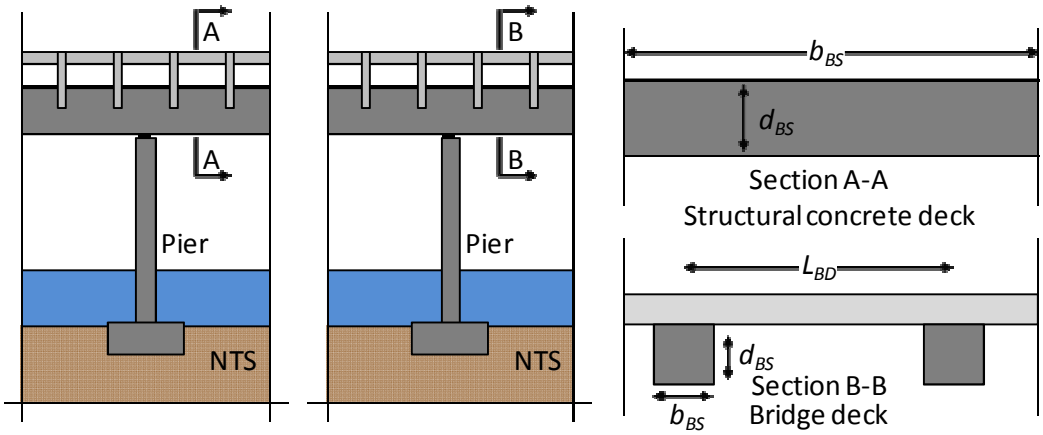

Figure A-8: Structural configuration of bridge superstructure.

$$V_{dBS} = 0.18 f'_{dcBS} b_{BS} \cdot d_{BS} \tag{A.29}$$

$$M_{uBS} = \frac{A'_{sBS} f_{dsBS}}{b_{BS}} \cdot \left(d_{BS} - \frac{(A_{sBS} - A'_{sBS}) f_{dsBS}}{2 \cdot 0.85 \cdot b_{BS} f'_{dcBS}} \right) + \frac{A'_{sBS} f_{dsBS}}{b_{BS}} \cdot (d_{BS} - d'_{BS}) \tag{A.30}$$

Where:

V_{dBS} = bridge superstructure ultimate direct shear capacity [N]

b_{BS} = bridge superstructure concrete compression face width [mm]

d_{BS} = distance from the extreme compression fiber to the centroid of the tensile reinforcement within the bridge superstructure [mm]

M_{uBS} = bridge superstructure ultimate moment resistance [Nmm]

A_{sBS} = tensile reinforcement area within the bridge deck width b_{BD} [mm^2]

$A_s'_{BS}$ = compression reinforcement area within the bridge deck width b_{BD} [mm^2]

d'_{BS} = distance from the extreme compression fiber to the compression reinforcement centroid of the bridge superstructure [mm]

f_{dsBS} = bridge superstructure reinforcement dynamic design stress [N/mm^2]

The forces applied to the bridge superstructure are a function of the physical reach of the given hazard. To analyze the avalanche hazard, Figure A-9, one can observe that the applied forces are assumed to be uniformly distributed across the bridge superstructure. Thus assuming the bridge superstructure responds as a simply supported beam, the maximum hazard induced direct shear and moment forces can be computed with Equations (A.31) and (A.32) (AISC, 1998, p. 4.190).

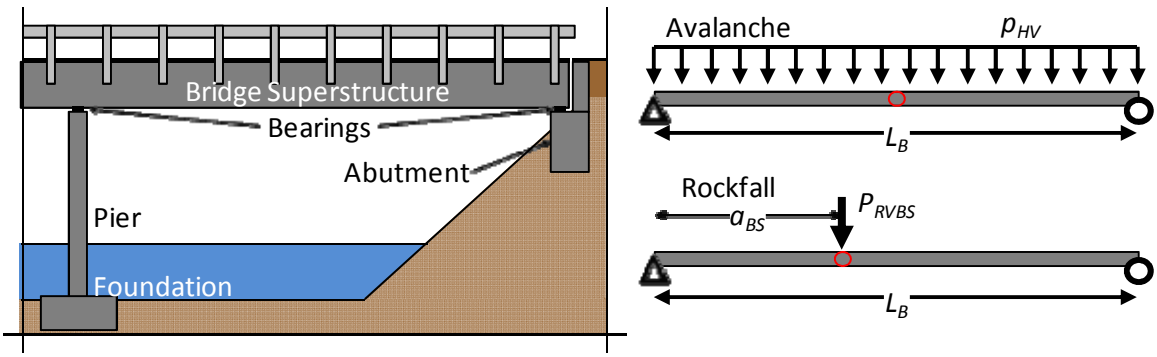

Figure A-9: Bridge superstructure loading and potential flexural hinge locations.

$$V_{ABS} = \frac{p_{AV} b_{BS} L_B}{2} \tag{A.31}$$

$$M_{ABS} = \frac{p_{AV} b_{BS} L_B^{\,2}}{8} \tag{A.32}$$

Where:

V_{ABS} = maximum bridge superstructure avalanche induced direct shear [N]
M_{ABS} = maximum bridge superstructure avalanche induced moment [Nmm]
L_B = bridge span length between two adjacent supports [m]

For the first bridge superstructure configuration and the second bridge superstructure configuration, when the bridge deck has sufficient strength to withstand the applied local hazard forces, b_{BS} is equal to the width of the bridge and the spacing between the bridge beams, respectively. Within the second bridge configuration, if the bridge deck does not have sufficient strength to withstand the applied hazard forces, a significant portion of the hazard force will be shed and the variable b_{BS} will be equal to the width of the bridge beam.

Shifting to assessing the rockfall hazard and considering the first bridge superstructure configuration, the induced rockfall forces are a function of the location of the rockfall impact point. By assuming the bridge superstructure responds as a simply supported beam, the maximum rockfall induced direct shear and moment forces can be calculated with Equations (A.33) and (A.34) (AISC, 1998, p. 4.192).

$$V_{RBS} = \max\left(\begin{array}{c} \frac{P_{RVBD} a_{BS}}{L_B} \\ \frac{P_{RBD}\left(L_B - a_{BS}\right)}{L_B} \end{array} \right) \tag{A.33}$$

$$M_{RBS} = \frac{P_{RVBD}\left(L_B - a_{BS}\right)\left(a_{BS}\right)}{L_B} \tag{A.34}$$

Where:

V_{RBS} = the bridge superstructure maximum rockfall induced direct shear [N]
M_{RBS} = the bridge superstructure maximum rockfall induced moment [Nmm]
a_{BS} = the lateral position of the rockfall impact point measured from the uphill gallery wall [m]

Expanding the rockfall hazard assessment to second bridge superstructure configuration, the forces imposed into the bridge beams are a function of whether the bridge deck fails under the applied rockfall hazard (thereby shedding a portion of the rockfall force) and the distance between the rockfall impact location and the closest bridge beam. If the bridge deck does fail, the force transferred to the bridge beam is equal to the maximum direct shear of the bridge deck as shown in Equations (A.35) and (A.36).

$$V_{RBS} = \max\left(\begin{array}{c} \frac{V_{RBD} a_{BS}}{L_B} \\ \frac{V_{RBD}\left(L_B - a_{BS}\right)}{L_B} \end{array} \right) \tag{A.35}$$

$$M_{RBS} = \frac{V_{RBD}\left(L_B - a_{BS}\right)\left(a_{BS}\right)}{L_B} \tag{A.36}$$

If the bridge deck has sufficient capacity to withstand the induced rockfall forces, the resulting bridge beam induced shear and flexural forces can be assessed with Equations (A.37) and (A.38).

$$V_{RBS} = \max\left(\begin{array}{c} \frac{P_{RVBD} a_{BS}\left(L_{BD} - a_{BD}\right)}{L_B L_{BD}} \\ \frac{P_{RBD}\left(L_B - a_{BS}\right)\left(L_{BD} - a_{BD}\right)}{L_B L_{BD}} \end{array}\right) \tag{A.37}$$

$$M_{RBS} = \frac{V_{RVBD}\left(L_B - a_{BS}\right)\left(a_{BS}\right)\left(L_{BD} - a_{BD}\right)}{L_B L_{BD}} \tag{A.38}$$

Through this structured process, one can verify if the bridge deck has enough capacity to absorb the directly applied hazard forces and if these members can transfer the applied hazard forces to the bridge beams. Additionally, this process highlights equations that can be employed to assess if the bridge beams have sufficient capacity to withstand these applied forces. It should be noted that while the detailed equations only address the concrete member capacity and the applied hazard forces, all additional forces including self weight, dead force and live force should also be considered within this assessment.

Bridge component failure assessment step E

The fifth bridge failure assessment step, step E: bearing resistance > applied superstructure forces, assesses if the bridge bearings have sufficient capacity to withstand the hazard imposed vertical uplift and the horizontal shifting forces. This assessment process first focuses on assessing the bridge bearing capacity to withstand hazard induced vertical uplift.

In assessing the bridge bearing vertical capacity, dynamic hazard and bearing frictional forces are neglected and the assessment focuses on the hazard static buoyancy forces, the bridge superstructure weight and the bearing vertical capacity. The only hazards which can impose buoyancy forces are liquid hazards and thus it is assumed only flood and torrent hazards can cause a bridge's bearings to vertically fail. In general, the vertical bearing capacity is assessed by subtracting the superstructure weight from the weight of the displaced hazard volume (buoyancy force) and confirming that this value is smaller than the total bearing vertical capacity, as shown in Figure A-10 and Equation (A.39).

$$B_{BV} > W_{DH} - W_{BS} \tag{A.39}$$

Where:

B_{BV} = the bridge bearing vertical capacity [kN]
W_{DH} = weight of the displaced hazard volume [kN]
W_{BS} = weight of the bridge superstructure [kN]

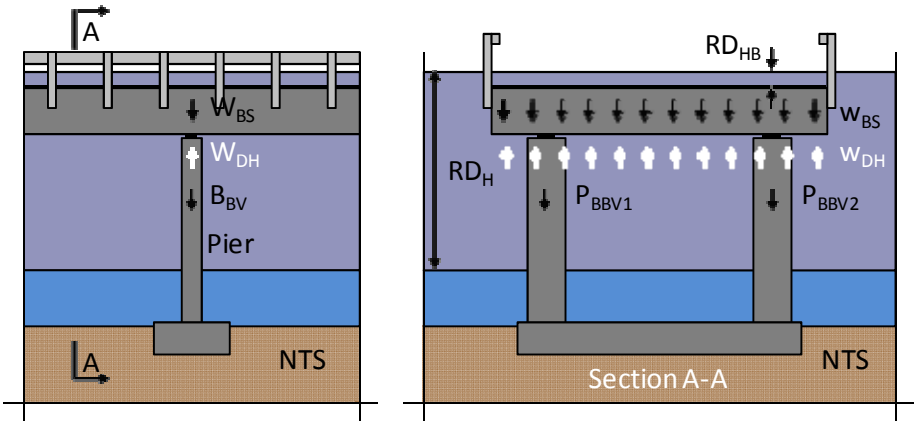

Figure A-10: Assessing the vertical capacity of bridge bearings to resist static buoyancy forces.

In detail, for the bridge depicted in Figure A-10, one can assess the bridge bearing vertical capacity, the weight of the displaced hazard volume and the bridge superstructure weight respectively with Equations (A.40), (A.41) and (A.42).

$$B_{BV} = \sum_{i}^{n} P_{BBV_i} \tag{A.40}$$

$$W_{DH} = (RD_H - C_B - RD_{HB})\rho_H b_{BS} L_{BT} = w_{DH} b_{BS} L_{BT} \tag{A.41}$$

$$W_{BS} = w_{BS} b_{BS} L_{BT} \tag{A.42}$$

Where:

P_{BBVi} = vertical capacity of bridge bearing *i* [kN]
R_{DH} = hazard running depth [m]
RD_{HB} = hazard running depth on top of the bridge superstructure [m]
L_{BT} = total bridge length measured from end to end or expansion joint to expansion joint [m]
ρ_H = hazard density [kN/m^3]
w_{DH} = distributed buoyancy force per square meter [kN/m^2]
w_{BS} = bridge superstructure weight per square meter [kN/m^2]

If the hazard buoyancy force exceeds the bridge superstructure weight and the bearing vertical capacity, it is assumed that the bridge superstructure will be lifted off its bearings resulting in the

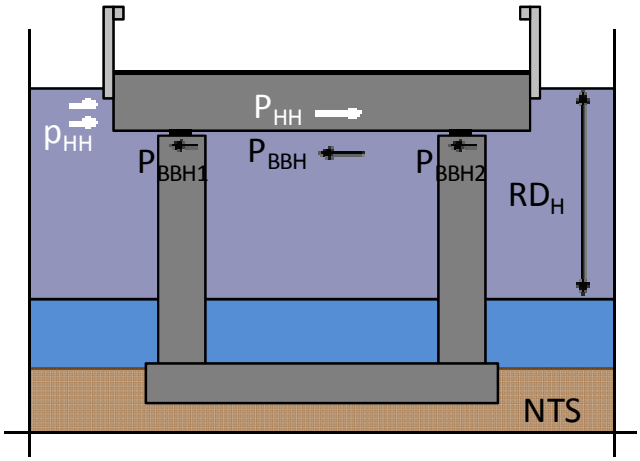

Figure A-11: Assessing the horizontal bridge bearing capacity to resist applied horizontal hazard forces.

complete loss of the bridge superstructure.

To assess the horizontal capacity of the bridge's bearings, the imposed equivalent static hazard forces are compared against the bridge bearing capacity, as shown in Figure A-11 and Equation (A.43). One should note that herein a bridge's horizontal bearing capacity is assumed to include the bridge bearing structural and frictional induced horizontal capacity and any secondary horizontal force paths, such as horizontal shear keys.

$$B_{BH} > P_{HH} \tag{A.43}$$

Where:

B_{BH} = total bridge bearing horizontal capacity [kN]

P_{HH} = total horizontal applied force [kN]

In detail, for the bridge cross section shown in Figure A-11, one can assess the bridge bearing horizontal capacity and the applied horizontal hazard forces with Equations (A.44) and (A.45).

$$B_{BH} = \sum_{i}^{n} P_{BBH_i} \tag{A.44}$$

$$P_{HH} = p_{HH} L_{BT} (R_{DH} - C_B) = p_{HH} A_{BSE} \tag{A.45}$$

Where:

P_{BBHi} = horizontal capacity of bridge bearing or force path *i* [kN]

p_{HH} = hazard horizontal pressure [kN/mm^2]

A_{BSE} = area of bridge superstructure exposed to the hazard [m^2]

If the applied horizontal force exceeds the total horizontal bridge bearing capacity, it is assumed that the bridge superstructure will laterally slide off its bearings resulting in the complete loss of the bridge superstructure.

Bridge component failure assessment step F

The sixth bridge failure assessment step, step F: horizontal resistance > applied horizontal force, focuses on assessing if the bridge superstructure globally has sufficient capacity to withstand the applied horizontal hazard forces. As the bridge is being loaded in its strong axis, it is assumed that the bridge superstructure has sufficient capacity to locally withstand the applied horizontal hazard forces. This assumption may not hold true for thin steel trusses, tall non-composite steel beams and tall thin-walled concrete girders. For such elements, the local horizontal capacity of the individual bridge superstructure elements should also be assessed, an analysis step not included within this document. Given these assumptions, the bridge superstructure shear and moment capacities considering the applied horizontal hazard forces can be determined, in general, with Equations (A.46) and (A.47) respectively.

$$V_{UBSH} > V_{HHBS} \tag{A.46}$$

$$M_{UBSH} > M_{HHBS} \tag{A.47}$$

Where:

V_{UBSH} = bridge superstructure ultimate direct horizontal shear capacity [kN]

V_{HHBS} = hazard induced horizontal shear force [kN]

M_{UBSH} = bridge superstructure ultimate horizontal moment capacity [kNm]

M_{HHBS} = hazard induced horizontal moment [kNm]

assuming the bridge deck is the primary contributor to the bridge superstructure horizontal stiffness and the tensile and compressive steel reinforcement are uniformly distributed across the bridge deck, for the bridge shown in Figure A-12, the bridge superstructure ultimate shear and moment strengths can be determined with Equations (A.48) and (A.50).

$$V_{UBSH} = 0.18 f'_{dcBD}\left(H_{BD}W_{BD} + (n-1)\left(A_{sBD} - A'_{sBD}\right)\right) \quad \text{(A.48)}$$

$$M_{UBSH} = \frac{0.18 f'_{dc}}{y}\left(\sum_{i=1}^{n} I_i\right) \quad \text{(A.49)}$$

$$M_{UBSH} = \frac{0.18 f'_{dc}}{y}\left(\begin{array}{l}\frac{1}{12}\left(W_{BD}{}^3 H_{BD} + (n-1)\left(A_{SBD}W_{BD}{}^2 + A'_{sBD}W_{BD}{}^2\right)\right) \\ +\left(W_{BD}H_{BD} + (n-1)\left(A_{sBD} + A'_{sBD}\right)\right)\left(\frac{W_{BD}}{2} - y\right)^2\end{array}\right) \quad \text{(A.50)}$$

Where:

f'_{dcBD} = the bridge deck dynamic ultimate compressive concrete strength [N/mm^2]
y = distance between the neutral axis and the extreme compression fiber [mm]
W_{BD} = bridge deck width [m]
H_{BD} = bridge deck height [m]
n = steel reinforcement to concrete modulus of elasticity ratio [ ]

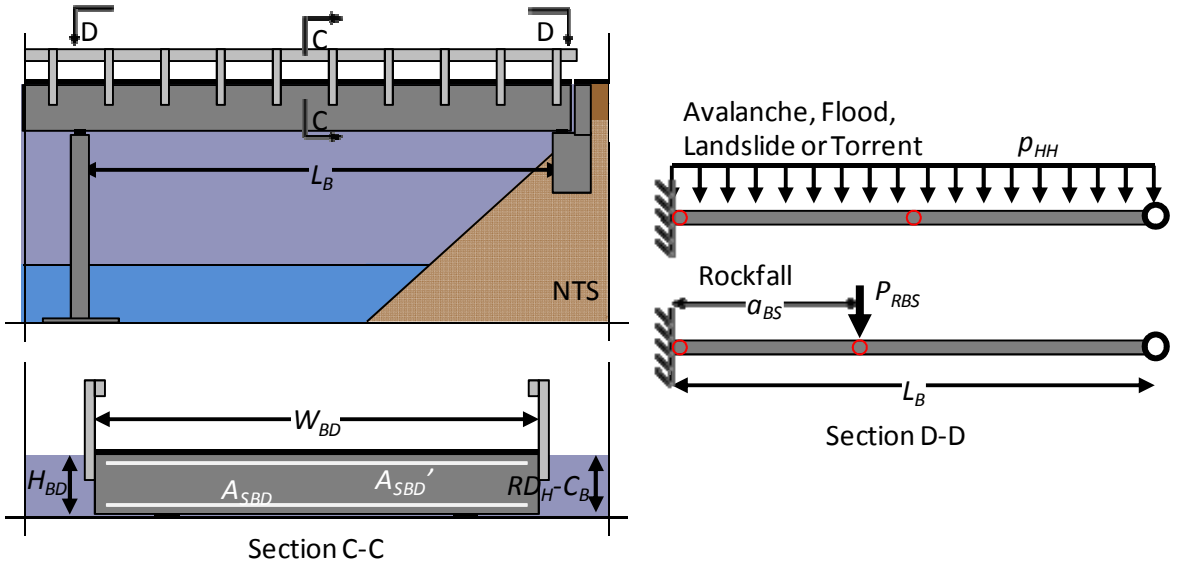

Figure A-12: Bridge superstructure horizontal loading and potential flexural hinge locations.

In determining the hazard induced horizontal global shear and moment forces, it is assumed each span of the bridge can be analyzed as a propped cantilever, as shown in Figure A-12.

For distributed hazards, avalanche, flood, landslide and torrent, it is assumed that the bridge superstructure is horizontal with the top surface of the hazard, thereby ensuring that the hazard is uniformly applied across the superstructure. Thus the hazard induced horizontal global shear and moment forces can be determined with Equations (A.51) and (A.52), respectively.

$$V_{HHBS} = \frac{5 p_{HH} \left(R_{DH} - C_B \right) L_B}{8} \tag{A.51}$$

$$M_{HHBS} = \frac{5 p_{HH} \left(R_{DH} - C_B \right) L_B{}^2}{8} \tag{A.52}$$

For the concentrated hazard, rockfall, and following the process employed to develop Equation (A.25), the applied horizontal force can be determined with Equation (A.53) and the induced shear and moment forces can be quantified with Equations (A.54) and (A.55)

$$P_{RHBS} = 2.8 r_R{}^{0.7} E_{BS}{}^{0.4} E_R{}^{0.6} \cos(\alpha_R) \tag{A.53}$$

Where:

P_{RHBS} = the rockfall horizontal force applied to the bridge deck [kN]
E_{BS} = the bridge superstructure modulus of elasticity [N/mm^2]

$$V_{RHBS} = \max \begin{pmatrix} \frac{P_{RHBS} a_{BS}{}^2}{2 L_B{}^3} \left(3 L_B - a_{BS} \right) \\ \frac{P_{RHBS} \left(L_B - a_{BS} \right)}{2 L_B{}^3} \left(3 L_B{}^2 - \left(L_B - a_{BS} \right)^2 \right) \end{pmatrix} \tag{A.54}$$

$$M_{RHBS} = \max \begin{pmatrix} \frac{P_{RHBS} a_{BS}{}^2}{2 L_B{}^3} \left(3 L_B - a_{BS} \right) \left(L_B - a_{BS} \right) \\ \frac{P_{RHBS} a_{BS} \left(L_B - a_{BS} \right)}{2 L_B{}^2} \left(2 L_B - a_{BS} \right) \end{pmatrix} \tag{A.55}$$

Where:

V_{RHBS} = the bridge superstructure maximum rockfall induced horizontal direct shear [N]
M_{RHBS} = the bridge superstructure maximum rockfall induced moment [Nmm]
a_{BS} = the longitudinal position of the rockfall impact point measured from the closest support or expansion joint [mm]

If the induced horizontal hazard shear or moment forces are found to exceed the bridge superstructure's horizontal capacity, disproving Equation (A.46) or (A.47), it is assumed that the bridge superstructure fails.

Bridge component failure assessment step G

The seventh bridge failure assessment step, pier resistance > applied horizontal pier forces, assesses if one or more of the given bridge's piers is overloaded by the hazard induced shear or flexure forces. As the bridge pier is being loaded in its strong axis, it is assumed that the bridge pier has sufficient capacity to locally withstand the applied horizontal hazard forces. Given this assumption, the bridge pier shear and moment capacities considering the applied horizontal hazard forces can be determined, in general, with Equations (A.56) and (A.57) respectively.

$$V_{UBPH} > V_{HHBP} \tag{A.56}$$

$$M_{UBPH} > M_{HHBP} \tag{A.57}$$

Where:

V_{UBPH} = bridge pier ultimate direct horizontal shear capacity [kN]
V_{HHBP} = hazard induced horizontal shear force [kN]
M_{UBPH} = bridge pier ultimate horizontal moment capacity [kNm]
M_{HHPH} = hazard induced horizontal moment [kNm]

Given the bridge pier shown in Figure A-13, assuming the bridge superstructure contribution to the bridge pier stiffness is negligible and assuming the bridge pier tensile and compressive steel reinforcement is uniformly distributed across the bridge pier, the bridge pier ultimate shear and moment strengths can be determined with Equations (A.58) and (A.60).

$$V_{UBPH} = 0.18\, f'_{dcBP}\left(D_{BP}W_{BP} + (n-1)\left(A_{sBP} - A'_{sBP}\right)\right) \tag{A.58}$$

$$M_{UBPH} = \frac{0.18\, f'_{dc}}{y}\left(\sum_{i=1}^{n} I_i\right) \tag{A.59}$$

$$M_{UBPH} = \frac{0.18\, f'_{dc}}{y}\left(\begin{array}{l}\frac{1}{12}\left(W_{BP}D_{BP}{}^{3} + (n-1)\left(A_{SBP}D_{BP}{}^{2} + A'_{sBP}D_{BP}{}^{2}\right)\right) \\ +\left(W_{BP}D_{BP} + (n-1)\left(A_{sBP} + A'_{sBP}\right)\right)\left(\frac{D_{BP}}{2} - y\right)^{2}\end{array}\right) \tag{A.60}$$

Where:

f'_{dcBP} = the bridge pier ultimate compressive concrete strength [N/mm^2]
W_{BP} = bridge pier width [m]
D_{BP} = bridge pier depth [m]
A_{sBP} = the bridge pier tensile reinforcement [mm^2]
A_{sBP}' = the bridge pier compression reinforcement [mm^2]

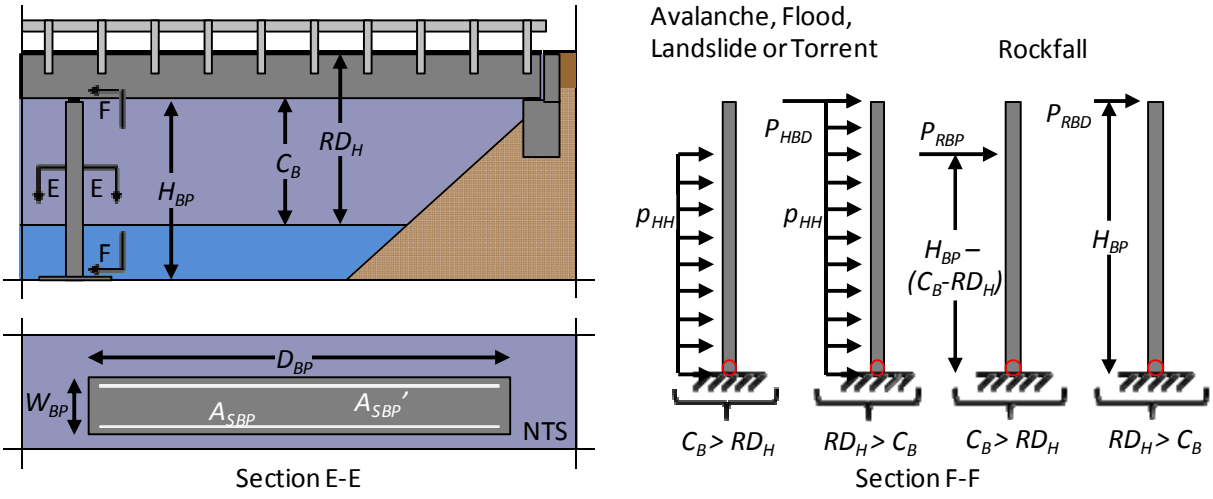

Figure A-13: Bridge pier horizontal loading and potential flexural hinge locations.

In determining the hazard induced horizontal global shear and moment forces, it is assumed the bridge pier can be modeled as a vertical cantilever, as shown in Figure A-13.

For the distributed hazards – avalanche, flood, landslide and torrent – the induced horizontal global shear and moment forces for hazards which do not surpass the bridge clearance can be quantified with Equations (A.61) and (A.62), respectively.

$$V_{HHBP} = p_{HH} 1.5 W_{BP} \left(H_{BP} - \left(C_B - RD_H \right) \right) \quad \text{(A.61)}$$

$$M_{HHBP} = \frac{3 p_{HH} W_{BP} \left(H_{BP} - \left(C_B - RD_H \right) \right)^2}{4} \quad \text{(A.62)}$$

If the given hazard does surpass the bridge clearance, these values are increased by the amount of hazard induced horizontal force is transferred through the bridge superstructure and into the bridge pier. Thus under such a condition, the horizontal global shear and moment forces can be determined with Equations (A.63) and (A.64).

$$V_{HHBP} = p_{HH} 1.5 W_{BP} H_{BP} + p_{HH} \frac{L_{BT}}{N_{BP} + 1} \left(RD_H - C_B \right) \quad \text{(A.63)}$$

$$M_{HHBP} = \frac{3 p_{HH} W_{BP} {H_{BP}}^2}{4} + \frac{p_{HH} L_{BT} \left(RD_H - C_B \right) \left(H_{BP} + RD_H - C_B \right)}{N_{BP} + 1} \quad \text{(A.64)}$$

For the concentrated hazard, rockfall, following the procedure employed to develop Equation (A.25) and assuming the rockfall impacts only the bridge pier, the applied horizontal force can be determined with Equation (A.65) and the induced shear and moment forces can be quantified with Equations (A.66) and (A.67).

$$P_{RHBP} = 2.8 {r_R}^{0.7} {E_{BP}}^{0.4} {E_R}^{0.6} \cos(\alpha_R) \quad \text{(A.65)}$$

Where:

P_{RHBP} = the rockfall horizontal force applied to the bridge pier [kN]
E_{BP} = the bridge pier modulus of elasticity [N/mm^2]

$$V_{RHBP} = P_{RHBP} \quad \text{(A.66)}$$

$$M_{RHBP} = P_{RHBP} \left(H_{BP} - \left(C_B - RD_H \right) \right) \quad \text{(A.67)}$$

Where:

V_{RHBP} = the bridge pier maximum rockfall induced horizontal direct shear [N]
M_{RHBP} = the bridge pier maximum rockfall induced moment [Nmm]

If the rockfall impacts the bridge superstructure rather than the bridge pier, the applied horizontal force can be determined with Equation (A.68) and the induced shear and moment forces can be quantified with Equations (A.69) and (A.70).

$$P_{RHBP} = \frac{2.8 {r_R}^{0.7} {E_{BS}}^{0.4} {E_R}^{0.6} \cos(\alpha_R) \left(L_B - a_{BS} \right) \left(3 {L_B}^2 - \left(L_B - a_{BS} \right)^2 \right)}{2 {L_B}^2} \quad \text{(A.68)}$$

$$V_{RHBP} = P_{RHBP} \quad \text{(A.69)}$$

$$M_{RHBP} = P_{RHBP} \left(H_{BP} + 0.5 \left(RD_H - C_B \right) \right) \quad \text{(A.70)}$$

If the induced horizontal hazard shear or moment forces are found to exceed the bridge pier's horizontal capacity, invalidating Equation (A.56) or (A.57), it is assumed that the bridge pier fails.

Bridge component failure assessment step H

The eighth and final bridge failure assessment step, clearance + structural height > hazard running depth, assesses if the bridge's running surface can potential become submerged in liquid or debris – thereby preventing free public usage of the infrastructure object. This failure assessment step can quantitatively be assessed with Equation (A.71).

$$C_B + d_{BS} > RD_H \tag{A.71}$$

If it is determined that Equation (A.71) is invalid for the given hazard intensity and bridge, it is assumed that the bridge will be submerged in liquid or debris.

Thus through applying the structured failure assessment process presented herein, one can systematically qualitatively and quantitatively determine if a bridge is vulnerable to a given hazard intensity and if so, which failure mode controls.

A.3 Culvert failure assessment procedure

Culverts are tubular objects constructed underneath roadway objects to ferry moving bodies of water unnoticed and unobserved underneath a given roadway, Figure A-14. When a culvert fails to perform as intended, water pools on the uphill side of the roadway and, unless the uphill water retention basin has adequate capacity for this retained water, the pooled water will overtop the roadway.

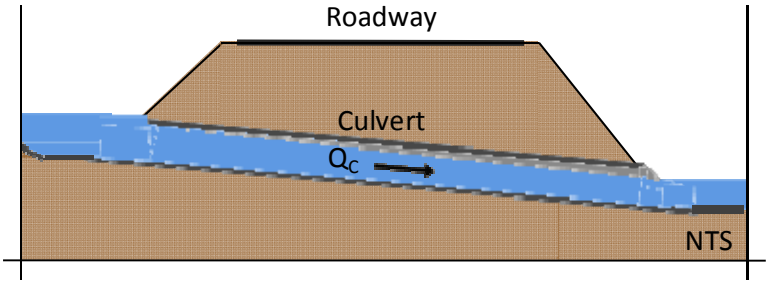

Figure A-14: A typical culvert configuration.

In Table 3-2, one can observe that a culvert object is assumed to potentially fail in 5 different hazard scenarios. When these hazards scenarios are analyzed as a group, two independent failure modes can be identified. These failure modes and their associated inducing hazards are presented in Table A-2.

Table A-2: Culvert failure modes and associated hazards.

	Potential Hazards				
Failure mode	**Avalanche**	**Flood**	**Landslide**	**Rockfall**	**Torrent**
Culvert buried in debris	x	-	x	x	x
Culvert capacity exceeded	-	x	-	-	-

In further analyzing these two potential failure modes, they can be arranged into a structured assessment process shown in Figure A-15.

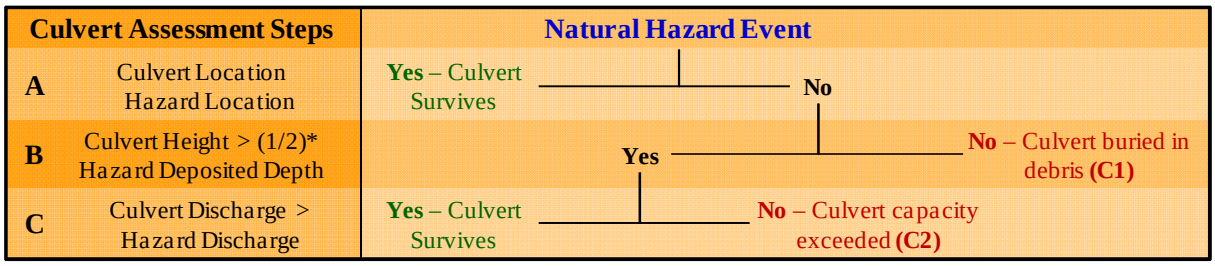

Figure A-15: Culvert component failure assessment process.

Culvert component failure assessment step A

To conduct the first step of the culvert failure assessment procedure, assessment step A: culvert location hazard location, one must conduct a geographic coincident analysis between all five hazards and the culvert location. Typically, it is during this phase of the analysis that the true scope of the culvert analysis becomes evident as typically only two to three of the potential five hazards are coincident with the culvert object.

Culvert component failure assessment step B

The second step, culvert height > (1/2)*hazard deposited depth, focuses on determining if the culvert can become blocked or partially blocked by avalanche, landslide, rockfall or torrent debris, as shown in Figure A-16. This assessment is formally conducted with Equation (A.72). It is herein assumed that if the deposited hazard debris exceeds one-half of the height of the culvert, the capacity of the culvert is so reduced that water will start to pool on the uphill side of the culvert and will eventually overtop the roadway.

$$DD_H > \frac{H_C}{2} \quad \{DD_H = DD_A \vee DD_L \vee DD_R \vee DD_T\} \tag{A.72}$$

Where:

H_C = height of the culvert inlet [m]
DD_H = hazard deposited depth [m]
DD_A = avalanche deposited depth [m]
DD_L = landslide deposited depth [m]
DD_R = rockfall deposited depth [m]
DD_T = torrent deposited depth [m]

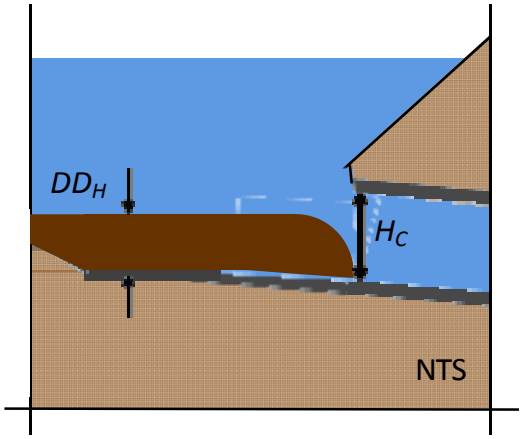

Figure A-16: Culvert potentially blocked by deposited debris.

Culvert component failure assessment step C

Turning to the third culvert assessment step, culvert discharge > hazard discharge, requires one to obtain flood hazard discharge data from the hazard intensity maps and to obtain the culvert design discharge from the KUBA database or calculate the culvert design discharge with Equation (A.73) (Normann, Houghtalen, & Johnston, 2001).

$$Q_C = \frac{a_c \cdot Rh^{2/3}\sqrt{2S_c \cdot g}}{n_c\sqrt{K_u}} \tag{A.73}$$

Where:

Q_C = culvert design discharge [m^3/s]
S_C = culvert slope [m/m]
a_C = culvert cross-sectional area [m^2]
Rh = hydraulic radius [m]
n_C = Manning's roughness coefficient for the given culvert [ ]
K_u = hydraulic constant (19.63) [ ]

Thus by applying this general culvert assessment process presented herein, one can qualitatively and quantitatively determine if any of the five considered hazards can induce a culvert to fail.

A.4 Gallery failure assessment procedure

Galleries are protection structures designed to shield roadways and railways from the affects of gravitational hazards - torrents, landslides, rockfalls and avalanches. Within this work, there are two different gallery configurations considered, Figure A-17. In the first configuration, the gallery uphill wall and roof are respectively doubly reinforced wall and slab elements. In the second configuration, the gallery uphill wall is composed of gallery wall structural members which span between and bear upon the gallery wall supports. Likewise, the gallery roof is composed of gallery roof structural members which span between and bear upon the gallery roof supports. Within both configurations, it is assumed that the gallery downhill wall is composed of a line of columns. Additionally, Figure A-17 presents two potential uphill wall exposures. In configuration 1, the uphill wall is completely embedded in the hillside while the uphill wall in configuration 2 is partially or completely exposed.

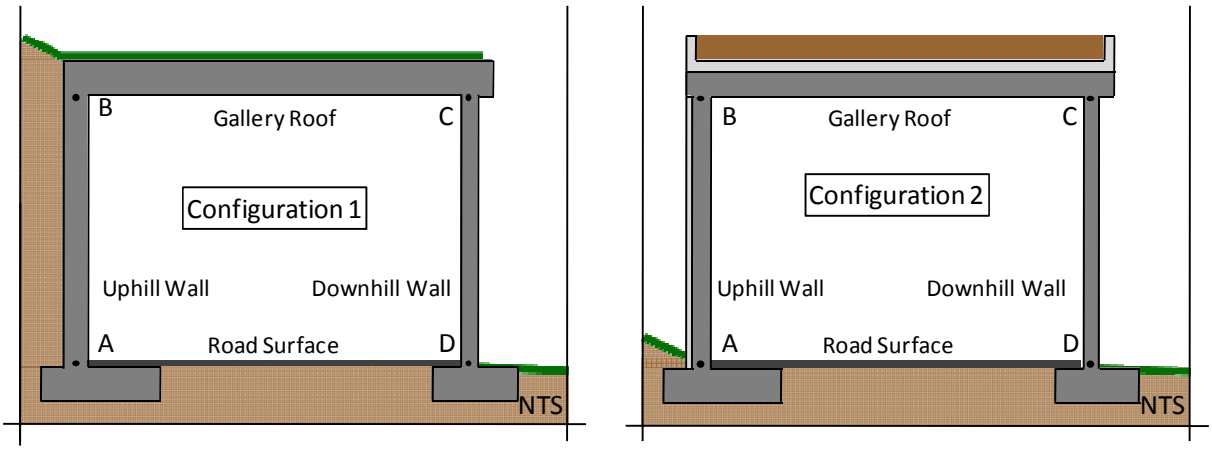

Figure A-17: Gallery configurations 1 and 2.

In Table 3-2, one can observe that 21 different hazard failure scenarios are considered for the gallery component. When these hazard scenarios are analyzed as a group, seven independent failure modes

can be identified. These failure modes and the hazards which can potentially induced each of these respective failure modes presented in Table A-3.

Table A-3: Gallery failure modes and associated hazards.

	Potential Hazards				
Failure mode	**Avalanche**	**Flood**	**Landslide**	**Rockfall**	**Torrent**
Foundation is undermined	-	x	x	-	-
Gallery wall is overloaded locally in shear or flexure	x	-	x	x	-
Gallery wall supports are overloaded in shear or flexure	x	-	x	x	-
Gallery roof is overloaded in shear or flexure	x	-	x	x	x
Gallery roof supports are overloaded in shear or flexure	x	-	x	x	x
Gallery frame laterally collapses	x		x	x	-
Gallery is 'flooded' with liquid or debris	-	x	-	-	x

In further analyzing the five hazards and the gallery's structural elements, these failure modes can be arranged into a structured assessment process shown in Figure A-18. In Figure A-18, one should note that failure modes 1, 3, 5, 6 and 7 are all global failure modes, while failure modes 2 and 4 are local failure modes. In modes 2 and 4, a portion of the structure does fail thereby shedding a part of the applied hazard force but these localized failures do not preclude the gallery from failing in an additional global failure mode.

Gallery component failure assessment step A

The first step of the gallery failure assessment procedure, assessment step A: gallery location ≠ hazard location, requires a geographic coincident analysis to be conducted between all five hazards

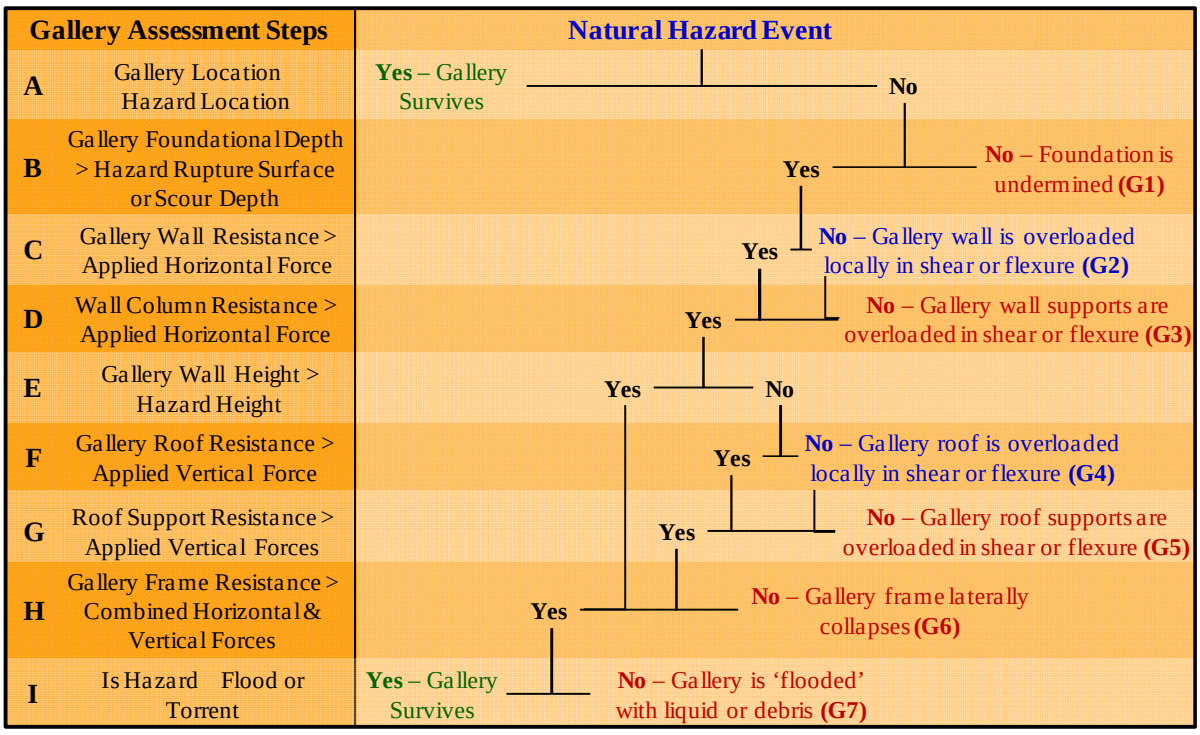

Figure A-18: Gallery component failure assessment process.

and the gallery location. Generally, it is during this phase that the true analysis scope is defined as typically only two or three hazards are coincident with the gallery component.

Gallery component failure assessment step B

The second step, gallery foundational depth > hazard rupture surface or scour depth, requires one to determine the gallery foundational depth, the landslide rupture surface depth and the flood scour depth, as shown in Figure A-19.

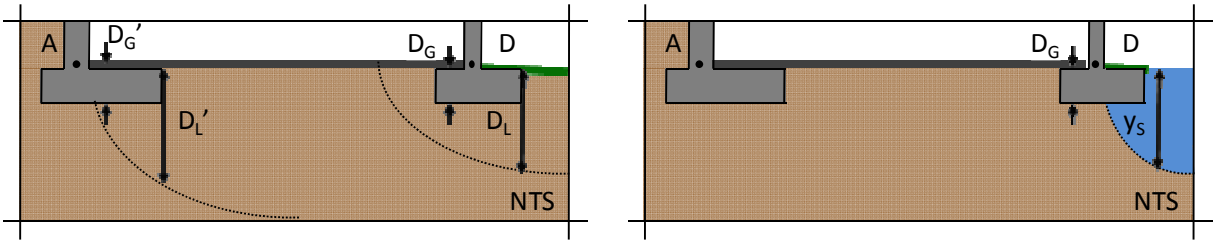

Figure A-19: Foundation undermined by landslide or flood hazards.

The uphill and downhill gallery foundational depths, respectively D_G *and* D_G', can be obtained from original design plans or from an onsite inspection. The landslide rupture surface depth at the uphill and downhill gallery wall foundations, D_L and D_L' respectively, should be assessed by an experienced geologist. While this assessment is typically general in nature, i.e. shallow or deep, such information can help to identify if the gallery foundations are below or above the landslide hazard. The flood scour depth, y_s, can be assessed by employing the scour assessment procedure detailed within the bridge assessment procedure or with other scour assessment procedures presented in the Evaluating Scour at Bridges manual (Richardson & Davis, 2001). In determining if the gallery foundational depth is exceeded, the uphill gallery foundation depth is compared against the local landslide rupture surface depth and the downhill gallery foundation depth is compared against the local landslide rupture surface depth and the flood scour depth.

Gallery component failure assessment step C

To conduct the next two analysis steps, C and D, one must assess to which hazards the uphill gallery wall element is exposed. If the gallery wall is embedded in the uphill slope, as is the case for gallery configuration 1, the gallery wall elements are not exposed to any of the potential three hazards – avalanche, landslide or rockfall – and thus analysis steps C and D are automatically positive. But if the uphill gallery wall extends above grade, as shown in the second gallery configuration, one must assess if the applied horizontal hazard forces can exceed the gallery wall structural strength. If either of these two capacity values are exceeded, it is assumed the gallery foundation fails.

Analysis step C, assesses if the applied horizontal hazard forces exceed the ultimate punching shear, direct shear or moment strengths of the gallery uphill wall elements, as shown in Figure A-20. This analysis step is completely applicable to the second gallery configuration in which the uphill gallery wall is composed of timber, concrete or steel structural wall members which span between and horizontally bear upon the wall columns.

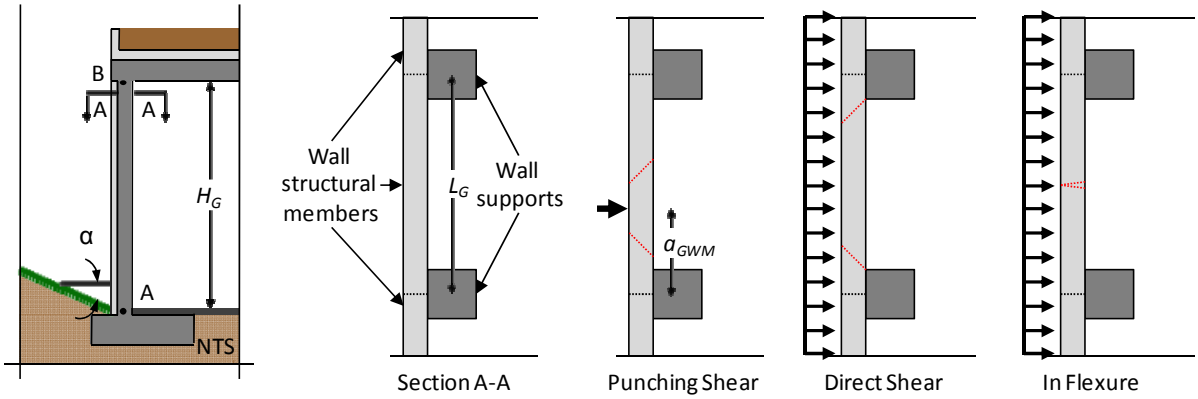

Figure A-20: Gallery wall or wall members overloaded in shear or flexure.

The analysis of the punching shear strength is also applicable to the gallery uphill wall in the first gallery configuration, but the ultimate direct shear and moment strengths for this first gallery configuration are considered within analysis step D. The structural punching shear, direct shear and moment capacity of the structural wall members within gallery configuration 2 can be assessed using Equations (A.1), (A.2) and (A.3) resulting in Equations (A.74), (A.75) and (A.76).

$$v_{cGWM} = 4\sqrt{f'_{dcGWM}} \tag{A.74}$$

$$V_{dGWM} = 0.18 f'_{dcGWM} b_{GWM} d_{GWM} \tag{A.75}$$

$$M_{uGWM} = \left(\frac{A'_{sGWM} f_{dsGWM}}{b_{GWM}} \cdot \left(d_{GWM} - \frac{\left(A_{sGWM} - A'_{sGWM}\right) f_{dsGWM}}{2 \cdot 0.85 \cdot b_{GWM} f'_{dcGWM}} \right) + \frac{A'_{sGWM} f_{dsGWM}}{b_{GWM}} \cdot \left(d_{GWM} - d'_{GWM}\right) \right) \tag{A.76}$$

Where:

v_{cGWM} = the gallery wall structural member punching shear stress capacity [N/mm^2]

f'_{dcGWM} = the gallery wall structural member dynamic ultimate concrete compressive strength [N/mm^2]

V_{dGWM} = the gallery wall structural member ultimate direct shear capacity [N]

b_{GWM} = the gallery wall structural member concrete compression face width [mm]

d_{GWM} = the distance from the extreme compression fiber to the centroid of the tensile reinforcement within the gallery wall structural member [mm]

M_{uGWM} = the gallery wall structural member ultimate moment resistance [Nmm]

A_{sGWM} = the gallery wall structural member tensile reinforcement area within the width b_{GWM} [mm^2]

$A_s'_{GWM}$ = the gallery wall structural member compression reinforcement area within the width b_{GWM} [mm^2]

d'_{GWM} = the distance from the extreme compression fiber to the centroid of the compression reinforcement within the gallery wall structural member [mm]

f_{dsGWM} = the gallery wall structural member reinforcement dynamic design stress [N/mm^2]

The first applicable hazard, avalanche hazard loading, is a uniformly distributed load and thus the critical gallery parameters are the gallery structural wall member's direct shear and moment capacities. Conservatively assuming the wall members are simply supported and the avalanche forces

are applied across the complete span of the structural wall member, the avalanche induced maximum shear and moment force can be calculated with Equations (A.77) and (A.78) respectively (AISC, 1998, p. 4.190).

$$V_{AGWM} = \frac{p_{AH} b_{GWM} L_G}{2} \tag{A.77}$$

$$M_{AGWM} = \frac{p_{AH} b_{GWM} L_G^{\,2}}{8} \tag{A.78}$$

Where:

V_{AGWM} = the gallery structural wall member maximum avalanche induced shear force [N]
M_{AGWM} = the gallery structural wall member maximum avalanche induced moment [Nmm]
b_{GWM} = the gallery structural wall member vertical width [mm]
L_G = the spacing distance between the gallery structural frames [mm]

Turning to the second applicable hazard, landslide hazard loading, is assumed to be uniformly distributed force and thus the critical parameters are likewise the gallery structural wall member's direct shear and moment capacities. These forces can be conservatively computed with Equations (A.77) and (A.78) by replacing the avalanche horizontal pressure (p_{AH}) with the landslide horizontal pressure (p_{LH}), thus resulting in Equations (A.79) and (A.80).

$$V_{LGWM} = \frac{p_{LH} b_{GWM} L_G}{2} \tag{A.79}$$

$$M_{LGWM} = \frac{p_{LH} b_{GWM} L_G^{\,2}}{8} \tag{A.80}$$

Where:

V_{LGWM} = the gallery structural wall member maximum landslide induced shear [N]
M_{LGWM} = the gallery structural wall member maximum landslide induced moment [Nmm]

The third and final applicable hazard, rockfall hazard forcing, is assumed to be a localized point force and thus the critical parameters are the gallery structural wall member's punching shear, direct shear and moment capacities. Assuming the gallery wall has a negligible cushion, the applied rockfall force can be computed with Equation (A.81) (Chikatamarla, 2007, pp. 11-12).

$$P_{RGWM} = 2.8 r_R^{\,0.7} E_{GWM}^{\,0.4} E_R^{\,0.6} \cos(\alpha_R) \tag{A.81}$$

Where:

P_{RGWM} = the rockfall force applied on the gallery roof member [kN]
E_{GWM} = the gallery wall member modulus of elasticity [N/mm^2]
α_{RH} = the rockfall angle of attack measured from the horizontal [rad]

As a rockfall is assumed to be a concentrated force, the initial critical parameter is a punching shear failure of the gallery wall which is applicable to both gallery configurations. Taking the example of a doubly reinforced concrete wall member, the applied horizontal rockfall punching shear force can be computed with Equation (A.82) (US Army, 1990, p. 4.40).

$$v_{RGWM} = \frac{P_{RGWM}}{2\pi d_{cGWM}\left(r_R + \frac{d_{GWM}}{2}\right)} \tag{A.82}$$

Where:

V_{RGWM} = the gallery wall member ultimate rockfall induced punching shear [N/mm^2]
d_{cGWM} = the distance between the centroids of the compression and tensile reinforcement within the gallery wall member [mm]
d_{GWM} = the distance between the extreme compression fiber and the centroid of the tensile reinforcement within the gallery wall member [mm]

Continuing with just the second gallery configuration, if the wall structural member has enough capacity to withstand the applied punching shear forces, the applied rockfall force is transferred to the gallery structural frames. This induces shear and flexural stresses in the gallery structural wall member which is a function of the location of the impact point. Thus the maximum rockfall induced shear and flexural forces in the gallery wall member can be respectively computed with Equations (A.83) and (A.84).

$$V_{RGWM} = \frac{P_{RGWM}\left(L_G - a_{GWM}\right)}{L_G} \tag{A.83}$$

$$M_{RGWM} = \frac{P_{RGWM}\left(L_G - a_{GWM}\right)a_{GWM}}{L_G} \tag{A.84}$$

Where:

V_{RGWM} = the gallery wall member maximum rockfall induced direct shear [N]
M_{RGWM} = the gallery wall member maximum rockfall induced moment [Nmm]

Thus through this process, one can determine if a gallery wall structural member will fall in punching shear, direct shear or moment overload.

Gallery component failure assessment step D

Turning to the fourth failure assessment step, gallery wall supports are overloaded in shear or flexure, requires one to assess if the applicable hazards – avalanche, landslide or rockfall – can exceed the shear or flexural strength of the gallery wall supports.

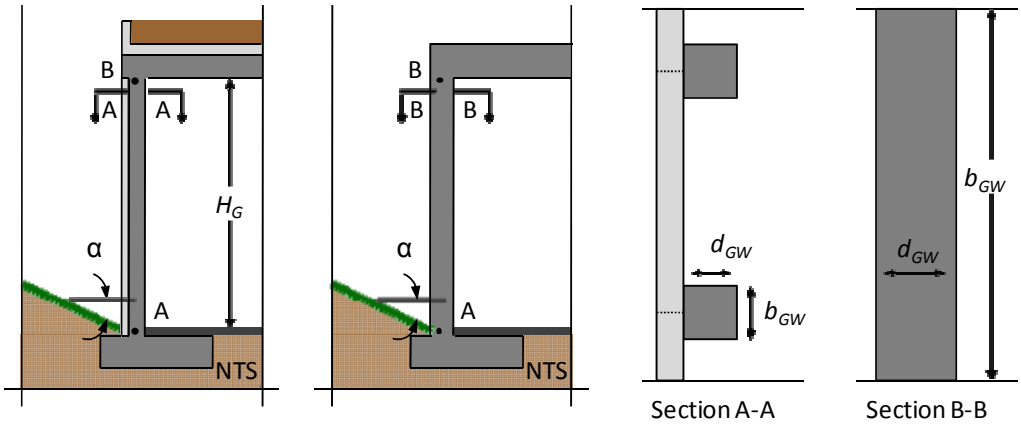

Figure A-21: Structured configuration of the uphill gallery wall.

For the first and second gallery configurations, assuming the gallery wall and gallery wall support, respectively, are doubly reinforced concrete members, each member's shear and flexural capacity being calculated using Equations (A.2) and (A.3) resulting in Equations (A.85) and (A.86). Please note the alternative definitions of the second gallery wall configuration width and depth variables, detailed in Figure A-21.

$$V_{dGW} = 0.18 f'_{dcGW} b_{GW} \cdot d_{GW} \tag{A.85}$$

$$M_{uGW} = \frac{A'_{sGW} f_{dsGW}}{b_{GW}} \cdot \left(d_{GW} - \frac{\left(A_{sGW} - A'_{sGW}\right) f_{dsGW}}{2 \cdot 0.85 \cdot b_{GW} f'_{dcGW}} \right) + \frac{A'_{sGW} f_{dsGW}}{b_{GW}} \cdot \left(d_{GW} - d'_{GW}\right) \tag{A.86}$$

Where:

f'_{dcGW} = the gallery wall dynamic ultimate concrete compressive strength [N/mm^2]
V_{dGW} = the gallery wall ultimate direct shear capacity [N]
b_{GW} = the gallery wall concrete compression face width [mm]
d_{GW} = the distance from the extreme compression fiber to the tensile reinforcement centroid within the gallery wall [mm]
M_{uGW} = the gallery wall ultimate moment resistance [Nmm]
A_{sGW} = the gallery wall tensile reinforcement area within the width b_{GWM} [mm^2]
$A_s'_{GW}$ = the gallery wall compression reinforcement area within the width b_{GWM} [mm^2]
d'_{GW} = the distance from the extreme compression fiber to the compression centroid reinforcement within the gallery wall [mm]
f_{dsGW} = the gallery wall reinforcement dynamic design stress [N/mm^2]

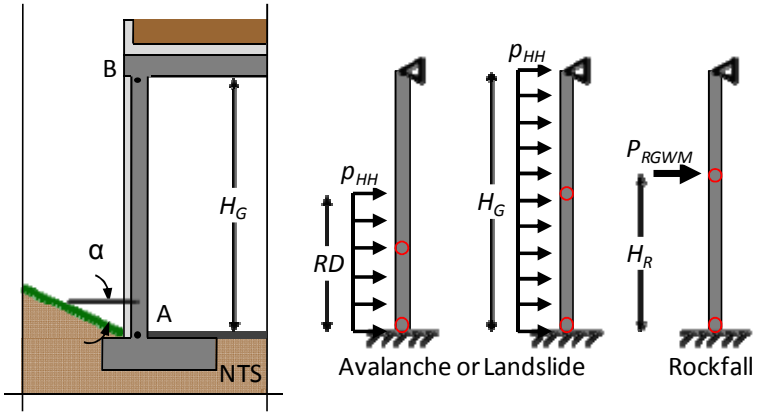

Figure A-22: Gallery wall loading and potential flexural hinge locations.

Graduating to the gallery wall supports, one can quickly observe that the hazard forces applied to the gallery wall supports are a function of how the gallery wall is loaded. Analyzing the avalanche and landslide hazards, Figure A-22, one can observe that applied forces are a function of the depth of the hazard and the exposed gallery width.

Thus assuming the gallery wall responds as a propped cantilever, the maximum avalanche or landslide induced direct shear and moment forces can be computed with Equations (A.87) and (A.88).

$$V_{HGW} = \frac{p_{HH} b_{GW} RD \left(3RD_H^{\,3} - 4RD_H^{\,2} + 4RD_H H_G - H_G^{\,3}\right)}{H_G^{\,3}} \tag{A.87}$$

$$M_{HGW} = \frac{p_{HH} b_{GW} RD_H \left(6RD_H{}^3 - 8RD_H{}^2 + 8RD_H H_G - RD_H H_G{}^2 - 2H_G{}^3\right)}{2H_G{}^2} \quad \text{(A.88)}$$

Where:

V_{HGW} = the gallery wall maximum hazard induced direct shear [N]
M_{HGW} = the gallery wall maximum hazard induced moment [Nmm]
p_{HH} = the applied landslide or avalanche horizontal pressure [N/mm^2]
RD_H = the landslide or avalanche running depth [m]
H_G = the gallery height [m]

When the gallery wall structural members have sufficient strength to withstand the applied hazard forces, b_{GW}, for the first and second gallery configurations, is equal to the length of the gallery section under analysis or the spacing between the gallery structural frames. Within the second gallery configuration, if the gallery wall structural members do not have sufficient strength to withstand the applied hazard forces, a significant portion of the hazard force will be shed, and the variable b_{GW} will be equal to the width of the wall support.

Turning to the rockfall hazard and considering the first gallery configuration, the induced rockfall forces are a function of the height of the rockfall impact point. By considering this parameter and by assuming the gallery wall responds as a propped cantilever, the maximum rockfall induced direct shear and moment forces can be calculated with Equations (A.89) and (A.90) (AISC, 1998, p. 4.194).

$$V_{RGW} = \max\begin{pmatrix} \frac{P_{RGWM} RD_R{}^2}{2H_G{}^3}\left(3H_G - RD_R\right) \\ \frac{P_{RGWM}\left(H_G - RD_R\right)}{2H_G{}^3}\left(3H_G{}^2 - \left(H_G - RD_R\right)^2\right) \end{pmatrix} \quad \text{(A.89)}$$

$$M_{RGW} = \max\begin{pmatrix} \frac{P_{RGWM} RD_R{}^2}{2H_G{}^3}\left(3H_G - RD_R\right)\left(H_G - RD_R\right) \\ \frac{P_{RGWM} RD_R\left(H_G - RD_R\right)}{2H_G{}^2}\left(2H_G - RD_R\right) \end{pmatrix} \quad \text{(A.90)}$$

Where:

V_{RGW} = the gallery wall maximum rockfall induced direct shear [N]
M_{RGW} = the gallery wall maximum rockfall induced moment [Nmm]

Expanding the rockfall hazard analysis to include the second gallery configuration, the forces induced into the gallery structural frame is a function of whether the gallery wall structural members fail under the applied rockfall hazard (thereby shedding the rockfall force) and the distance between the rockfall impact location and the closest gallery structural frame. If this condition controls, the force transferred to the gallery structural frame is equal to maximum direct shear of the gallery wall structural members as is shown in Equations (A.91) and (A.92).

$$V_{RGW} = \max\begin{pmatrix} \frac{V_{RGWM} RD_R{}^2}{2H_G{}^3}\left(3H_G - RD_R\right) \\ \frac{V_{RGWM}\left(H_G - RD_R\right)}{2H_G{}^3}\left(3H_G{}^2 - \left(H_G - RD_R\right)^2\right) \end{pmatrix} \quad \text{(A.91)}$$

$$M_{RGW} = \max\begin{pmatrix} \frac{V_{RGWM} RD_R{}^2}{2H_G{}^3}\left(3H_G - RD_R\right)\left(H_G - RD_R\right) \\ \frac{V_{RGWM} RD_R\left(H_G - RD_R\right)}{2H_G{}^2}\left(2H_G - RD_R\right) \end{pmatrix} \quad \text{(A.92)}$$

But if the gallery wall structural members have sufficient capacity to withstand the induced rockfall forces, the resulting gallery structural frame induced forces can be assessed with Equations (A.93) and (A.94).

$$V_{RGW} = \max\begin{pmatrix} \frac{P_{RGWM} RD_R{}^2\left(3H_G - RD_R\right)\left(L_G - a_{GWM}\right)}{2H_G{}^3 L_G} \\ \frac{P_{RGWM}\left(H_G - RD_R\right)\left(3H_G{}^2 - \left(H_G - RD_R\right)^2\right)\left(L_G - a_{GWM}\right)}{2H_G{}^3 L_G} \end{pmatrix} \quad \text{(A.93)}$$

$$M_{RGW} = \max\begin{pmatrix} \frac{P_{RGWM} RD_R{}^2\left(3H_G - RD_R\right)\left(H_G - RD_R\right)\left(L_G - a_{GWM}\right)}{2H_G{}^3 L_G} \\ \frac{P_{RGWM} RD_R\left(H_G - RD_R\right)\left(2H_G - RD_R\right)\left(L_G - a_{GWM}\right)}{2H_G{}^2 L_G} \end{pmatrix} \quad \text{(A.94)}$$

These potentially induced hazard forces are then combined with the standard self, dead and live forces normally carried by the gallery to assess if the gallery wall supports capacity is exceeded.

Thus through this structured two step analysis process, one can ascertain if the gallery wall structural members have sufficient capacity to withstand the directly applied hazard forces and if they can transfer these forces to the gallery wall supporting members. Furthermore, one can determine if the gallery wall supporting members likewise have sufficient capacity to withstand these applied hazard forces. In conducting this assessment, one should keep an open mind to additionally imposed self, dead or live forces. Where such additional forces do exist, they should be included in this assessment.

Gallery component failure assessment step E

With the capacity of the gallery wall verified, the focus of analysis then progresses to gallery roof –

analysis steps E, F and G. In Table A-3, one can observe that four hazards, avalanche, flood, landslide and torrent hazards, can potential induce the gallery roof to fail. The first step of this analysis is to confirm if the given hazard comes in contact with the gallery roof, Equation (A.95).

$$H_G{}' > RD_H \quad \text{(A.95)}$$

Where:

H_G' = the uphill gallery wall height measured from the surrounding earth [m]

For the four hazards, avalanche, landslide, rockfall and torrent, the hazard running depth respectively takes the form of the avalanche running depth RD_A, the landslide running depth RD_L, the rockfall running height H_R, and the thickness of the torrent T_D.

Gallery component failure assessment step F

Once it has been confirmed that the hazard does come in physical contact with the gallery roof, the process of assessing the structural capacity of the gallery roof begins, Figure A-23. This process parallels the process employed to assess the structural capacity of the gallery wall by first assessing the structural capacity and induced forces within the gallery roof members.

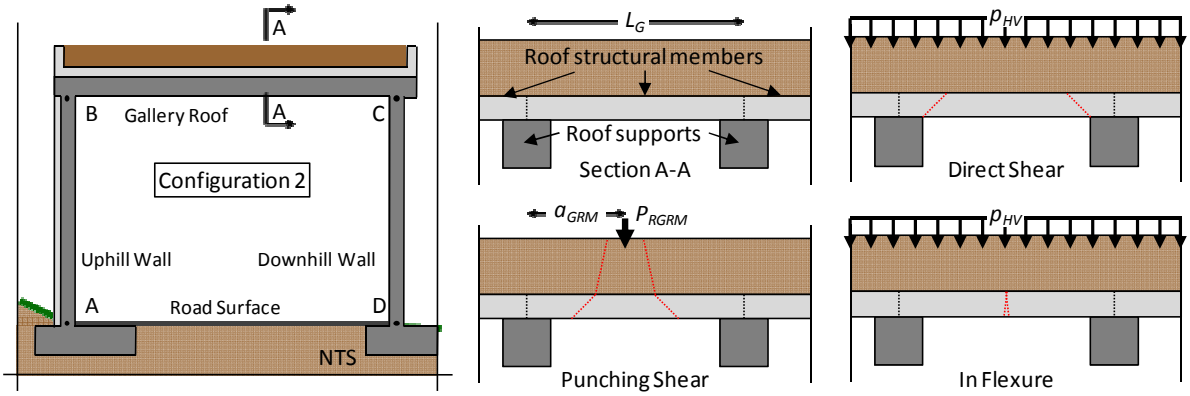

Figure A-23: Gallery roof or wall members overloaded in shear or flexure.

Considering the first gallery configuration, the punching shear strength can be determined with Equation (A.96) and considering the second gallery configuration and assuming the gallery roof structural member is composed of a doubly reinforced concrete member, the punching shear, direct shear and moment capacity can be respectively computed with Equations (A.97), (A.98) and (A.99).

$$v_{cGR} = 4\sqrt{f'_{dcGR}} \quad \text{(A.96)}$$

$$v_{cGRM} = 4\sqrt{f'_{dcGRM}} \quad \text{(A.97)}$$

$$V_{dGRM} = 0.18 f'_{dcGRM} b_{GRM} d_{GRM} \quad \text{(A.98)}$$

$$M_{uGRM} = \frac{A'_{sGRM} f_{dsGRM}}{b_{GRM}} \cdot \left(d_{GRM} - \frac{(A_{sGRM} - A'_{sGRM}) f_{dsGRM}}{2 \cdot 0.85 \cdot b_{GRM} f'_{dcGRM}} \right) + \frac{A'_{sGRM} f_{dsGRM}}{b_{GRM}} \cdot (d_{GRM} - d'_{GRM}) \quad \text{(A.99)}$$

Where:

v_{cGR} = the gallery roof punching shear stress capacity [N/mm^2]

f'_{dcGR} = the gallery roof dynamic ultimate concrete compressive strength [N/mm^2]

v_{cGRM} = the gallery roof structural member punching shear stress capacity [N/mm^2]

f'_{dcGRM} = the gallery roof structural member dynamic ultimate concrete compressive strength [N/mm^2]

V_{dGRM} = the gallery roof structural member ultimate direct shear capacity [N]

b_{GRM} = the gallery roof structural member concrete compression face width [mm]

d_{GRM} = the distance from the extreme compression fiber to the centroid of the tensile reinforcement within the gallery roof structural member [mm]

M_{uGRM} = the gallery roof structural member ultimate moment resistance [Nmm]

A_{sGRM} = the gallery roof structural member tensile reinforcement area within the width b_{GRM} [mm^2]
$A_s'_{GRM}$ = the gallery roof structural member compression reinforcement area within the width b_{GRM} [mm^2]
d'_{GRM} = the distance from the extreme compression fiber to the centroid of the compression reinforcement within the gallery roof structural member [mm]
f_{dsGRM} = the gallery roof structural member reinforcement dynamic design stress [N/mm^2]

Three of the four applicable hazards – avalanche, landslide and torrent – can be assumed to be uniformly distributed forces and thus it can be assumed that the gallery roof structural members will not fail in punching shear. Additionally, assuming the gallery roof structure members perform as fixed-fixed beams, the induced maximum shear and moment forces can be computed with Equations (A.100) and (A.101) (AISC, 1998, p. 4.195).

$$V_{HGRM} = \frac{p_{HV} b_{GRM} L_G}{2} \tag{A.100}$$

$$M_{HGRM} = \frac{p_{HV} b_{GRM} L_G^{\ 2}}{12} \tag{A.101}$$

Where:

V_{HGRM} = the gallery structural roof member maximum hazard induced shear [N]
M_{HGRM} = the gallery structural roof member maximum hazard induced moment [Nmm]
b_{GRM} = the gallery structural roof member horizontal width [mm]

For the avalanche and landslide hazards, the hazard vertical pressure can be computed from the avalanche and the landslide horizontal pressures by considering the uphill slope as is shown in Equations (A.102) and (A.103).

$$p_{AV} = p_{AH} \tan(\alpha_G) \tag{A.102}$$

$$p_{LV} = p_{LH} \tan(\alpha_G) \tag{A.103}$$

Where:

p_{LV} = the landslide vertical pressure [N/mm^2]
α_G = the gallery uphill slope [rad]

For the torrent hazard, the vertical pressure is a function of the torrent deposited depth as shown in Equation (A.104).

$$p_{TV} = d_T DD_T \tag{A.104}$$

Where:

P_{TV} = the torrent vertical pressure [N/mm^2]
d_T = the deposited torrent debris density [N/m^3]

Turning to the rockfall hazard, the force imposed on the gallery roof can be computed with Equation (A.105).

$$P_{RGRM} = 2.8 H_{GRC}^{\ -0.5} \tan(\phi_{GRC}) E_{GRC}^{\ 0.4} r_R^{\ 0.7} E_R^{\ 0.6} \sin(\alpha_R) \tag{A.105}$$

Where:

P_{RGRM} = the rockfall force applied on the gallery roof member [kN]

H_{GRC} = the height of the gallery roof cushioning material [mm]
φ_{GRC} = the gallery roof cushioning material internal friction angle [rad]
E_{GRC} = the gallery roof cushioning material modulus of elasticity [N/mm^2]

Thus, the respective induced punching shear, direct shear and moment forces are a function of the location of the rockfall impact point and can be calculated with Equations (A.106), (A.107), and (A.108) (Chikatamarla, 2007, pp. 11-12).

$$v_{RGRM} = \frac{P_{RGRM}}{2\pi d_{cGRM}\left(r_R + \frac{d_{GRM}}{2}\right)} \tag{A.106}$$

$$V_{RGRM} = \frac{P_{RGRM}\left(L_G - a_{GRM}\right)}{L_G} \tag{A.107}$$

$$M_{RGRM} = \frac{P_{RGRM}\left(L_G - a_{GRM}\right)a_{GRM}}{L_G} \tag{A.108}$$

Where:

v_{RGRM} = the gallery roof member ultimate rockfall induced punching shear [N/mm^2]
V_{RGRM} = the gallery roof member maximum rockfall induced direct shear [N]
M_{RGWM} = the gallery roof member maximum rockfall induced moment [Nmm]
a_{GRM} = the horizontal position of the rockfall impact point measured from the closest gallery roof structural frame [mm]
d_{cGRM} = the distance between the centroids of the compression and tensile reinforcement within the gallery roof member [mm]
d_{GRM} = the distance between the extreme compression fiber and the centroid of the tensile reinforcement within the gallery roof member [mm]

These potentially induced hazard forces are then combined with the standard self, dead and live forces normally carried by the gallery to assess if the gallery roof structural members' capacity is exceeded.

Gallery component failure assessment step G

Turning to the seventh failure assessment step, gallery roof supports are overloaded in shear or flexure, requires one to assess if the applicable hazards – avalanche, landslide, rockfall or torrent – can exceed the shear or flexural strength of the gallery roof supports. For the first and second gallery configurations, assuming the gallery roof and gallery roof support, respectively, are doubly reinforced concrete members, each member's shear and flexural capacity can be calculated using Equations (A.2) and (A.3) resulting in Equations (A.109) and (A.110). Please note the alternative definitions of the second gallery roof configuration width and depth variables, detailed in Figure A-24.

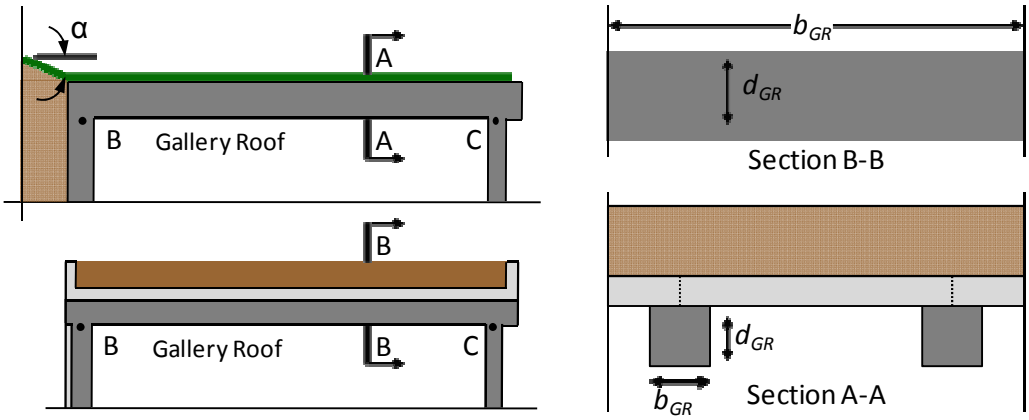

Figure A-24: Structural configuration of the gallery roof.

$$V_{dGR} = 0.18 f'_{dcGR} b_{GR} \cdot d_{GR} \qquad \text{(A.109)}$$

$$M_{uGR} = \frac{A'_{sGR} f_{dsGR}}{b_{GR}} \cdot \left(d_{GR} - \frac{(A_{sGR} - A'_{sGR}) f_{dsGR}}{2 \cdot 0.85 \cdot b_{GR} f'_{dcGR}} \right) + \frac{A'_{sGR} f_{dsGR}}{b_{GR}} \cdot (d_{GR} - d'_{GR}) \qquad \text{(A.110)}$$

Where:

V_{dGR} = the gallery roof ultimate direct shear capacity [N]
b_{GR} = the gallery roof concrete compression face width [mm]
d_{GR} = the distance from the extreme compression fiber to the tensile reinforcement centroid within the gallery roof [mm]
M_{uGR} = the gallery roof ultimate moment resistance [Nmm]
A_{sGR} = the gallery roof tensile reinforcement area within the width b_{GRM} [mm^2]
$A_s'_{GR}$ = the gallery roof compression reinforcement area within the width b_{GRM} [mm^2]
d'_{GR} = the distance from the extreme compression fiber to the compression reinforcement centroid within the gallery roof [mm]
f_{dsGR} = the gallery roof reinforcement dynamic design stress [N/mm^2]

The forces applied to the gallery roof supports are a function of the physical reach of the hazard. To analyze the avalanche, landslide and torrent hazards, Figure A-25, one can observe that the applied forces can be assumed to be uniformly distributed across the gallery roof. Thus assuming the gallery roof responds as a propped cantilever, the maximum hazard induced direct shear and moment forces can be computed with Equations (A.111) and (A.112) (AISC, 1998, p. 4.193).

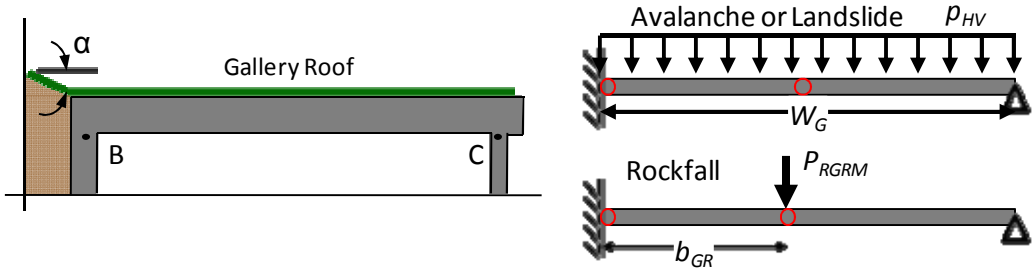

Figure A-25: Gallery roof loading and potential flexural hinge locations.

$$V_{HGR} = \frac{5 p_{HV} b_{GR} W_G}{8} \qquad \text{(A.111)}$$

$$M_{HGR} = \frac{5 p_{HV} b_{GR} W_G^{\ 2}}{8} \tag{A.112}$$

Where:

V_{HGR} = the gallery roof maximum hazard induced direct shear [N]
M_{HGR} = the gallery roof maximum hazard induced moment [Nmm]
W_G = the gallery width [m]

When the gallery roof structural members have sufficient strength to withstand the applied hazard forces, b_{GR}, for both the first and second gallery configurations is equal to the length of the gallery section under analysis or the spacing between the gallery structural frames. Within the second gallery configuration, if the gallery roof structural members do not have sufficient strength to withstand the applied hazard forces, a significant portion of the hazard force will be shed and the variable b_{GR} will be equal to the width of the roof support.

Shifting to assessing the rockfall hazard and considering the first gallery configuration, the induced rockfall forces are a function of the location of the rockfall impact point. By assuming the gallery roof responds as a propped cantilever, the maximum rockfall induced direct shear and moment forces can be calculated with Equations (A.113) and (A.114) (AISC, 1998, p. 4.194).

$$V_{RGR} = \max\left\{\begin{array}{c} \frac{P_{RGRM} b_{GR}^{\ 2}}{2W_G^{\ 3}}\left(3W_G - b_{GR}\right) \\ \frac{P_{RGRM}\left(W_G - b_{GR}\right)}{2W_G^{\ 3}}\left(3W_G^{\ 2} - \left(W_G - b_{GR}\right)^2\right) \end{array}\right\} \tag{A.113}$$

$$M_{RGW} = \max\left\{\begin{array}{c} \frac{P_{RGRM} b_{GR}^{\ 2}}{2W_G^{\ 3}}\left(3W_G - b_{GR}\right)\left(W_G - b_{GR}\right) \\ \frac{P_{RGRM} b_{GR}\left(W_G - b_{GR}\right)}{2W_G^{\ 2}}\left(2W_G - b_{GR}\right) \end{array}\right\} \tag{A.114}$$

Where:

V_{RGR} = the gallery roof maximum rockfall induced direct shear [N]
M_{RGR} = the gallery roof maximum rockfall induced moment [Nmm]
b_{GR} = the lateral position of the rockfall impact point measured from the uphill gallery wall [m]

Expanding the rockfall hazard assessment to second gallery configuration, the forces imposed into the gallery roof supports are a function of whether the gallery roof structural members fail under the applied rockfall hazard (thereby shedding a portion of the rockfall force) and the distance between the rockfall impact location and the closest gallery roof support. If this condition controls, the force transferred to the gallery roof support is equal to the maximum direct shear of the gallery roof structural members as shown in Equations (A.115) and (A.116).

$$V_{RGW} = \max\left\{\begin{array}{c} \frac{V_{RGRM} b_{GR}^{\ 2}}{2W_G^{\ 3}}\left(3W_G - b_{GR}\right) \\ \frac{V_{RGRM}\left(W_G - b_{GR}\right)}{2W_G^{\ 3}}\left(3W_G^{\ 2} - \left(W_G - b_{GR}\right)^2\right) \end{array}\right\} \tag{A.115}$$

$$M_{RGR} = \max\left\{\begin{array}{l} \frac{V_{RGRM} b_{GR}^{\ 2}}{2W_G^{\ 3}}\left(3W_G - b_{GR}\right)\left(W_G - b_{GR}\right) \\ \frac{V_{RGRM} b_{GR}\left(W_G - b_{GR}\right)}{2W_G^{\ 2}}\left(2W_G - b_{GR}\right) \end{array}\right\} \quad \text{(A.116)}$$

If the gallery roof structural members have sufficient capacity to withstand the induced rockfall forces, the resulting gallery roof support induced shear and flexural forces can be assessed with Equations (A.117) and (A.118).

$$V_{RGR} = \max\left\{\begin{array}{c} \frac{P_{RGRM} b_{GR}^{\ 2}\left(3W_G - b_{GR}\right)\left(L_G - a_{GRM}\right)}{2W_G^{\ 3} L_G} \\ \frac{P_{RGRM}\left(W_G - b_{GR}\right)\left(3W_G^{\ 2} - \left(W_G - b_{GR}\right)^2\right)\left(L_G - a_{GRM}\right)}{2W_G^{\ 3} L_G} \end{array}\right\} \quad \text{(A.117)}$$

$$M_{RGR} = \max\left\{\begin{array}{c} \frac{P_{RGRM} b_{GR}^{\ 2}\left(3W_G - b_{GR}\right)\left(W_G - b_{GR}\right)\left(L_G - a_{GRM}\right)}{2W_G^{\ 3} L_G} \\ \frac{P_{RGRM} b_{GR}\left(W_G - b_{GR}\right)\left(2W_G - b_{GR}\right)\left(L_G - a_{GRM}\right)}{2W_G^{\ 2} L_G} \end{array}\right\} \quad \text{(A.118)}$$

Through this structural process, one can verify if the gallery roof structural members have enough capacity to absorb the directly applied hazard forces and if these members can transfer the applied hazard forces to the gallery roof supporting members. Additionally, this process highlights equations that can be employed to assess if the gallery roof supporting members have sufficient capacity to withstand these applied forces. It should be noted that while the detailed equations only address the concrete member capacity and the applied hazard forces, all additional forces including self weight, dead force and live force should also be considered within this assessment.

Gallery component failure assessment step H

Turning to the eighth assessment step, assessing the gallery frame capacity to resist the applied horizontal and vertical forces induced by avalanche, landslide and rockfall hazards, requires one to quantify the gallery frame properties and the applied hazard forces. To quantify the gallery frame properties, it is assumed that the moment of inertia of each gallery wall is equal to the average of the uphill and downhill wall moment of inertias and that the gallery responds globally as a rigid frame to applied horizontal and vertical forces. Thus, assuming the gallery walls and roof are doubly reinforced concrete members, the moment of inertia of each element can be computed with Equation (A.119) and the average wall moment of inertia can be computed with Equation (A.120) (Merritt, Loftin, & Ricketts, 1996, pp. 8.43-44).

$$I = \left(d - d \cdot k\right)^2 A_s + \left(d \cdot k - d'\right)^2 A' + \left(d \cdot k\right)^3 \frac{b}{3} \quad \text{(A.119)}$$

$$\bar{I}_{GW} = \frac{I_{GW} + I'_{GW}}{2} \quad \text{(A.120)}$$

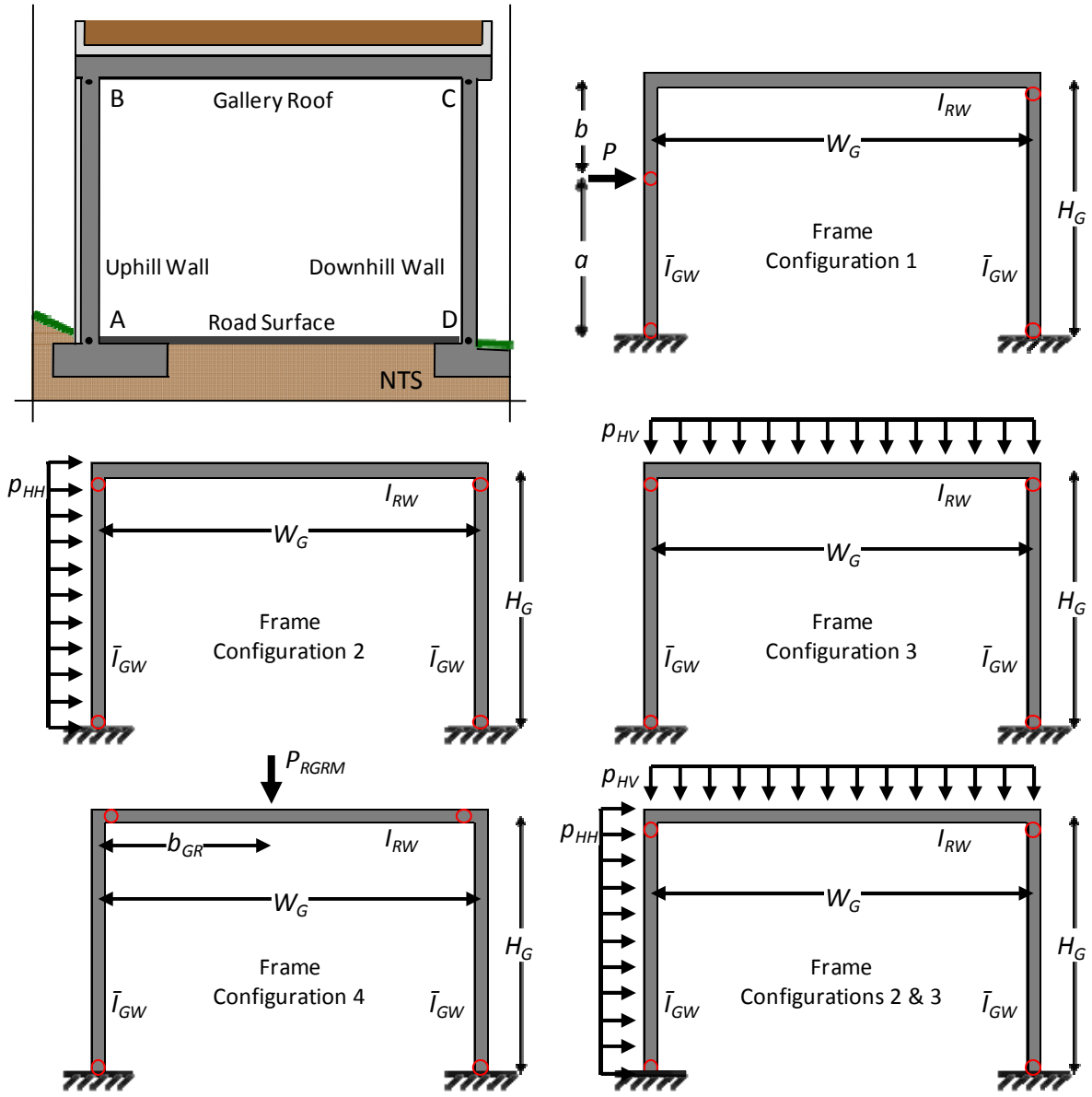

Figure A-26: Gallery frame loading and potential flexural hinge locations.

When one considers the three different hazards, there are four different ways these loading configurations can load in the rigid gallery frame. The first configuration, detailed in Figure A-26, addresses an avalanche, landslide or rockfall hazard impacting but not overtopping the uphill wall of the gallery. The hazard induced axial, shear, and moment gallery wall forces can be computed with Equations (A.121), (A.122) and (A.123).

$$A_{GW} = \frac{3 \cdot P \cdot a^2 I_{GR}}{H_G W_G (6 I_{GR} + I_{GW})} \tag{A.121}$$

$$V_{GW} = \frac{P\left(\left(2{H_G}^3 - a{H_G}^2\right)\left(I_{GR} + 2I_{GW}\right) + a \cdot b \cdot H_G I_{GW} + a \cdot b^2 \left(I_{GW} + I_{GR}\right) - a^2 b \cdot I_{GR}\right)}{2{H_G}^3 \left(I_{GR} + 2I_{GW}\right)} \tag{A.122}$$

$$M_{GW} = \frac{-P \cdot a \begin{pmatrix} H_G b\left(6I_{GW}I_{GR} + {I_{GW}}^2\right) + b^2\left(I_{GW} + 6I_{GR}\right)\left(I_{GW} + I_{GR}\right) \\ +{H_G}^2\left(6I_{GR} + I_{GW}\right)\left(I_{GR} + 2I_{GW}\right) - 3aH_G\left({I_{GR}}^2 + 2I_{GR}I_{GW}\right) \end{pmatrix}}{{H_G}^2\left(I_{GR} + 2I_{GW}\right)\left(6I_{GR} + I_{GW}\right)} \quad \text{(A.123)}$$

Where:

A_{GW} = the hazard induced axial wall forces [kN]

V_{GW} = the hazard induced shear wall forces [kN]

M_{GW} = the hazard induced moment wall forces [kNm]

	Avalanche	**Landslide**	**Rockfall**
P	$RD_A p_{AH} b_{GW}$	$RD_L p_{LH} b_{GW}$	P_{RGWM}
a	$RD_A/2$	$RD_L/2$	H_R
b	H_G-$RD_A/2$	H_G-$RD_L/2$	H_G-H_R

The second configuration, detailed in Figure A-26, addresses an avalanche or landslide hazard reaching or exceeding the top of the gallery wall. The induced axial, shear and moment gallery wall forces can be computed with Equations (A.124), (A.125) and (A.126).

$$A_{GW} = \frac{p_{HH} b_{GW} {H_G}^2 I_{GR}}{W_G\left(6I_{GR} + I_{GW}\right)} \quad \text{(A.124)}$$

$$V_{GW} = \frac{p_{HH} b_{GW} H_G}{8}\left(\frac{6I_{GR} + 13I_{GW}}{I_{GR} + 2I_{GW}}\right) \quad \text{(A.125)}$$

$$M_{GW} = \frac{p_{HH} b_{GW} {H_G}^2}{24}\left(\frac{30{I_{GR}}^2 + 73I_{GR}I_{GW} + 15{I_{GW}}^2}{\left(I_{GR} + 2I_{GW}\right)\left(6I_{GR} + I_{GW}\right)}\right) \quad \text{(A.126)}$$

The third configuration, detailed in Figure A-26, addresses an avalanche or landslide hazard blanketing the roof of a gallery inducing axial, shear and moment gallery wall forces. These forces can be computed with Equations (A.127), (A.128) and (A.129).

$$A_{GW} = \frac{p_{HV} b_{GRM} W_G}{2} \quad \text{(A.127)}$$

$$V_{GW} = \frac{p_{HV} b_{GRM} {W_G}^2 I_{GW}}{4H_G\left(I_{GR} + 2I_{GW}\right)} \quad \text{(A.128)}$$

$$M_{GW} = \frac{p_{HV} b_{GRM} {W_G}^2 I_{GW}}{12\left(I_{GR} + 2I_{GW}\right)} \quad \text{(A.129)}$$

The fourth configuration, detailed in Figure A-26, addresses a rockfall point force hazard impacting the roof of a gallery and inducing axial, shear and moment gallery wall forces. These forces can be computed with Equations (A.130), (A.131) and (A.132).

$$A_{GW} = \frac{P_{RGRM}\left(H_G - b_{GR}\right){W_G}^2\left(6I_{GR} + I_{GW}\right) + b_{GR} I_{GW}\left(H_G - 2b_{GR}\right)}{{W_G}^3\left(6I_{GR} + I_{GW}\right)} \quad \text{(A.130)}$$

$$V_{GW} = \frac{3P_{RGRM} b_{GR} \left(W_G - b_{GR}\right) I_{GW}}{2H_G W_G \left(I_{GR} + 2I_{GW}\right)} \tag{A.131}$$

$$M_{GW} = \frac{P_{RGR} b_{GR} \left(W_G - b_{GR}\right) I_{GW} \left(I_{GR} \left(5W_G + 2b_{GR}\right) - I_{GW} \left(W_G - 4b_{GR}\right)\right)}{W_G{}^2 \left(I_{GR} + 2I_{GW}\right)\left(6I_{GR} + I_{GW}\right)} \tag{A.132}$$

If the considered gallery follows gallery configuration 2 and is exposed to avalanche or landslide hazards which exceed the height of the gallery wall height, Equation (A.95), one must consider the potential for horizontal and vertical hazard loading. This can be accomplished by superimposing frame loading configurations 2 and 3 as detailed in Figure A-26.

These potentially induced gallery frame hazard forces are then combined with the standard self, dead and live forces normally carried by the gallery to assess if the gallery frame capacity is exceeded.

Gallery component failure assessment step I

If the gallery has sufficient capacity to structurally withstand the applied hazard forces, one must assess if the gallery can become inundated with flood waters or torrent debris, assessment step I, thereby denying public use of the gallery 'protected' roadway. Such assessment is conducted by further analyzing the hazard-object coincident analysis to determine if and to what extent the gallery object can become inundated.

By applying the general gallery assessment process presented herein, one can qualitatively and quantitatively determine which of the five considered hazards can induced the gallery to fail.

A.5 Retaining wall failure assessment procedure

Retaining walls are hardened structural objects constructed to hold back earthen embankments above or below roadways,

Table A-4.

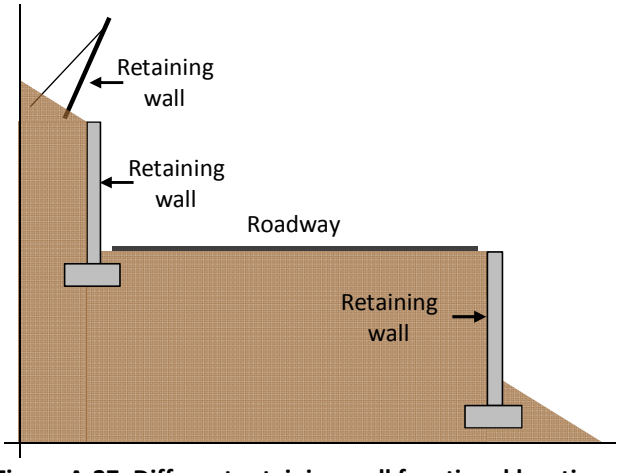

Figure A-27: Different retaining wall functional locations.

Herein, the term 'retaining wall' is extended to also include additional restraint oriented protective objects whose primary objective is restrain static or dynamic forces (e.g. avalanche barriers, check dams, levies, rockfall fences). When a retaining wall fails to perform as designed, the given hazard either breaks through or overtops the given retaining wall.

Table A-4: Retaining wall failure modes and associated hazards.

	Potential Hazards				
Failure mode	**Avalanche**	**Flood**	**Landslide**	**Rockfall**	**Torrent**
Foundation is undermined	-	x	x	-	-
Retaining wall is overloaded locally in shear	-	-	-	x	-
Retaining wall is overloaded globally in shear or flexure	x	x	x	x	x
Retaining wall foundation is overturned	x	x	x	x	x
Hazard flows over retaining wall	x	x	x	x	x

In

Table A-4, one can observe that it is assumed a retaining wall can fail in 18 different hazard scenarios. When these hazard scenarios are analyzed as a group, five independent failure modes can be identified. These failure modes can, in turn, be arranged into a structure assessment process, as shown in Figure A-28.

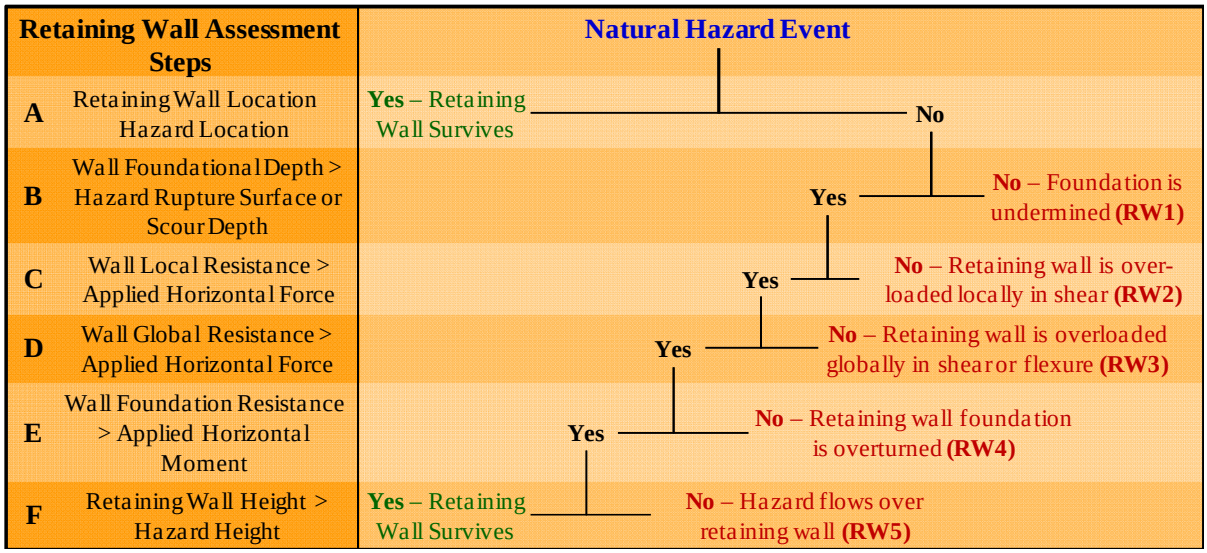

Figure A-28: Retaining wall component failure assessment process.

Retailing wall component failure assessment step A

The first step of the retaining wall failure assessment procedure, assessment step A: retaining wall location ≠ hazard location, requires a geographic coincident analysis to be conducted between the five potential hazards and the given retaining wall's location. Typically, it is during this phase of analysis that the true scope of the retaining wall failure assessment becomes evident as typically only two or three of the potential five hazards are coincident with the given retaining wall's location.

Retailing wall component failure assessment step B

The second step, wall foundation depth > hazard rupture surface or scour depth, focuses on determining if the retaining wall foundation can become compromised by a landslide or flood induced scour, as depicted in Figure A-29 and quantitatively assessed in Equation (A.133).

Where:

D_{RWF} = retaining wall foundation depth [m]

D_H = hazard rupture surface depth at the retaining wall location [m]

The landslide rupture surface depth should be assessed by an experienced geologist. While this assessment is commonly conducted in a general nature, i.e. shallow or deep, such information can

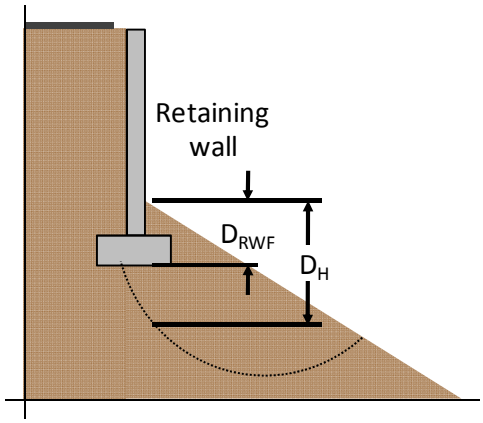

Figure A-29: Retaining wall foundation undermined by landslide or flood hazards.

$$D_{RWF} > D_H \tag{A.133}$$

help to identify if the retaining wall foundations are above or below a potential landslide rupture surface. The potential scour depth can be assessed using the procedure presented in the bridge pier scour assessment or through alternative procedures presented in Evaluating Scour at Bridges manual (Richardson & Davis, 2001).

Retailing wall component failure assessment step C

The third retaining wall failure assessment step, wall local resistance > applied horizontal force, determines if the retaining wall's internal resistance is sufficient to prevent a local punching shear failure, Figure A-30. In retaining walls, local punching shear is assumed to only be potentially present in above ground retaining walls and is assumed to only be induced by rockfall hazards. Within these assumptions, the potential punching shear failure mode can be quantitatively assessed with Equation (A.134).

$$v_{cRW} > v_{RRW} \tag{A.134}$$

Where:

v_{cRW} = retaining wall punching shear stress capacity [N/mm^2]
v_{RRW} = rockfall induced punching shear stress [N/mm^2]

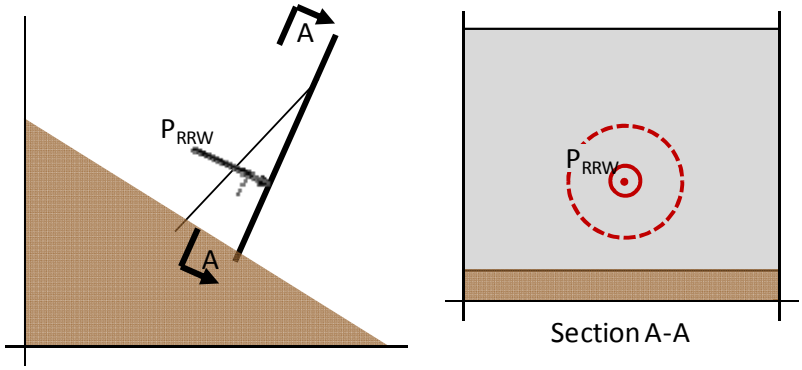

Figure A-30: Rockfall punching shear loading of a retaining wall.

The retaining wall punching shear stress capacity is commonly a key design parameter of retaining walls, particularly rockfall nets, and should be readily available on the given retaining wall's design

plans. The rockfall force applied to the retaining wall can be quantified with Equation (A.135) and the rockfall induced punching shear stress for a rockfall net and a concrete wall can be determined with Equations (A.136) and (A.137) respectively.

$$P_{RRW} = 2.8 r_R^{0.7} E_{RW}^{0.4} E_R^{0.6} \cos(\alpha_{RRW}) \quad \text{(A.135)}$$

Where:

P_{RRW} = the rockfall force applied on the retaining wall [kN]

E_{RW} = the retaining wall modulus of elasticity [N/mm^2]

α_{RRW} = the rockfall angle of attack measured from a line perpendicular to the retaining wall surface [rad]

$$v_{RRW} = \frac{P_{RRW}}{2 r_R \pi} \quad \text{(A.136)}$$

$$v_{RRW} = \frac{P_{RRW}}{2\pi d_{cRW}\left(r_R + \frac{d_{RW}}{2}\right)} \quad \text{(A.137)}$$

Where:

d_{cRW} = the distance between the retaining wall compression and tensile reinforcement centroids [mm]

d_{RW} = the distance between the retaining wall extreme compression fiber and tensile reinforcement centroid [mm]

If the rockfall induced punching shear exceeds the retaining wall punching shear capacity, it is assumed that the retaining wall along the entire width of the given rockfall hazard experiences failure.

Retailing wall component failure assessment step D

The fourth retaining wall failure assessment step, wall global resistance > applied horizontal force, assesses if the given retaining wall has sufficient global shear or flexural capacity to resist the applied hazard loading. The approach employed in this analysis is controlled by the type of hazard under consideration.

If the hazard is a mass movement hazard (avalanche, landslide, rockfall), it is herein assumed the retaining wall can be modeled as a simply supported beam and the applied avalanche and landslide hazard loads are uniformly distributed along the height of the hazard, as shown in Figure A-31.

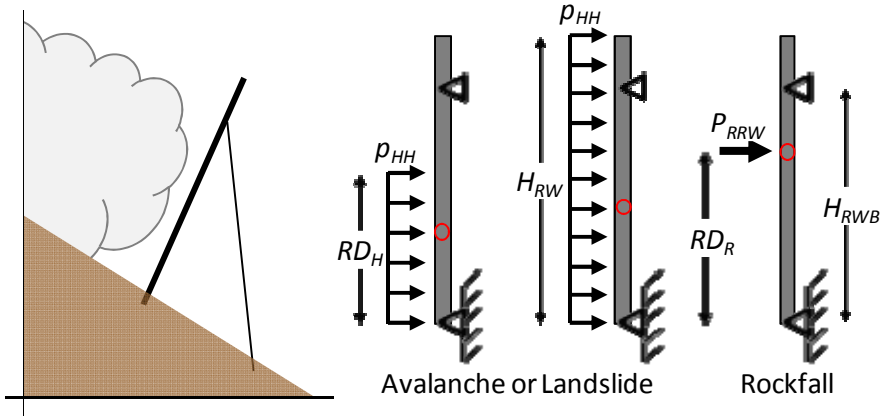

Figure A-31: Assessing retaining wall global resistance to the applied mass movement hazard force.

With a simply supported beam one needs to confirm that the retaining wall brace, retaining wall shear and retaining wall moment all have sufficient capacity to withstand the applied hazard forces. These different elements can be assessed, in general, with Equations (A.138), (A.139) and (A.140), respectively.

$$R_{URW} > R_{HRW} \tag{A.138}$$

$$V_{URW} > V_{HRW} \tag{A.139}$$

$$M_{URW} > M_{HRW} \tag{A.140}$$

Where:

R_{URW} = the retaining wall brace ultimate capacity assessed parallel to the slope [kN]
R_{HRW} = the retaining wall brace maximum hazard induced force assessed parallel to the slope [kN]
V_{URW} = the retaining wall ultimate shear capacity [kN]
V_{HRW} = the retaining wall maximum hazard induced shear [kN]
M_{URW} = the retaining wall ultimate moment capacity [kNm]
M_{HRW} = the retaining wall maximum hazard induced moment [kNm]

The retaining wall brace, retaining wall shear, and retaining wall moment ultimate capacities are best obtained from the given retaining wall's design plans or from an experienced practitioner as there are numerous different retaining wall types and configurations.

For avalanche and landslide hazards, the retaining wall maximum induced brace, shear and moment forces can be obtaining using Equations (A.141), (A.142) and (A.143), respectively (AISC, 1998, pp. 4-191,198).

$$R_{HRW} = \frac{p_{HH} W_H {RD_H}^2}{2H_{RWB}} \tag{A.141}$$

$$V_{HRW} = \begin{cases} \dfrac{p_{HH}\left(RD_H - H_{RWB}\right)}{2H_{RWB}}\left(3H_{RWB} - RD_H\right) & \left(H_{RWB} \geq RD_H\right) \\ \dfrac{p_{HH} W_H}{2H_{RWB}}\left({H_{RWB}}^2 + \left(RD_H - H_{RWB}\right)^2\right) & \left(RD_H > H_{RWB}\right) \end{cases} \tag{A.142}$$

$$M_{HRW} = \begin{Bmatrix} \dfrac{p_{HH}\left(RD_H - H_{RWB}\right)^2}{8H_{RWB}^{\ 2}}\left(3H_{RWB} - RD_H\right)^2 & \left(H_{RWB} \geq RD_H\right) \\ \max\begin{Bmatrix} \dfrac{p_{HH}W_H}{8H_{RWB}}\left(H_{RWB} + RD_H\right)^2\left(2H_{RWB} - RD_H\right)^2 \\ \dfrac{p_{HH}W_H\left(RD_H - H_{RWB}\right)^2}{2} \end{Bmatrix} & \left(RD_H > H_{RWB}\right) \end{Bmatrix} \quad \text{(A.143)}$$

Where:

H_{RWB} = the height of the retaining wall brace [m]

For a rockfall hazard, the retaining wall maximum induced brace, shear and moment forces can be obtaining using Equations (A.144), (A.145) and (A.146), respectively (AISC, 1998, pp. 4-192,199).

$$R_{RRW} = \frac{P_{RRW}RD_R}{H_{RWB}} \quad \text{(A.144)}$$

$$V_{RRW} = \begin{Bmatrix} \max\begin{Bmatrix} \dfrac{P_{RRW}\left(H_{RWB} - RD_R\right)}{H_{RWB}} \\ \dfrac{P_{RRW}RD_R}{H_{RWB}} \end{Bmatrix} & \left(H_{RWB} \geq RD_R\right) \\ P_{RRW} & \left(RD_R > H_{RWB}\right) \end{Bmatrix} \quad \text{(A.145)}$$

$$M_{RRW} = \begin{Bmatrix} \dfrac{P_{RRW}RD_R\left(H_{RWB} - RD_R\right)}{H_{RWB}} & \left(H_{RWB} \geq RD_R\right) \\ P_{RRW}\left(RD_R - H_{RWB}\right) & \left(RD_R > H_{RWB}\right) \end{Bmatrix} \quad \text{(A.146)}$$

In this global assessment of the retaining wall, the process through which the hazard force is distributed across two or more vertical retaining wall supports has not be considered within this assessment process, as the above included assessment process has assumed the hazard coincides with the vertical retaining wall member under consideration. For additional information concerning the hazard force distribution between and among two or more vertical supports, please consult the gallery wall assessment procedure.

Thus through the assessment process included above, one can quantify if the retaining wall has sufficient capacity to withstand the imposed mass movement hazard forces.

If the hazard is a flood or torrent hazard, it is herein assumed the retaining wall can be modeled as a cantilever and the applied hazard loading follows a hydrostatic distribution along the depth of the hazard, as shown in Figure A-32.

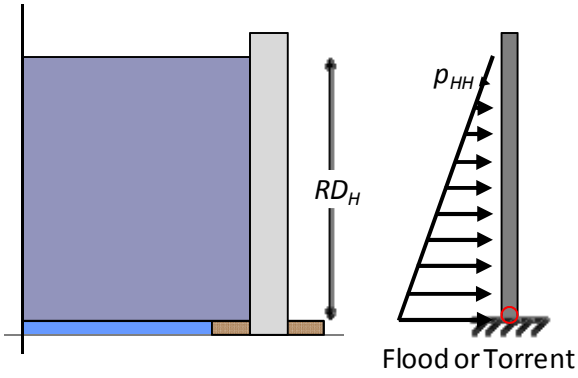

Figure A-32: Assessing retaining wall global resistance to the applied flood or torrent hydrostatic hazard force.

With a cantilever beam, one needs to confirm that the retaining wall has sufficient shear and moment capacity to withstand the applied hazard forces. These two parameters can be assessed, in general, with Equations (A.139) and (A.140), respectively.

The retaining wall shear and retaining wall moment ultimate capacities are best obtained from the given retaining wall's design plans or from an experienced practitioner as there are numerous different retaining wall types and configurations.

The retaining wall maximum induced shear and moment forces for flood and torrent, assuming the hazard forces are purely hydrostatic, can be obtaining using Equations (A.147) and (A.148) respectively (AISC, 1998, pp. 4-196).

$$V_{HRW} = \max\left\{\begin{array}{c}\frac{\gamma_H W_{RW} RD_H{}^2}{2} \\ \frac{\gamma_H W_H RD_H{}^2}{2}\end{array}\right\} \quad \text{(A.147)}$$

$$M_{HRW} = \max\left\{\begin{array}{c}\frac{\gamma_H W_{RW} RD_H{}^3}{6} \\ \frac{\gamma_H W_H RD_H{}^3}{6}\end{array}\right\} \quad \text{(A.148)}$$

Where:

W_{RW} = the retaining wall width [m]
W_H = the hazard width [m]
γ_H = the hazard's specific gravity [kN/m^3]

Thus through the assessment process included above, one can quantify if the retaining wall has sufficient capacity to withstand the imposed flood or torrent hazard forces.

Retailing wall component failure assessment step E

The fifth retaining wall failure assessment step, wall foundation resistance > applied horizontal moment, assesses if the retaining wall foundation can potential be overturned by the imposed hazard forces. In general, the overturning capacity of a retaining wall foundation can be assessed with Equation (A.149).

$$M_{URWF} > M_{HRWF} \quad \text{(A.149)}$$

Where:

M_{URWF} = the retaining wall foundation ultimate moment capacity [kNm]

M_{HRWF} = the retaining wall foundation maximum hazard induced moment [kNm]

Considering the retaining wall configuration shown in Figure A-31, the maximum hazard imposed moment on the retaining wall foundation can be quantified with Equation (A.150) as presented in Figure A-33.

$$M_{HRWF} = \begin{Bmatrix} \max\left\{ \begin{matrix} \frac{p_{HH} W_H RD_H^{\,2}}{2} \\ \frac{p_{HH} W_{RW} RD_H^{\,2}}{2} \end{matrix} \right\} & \left(Avalanche \vee Landslide\right) \\ P_{RRW} RD_R & \left(Rockfall\right) \end{Bmatrix} \quad \text{(A.150)}$$

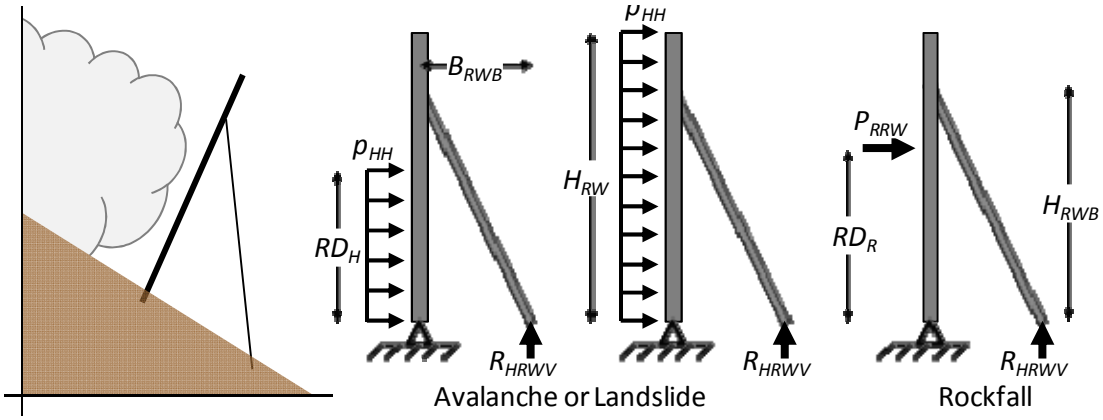

Figure A-33: Assessing the retaining wall foundation to the applied mass movement or rockfall hazard.

The retaining wall foundation ultimate moment capacity can be assessed, in terms of the reaction perpendicular to the slope and negating the self weight of the retaining wall, with Equation (A.151).

$$M_{URWF} = R_{HRWV} B_{RWB} \quad \text{(A.151)}$$

As there are numerous different retaining wall and brace foundation configurations which are in turn influenced by the local soil conditions, thus the vertical capacity of both the retaining wall and brace need to be obtained from the retaining wall plans or independently assessed by a trained foundation specialist.

If it is found that the imposed hazard forces do cause the retaining wall foundations to be over turned, it is herein conservatively assumed that retaining wall along the entire width of the given mass movement hazard will also be overturned.

Considering the retaining wall configuration shown in Figure A-32 for the flood and torrent hazards, the maximum hazard imposed moment on the retaining wall foundation can be quantified with Equation (A.152), as presented in Figure A-34.

$$M_{HRWF} = M_{HRW} = \max\left\{ \begin{matrix} \frac{\gamma_H W_{RW} RD_H^{\,3}}{6} \\ \frac{\gamma_H W_H RD_H^{\,3}}{6} \end{matrix} \right\} \quad \text{(A.152)}$$

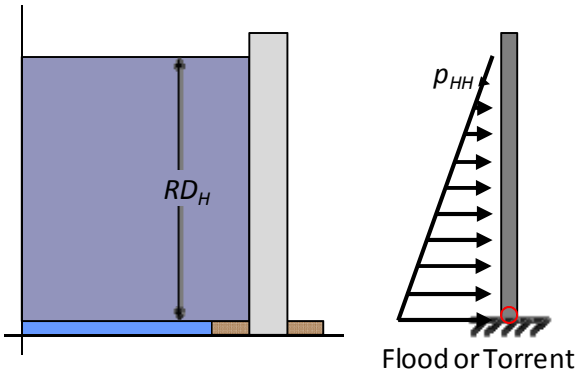

Figure A-34: Assessing retaining wall foundation to the applied flood and torrent hazard forces.

The retaining wall foundation ultimate moment capacity is a direct function of the type of retaining wall foundation employed and the local geological conditions, thus the moment capacity of the retaining wall needs to be obtained from the retaining wall plans or independently assessed by a trained foundation specialist.

If it is found that the imposed hazard forces do cause the retaining wall foundations to be over turned, it is herein conservatively assumed that retaining wall along the entire width of the given flood or torrent hazard will also be overturned as long as the other retaining wall sections have equal or lesser moment capacities.

Retailing wall component failure assessment step F

Turning to the sixth and last retaining wall assessment step, retaining wall height > hazard height, assesses if the retaining wall is physically overtopped by the given hazard. This step is rather straightforwardly assessed with Equation (A.153).

$$H_{RW} > RD_H \tag{A.153}$$

If the hazard does not overtop the given retaining wall, it is assumed that the retaining wall survives and the given hazard is effectively restrained.

Thus through applying this retaining wall failure assessment process and the detailed assessment procedure detailed herein, one can qualitatively and quantitatively determine if and in what failure mode a retaining wall can potentially experience a failure due to any of the five considered hazards.

A.6 Roadway failure assessment procedure

Roadways include highways, roadways and small country lanes and comprise more than ninety-five percent of the road transportation network. Roadway objects are constructed by leveling the given location to a smooth grade, placing an appropriate gravel-based foundation and laying an asphalt or concrete roadway surface. While roadway objects, in comparison to all other objects, are by and large constructed in less hazard risk prone locations, these objects have negligible resistance, beyond their given location, to natural hazards. In consulting the five hazards, it is herein assumed that a roadway object can fail in seven different failure scenarios, as presented in Table A-5. When these seven potential failure scenarios are assessed as a group, two independent failure modes can be identified – specifically the roadway foundation can become compromised or the roadway can become buried in liquid or debris.

Table A-5: Roadway failure modes and associated hazards.

	Potential Hazards				
Failure mode	**Avalanche**	**Flood**	**Landslide**	**Rockfall**	**Torrent**
Roadway foundation compromised	-	x	x	-	-
Roadway buried in liquid or debris	x	x	x	x	x

As a roadway's only internal resistance to natural hazards is its location, roadway objects are commonly locally strengthened by constructing supporting culvert and retaining wall objects respectively under and above or below a given roadway in locations where the roadway object transects significant transverse grades, crosses small moving bodies of water, runs parallel to known flood or torrent hazard zones, or crosses recognized avalanche, landslide or rockfall hazard zones.

Considering the positive influence culvert and retaining wall supporting objects can have on roadway object resistance and the two potential failure modes presented in Table A-5, these two failure modes can be arranged into a structured assessment process presented in Figure A-35.

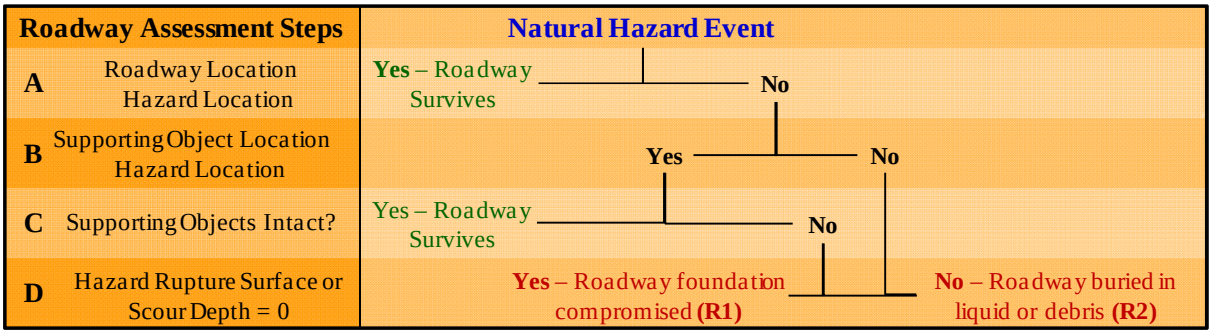

Figure A-35: Roadway component failure assessment process.

Roadway component failure assessment step A

The first step of the roadway failure assessment procedure, assessment step A: roadway location ≠ hazard location, requires a geographic coincident analysis to be conducted between the locations of the five potential hazards and the location of the given roadway object. It is during this phase of analysis that the true scope of the roadway failure assessment becomes evident, as typically only two or three of the potential five hazards are coincident with the given roadway object.

Roadway component failure assessment step B

In the second step of the roadway failure assessment procedure, assessment step B: supporting object location ≠ hazard location, a geographic coincident analysis is conducted between the given roadway object location, the hazard location and the supporting object location. If it is found that the supporting object is geographically coincident with the given hazard effecting the roadway object, the failure assessment process graduates to assessing the supporting object's capacity in step C, and if not, the assessment process transitions to assessment step D.

Roadway component failure assessment step C

In the third step, assessment step C: supporting objects intact?, focuses on assessing if the supporting objects coincident with the given hazards effecting the studied roadway object has sufficient capacity to withstand the applied hazard forces. This is determined by conducting a failure assessment for the respective component and hazard. If it is found that the supporting object does in fact have sufficient capacity to withstand the applied hazard forces, it is herein assumed that the hazard will be prevented from coming in contact with given roadway and thus the roadway survives.

If it is found that the supporting object does not have sufficient capacity and experiences either structural or functional failures, it is herein assumed that the complete hazard intensity is transitioned directly onto the roadway.

Roadway component failure assessment step D

The fourth and final assessment step, hazard rupture surface or scour depth = 0, assesses if the roadway foundation can become compromised by a landslide or flood induced scour, as depicted in Figure A-36 and quantitatively assessed in Equation (A.154).

$$D_L = 0 \qquad \text{(A.154)}$$

As it is herein assumed that roadway objects have negligible foundational depths, if the landslide or scour depth at the roadway location exceeds a value of 0 at and location under the roadway, it is

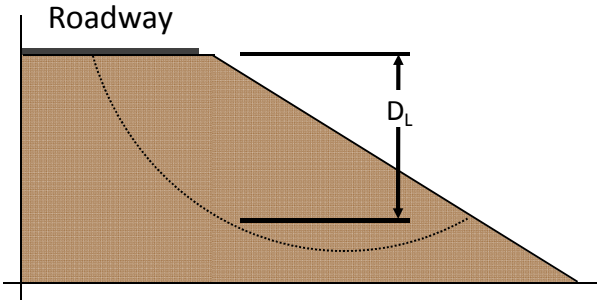

Figure A-36: Roadway foundation undermined by landslide or flood hazards.

herein assumed that the roadway foundation will be undermined along the width of the flood induced scour or landslide hazard. The landslide rupture surface depth should be assessed by an experienced geologist. While this assessment is commonly conducted in a general nature, i.e. shallow or deep, such information can help to identify if the retaining wall foundations are above or below a potential landslide rupture surface. The potential scour depth can be assessed using the procedure presented in the bridge pier scour assessment or through alternative procedures presented in the Evaluating Scour at Bridges manual (Richardson & Davis, 2001).

If the analysis conducted in fourth step of the roadway failure assessment validates Equation (A.154), it is herein assumed that the roadway object is structurally intact but the given roadway object is buried under the liquid or debris causing the roadway to be functionally inoperable along the entire width of the hazard.

Through applying this roadway failure assessment process and the detailed assessment included herein, one can qualitatively and quantitatively determine if and in what failure mode a roadway, and its supportive objects, can potentially experience a failure due to any of the five considered hazards.

A.7 Tunnel failure assessment procedure

Tunnels are hardened structural objects constructed to pass roadways and railways through or under a masses of earth, rock or water. Tunnel objects are constructed either through a cut and cover process or by cutting a passageway through the in situate earth and rock. Within this immediate work, it is assumed that the buried nature of the tunnel component protects and precludes it from

potential avalanche, landslide and rockfall hazards. Therefore the process of assessing the failure of a tunnel object, focuses on the potential functional failure modes.

Table A-6: Tunnel failure modes and associated hazards.

	Potential Hazards				
Failure mode	**Avalanche**	**Flood**	**Landslide**	**Rockfall**	**Torrent**
Tunnel is 'flooded' with liquid or debris	-	x	-	-	x
Tunnel and utilities 'flooded' with liquid or debris	-	x	-	-	x

In Table 3-2, one can observe that it is assumed a tunnel object can fail in 4 different hazard scenarios. When these hazard scenarios are analyzed as a group, two independent failure modes can be identified, – specifically the inundation of the tunnel itself with liquid or debris or the inundation of the tunnel lighting and ventilation utilities with liquid or debris, Table A-6. These two failure modes can be arranged into a structured assessment process presented in Figure A-37.

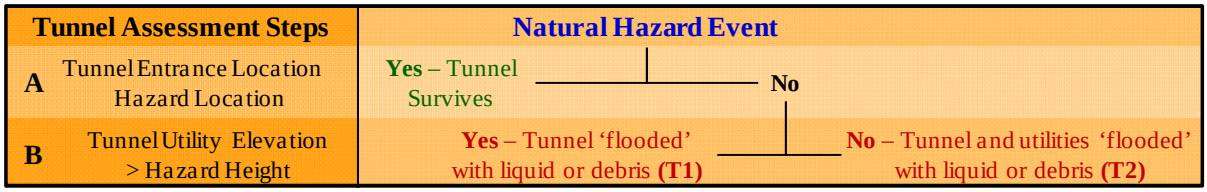

Figure A-37: Tunnel component failure assessment process.

Tunnel component failure assessment step A

The first step of the tunnel failure assessment process, assessment step A: tunnel entrance location ≠ hazard location, requires a geographic coincident analysis to be conducted between the two potential hazards, flood and torrent, and the tunnel entrance locations. If either of the two hazards are coincident with either of the tunnel entrances, and precluding any significant tunnel slopes, the tunnel is assumed to be inundated along its entire length.

Tunnel component failure assessment step B

With the coincident analysis conducted, the assessment then graduates to assessing the level of damage exacted upon the tunnel. The second tunnel assessment step determines if the tunnel utilities, including electrical, communication and ventilation utilities, are also inundated with the flood or torrent hazards. This assessment is conducted with Equation (A.155) and detailed in Figure A-38.

$$H_{TU} > \begin{pmatrix} DD_T \\ H_F \end{pmatrix} \quad \text{(A.155)}$$

Where:

H_{TU} = the height of the lowest tunnel electrical, communication or ventilation utilities [m]

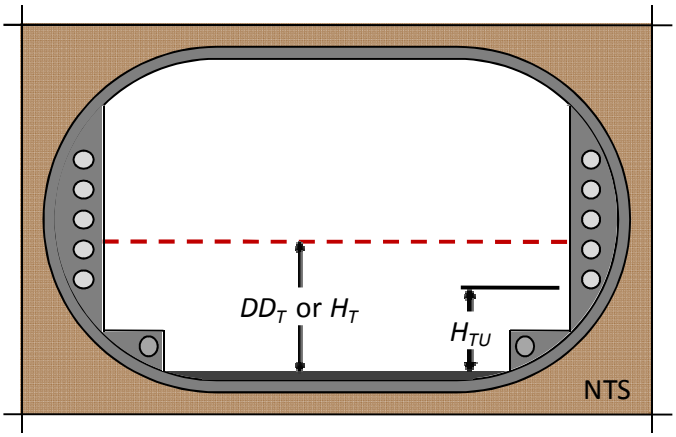

Figure A-38: General tunnel configuration.

Thus through this general tunnel assessment process and the detailed assessment process presented herein, one can qualitatively and quantitatively determine if a tunnel can potentially experience a functional failure due to the considered hazards – flood and torrent.

B Limits of Analytical Risk Management

B.1 Managing risk sources in civil engineering

Risk sources within the civil engineering and construction industries are managed and mitigated as in any other industries but in these domains, the most common risk management activities are integrated into the building codes and standards. These risk management policies and approaches are developed through a highly empirical process employing system, elemental and material testing. With these manuals, civil engineers are able to analyze a structure, be it a bridge or a building, and determine if it has the structural capacity to withstand the anticipated forces. Unfortunately these codes do have their limitations and where these limitations are breached, professional modes of practice take the place of formalized codes.

B.2 Expanding the limits of formalized codes – the life quality index

One such area in which the building code limits are surpassed is in evaluating what is an acceptable level of investment to advert the loss of a life. As highlighted by Tengs et. al. in their cross comparison of the cost-effectiveness of five-hundred life-saving interventions which have been either fully implemented, partially implemented or not implemented, the cost-effectiveness of life saving interventions can vary significantly from a net gain on investment in fields such as drug and alcohol treatment to a potential net investment cost of tens of millions of dollars per life saved in the fields of chemical and radiation control (Tengs, et al., 1995).[14]

While it is good to see that cost-effectiveness is being actively considered in practical decision making, the cost-effectiveness range of these risk reduction measures leaves the question of an acceptable maximum cost-effectiveness limit unanswered. The variance of risk reduction measures from project to project even within the same industry has further complicated the civil engineer's task of designing a `safely operating´ structure for it has become difficult if not impossible to define what is a `safe enough´ safely operating structure.

One approach for determining the acceptable level of life-saving investment is the Life Quality Index (LQI) developed by Nathwani, Lind and Pandey (1997). The motivation for developing the LQI was to improve "the overall public welfare by reducing risk to life in a cost-effective manner" for in the words of the LQI developers one should choose the "prospect to save life or produce wealth if no alternative presents a greater life expectancy net or work-time cost." (Pandey, Nathwani, & Lind, 2006, pp. 342, 352).

B.3 Life quality index theoretical foundation

The theoretical foundation of the LQI is constructed on four key tenets:

[14] It should be noted that in a subsequent letter to the editor submitted by a representative of the United States Environmental Protection Agency (EPA), it was stated that of the eleven EPA related life-saving interventions included in the cross comparison, only two – radionuclide regulations in underground uranium mines ($101,600[14]/life) and in elemental phosphorous plants ($11,400,000/life) – were actually implemented. In all other cases, "a control option less costly than that listed was adopted, or a decision was made not to regulate at all." (Puskin & Bunger, 1996, p. 131)

1) Risk reduction funds should be equally distributed.
2) Risk management decisions should be accountable and transparent.
3) Potential adversely affected individuals should be fairly compensated.
4) The amount of investment should reflect society's work to leisure equilibrium. (Nathwani, Lind, & Pandey, 1997)

Equal distribution of risk reduction funds

The first theoretical LQI tenet posed by the LQI developers is that risk reduction funds, which are assumed to be a fixed and scarce commodity, should be invested "in an impartial manner, since gain in life expectancy is valued equally, irrespective of who gets it." If such an approach were to be implemented in practice, the LQI developers take the view point that the available resources would purchase the maximum benefit for the general society (Nathwani, Lind, & Pandey, 1997).

Supporting this argument, the LQI developers have highlighted the investment dichotomy between treating the effects of water born diseases in the developing world and chemical regulatory standards in industrialized countries. In particular, the LQI developers note that in 1993 diarrheal diseases took the lives of approximately 3 million children the loss of which could have been prevented through the dissemination of food safety education, hygienic behavior promotion and administration of oral rehydration salts (ORS) amounting to a total investment of $1.03/life saved (World Health Organization, 2007) (Nathwani, Lind, & Pandey, 1997). This and other similar needs were left unfulfilled while multi-million dollar regulatory investments per life saved such as radionuclide emission control at elemental phosphorous plants ($11.84 million/life saved), strengthening buildings in earthquake regions (23 million/life saved), and chloroform reduction at 70 pulp and paper mills ($19.3 million/life saved) were being required by law (Tengs, et al., 1995).

Accountability principle

The LQI developers' second tenet is an "Accountability Principle" in which "Decisions for the public in regard to health and safety must be open, quantified, defensible, consistent and applied across the complete range of hazards to life." The authors continue to state that "(t)here is a need for a single, clear process for managing risks affecting the public. Once known and accepted, this rationale removes day-to-day decisions about risk from the political arena where they do not belong." (Nathwani, Lind, & Pandey, 1997, p. 23) In the view of the LQI developers, this unified industry standard would give the practitioners the tools and support they need for making difficult decisions concerning allocating life-saving investment funds.

Currently within the science and engineering practice, cost-benefit analysis is actively used but as is commonly said `the devil is in the details' with the various risk assessments considering, weighing or even ignoring the direct and indirect risk elements (National Resarch Council, 1983). This has introduced confusion and uncertainty within society who has begun to question the processes and analyzes decision makers employ in reaching their decisions. This has resulted in society losing faith in the decision maker's priorities and thus society commonly reverts to the precautionary principle – demanding additional regulations and regulatory processes which, in turn, further widens the cost differential among life-saving interventions (Slovic, 1999).

Fair compensation

The third foundational tenet posed by the LQI developers is that potential losers of life-saving investment reallocations can be transformed into non-losers through the allocation of secondary

compensation (Nathwani, Lind, & Pandey, 1997). The developers employ the Kaldor-Hicks Efficiency Principle which defines an efficient situation as a situation in which the winners can in theory compensate the losers but that compensation is not required to actually be transferred (Wikipedia, 2008). Through using this approach, the developers state "the cost of a project and affected individuals who bear the additional risk are compensated. This compensation if it is viewed as fair by those affected, transforms the potential losers into non-losers thus making the policy for all at least neutral." (Nathwani, Lind, & Pandey, 1997)

One commonly sighted example of a Kaldor-Hicks efficient situation is the introduction of additional risk exposure tasks for factory workers. In this environment, factory workers are commonly compensated for exposure to dangerous situations with additional compensation or danger pay. From the viewpoint of the Kaldor-Hicks efficient situation if the employees accept these employment conditions – exposure to the dangerous situations for the associated financial compensation – the potential losers are transferred into non-losers (Viscusi & O'Connor, 1984).

Ratio of work to leisure

The last tenet posed by Nathwani and his coauthors is that life-saving investment should "reflect peoples' revealed preference for the work/non-work (leisure) time ratio" (Pandey, Nathwani, & Lind, 2006, p. 342). The LQI developers state that such a work/leisure balance is reached by workers in a similar fashion as the way in which consumers choose between consumption and leisure – through the marginal rate of substitution. Per this argument developed by Nathwani and his colleagues, a worker determines how many hours he should work each week, how many weeks he should work each year and how many years he should work in a life-time by directly considering the marginal rate of substitution of gains from potential additional work offsetting the potential loss of leisure time. Thus, in the view of the LQI developers, the ratio of working time to leisure time is a direct reflection of how much time the average worker is willing to forfeit for the resulting gain.

Upon these four fundamental tenets, the LQI developers have employed macroeconomic and mathematical derivation processes to formulate the Life Quality Index. While these derivation steps are not directly included herein, the specific derivation steps and reasoning can be found within (Nathwani, Lind, & Pandey, 1997) (Pandey, Nathwani, & Lind, 2006).

B.4 The life quality index

B.4.1 The life quality index equation

The life quality index for a given country is a function of the gross domestic product (GDP) per capita (the annual financial resources at the given country's disposal), the life expectancy (a reflection of the number of working years a person can contribute) and the proportion of an individual's lifetime invested in working within the given country. The original formulation of the LQI is:

$$L_o = g^w e^{(1-w)} \tag{B.1}$$

Where:

L_0 = the original life quality index [$/person]
g = the real gross domestic product per capita [$/person/year]
e = the life expectancy at birth [years]
w = the average amount of an individual's lifetime invested in working [ ]

Thus, the LQI is calculated by raising the gross domestic product per capita (*g*) by the proportion of time spent working (*w*) and multiplying this quantity by the life expectancy at birth (*e*) raised by the proportion of time spent in non-work related activities (1-*w*) (Nathwani, Lind, & Pandey, 1997).

As this index is a function of the productivity (*g*), the length of time a given individual can contribute to society by working (the life expectancy *e*) and the ratio between substituting additional work for less leisure time and vice versa (*w*), the LQI increases as a society's annual production and life expectancy increases and decreases as the society moves to substituting additional leisure for a reduction in work.

In 2004, two of the original LQI developers released a secondary life quality indicator by considering work-leisure tradeoffs, such that:

$$L = g^{\frac{w}{1-w}} e = L_o^{\frac{1}{1-w}} \tag{B.2}$$

Where:

L = redefined LQI considering work-leisure tradeoffs (Pandey & Nathwani, 2004)

This redefined LQI formulation will be subsequently referred to as the LQI or *L* and will be the equation employed in all subsequent discussions, analyzes and examples. In this LQI formulation, the economic production of a given country is raised by the country's ratio of working to leisure activities and multiplied by the country's life expectancy.

Example B-1 - Calculate the Life Quality Index for a country:

Taking the country of Switzerland in 2004 for example, where the real GDP per capita (*g*) is $50,387 (IMF, 2007), life expectancy at birth is 81.304 years (World Health Organization, 2007), and the ratio of work time is 0.1376[15] and employing Equation (B.2):

$$L = g^{\frac{w}{1-w}} e = (\$50387)^{\frac{0.1376}{1-0.1376}} (81.304 years)$$

Resulting in a Life Quality Index of 457.50.

In this form, the LQI is just what its name implies, a social index and indicator which can be used to track the economic and life expectancy developments of a country in time and to compare the economic and life expectancy developments of various countries against one another.

B.4.2 Deriving the maximum life-saving investment

Where the potential application of the LQI for the civil engineering community becomes evident is when one considers how the LQI fluctuates in time as a function of changes in the life expectancy and GDP per capita. These life expectancy and financial modifications can be considered as the implications of additional safety measures. This form of the LQI is determined by taking the derivative of the LQI, by assuming the work to leisure ratio remains constant in the face of changing life expectancy, resulting in:

$$dL = \frac{w}{1-w} g^{\frac{w}{1-w}-1} dg \cdot e + g^{\frac{w}{1-w}} de \tag{B.3}$$

[15] 0.1376 = [(40 hours/week)(50 weeks/year)(49 years/life)] / [(24 hours/day)(365 days/year)(81.304 years/life)

Where:

de = the new safety regulation impact on the life expectancy at birth
dg = the financial investment required to implement this new safety regulation per exposed individual
dL = the change of the LQI as a function of a new safety regulation

Normalizing both sides with respect to the LQI produces:

$$dL = \frac{\frac{w}{1-w} g^{\frac{w}{1-w}-1} dg \cdot e + g^{\frac{w}{1-w}} de}{g^{\frac{w}{1-w}} e} \tag{B.4}$$

Which simplifies to:

$$\frac{dL}{L} = \frac{\frac{w}{1-w} \cdot dg}{g} + \frac{de}{e} \tag{B.5}$$

For a regulation to be beneficial, the *dL*, the change of the life quality index, must be greater than zero, thus:

$$\frac{\frac{w}{1-w} dg}{g} + \frac{de}{e} \geq 0 \tag{B.6}$$

Finally, solving for the required financial investment (*dg*) per individual protected yields:

$$dg = -\frac{g \cdot de}{\frac{w}{1-w} \cdot e} \tag{B.7}$$

The authors of the LQI propose this value, *dg*, is the maximum optimal life-saving investment applied to save, *de*, number of lives that can be sustained by a country with an annual production *g*, a life expectancy *e* and a work to leisure ratio of *w*.

Example B-2 - Calculate the maximum optimal life-saving investment for Switzerland:

Continuing with the Switzerland example introduced in Example B-1, calculate the maximum optimal investment that should be expended to implement a safety regulation which reduces the risk to life uniformly by $1 \cdot 10^{-6}$.

The maximum optimal investment is determined with Equation (B.7). This equation requires one to obtain or calculate the variables *g*, *e*, *w* and *de*. The first three variables *g*, *e* and *w* were calculated as \$50,287, 80.304 years and 0.1376 respectively in Example B-1, but the impact of the new safety regulation on the life expectancy (*de*) must be determined by calculating the life-expectancy change induced by the new regulation.

The Switzerland 2004 life-table is presented in Example B-1 where:

Table B-1: Calculate Switzerland 2004 life table.

Age interval x	Interval duration n_x	Death rate factor [WHO 2007] a_x	Observed death rate [WHO 2007] M_x	Probability of death q_x	Number of survivors l_x	Number of deaths d_x	Total number of years lived in age interval L_x	Total number of years lived beyond age x T_x	Life expectancy (years) e_x
'<1'	1	0.1	0.00424	0.004224	100000	422	99620	8130415	81.3041514
'1-4'	4	0.4	0.00019	0.00076	99578	76	398129	8030795	80.648603
'5-9'	5	0.5	0.00011	0.00055	99502	55	497373	7632666	76.7086982
'10-14'	5	0.5	0.00011	0.00055	99447	55	497100	7135293	71.7495242
'15-19'	5	0.5	0.00034	0.001699	99393	169	496541	6638194	66.7876219
'20-24'	5	0.5	0.00053	0.002646	99224	263	495462	6141653	61.8970039
'25-29'	5	0.5	0.00045	0.002247	98961	222	494250	5646191	57.0546148
'30-34'	5	0.5	0.00053	0.002646	98739	261	493040	5151941	52.1775009
'35-39'	5	0.5	0.00081	0.004042	98477	398	491392	4658900	47.3093209
'40-44'	5	0.5	0.00118	0.005883	98079	577	488955	4167508	42.4911669
'45-49'	5	0.5	0.00198	0.009851	97502	961	485111	3678554	37.7278129
'50-54'	5	0.5	0.00293	0.014543	96542	1404	479199	3193443	33.0783032
'55-59'	5	0.5	0.00464	0.022934	95138	2182	470235	2714243	28.5295809
'60-64'	5	0.5	0.00732	0.035942	92956	3341	456427	2244009	24.1405545
'65-69'	5	0.5	0.0113	0.054948	89615	4924	435764	1787582	19.9473634
'70-74'	5	0.5	0.01844	0.088137	84691	7464	404793	1351817	15.9617972
'75-79'	5	0.5	0.03206	0.148405	77226	11461	357480	947024	12.2629584
'80-84'	5	0.5	0.06078	0.263814	65766	17350	285453	589544	8.96432522
'85-89'	5	0.5	0.11008	0.431619	48416	20897	189836	304091	6.28082593
'90-94'	5	0.4	0.18857	0.602187	27519	16571	87879	114255	4.15191671
'95-99'	5	0.3	0.30721	0.740181	10947	8103	26376	26376	2.40936569
'100+'	2.1	1	0.47403	0.995463	2844	2831	0	0	0

$$q_x = \frac{n_x M_x}{1 + n_x(1 - a_x)M_x} \tag{B.8}$$

$$l_{x+n_{x+1}} = l_x(1 - q_x) \tag{B.9}$$

$$d_x = q_x l_x \tag{B.10}$$

$$L_x = n_x(l_{x+n_{x+1}} + a_x d_x) \tag{B.11}$$

$$T_x = T_{x+n_x} + L_x \tag{B.12}$$

$$e_x = \frac{T_x}{l_x} \tag{B.13}$$

Therefore prior to implementing this additional theoretical safety regulation, the life expectancy in Switzerland is 81.3042 years. The post implementation observed death rate is calculated by uniformly reducing the observed death rate for each time increment by the regulation's global impact, *dM*, which in this example is equal to $-1 \cdot 10^{-6}$.

$$M_{x1} = M_x\left(1 + \frac{dM}{M_x}\right) \tag{B.14}$$

Once the modified death rates (M_{x1}) for each increment have been calculated, the resulting post-implementation life expectancy, shown in

Table B-2, is then calculated following the process presented in Equations (B.8) to (B.13). Lastly, the change in life expectancy at birth is:

$$de = e_{x1} - e_x \tag{B.15}$$

Table B-2: Modified 2004 life table for Switzerland.

Age interval x	Interval duration n_x	Death rate factor [WHO 2007] a_x	Modified death rate M_{x1}	Modified probability of death q_{x1}	Modified number of survivors l_{x1}	Modified number of deaths d_{x1}	Modified total number of years lived in age interval L_{x1}	Modified total number of years lived beyond age x T_{x1}	Modified life expectancy (years) e_{x1}
'<1'	1	0.1	0.004239	0.004223	100000	422	99620	8130756	81.3075591
'1-4'	4	0.4	0.000189	0.000756	99578	75	398130	8031136	80.6519439
'5-9'	5	0.5	0.000109	0.000545	99502	54	497377	7633006	76.7117253
'10-14'	5	0.5	0.000109	0.000545	99448	54	497106	7135629	71.7521817
'15-19'	5	0.5	0.000339	0.001694	99394	168	496550	6638523	66.7899344
'20-24'	5	0.5	0.000529	0.002642	99226	262	495473	6141974	61.8989983
'25-29'	5	0.5	0.000449	0.002242	98964	222	494263	5646500	57.0563167
'30-34'	5	0.5	0.000529	0.002642	98742	261	493056	5152237	52.1789333
'35-39'	5	0.5	0.000809	0.004037	98481	398	491411	4659180	47.310508
'40-44'	5	0.5	0.001179	0.005878	98083	577	488975	4167770	42.4921339
'45-49'	5	0.5	0.001979	0.009846	97507	960	485134	3678795	37.7285845
'50-54'	5	0.5	0.002929	0.014539	96547	1404	479225	3193661	33.0789045
'55-59'	5	0.5	0.004639	0.022929	95143	2182	470262	2714436	28.530036
'60-64'	5	0.5	0.007319	0.035937	92962	3341	456456	2244174	24.140887
'65-69'	5	0.5	0.011299	0.054943	89621	4924	435794	1787719	19.947596
'70-74'	5	0.5	0.018439	0.088132	84697	7465	404822	1351925	15.9619509
'75-79'	5	0.5	0.032059	0.148401	77232	11461	357508	947103	12.2630531
'80-84'	5	0.5	0.060779	0.26381	65771	17351	285477	589595	8.96437865
'85-89'	5	0.5	0.110079	0.431615	48420	20899	189852	304118	6.28085358
'90-94'	5	0.4	0.188569	0.602185	27521	16573	87887	114266	4.15192936
'95-99'	5	0.3	0.307209	0.74018	10948	8104	26379	26379	2.40936975
'100+'	2.1	1	0.474029	0.995461	2845	2832	0	0	0

In this example, the change in life expectancy *de* = 81.3075591-81.3041514 or 0.0034077 years.

Substituting these values into Equation (B.7), the maximum optimal life-saving investment is:

$$dg = \frac{\$50387 \cdot 0.0034077\,years}{\frac{0.1376}{1-0.1376} \cdot 80.304\,years} = \$13.25\,/\,person$$

Thus if this safety regulation were to be applied to 1 million Swiss residents (thereby saving on statistical life), the resulting maximum optimal life-saving investment would be $13.25*1,000,000 or $13.25 million.

B.4.3 Gaining a global perspective

To gain a perspective of how the optimal life-saving investment varies around the globe, the calculation presented in Example B-2 was repeated for 189 additional countries. Some countries, like Demark, Iceland or Ireland have GDP per capitas, life expectancies and work to leisure ratios within 6.5% of Switzerland's. Other countries, like Bolivia, Cambodia, Chad, India and South Africa have GDP per capitas 10% to 1% of Switzerland's GDP, life expectancies 58% to 80% lower than Switzerland's life expectancy and work to leisure ratios 9 to 25% higher than Switzerland's work to leisure ratio.[16]

[16] Please note: the work to leisure calculation assumes a work week of 40 hours, a retirement age of 65 and in instances where life expectancy is lower than 65, the life expectancy is used as the maximum work age.

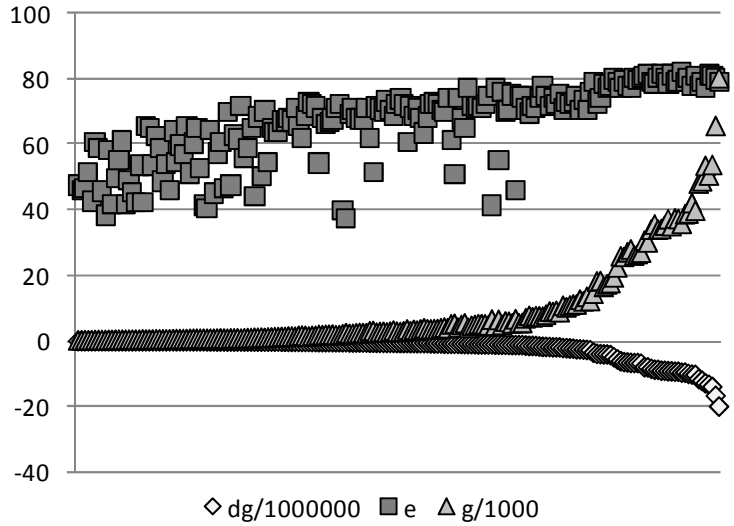

Figure B-1: Optimal life-saving investment (*dg*), life expectancy (*e*) and GDP per capita (*g*) plotted across the data set.

In Figure B-1, the optimal life-saving investment per 1 million individuals ($dg/1{\cdot}10^6$), the life expectancy (*e*) and the GDP per capita (*g*) for each of the 190 representative countries have been sorted by increasing the *dg* values (please note that as *dg*, the optimal life-saving investment, is an expenditure, it is shown as a negative value). In Figure B-1, one can see that over 60 percent of the countries in the studied data set, the GDP per capita and the optimal life-saving investment are just slightly increasing, while the life-expectancy for these same countries exhibits strong growth.

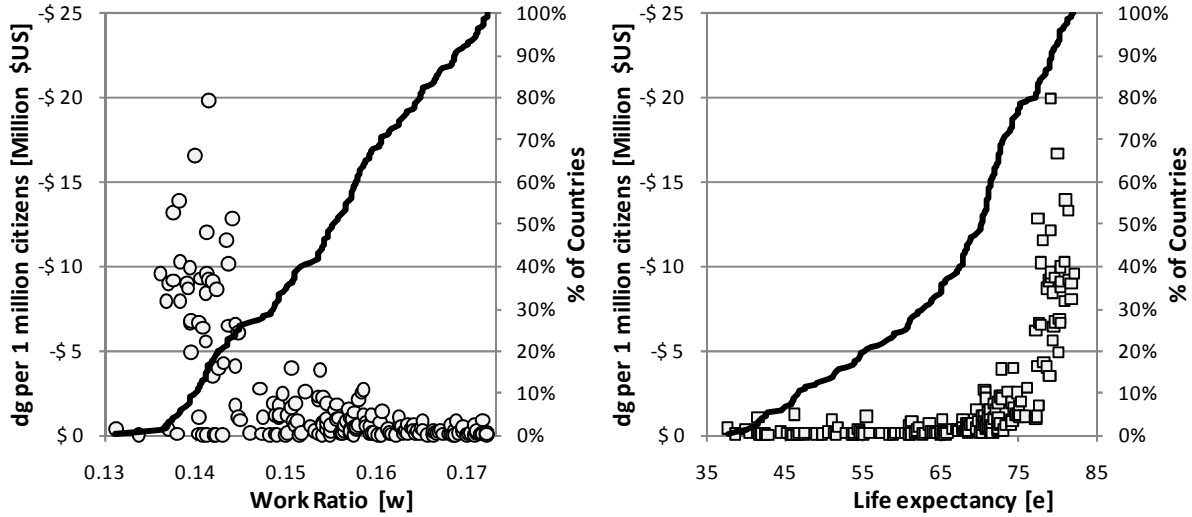

Figure B-2: The optimal life-saving investment per one million citizens (shown in millions of dollars) plotted against a) Work to leisure ratio (*w*), b) Life Expectancy (*e*)

Interestingly enough, during the last 40% of the data set, the GDP per capita and optimal life-saving investment show exponential growth while the life-expectancy growth slows.

Looking at the individual variable influence upon the resulting optimal life-saving investment, it can be seen in Figure B-2a that the work to leisure ratio (*w*) has no significant correlation with the optimal life-saving investment. In Figure B-2b one can observe that below a life expectancy of 70 years of age, the optimal life-saving investment is consistently low. It is only when the life-expectancy surpasses 70 years of age that the optimal life-saving investment exponentially increases.

Furthermore, in Figure B-3, one can observe that the change in life expectancy (*de*) increases linearly with an increasing original life-expectancy (*e*). From these two figures, one can observe that as the potential length of life increases, the associated optimal life-saving investment and the resulting change in life expectancy also increases.

From this cross country analysis, one can observe that the optimal life-saving investment is a function of the given country's GDP per capita, life expectancy, and work to leisure ratio. A large portion of the world, the developing countries in particular, has a relative low and consistent optimal life-saving investment reflecting the limited resources available to the given countries. As additional financial and human production resources become available (GDP per capita and life expectancy increases) the optimal life-saving investment increases at an exponential rate. Through the LQI approach, analytical risk analysts can compute the optimal life-saving intervention costs for various countries around the globe and through applying this approach they can ensure the life-saving investment does not outstretch the country's available resources.

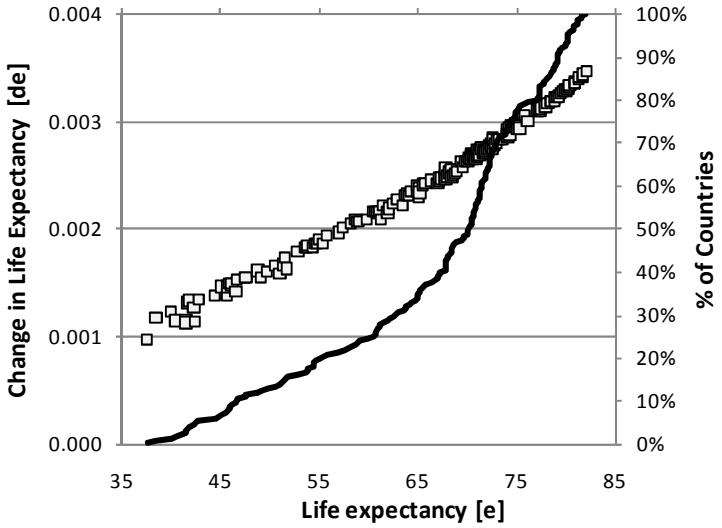

Figure B-3: The change in life expectancy (*de*) plotted against the Life expectancy (*e*)

B.5 Applications of the LQI in industry[17]

The life quality index and the derived optimal life-saving investment have been employed as a fundamental element in the cost benefit analysis of a number of different risk decision processes including in regulating particulate matter and ozone levels in Canada, in evaluating various nuclear safety options, in determining the acceptable level of investment to advert traffic and road accidents and in formulating an inspection planning regime for offshore production facilities.

Regulating particular matter and ozone levels in Canada

Ozone molecules and particulate matter (including soot, acids, sulphates and nitrates) pose a threat to life, for these particles penetrate deep into lungs blocking and damaging the individual's bronchi and alveolar sacs – reducing the individual's lung capacity. If exposure time and levels persist,

[17] Please note: the life quality index and optimal life saving investment values stated within this section are directly from their respective source documents. The respective calculation values and approaches have not been updated to match the calculation approaches presented in Equation (B.2). Lastly, the dollar valuations have not been updated to reflect inflation.

significant lung damage can accumulate, contributing to an increased risk to life of the individual (Pope, et al., 1995). In Canada, the particulate matter and ozone standards are first formulated by the Standards Development Committee which are then submitted to and ratified by the Canadian Council of Ministers of the Environment.

In 2000, the Canadian Standards Development Committee employed a cost benefit analysis based upon the Air Quality Valuation Model to estimate health benefits associated with pollution reduction, the LQI optimal life-saving investment to formulate a financial valuation for each life saved and the U.S. EPA data to estimate the cost and emission regulation efficiency options for various air particulate and ozone regulations ranging from $PM_{10}/PM_{2.5}$ = 70/35 to 50/25 mg/m^3 and 70 to 60 ppb respectively. This cost benefit analysis found that when evaluated independently, the most stringent particulate regulation level $PM_{10}/PM_{2.5}$ = 50/25 was still cost effective with an estimated cost of $1.6 billion, an avoided mortality savings of $12.3 billion and a cost benefit ratio of 7.7 while the most liberal ozone regulation 70 ppb was cost effective with an estimated implementation cost of $790 million, an avoided mortality savings of $740 million and a cost benefit ratio of 0.9. A potential composite particulate-ozone regulation was reached by combining to slightly less stringent regulation options resulting in a $PM_{10}/PM_{2.5}$/ozone = 60/30/65 regulation limits with a joint estimated cost of $2.41 billion, an avoided mortality savings of $8.16 billion and a cost benefit ratio of 3.3 (Pandey & Nathwani, 2003).

Selecting nuclear safety programs for Canadian nuclear reactors

A number of Canadian nuclear reactors are envisioned to reach the end of their service lives within the next 15 years. To continue operating these reactors, cost effective refurbishment solutions must be found – otherwise the most cost effective solution will be to decommission the facilities. A key element in evaluating the cost effectiveness of the various refurbishment options is selecting refurbishment options which efficiently meet the plant worker and neighboring population radiation exposure limits. The worker age-adjusted low-level ionizing radiation mortality risk is estimated at 0.026 lives/Sv (National Academy of Sciences, 1990)

To evaluate the various ionizing radiation reduction options, the investigators computed the relative change in life expectancy of a 35 year old worker exposed to 1 mSv/year/person over a 30 year professional life. The resulting change in life expectancy (*de/e*) was equal to $5.1982*10^{-4}$. Likewise the optimal life-saving investment for the 35 year old worker was computed to be 112.9 $/year/person/Sv with a total compensation of 4967 $/person/Sv for the remaining expected 44 years of life. The investigators then compared the cost of the safety measures installed during construction of a typical plant against the financial equivalent lost of life adverted by the active functioning of said safety measures (considering population distribution near the plant and local environmental conditions affecting radiation dispersion) and found that the safety improvement costs ($1.7 billion) are justified to advert the expected mean population dose of 1300-1400 Sv (Ontario Hydro, 1987) (Pandey & Nathwani, 2003).

Roadway maintenance and safety in the Netherlands

The quality of a roadway surface, the roadway skid resistance and tire rut depth, is a function of the amount of invested upkeep maintenance. The roadway surface quality influences the number of road accidents and fatalities with the surface quality being inversely related with the number of accidents and fatalities. In this specific case, the risk managers explored if the current level of road maintenance was justified against the potential number of adverted accidents and fatalities.

Considering the road segment in question, the risk managers determined that reducing the level of annual maintenance at a savings of 20€ million would result in 6 additional depths per year. In applying the life quality index and through considering non-fatal accident related costs, the risk managers determined the additional loss of life and damage costs would total 39€ million – far exceeding the saved maintenance investment. Thus from the application of the LQI, the risk managers were able to confirm that the current level of maintenance is appropriate and necessary (Pandey, van Noortwijk, & Klatter, 2006).

Inspection planning for offshore production facilities

Fixed offshore welded steel structures – commonly used in oil production operations – are highly susceptible to fatigue crack development. Direct or indirect visual inspection of the steel members and welded connections can be employed to verify the occurrence and developmental extent of potential cracks. Unfortunately, these cost prohibitive preventative measure can quickly jeopardize the financial stability of such offshore structures. Thus, risk-based assessments are employed in developing inspection regimes.

In the case at hand, the inspection plan developers employed a LQI based risk assessment approach which considered potential personal, environmental and ecological risks. Through applying this approach, the development team was able to formulate an optimal inspection plan which fulfilled the stated acceptance criteria which included the LQI valuation of life (Faber, Straub, & Goyet, 2003).

From these examples, one can observe that current complex engineering decision processes in a wide range of technical domains and geographic locations can be addressed through applying a life quality index based risk assessment. This can aid risk analysts in arriving at analytically optimal decisions that balance available resources against the implement life-saving regulations.

B.6 Investigating the validity of the LQI theoretical foundation

B.6.1 LQI: The solution?

If engineering decisions including such items as particulate matter and ozone pollution regulation, nuclear safety programs in Canadian nuclear reactors, roadway maintenance investment and offshore production facility inspection planning fulfill if not surpass the LQI optimal life-saving investment requirements, why is there still such significant public concern and distrust of the decisions set forth by risk managers (Slovic, 1999)? It is proposed that this public concern and potential distrust is a direct product of the different risk assessment approaches employed by technical risk managers and the experiencing public.

B.6.2 Equally distributed risk reduction funds

On the surface, the argument of equally distributed life-saving interventions to obtain the largest gain, without considering who the recipient is sounds reasonable, but the LQI developers made two flawed assumptions counterintuitive to human nature in formulating this tenet. The LQI developers have assumed:

a) safety expenditure is directly transferable between risk sources
b) individuals are capable of impartially allocating life-saving investment

To detail this, first reanalyze the differences between the developing world diarrheal disease life saving investment (an investment of $1.03/saved) verses chloroform reduction at 70 pulp and paper mills (an investment of $19.3 million/life saved). The implementation of additional chloroform reduction will place an additional financial burden on these 70 mills making the paper and paper products produced at these mills less price competitive, if not making their sale economically unviable. In a non-commoditized market, these additional regulations will raise the consumer unit price of paper and paper products. But the question that rests on this situation is, if these regulations were removed and these lower regulation production savings were passed onto the consumer, would the consumers freely transfer the saved money to an alternative risk source thereby reinvesting these funds to reduce other risks to life such as combating diarrheal diseases in the developing world? Such a reinvestment would by no-means not be warranted for, as mentioned earlier, diarrheal diseases take the lives of over 3 million children each year and to prevent each lost life cost the investment of $1.03/life saved. Unfortunately, it is highly unlikely that the consumer would freely transfer the saved funds to alternative risks if such stringent regulations, like chloroform regulations at 70 pulp and paper mills were to be reduced. It is more likely in this deregulated market that the paper producers would just strive to increase their respective market shares and profits while the consumers would strive to increase the quantity and quality of goods purchased – each directly bypassing the potential reinvestment of limited life-saving funds. It is proposed that this potential reinvestment of life-saving funds is not considered by the consumer because when purchasing paper products, the consumer does not observe the regulation-based life-saving investment or the reduction of harmful pollutants; he only sees the quality and price of the paper product and therefore only considers financial and quality purchasing reallocations when the price is reduced.

The second assumption made by the LQI developers is that individuals are capable of impartially allocating life-saving investments. In a perfectly utopian society, each individual facing an equivalent normalized risk would be valued equally, but in reality when it comes to life saving investments, allocating life-saving investment is as much a product of the valuation context as the risk source.

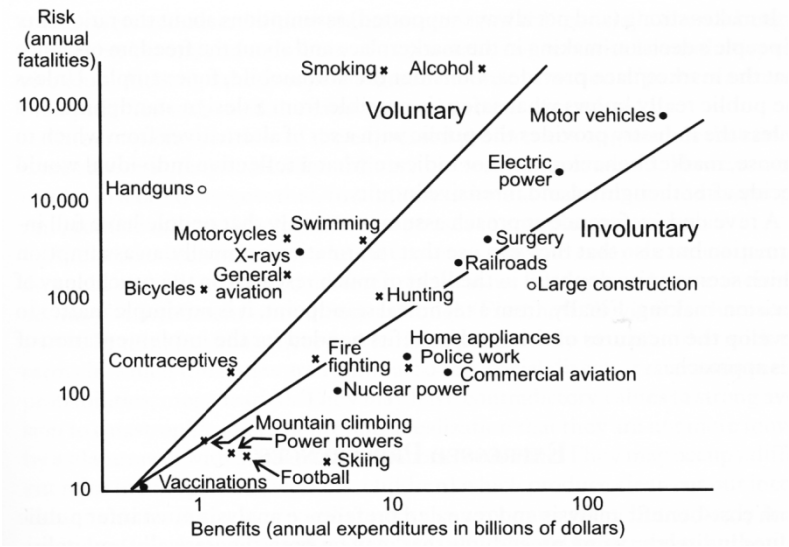

Figure B-4: Risks as a function of benefits with voluntary (x) and involuntary (•) risks.

Figure B-4 presents a cross comparison of the benefits (annual expenditures in billions of dollars versus the risks (annual fatalities) of 25 different risk sources (Fischhoff, Slovic, & Lichtenstein, 2004).

Within this figure the voluntary risks (e.g. swimming and alcohol consumption) are represented with an x, the involuntary risks (e.g. nuclear power and commercial aviation) are represented with a filled circle and the inconclusive risks (i.e. handguns and large construction) are represented with open circles. From this figure, one can observe that a significant dispersion in the amount of money invested in combating the various risk sources. Furthermore, more resources are invested on average in combating involuntary risk sources in comparison to voluntary experienced risk sources.

Such contextual influence over the risk valuation is also apparent in a research study conducted by Michael Siegrist (1997) who asked a group of individuals to state the amount they were willing to allocate for a safer medicine. The key element of this experiment was that stated valuations for risks represented as probabilities (e.g. 0.0006) were compared against risks represented as frequencies (600 in 1,000,000). Dr. Siegrist found that risks presented in a frequency format were consistently allocated a higher value than risks represented in a probability format.

If such societal valuations are blindly ignored rather than directly addressed, the employed technical risk management policy may be incongruent with society's expectations – creating an environment of distrust between the public and the risk manager.

B.6.3 Accountability principle

The LQI developers' second tenet is that a unified rationale should be developed for taking action in society's interest for managing risks affecting the public. They then propose that once this rationale is known and accepted, this rationale should remove the day-to-day risk decisions from the political arena where, in LQI developers' opinion, they do not belong.

While, it is important to develop a unified rationale for managing risks affecting the public, it is essential that this process involve direct public participation or at least a public vetting stage rather than unilaterally removing the day-to-day risk decisions from the political arena, as is proposed by the LQI developers. Since the direct result of well or poorly managed risks is the increase or decrease of public health and safety, this process by all means should involve the people who are directly affected – the public and associated stakeholders.

Indirect and direct public participation in governmental decisions has been a key element of direct and representational democracies for centuries. Recently, one approach to further foster public and stakeholder involvement has been the formation of deliberative democracies – governmental bodies composed of common citizens who discuss, deliberate, formulate and manage the implementation of policy decisions for issues commonly relegated to formal governmental bodies (Fung & Wright, 2003). Two poignant examples of deliberative democracies are the formulation of environmental regulations within the United States and the management of local communities in Kerala, India.

Within the United States the bulk of environmental regulations are formulated by the Environmental Protection Agency (EPA), a federal governmental body. One of the primary legislative policies employed by the EPA is the Endangered Species Act (ESA) which forbids any government agency, corporation or citizen from harming or harassing endangered and threaten species or their respective environments. While these regulations do prevent communities from negligently altering the environments of endangered or threaten species, it also prevents communities from taking actions which improve an endangered or threaten species' environment. It is within this former case that Habitat Conservation Plans (HCPs), a form of deliberative democracy, has fostered. Habitat conservation plans are conservation oriented land use plans which have been tailored to meet the

environmental and economic constraints of the given location. The development of HCPs has shown that when multiple economic, political, environmental and civic stakeholders are each individually motivated to participate in creating a HCP, the end result is a sound marriage between the environmental and economic constraints of the given region. But where only one or two stakeholders motivated to participate, commonly a land-owner or natural resource extraction company, the resulting HCP is significantly slanted towards meeting the economic interests of the involved stakeholders (Karkkainen, 2003).

In Kerala, one of India's 28 states, a five year deliberative democracy pilot program was conducted between 1996 and 2001. Within this program, forty percent of the state's developmental investment funds were allocated directly to over 1200 newly created Local Self-Governing Institutions (LSGIs). Each LSGI was comprised of citizen volunteers from the respective local area. These volunteers, who were commonly first given informal civic training, were charged with assessing the local community's developmental needs and formulating development related projects. Through the course of the five year program, it was found that when adequate civic training was provided, the LSGIs helped to greatly improve the efficiency and applicability of the development investment. Instances where the civic training resources were scarce due to financial or political constraints, the quality of the developmental investment also suffered (Isaac & Heller, 2003).

These two example cases show that public involvement, particularly when the local citizens are personally motivated and given informal civics training, can be an asset, rather than a potential complication to be avoided, for formulating public decisions.

In formulating their accountability principle, The LQI developers add the condition that once this process is known and accepted, the process will be removed from the political arena. The developers fail to consider that public acceptance for a process is highly sensitive to public trust and public trust is fueled by transparency and public interaction (Freudenburg, 2003). By removing this risk management process from the public realm, the developers are undermining public interaction and are developing a ripe environment for diminished public trust and potential rejection of this proposed process (Frewer, 2003).

Lastly, in assessing and mitigating extremely rare risks (i.e. the safe functioning of a nuclear power plant, environmental regulation, mitigating natural risks) the information contained and discussed within the analytical risk assessment process is commonly the only venue through which the general public can be exposed to analytical risk information. If this sole remaining avenue for accessing the truth and reanchoring one's experience-based risk assessment is removed, the general public will be completely adrift – left to the whims and currents of the media and popular viewpoints (Leiss, 2003). In such an ostracized environment, it is not surprising that the general public's experience-based risk assessment can significantly differ from the practitioner's analytical risk assessment.

B.6.4 Fair compensation

The third tenet posed by the LQI developers is that potential losers of life-saving investment reallocations can be turned into non-losers through the allocation of secondary compensation if the compensation is viewed as fair by those affected. In forming this tenet, the LQI developers fail to consider the limitation that stakeholders in public risk decisions, particularly potential losers, are seldom in a position where they can freely express their opinions and demand what they believe is 'fair' compensation.

Within the factory worker example presented earlier, the acceptance of the risky working environment and the associated danger pay without confirmation that alternative employment choices and opportunities are in fact available to the factory workers is a prime example of negative liberty – the workers have liberty from oppression (the ability not to work in the elevated hazardous work environment) but the costs of this liberty (leaving the job) is not considered (Wikipedia, 2008). The intricacies of negative liberty have been extensively studied by Amartya Sen who in analyaing the causal forces of famines has shown that famines are commonly caused not by the shortage of food but by the inability of the starving population to purchase or acquire food (Sen, 1981). The individuals starving in a famine are free to choose (they have liberty) but their choice was constrained by their financial situation. Thus the only choice they had was to starve to death (negative liberty). Without positive liberty – "the opportunity and ability to fulfill one's own potential" – the choice made by the factory worker or by the starving citizen can by no means be viewed as 'fair' (Wikipedia, 2008). Thus to actually transfer potential losers into non-losers through secondary compensation, one must transparently engage the general public or given group in active discussion and interaction in an environment devoid of the negative liberty constraints thereby ensuring the given group has the knowledge and the capacity to evaluate and freely accept or reject the offered compensation. Only under such situations can chosen compensation be deemed `fair´ compensation.

B.6.5 A solution for the LQI?

From these investigations and discussions, one can observe that a large range of information, capability and political barriers can undermine the validity and applicability of the LQI theoretical tenets. In face of these barriers one is faced with the question of which way to proceed –

1) Employ an LQI based analytical risk management approach by declaring these barriers as non-consequential and proceed unilaterally in managing risks in conformance with the LQI thereby removing the day-to-day risk decisions from the political arena where, in LQI developers' opinion, they do not belong.
2) Employ a populist risk management approach by minimizing the analytical practitioners' influence in the risk management process and transferring the risk management approach over to the political establishment and the general civic communities.
3) Develop the basis for a joint socially and analytically optimal risk management approach by declaring a need for a analytically based risk management approach and investigating how the management of the risk source contextual elements can influence society's experience-based risk assessment.

This first option, declaring the capability and political barriers non-consequential and proceeding unilaterally in managing risks in conformance with the LQI recommended investment levels is a relatively compact and actionable solution for the risk assessment, decision formation and policy implementation would be all conducted by the same entity – the analytical practitioner. Unfortunately, this option wrests the risk management process from the social and political realms and hence if the developed decisions prove contrary to society's desires or concerns the resulting reactionary response could significantly undermine, if not outright jeopardize, the analytical practitioner's participation in the risk management process.

The second option, transferring the risk management approach over to the political establishment and general civil communities has been proven to be a valid solution for managing issues in which multiple stakeholders have a strong motive to be involved in the deliberative process and where sufficient civic training and support is provided. Thus this approach should be valid for making very geographically, temporally and subject focused risk decisions – such as determining the location of a power plant. Unfortunately the stakeholders' personal interest or analytical expertise may be exceeded when the technical aspects of the risk source passes either into less contentious or more complex technical aspects, undermining the risk management body.

The third option – declaring a need for a analytical based risk management approach but investing time and resources into researching how the management of the risk source contextual elements can influence the social experience-based risk assessment would facilitate the analytical risk manager in contextualizing and tuning the risk management policies to meet society's concerns while maintaining the majority of the risk management tasks within the same entity – the analytical practitioner.

This third option is the perspective and approach actively employed in this work.

B.7 A Path Forward – Investigating the Dynamics of Experience-Based Risk Assessment

Chapters 5, 6 and 7 lay the foundation for building a bridge connecting the analytical and social experienced-based aspects of risk management. The three main steps of this methodological construction project are:

1) Developing a quantitative model from key findings within the psychology and sociology fields to simulate an individual's social experience-based risk responses to sequence of events (Chapter 5).
2) Employing this quantitative model to simulate the experience-based risk assessment responses to different risk management approaches – with addressing particular attention to how the risk source event magnitude and societal risk source interaction frequency influences the social experience-based risk assessment. (Chapter 6).
3) Proposing and assessing the feasibility of a methodology for documenting the personal experience-based assessment of risk (Chapter 7).

C The psychology of person constructs[18]

Personal concepts – General constraints:

- Dichotomy corollary – A person's construction system is composed of a finite number of dichotomous constructs.
- Choice corollary – A person chooses for himself that alternative in a dichotomized construct though which he anticipates the greater possibility for extension and definition of his system.
- Range corollary – A construct is convenient for the anticipation of a finite range of events only.

Personal concepts – Interaction evaluation mechanism:

- Construction corollary – A person anticipates events by construing their replications.

Post-evaluation benchmark reformation:

- Experience corollary – A person's construction system varies as he successively construes the replications of events.
- Modulation corollary – the variation in a person's construction system is limited by the permeability of the constructs within whose range of convenience the variants lie.
- Organization corollary – Each person characteristically evolves, for his convenience in anticipating events, a construction system embracing ordinal relationships between constructs.
- Fragmentation corollary – A person may successively employ a variety of construction subsystems which are inferentially incompatible with each other.

Societal concepts:

- Individuality corollary – Persons differ from each other in their construction of events.
- Commonality corollary – To the extent that one person employs a construction of experience which is similar to that employed by another, his psychological processes are similar to those of the other person.
- Sociality corollary – To the extent that one person construes the construction processes of another, he may play a role in a social process involving the other person. (Kelly G. A., 1963, pp. 103-104)

[18] Note, the corollaries have been reordered and separated into the subject titles to improve clarity.

D Works cited

24 Heures. (2003, July 11). Letters to the Editor: Réactions au drame du Grand-Pont. *24 Heures* , p. 30.

Aargau, C. o. (2007, April 17). Flood identification hazard maps. Aarau, Aargau, Switzerland.

Adey, B. (2008). ASTRA risk management approach. (J. Birdsall, Interviewer)

AISC. (1998). *Manual of Steel Construction - Load and Resistance Factor Design* (2nd Edition ed., Vol. 1). American Institute of Steel Construction.

Ang, A. H., & Tang, W. H. (1984). *Probability Concepts in Engineering Planning and Design* (Vols. II Decision, Risk and Reliability). New York: John Wiley & Sons.

Antonoff, L. (2003, July 9). On aurait dit un vrai jeu de quilles. *24 Heures* , p. 2.

AP. (2006, November 30). *Homeland Security assigns terror scores to travelers.* Retrieved 12 14, 2006, from CNN.com: http://www.cnn.com/2006/TRAVEL/11/30/traveler.screening.ap/index.html

ASCE. (2005). *Infrastructure Report Card 2005*. Retrieved Febuary 2008, 2008, from American Society of Civil Engineers: http://www.asce.org/reportcard/2005

ASTRA. (2008). *Effectiveness of inteventions.* Bern: Swiss national roads office.

Axhausen, K. W., Zimmermann, A., Schönfelder, S., Rindsfüser, G., & Haupt, T. (2002). Observing the rhythms of daily life: A six-week travel diary. *Transportation , 29* (2), 95-124.

Bargh, J. A., & Chartand, T. L. (1999). The unbearable automaticity of being. *American Psychologist , 54* (7), 462-479.

Bédat, A. (2003, October 15). L'interrogatoire du conducteur fou. *L'illustré* , p. 34.

Bernoulli, D. (1954). Exposition of a New Theory of the Measurement of Risk. *Econometrica , 22* (1), 23-36.

Birdsall, J. D., & Brühwiler, E. (2006a). Affect-based approach: quantifying user costs related to infrastructure. In T. Vogel, N. Mojsilovic, & P. Marti (Ed.), *6th International PhD Symposium in Civil Engineering.* Zurich: ETH Zurich Publications.

Birdsall, J. D., & Brühwiler, E. (2006). Changing perceptions: managing civil infrastructure in a post-intentional action environment. In C. G. Soares, & E. Zio (Ed.), *International Symposium Proceedings - Safety and Reliability for Managing Risk* (pp. 1257-1263). Estoril, 18-22 September: Taylor & Francis.

Birdsall, J. D., & Brühwiler, E. (2006b). Changing perceptions: managing civil infrastructure in a post-intentional action environment. In C. G. Soares, & E. Zio (Ed.), *International Symposium Proceedings - Safety and Reliability for Managing Risk* (pp. 1257-1263). Estoril, 18-22 September: Taylor & Francis.

Birdsall, J. D., & Brühwiler, E. (2006). Harnessing social perception of a bridge's condition. In P. Cruz, D. Frangopol, & N. LC (Ed.), *3rd International Conference on Bridge Maintenance, Safety and Management.* Porto: Taylor & Francis.

Birdsall, J. D., & Brühwiler, E. (2006a). Harnessing social perception of a bridge's condition. In P. Cruz, D. Frangopol, & N. LC (Ed.), *3rd International Conference on Bridge Maintenance, Safety and Management.* Porto: Taylor & Francis.

Birdsall, J., & Brühwiler, E. (2007). Methods for documenting the personally constructed reality of risk. *International Symposium: Safety and Reliability* (pp. 25-27). Stavenger: Taylor & Francis.

Boeree, C. G. (1997). *Personality Theories.* Retrieved May 21, 2008, from George Kelly: http://www.ship.edu/~cgboeree/kelly.html

Brehmer, B. (1970). Note on the effect of velocity on perceived duration. *Scandinavian Journal of Psychology , 11*, 157-160.

Brickman, P., & Campbell, D. T. (1971). Hedonic relativism and planning the good society. In M. H. Appley (Ed.), *Adaptation-level theory* (pp. 287-302). New York: Academic Press.

Bridge Safety Assurance. (2008, June 9). *Bridge Safety Assurance Manuals*. Retrieved June 9, 2008, from New York State Department of Transportation: https://www.nysdot.gov/portal/page/portal/divisions/engineering/structures/manuals

Canton de Vaud. (2006, March 3). *Stastique Lausanne*. Retrieved April 25, 2008, from http://www.scris-lausanne.vd.ch/

Charles, D. (2006, September 25). *Technology - GPS is smartening up your cell phone.* Retrieved December 7, 2007, from NPR - Morning Edition: http://www.npr.org/templates/story/story.php?storyId=6097216

Chikatamarla, R. (2007). *Optimisation of cushion materials for rockfall protection galleries.* Zurich: Swiss Federal Institute of Technology Zurich.

Cho, Y. H., Kim, J. K., & Kim, S. H. (2002). A personalized recommender system based on web usage mining and decision tree induction. *Expert Systems with Applications , 23* (3), 329-342.

Co, P. (2004, Febuary 13). Drame du Grand-Pont: l'hypothèse du malaise est exclue. *24 Heures* , p. 27.

Combremont, P. (2003, July 9). Fauchés et précipités dans le vide. *24 heures* , p. 2.

Csikszentmihalyi, M., & Hunter, J. (2003). Happiness in everyday life - the uses of experience sampling. *Journal of Happiness Studies , 4* (2), 185-199.

Csikszentmihalyi, M., Larson, R., & Prescott, S. (1977). The ecology of adolescent activity and experience. *Journal of Youth and Adolescence , 6* (3), 281-294.

Egli, T. (2005). *Objektschutz gegen gravitative Naturgefahren.* Bern: Vereinigung Kantonaler Feuerversicherungen VKF.

ESRI. (2006). ESRI ArcInfo. http://www.esri.com.

Eyer, W. (2007a, July 11). General natural hazard risk assessment discussions. (J. Birdsall, Interviewer)

Eyer, W. (2007). *Rapport explicatif: Cadastre des événements StorMe.* Fribourg: Service des Forêts et de la faune, Canton de Fribourg.

Faber, M. H., Straub, D., & Goyet, J. (2003). Unified approach to risk-based inspection planning for offshore production facilities. *Journal of Offshore Mechanics and Artic Engineering , 125* (2), 126-131.

FCC. (2007, December 7). *Enhanced 911 - Wireless Services*. Retrieved December 7, 2007, from http://www.fcc.gov/pshs/911/enhanced911/Welcome.html

FEMA. (2002). *A Guide to Using HAZUS for Mitigation.* Washington DC: The Federal Emergency Management Agency.

FEMA. (2007). *HAZUS-MH MR3 - Multi-Hazard Loss Estimation Methodology - Flood Model - Technical Manual.* Washington D.C.: Federal Emergency Management Agency.

FEMA. (2004). *Using HAZUS-MH for Risk Assessment - FEMA 433.* Washington DC: FEMA.

FHWA. (1995). *Recording and Coding Guide for the Structure Inventory and Appraisal of the Nation's Bridges.* Washington DC: Federal Highway Administration.

Fischhoff, B., Slovic, P., & Lichtenstein, S. (2004). Weighing the risks: Which risks are acceptable? In P. Slovic, *The Perception of Risk* (pp. 121-136). London: Earthscan Publications.

Fontaine, M. D., & Smith, B. L. (2004). *Improving the effectiveness of traffic monitoring based on wireless location technology.* Virginia: Virginia Transportation Research Council Final Report.

Frederick, S., & Loewenstein, G. (2003). Hedonic Adaptation. In D. Kahneman, E. Diener, & N. Schwarz, *Well-being: The foundations of hedonic psychology* (pp. 302-329). New York: Russell Sage Foundation.

Freudenburg, W. R. (2003). Institutional failure and the organizational amplification of risks: The need for a closer look. In N. Pidgeon, R. E. Kasperson, & P. Slovic, *The Social Amplification of Risk* (pp. 102-122). Cambridge: Cambridge University Press.

Frewer, L. J. (2003). Trust transparency and social context: Implications for social amplification of risk. In N. Pidgeon, R. E. Kasperson, & P. Slovic, *The Social Amplification of Risk* (pp. 123-137). Cambridge: Cambridge University Press.

Frey, K., Gerber, P., Kost, M., & Schneeberger, B. (2005). *Teilprojekt AGB 101: Voranalyse.* Bern, Switzerland: Bundesamt für Strassen (ASTRA).

Frick, M., & Aeberhard, B. (2008). *Gefahrenbeurteilung, Risikoanalyse, Massnahmenplanung Naturgefahren Mationalstrassen Kanton Bern (Risk assessment, risk analysis, natural hazard mitigation planning for the Berne Cantonal Federal Highways).* Berne: Tiefbauamt des Kantons Berne & Bundesamt für Strassen.

Fung, A., & Wright, E. O. (2003). *Deepening Democracy: Institutional Innovations in Empowered Participatory Governance.* London: New Left Books.

Garmin. (2006). *Forerunner 205/305 Owner's Manual.* Taiwan: Garmin Publications.

Genevay, Y. (2003, July 9). *Le Matin Online*. Retrieved Febuary 8, 2006, from En Images: http://www.lematin.ch/nwmatinhome/nwmatinhome/nwmatinheadactu/actu_suisse/une_voiture_tombe.diashowcontent.html

Giamboni, M. (2007). *SilvaProtect-CH - Phase 1.* Bern: Gefährenprävention, Bundesamt für Umwelt (BUFA).

Google. (2006). *Google Earth*. Retrieved January 30, 2006, from Google earth beta 3: http://earth.google.com

Gramlich, E. M. (1994). Infrastructure investment: A review essay. *Journal of Economic Literature , 32* (3), 1176-1196.

Hajdin, R. (2001). KUBA-MS: The Swiss Bridge Management System. In P. C. Chang (Ed.), *Structures 2001 - A Structural Engineering Odyssey.* Washington DC: American Society of Civil Engineers.

Hajdin, R., Axhausen, K., Bell, M., Birdsall, J., & Erath, A. (2008). *Consideration of vulnerability in the management of Swiss transportation infrastructure.* Berne: Swiss National Science Foundation - Sustainable Development of the Built Environment - National Research Program NRP54.

Hartle, R. A., Ryan, T. W., Mann, E. J., Danovich, L. J., Sosko, W. B., & Bouscher, J. W. (2002). *Bridge Inspector's Reference Manual.* Arlington: Federal Highway Administration.

Hartle, R. A., Thomas, R. W., Mann, E. J., Danovich, L. J., Sosko, W. B., & Bouscher, J. W. (2002). *Bridge Inspector's Reference Manual* (Vol. 1). Federal Highway Administration.

IMF. (2007). *World economic outlook database*. Retrieved January 8, 2008, from http://www.imf.org/external/pubs/ft/weo/2007/01/data/WEOApr2007all.xls

Intille, S. S., Rondoni, J., Kukla, C., Ancona, I., & Bao, L. (2003). A context-aware experience sampling tool. In G. Cockton, & P. Korhonen (Ed.), *Human Factors in Computing Systems.* Fort Lauderdale: ACM Press.

Isaac, T. T., & Heller, P. (2003). Democracy and Development: Decentralized Planning in Kerala. In A. Fung, & E. O. Wright, *Deepening Democracy: Institutional Innovations in Empowered Participatory Governance* (pp. 77-110). London: New Left Books.

Kahneman, D. (2000). Evaluation by moments: Past and future. In D. Kahneman, & A. Tversky, *Choices, Values and Frames* (pp. 693-708). New York: Cambridge University Press.

Kahneman, D. (2003). Maps on bounded rationality: Psychology for behavioral economists. *The American Economic Review , 93* (5), 1449-1475.

Kahneman, D., & Miller, D. (2002). Norm theory - comparing reality to its alternatives. In T. Gilovich, D. Griffin, & D. Kahneman, *Heuristics and Biases* (pp. 348-366).

Kahneman, D., & Tversky, A. (1979). Prospect theory - an analysis of decision under risk. *Econometrica , 47* (2), 263-292.

Kahneman, D., Diener, E., & Schwarz, N. (1999). Preface. In D. Kahneman, E. Diener, & N. Schwarz, *Well-being: the foundations of hedonic psychology* (pp. 26-39). New York: Russell Sage Foundation.

Kahneman, D., Krueger, A. B., Schkade, D. A., Schwarz, N., & Stone, A. A. (2006). A survey method for characterizing daily life experience - the day reconstruction method. *Science , 306* (5702), 1908-1910.

Karkkainen, B. C. (2003). Toward ecologically sustainable democracy? In A. Fung, & E. O. Wright, *Deepening Democracy - Instiutional Innovations in Empowered Participatory Governance* (pp. 208-224). London: New Left Books.

Kelly, G. A. (1963). *A Theory of Personality - The Psychology of Personal Constructs.* New York: W.W. Norton & Company Inc.

Kelly, G. A. (1955). *A Theory of Personality: The Psychology of Personal Constructs.* New York, New York: W.W. Norton & Company Inc.

Landfried, P. (2006, November 22). *Privacy Impact Assessment for the Automated Targeting System.* Retrieved December 7, 2007, from US Department of Homeland Security Report: http://www.dhs.gov/xlibrary/assets/privacy/privacy_pia_cbp_ats.pdf

Lausanne Tourisme. (2003). *City Map* .

Le Journal, 1. (Composer). (2003b). Accident spectaculaire à Lausanne: deux morts. [T. S. Romande, Conductor]

Le Journal, 1. (Composer). (2003a). La sécurité sur les ponts de Lausanne mise en cause. [T. S. Romande, Conductor]

Le Matin Online. (2003a, July 9). *Le Matin Online*. Retrieved August 2, 2006, from Une voiture tombe du Grand Pont: http://www.lematin.ch/nwmatinhome/nwmatinheadactu/actu_suisse/une_voiture_tombe.html

Le Temps. (2005, November 24). L'irresponsabilité écartée le drame du Grand-Pont a son coupable. *Le Temps* .

Leiss, W. (2003). Searching for the public policy relevance of the risk amplification framework. In N. Pidgeon, R. E. Kasperson, & P. Slovic, *The Social Amplification of Risk* (pp. 355-373). Cambridge: Cambridge University Press.

Loat, R. (2007). *Hazard mapping in Switzerland.* Bern: Gefährenprävention, Bundesamt für Umwelt (BAFU).

Lowe, P. A., Scheffey, C. F., & Lam, P. (1991). *Inventory of Lifelines in the Cajon Pass, California.* Washington, D.C.: Federal Emergency Management Agency.

Mahoney, M. J. (2003). *Constructive Psychotherapy: A Practical Guide.* New York, New York: The Guilford Press.

Meier, A. (2008, April 18). Natural hazard risk activities at SBB. (J. Birdsall, Interviewer)

Merritt, F. S., Loftin, M. K., & Ricketts, J. T. (1996). *Standard Handbook for Civil Engineers* (4th Edition ed.). New York: McGraw-Hill.

Mologogo. (2007, December 7). Retrieved December 7, 2007, from http://www.mologogo.com/

Muhieddine, F. (2003, October 21). Le Grand-Pont sera sécurisé. *Le Matin Suisse* , p. 9.

Nathwani, J., Lind, N., & Pandey, M. (1997). *Affordable Safety By Choice: The Life Quality Method.* Waterloo, Ontario: Institute for Risk Research.

National Academy of Sciences. (1990). *Health effects of exposure to low levels of ionizing radiation (BEIR V).* Washington, DC: Nathional Academy Press.

National Office of Topography Swisstopo. (2008, February 14). *Vector25.* Retrieved February 14, 2008, from Swisstopo: http://www.swisstopo.admin.ch/internet/swisstopo/en/home/products/landscape/vector25.html

National Resarch Council. (1983). *Risk Assessment in the Federal Government: Managing the Process.* Washington, DC: National Academy Press.

Normann, J. M., Houghtalen, R. J., & Johnston, W. J. (2001). *Hydraulic design of highway culverts* (2nd Edition ed.). Washington, D.C.: Federal Highway Administration National Highway Institute.

Okeil, A. M., & Cai, C. S. (2008). Survey of short- and medium-span bridge damage induced by hurricane katrina. *Journal of Bridge Engineering* , 377-387.

Omar, M. (2001, Nov 13). The long and winding road to women's transportation solutions. *The Economist* .

Ontario Hydro. (1987). *Darlington NGS probablistic safety evaluation: summary report.* Toronto, Ontario: Ontario Hydro.

Pandey, M., & Nathwani, J. (2003). A conceptual approach to the estimation of societal willingness-to-pay for nuclear safety programs. *Nuclear Engineering and Design , 224*, 65-77.

Pandey, M., & Nathwani, J. (2003). Canada wide standard for particulate matter and ozone cost-benefit analysis using a life qulaity index. *Risk Analysis , 23*, 55-67.

Pandey, M., & Nathwani, J. (2004). Life quality index for the estimation of societal willingness-to-pay for safety. *Structural Safety , 26*, 181-199.

Pandey, M., Nathwani, J., & Lind, N. (2006). The derivation and calibration of the life-quality index (LQI) from economic principles. *Structural Safety* (28), 341-360.

Pandey, M., van Noortwijk, J., & Klatter, H. (2006). The potential applicability of the life-quality index to maintenance optimization problems. In P. Cruz, D. Frangopol, & L. Neves (Ed.), *Bridge Maintenance, Safety, Management, Life-Cycle Performance and Cost.* London: Taylor & Francis Group.

Passer, C., & Bédat, A. (2005, November 2). Voiture folle chauffard fou? *L'Illustré* , p. 46.

Patidar, V., Labi, S., Sinha, K. C., & Thompson, P. (2007). *Multi-objective optimization for bridge management systems.* Washington D.C.: National Cooperative Highway Research Program - Transportation Research Board.

Pope, C., Thun, M., Namboodiri, M., Dockery, D., Evans, J., Speizer, F., et al. (1995). Particulate air pollution as a predictor of mortality in the prospective study of U.S. adults. *American Journal of Respiratory and Critical Care Medicine , 115*, 669-775.

Prin, M.-S. (2005, August 25). Le Grand-Pont va retrouver de vraies barrières. *24 Heures* , p. 21.

Puskin, J. S., & Bunger, B. (1996). Comments on Tengs et al., "Comparative Study of the Cost-Effectiveness of Life-Saving Interventions". *Risk Analysis , 16* (2), 131.

Rapport du Jury. (2005). *Grand Pont - Lausanne Railing Replacement.* Lausanne: Service d'Achitecture.

Resse, S., King, A., Bell, R., & Schmidt, J. (2007). Regional RiskScape: A multi-hazard loss modelling tool. In L. Oxley, & D. Kulasiri (Ed.), *MODSIM 2007 International Congress on Modelling and Simulation.* (pp. 1681-1687). Modelling and Simulation Society of Australia and New Zealand.

Richardson, E. V., & Davis, S. R. (2001). *Evaluating Scour at Bridges.* Washington, DC: Federal Highway Administration.

Rime, M. (2004, April 10). Le Grand-Pont retrouvera ses barrières d'antan. *24 Heures* , p. 23.

Risk Map. (2007, March 23). *Risk Map Germany*. Retrieved September 15, 2008, from EDIM Universität Karlsruhe: http://www.cedim.de/english/166.php

Rivers, L., & Arvai, J. (2007). Win some, lose some: The effect of chronic losses on decision making under risk. *Journal of Risk Research , 10* (8), 1085-1099.

SBB. (2008, October 7). *SBB Infrastructure*. Retrieved October 7, 2008, from SBB: http://mct.sbb.ch/mct/en/infra-ueber_uns/infra-i_zahlen.htm

SCDOT. (2008, May 9). *South Carolina traffic polling and analysis system*. Retrieved May 9, 2008, from http://dbw.scdot.org/Poll5WebAppPublic/wfrm/wfrmHomePage.aspx

Schwarz, N. (1987). *Stimmung als Information - Untersuchungen zum Einfluss von Stimmungen auf die Bewertung des eigenen Lebens (Mood as information on the impact of moods on evaluations of one's life).* Heidelberg: Springer-Verlag.

Sen, A. (1981). *Poverty and Famines: An Essay on Entitlement and Deprivation.* New York: Oxford University Press.

Siegrist, M. (1997). Communicating low risk magnitudes: incidence rates expressed as frequency versus rates expressed as probability. *Risk Analysis , 17* (4), 507-510.

Simon, H. A. (1957). *Models of Man: Social and Rational.* New York: Wiley.

Slovic, P. (1999). Trust emotion sex politics and science: surveying the risk-assessment battlefield. *Risk Analysis , 19* (4), 689-701.

Slovic, P., Finucane, M. L., Peters, E., & MacGregor, D. G. (2002). The affect heuristic. In T. Gilovich, D. Griffin, & D. Kahneman, *The Psychology of Intuitive Judgement* (pp. 297-420). New York: Cambridge University Press.

Smith, B. L., Zhang, H., Fontaine, M. D., & Green, M. W. (2003). Wireless location technology-based traffic monitoring - critical assessment and evaluation of an early-generation system. *Journal of Transportation Engineering , 130* (5), 576-584.

Smyth, J. M., & Stone, A. A. (2003). Ecological momentary assessment research in behavioral medicine. *Journal of Happiness Studies , 4* (1), 35-52.

Souders, M. (1966). *The Engineers Companion.* New York: John Wiley & Sons.

Spiegel, K., Knutson, K., Leproult, R., Tasali, E., & Van, E. (2005). Sleep loss - a novel risk factor for insulin resistance and Type 2 diabetes. *Journal of Applied Physiology , 99* (5), 2008-2019.

Stone, A. A., Shiffman, S. S., & DeVries, M. W. (1999). Ecological momentary assessment. In D. Kahneman, E. Diener, & N. Schwarz (Eds.), *Well-being - the foundations of hedonic psychology* (pp. 26-39). New York: Russell Sage Foundation.

Swissdox. (2006, March 30). *Votre partenaire pour la researche d'informations*. Retrieved April 23, 2008, from Swissdox: http://www.swissdox.ch

Tengs, T. O., Adams, M. E., Pliskin, J. S., Gelb Safran, D., Siegel, J. E., Weinstein, M. C., et al. (1995). Five-Hundred Life-Saving Interventions and Their Cost-Effectiveness. *Risk Analysis , 15* (3), 369-390.

The Economist. (2007, August 9). America's creaking infrastructure - a bridge too far gone. *The Economist* .

The Economist. (1999, December 16). Reverse Gear. *The Economist* .

The Economist. (2005, January 6). The long and expensive road. *The Economist* .

The Economist. (1998, September 3). The unbridgeable gap. *The Economist* .

Thompson, P. D., Small, E. P., Johnson, M., & Marshal, A. R. (1998). The Pontis Bridge Management System. *Structural Engineering International , 8* (4), 303-308.

Tversky, A., & Kahneman, D. (1974). Judgment under uncertainty: Heuristics and biases. *Science , 185* (4157), 1124-1131.

US Army. (1990). *Structures to Resist the Effects of Accidental Explosions.* Retrieved June 18, 2008, from Department of Defense Explosive Saftey Board: http://www.ddesb.pentagon.mil/tm51300.htm

US Department of Transportation - Federal Highway Administration. (2008, February 14). *Highway Statistics 2005.* Retrieved Febuary 14, 2008, from US Departmetn of Transportation: http://www.fhwa.dot.gov/policy/ohim/hs05/index.htm

Vickerman, R. (2004). Maintenance incentives under different infrastructure regimes. *Utilities Policy , 12*, 315-322.

Viscusi, W. K., & O'Connor, C. J. (1984). Adaptive responses to chemcial labeling: are workers Bayesian decision makers? *The American Economic Review , 74* (5), 942-956.

von Glasersfeld, E. (1996). The conceptual construction of time. In H. Helfrich (Ed.), *Proceedings of the International Symposium - Mind and Time.* Neuchâtel, 8-10 September: Hogrefe & Huber.

Vrtic, M., Fröhlich, P., Schüssler, N., Dasen, S., Erne, S., Singer, B., et al. (2005). *Erzeugung neuer Quell-/Zielmatrizen im Personenverkehr.* Swiss Federal Department for Environment, Transport, Energy and Communication. Zurich: Swiss Federal Office for Spatial Development, Swiss Federal Roads Authority and Swiss Federal Office of Transpot.

Wikipedia. (2007, December 10). *Global Positioning System*. Retrieved December 10, 2007, from Wikipedia - The free Encyclopedia: http://en.wikipedia.org/wiki/Global_positioning_system

Wikipedia. (2008). *Kaldo-Hicks Efficiency*. Retrieved January 8, 2008, from http://en.wikipedia.org/wiki/Kaldor-Hicks

Wikipedia. (2008). *Negative Liberty.* Retrieved January 10, 2008, from Wikipedia: http://en.wikipedia.org/wiki/negative_liberty

Wikipedia. (2008). *Positive Liberty.* Retrieved January 10, 2008, from Wikipedia: http://www.wikipedia.org/wiki/positive_liberty

Wolf, J. (2004). Applications of new technologies in travel surveys. In P. Stopher, & C. Strecher (Ed.), *International Conference Proceedings - Travel survey methods.* Costa Rica, 1-6 August.

World Health Organization. (2007). *Life tables for WHO member states*. Retrieved January 8, 2008, from http://www.who.int/whosis/database/life_tables/life_tables.cfm

Ygnance, J. L., Remy, J. G., Bosseboeuf, J. L., & Da Fonseca, V. (2000). *Travel time estimates on Rhone corridor network using cellular phones as probes: phase 1 technology assessment and preliminary results.* Arcueil: INRETS report.

Zingg, C. (2003b, July 11). Il meurt terrassé par l'émotion. *Le Matin Suisse* , p. 4.

Zingg, C. (2003a, July 9). *Le Matin*. Retrieved August 2, 2006, from Après avoir soigné, il faut parler: http://www.lematin.ch/nwmatinhome/nwmatinheadactu/actu_suisse/_apres_avoir_soigne,.html

James D Birdsall CV

Avenue des Cerisiers 6, Pully, 1009, Switzerland +41.(0)79.756.63.01 james.birdsall@epfl.ch

EDUCATION & PROFESSIONAL EXPERIENCE

Research Consultant, Assessing Swiss Transport Infrastructure Vulnerability, March 2007 - December 2008
Infrastructure Management Consultants (IMC), Zurich, Switzerland

- Failure modes due to sudden events are not considered by current Swiss infrastructure management approaches; correcting this weakness by doctoral research as a key consultant; developing and validating a vulnerability assessment methodology which can be easily integrated into existing infrastructure management programs; implementation of this research will significantly improve the management of Switzerland's transportation networks by allowing transportation network agencies to assess, quantify and work to correct the sources of vulnerability within their networks.
- Funding: Swiss National Science Foundation

Doctorate of Science in Civil Engineering, September 2004 – December 2008
Ecole Polytechnique Fédérale de Lausanne, Lausanne, Switzerland

- **"The Responsive Approach: An Integrated Socially-Sustainable Technically-Optimal Management Approach"**
  Within the public and quasi-public business sectors, long-term life cycle cost optimal solutions are only viable if public support is guaranteed. This does not reflect reality. By combining life cycle cost and vulnerability analyses with mapping the change of individual perceptions resulting from ongoing interactions within a given system, this weakness of traditional life cycle analysis can be prevented using elements of social-psychology and behavioral economics to create a more sustainable infrastructure management approach.
- Honors: EPFL University Scholar (complete funding for four year doctorate)

Structural Engineer, Bridge and Tunnel Division, June 2002-July 2004
Parsons Corporation, New York, New York, United States of America

- Spearheaded the development of an in-house blast assessment and mitigation team which analyzed conceptual designs of client sites.
- World Trade Center PATH Station Reconstruction, New York City, USA
  - Acted as a liaison between stakeholder clients for vetting conceptual designs
  - Co-Organized a stakeholder workshop to identify financial and project schedule risks
  - Assisted estimation team in meeting critical deliverables
- Emergency Retrofit of Waldo-Hancock Suspension Bridge Main Cables, Maine, USA
  - Part of four member team charged with developing an approach and procedure for a 100 day emergency retrofit required to avert the imminent failure of the main cables of a 622m suspension bridge.
  - Acted as an inspector and onsite consultant for fabrication, installation, and implementation of the developed procedure.
- Alfred Zampa Memorial Bridge, San Francisco, California, USA
  - Successfully refuted a $12 million claim (20% of the total contract) filed by the steel deck fabricator against Parsons Corporation and the State of California for additional and unanticipated work by creating a video detailing how the fabricator instigated the additional work by employing a non-standard fabrication procedure against the advice of Parsons Corporation.
  - Collaborated with a tight knit team to provide real-team fabrication review and onsite support for the construction of the 1056m suspension bridge.

Master of Science in Civil Engineering, GPA: 3.63/4.0, January 2001-June 2002
Lehigh University, Bethlehem, Pennsylvania, United States of America

- Developed a state-of-the-art conceptual design of an elevated fiber reinforced composite light railway for Bombardier Transportation which can be completely prefabricated and assembled onsite – significantly reducing costly onsite construction.
- Honors: Lehigh University Presidential Scholar (one year tuition funding), Magna cum laude

Structural Engineering Intern, Bridge and Tunnel Division, June 2001-August 2001
Parsons Corporation, New York, New York, United States of America

Bachelor of Science in Civil Engineering, GPA: 3.71/4.0, Department Rank: 2/39, September 1997-June 2001
Lehigh University, Bethlehem, Pennsylvania, United States of America

- Honors: Magna cum laude, Dean's List All Four Years

PUBLICATIONS

Birdsall, JD & Hajdin, R. Submitted. Vulnerability Assessment of Individual Infrastructure Objects Subjected to Natural Hazards. 10th International Bridge and Structure Management Conference. Buffalo, 20-22 October, 2008.

Birdsall, JD, Hajdin, R, Erath, A & Axhausen, K. 2007. **Assessing infrastructure vulnerability to sudden events**. INFRADAY 2007: 6th Conference on applied infrastructure research. Berlin, 5-6 October.

Birdsall, JD & Brühwiler, E. 2007. **Methods for documenting the personally constructed reality of risk**. International Symposium Proceedings: Safety and reliability for managing risk. Stavanger, Norway, 25-27 June.

Birdsall, JD & Brühwiler, E. 2006. **Changing perceptions: Managing civil infrastructure in a post-intentional action environment**. In Carlose Guedes Soares & Enrico Zio (editors), International Symposium Proceedings: Safety and reliability for managing risk, Estoril, 18-22 September 2006, London: Taylor & Francis.

Birdsall, JD. 2006. **Affect-based approach: Quantifying user costs related to infrastructure**. In Thomas Vogel, Nebojša Mojsilovi, Peter Marti (editors), 6th International PhD Symposium in Civil Engineering, Zürich, 23-26 August 2006, SP-015, Zürich: IBK Publikation.

Birdsall, JD & Brühwiler, E. 2006. **Harnessing social perception of a bridge's condition**. In Paulo J.S. Cruz, Dan M Frangopol and Luis C Neves (editors), Proceedings of the 3rd International Conference on Bridge Maintenance, Safety and Management, Porto, 16-19 July 2006, London: Taylor & Francis.

Birdsall, JD. 2002. **Structural Guideways: Advanced Materials and New Structural Systems**. Master's Thesis, Lehigh University, Dr. John L. Wilson & Dr. Ben Yen (advisors).

PRESENTATIONS

Assessing infrastructure vulnerability to sudden events. INFRADAY 2007: 6th Conference on applied infrastructure research. Berlin, 5-6 October 2007.

Changing perceptions: Managing civil infrastructure in a post-intentional action environment. International Symposium: Safety and reliability for managing risk, Estoril, 18-22 September 2006.

Affect-based approach: Quantifying user costs related to infrastructure. 6th International PhD Symposium in Civil Engineering, Zürich, 23-26 August 2006.

Defining Life in civil engineering life-cycle analysis. Structures Institute, Ecole Polytechnique Fédérale de Lausanne, 1 December 2005.

AWARDS

Ecole Polytechnique Fédérale de Lausanne University Scholar, September 2004-December 2008
Fully funded doctoral program for all four years.

Lehigh University Presidential Scholar, September 2001-June 2002
One year tuition funded, awarded for undergraduate scholastic achievement

Phi Beta Kappa Honor Society, March 2001

Inducted into the liberal arts and sciences honor society Phi Beta Kappa for undergraduate academic achievement.

CE News 2001 Star Student, December 2000

Ranked as one of the top 15 2001 United States of America civil engineering graduates by CE News a leading industry journal

Chi Epsilon Honor Society, December 2000

Inducted into the civil engineering honor society Chi Epsilon for undergraduate academic achievement.

Tau Beta Pi Honor Society, November 2000

Inducted into Tau Beta Pi honor society for undergraduate engineering academic achievement.

National Honor Society, December 1996

Inducted into Chatham High School's chapter of the National Honor Society for my high school academic achievement.

Eagle Scout, September 1994

Attained the rank of Eagle Scout – the highest award a scout can achieve in the Boy Scouts of America.

LEADERSHIP

Swiss Sustainable Development of the Built Environment Advisory Council, March 2007-December 2008

Active member of an inter-disciplinary team charged with advising the Swiss government semi-annually on pro-sustainability policies, research activities, and investments.

Scots Kirk of Lausanne Congregational Board Member, December 2005-December 2008

Elected to the congregational board of the Scots Kirk of Lausanne. As a board member I review and vote on budgetary and maintenance policies.

Habitat for Humanity Alternative Spring Break Faculty Advisor, March 2002

Lead 12 students on a week-long Habitat for Humanity trip.

Lehigh Christian Community Church founding member, January 2000-January 2002

Helped found an all student organized, contemporary Christian Church which hold weekly praise worship services on Lehigh University's campus.

Served as facilities manager and helped meet the church's facilities needs as it grew from 10 initial students to a congregation of over 150 students.

Chi Epsilon Vice President, December 2000-May 2001

Elected vice president of Lehigh University's civil engineering honor society Chi Epsilon

Represented the Lehigh chapter at the Chi Epsilon annual conference in Madison, Wisconsin.

Boy Scout Leadership Roles, September 1990-1997

Contributed to the growth and development of my fellow scouts by holding numerous leadership roles in my local troop.

Taught and lead over 45 young men in weekly scouting meetings and monthly weekend outings.

LANGUAGES English (native language), French (conversational)

PROFESSIONAL AFFILIATIONS American Society of Civil Engineers, European Safety and Reliability Association, Tau Beta Pi

INTERESTS: I enjoy running 10k and ½ marathons to keep my body and mind fit.